UNIVERSITY OF THE WITWATERSRAND, JOHANNESBURG

Doctoral Thesis

Modelling vector-borne diseases: epidemic and inter-epidemic activities with application to Rift Valley fever

Author:

Sansao Agostinho Pedro

Student number:763473

Supervisors:

Prof. Shirley Abelman

Dr. Henri E.Z. Tonnang

A Thesis submitted to the Faculty of Science in fulfilment of the requirements for the degree of Doctor of Philosophy

School of Computer Science and Applied Mathematics

Declaration of Authorship

I declare that this Thesis titled 'Modelling vector-borne diseases: epidemic and inter-epidemic activities with application to Rift Valley fever' is my own, unaided work. It is being submitted for the Degree of Doctor of Philosophy at the University of the Witwatersrand, Johannesburg. It has not been submitted before for any degree or examination at any other University.

Signed: _____

Date: _____

"Brethren, I do not count myself to have apprehended; but one thing I do, forgetting those things which are behind and reaching forward to those things which are ahead,"

Ap. Paul in Philippians 3:13, NKJV.

Abstract

In this thesis in order to study the complex dynamics of Rift Valley fever (RVF) we combine two modelling approaches: equation-based and simulation-based modelling. In the first approach we first formulate a deterministic model that includes two vector populations, *Aedes* and *Culex* mosquitoes with one host population (livestock), while considering both horizontal and vertical transmissions. An easy applicable expression of the basic reproduction number, R_0 is derived for both periodic and non-periodic environment. Both time invariant and time varying uncertainty and sensitivity analysis of the model is carried out for quantifying the attribution of model output variations to input parameters over time and novel relationships between R_0 and vertical transmission are determined providing important information useful for improving disease management.

Then, we analytically derive conditions for stability of both disease-free and endemic equilibria. Using techniques of numerical simulations we perform bifurcation and chaos analysis of the model under periodic environment for evaluating the effects of climatic conditions on the characteristic pattern of disease outbreaks. Moreover, extending this model including vectors other than mosquitoes (such as ticks) we evaluate the possible role of ticks in the spread and persistence of the disease pointing out relevant model parameters that require further attention from experimental ecologists to further determine the actual role of ticks and other biting insects on the dynamics of RVF. Additionally, a novel host-vector stochastic model with vertical transmission is used to analytically determine the dominant period of disease outbreaks with respect to vertical transmission efficiency. Then, novel relationships among vertical transmission, invasion and extinction probabilities and R_0 are determined.

In the second approach a novel individual-based model (IBM) of complete mosquito life cycle built under daily temperature and rainfall data sets is designed and simulated. The model is applied for determining correlation between abundance of mosquito populations and rainfall regimes and is then used for studying disease inter-epidemic activities. We find that indeed rainfall is responsible for creating intra- and inter-annual variations observed in the abundance of adult mosquitoes and the length of gonotrophic cycle, number of eggs laid per blood meal, adults age-dependent survival and flight behaviour are among the most important features of the mosquito life cycle with great epidemiological impacts in the dynamics of RVF transmission. These indicators could be of great epidemiological significance by allowing disease control program managers to focus their efforts on specific features of vector life cycle including vertical transmission ability and diapause. We argue that our IBM model is an ideal extendible framework useful for further

investigations of other relevant host-vector ecological and epidemiological questions for providing additional knowledge important for improving the length and quality of life of humans and domestic animals.

To my lovely family:
my wife Albertina Pedro and our daughters Sanny Ebenezer and Keila Immanuel; and my parents Carnada and Agostinho. For their unconditional love, encouragement, support and prayers!

Acknowledgements

Praise and glory be to the living Jehovah God for giving me such opportunity to undertake my PhD studies in the hands of such special supervisors.
I am indebted to my main supervisors Prof. Shirley Abelman and Dr. Henri Tonnang for their support and guidance throughout the conduct of this study. Working with them has allowed to me grow as a researcher and to explore my potential as a graduate student. I am grateful for their tireless dedication, encouragements and help along the way. Special thanks to Dr. Henri with whom I spent much more time at the International Centre of Insect Physiology and Ecology (ICIPE), in particular, during our weekly meetings. Most of the time I was not at Wits but I always felt like I am there and close. Thank you Prof. Shirley for making me feel comfortable in all our discussions and communications.
I would like to express my deepest thanks to my co-supervisor Dr. Rosemary Sang at ICIPE for fruitful discussions on the ecological and epidemiological aspects of vectors and hosts involved in the transmission of Rift Valley fever (RVF). I benefited a lot from her expertise as well as from Drs Baldwin Torto and David Tchouassi also from ICIPE for their comments. My special gratitude to Prof. Uta Berger for hosting me for 5 months at the Institute of Forest Growth and Forest Computer Sciences, Dresden University of Technology as a research visitor for developing a RVF individual-based model (IBM). Many thanks to her lab team for allowing me to enjoy their company and learn from their experience. Special appreciation to Adewole who received me as brother and helped me to settle down. Special thanks to my friend and Master's supervisor Prof. Jean Tchuenche for being by my side encouraging me to go forward and for reading and commenting on my manuscripts.
I also want to express my gratitude to ICIPE Capacity Building and Institutional Development group headed by Dr. Robert Skilton for their academic and administrative support. They were all ready to serve us and take good care of us. I extend my appreciation to the ICIPE student community for their friendship and for giving me a chance to learn to serve the community as the president of the ICIPE Scholars Association (IScA) from July 2014 to July 2015.
To my fellows in the research group: Sizah, Ben, Ritter and Frank thank you all for fruitful discussions during our weekly meetings. Special thanks to Frank with whom we spent much more time together trying to find some sense of our labour. Thank you for allowing me to benefit from your vast experience in numerical analysis. I am grateful to the IT team at ICIPE for their support.
I will never know how to say thank you to my special family. Thanks to my wife for her unconditional love, patience, tolerance, support and encouragement along this experience in a foreign land. To our first born for always allowing me to go abroad to bring her dresses. Special thanks to my parents, brothers and in laws who tirelessly supported us while abroad. Thank you all for your support and

many thanks to our church members and friends for their support in prayers.
Last but not least, I am grateful for the financial support from the Germany Academy Exchange Service (DAAD) with code number: A/13/95234 through the African Regional Postgraduate Programme in Insect Science (ARPPIS) based at ICIPE. I extend my appreciation to Eduardo Mondlane University, Mozambique for granting me study leave to pursue my PhD.

Contents

[1]This chapter has been published: S.A. Pedro et al., Uncertainty and sensitivity analysis of a Rift Valley fever model, Applied Mathematics and Computation (2016), http://dx.doi.org/10.1016/j.amc.2016.01.003

[2]This chapter has been published: Pedro SA, Abelman S, Ndjomatchoua FT, Sang R, Tonnang HEZ (2014) Stability, Bifurcation and Chaos Analysis of Vector-Borne Disease Model with Application to Rift Valley Fever. PLoS ONE 9(10): e108172. doi:10.1371/journal.pone.0108172

[3]This chapter has been published: S. A. Pedro et al. The role of *Hyalomma Truncatum* on the dynamics of Rift Valley fever. Insights from a mathematical epidemic model. Acta Biotheor. 64(3) 2016. DOI 10.1007/s10441-016-9285-0

[4]This chapter has been submitted to: PLOS Neglected Tropical Diseases

List of Figures

List of Tables

Abbreviations

RVF	**R**ift **V**alley **f**ever
RVFV	**R**ift **V**alley **f**ever **v**irus
ENSO	**E**l **N**ino **S**outhern **O**scillation
ODE	**O**rdinal **D**ifferential **E**quation
SDE	**S**tochastic **D**ifferential **E**quation
ABM	**A**gent **B**ased **M**odel
IBM	**I**ndividual **B**ased **M**odel
CDC	**C**enter for **D**isease prevention and **C**ontrol
IEP	**I**nter **E**pidemic **P**eriod
GAS	**G**lobal **A**ssymptotic **S**tability
LAS	**L**ocal **A**ssymptotic **S**tability

Symbols

$\mathbb{R}$	The set of real numbers
$\mathbb{R}_+$	The set of nonnegative real numbers
$\mathbb{R}^n$	The space of column vectors of size n of real numbers
$\mathbb{R}^n \times \mathbb{R}^n$	The space of $n \times n$ matrices of real numbers
C^1	The space of continuously differentiable functions
x	Is a vector in $\mathbb{R}^n$
$\dot{x}$	The derivative of each entry of vector x
$\bar{x}$	Represent an upper bound of vector x
R_0	The basic reproductive number

Chapter 1

Introduction

For many years there has been great interest in trying to understand what are the rules that govern the spread, emergence, re-appearance and even persistence of diseases. The emergence of infectious diseases has become a phenomenon of great concern, especially in the case of vector-borne viral zoonoses that occasionally give rise to human epidemics such as West Nile fever, Rift Valley fever (RVF) and Japanese encephalitis [7]. For the past few decades the occurrence of RVF outbreaks in endemic areas (sub-Saharan Africa) [8, 9], its emergence outside this region [10, 11] and its potential for global spread [12], has become a major concern for public health authorities worldwide [3]. RVF occurs at irregular intervals and the disease causes high mortality and abortion in domestic livestock, and significant morbidity and mortality in humans [13], with devastating economic impact particularly in vulnerable African communities with low resilience to economic and environmental challenges [1, 11, 14]. Therefore, use of sound knowledge regarding the dynamics of diseases and an understanding of the changing roles and relationships among the drivers and the constraints on their spread [15] are needed for optimizing and improving existing disease control interventions.

1.1 Background

1.1.1 Vector-borne diseases

Vector-borne diseases belong to a class of infectious diseases transmitted by the bite of infected arthropod species, such as mosquitoes, ticks, triatomine bugs, sandflies, and blackflies [16]. Transmission mechanisms underlying these diseases have been well understood for more than a century. However, vector-borne diseases continue to pose a significant burden worldwide [17]. Vector-borne diseases account for more than 17% of all infectious diseases, causing more than 1 million deaths annually [16]. The development of vector resistance to insecticides, changes in public health programs, climate change, changes in agricultural practices, the increased mobility of humans, and urban growth are all factors that contribute

to the difficulty in controlling and eliminating vector-borne diseases [18]. They have been responsible for the underdevelopment or non-development of large areas of the tropics, especially in African countries with low resilience to economic and environmental challenges. RVF is among the most vector-borne diseases that disproportionately affect poor and marginalized populations in Sub-Saharan Africa. The disease mainly affects livestock with severe socio-economic impacts in affected countries resulting from cessation of trade in ruminants, livestock products and livestock deaths [19]. RVF is listed as one of the neglected tropical diseases and for many years received less attention as it was considered a disease of livestock and wildlife only. This situation can also be reflected from the fact that there are about 1,415 known human pathogens while only about 616 pathogens of livestock are known [20]. Similarly, very few infectious diseases of wildlife are known or studied in any detail, and yet wildlife reservoirs may be important sources of novel emerging human infections [21]. Further, the disease presents significant differences in the ecology and transmission patterns of the virus in endemic regions [3]. Therefore, understanding how to model transmission and persistence of vector-borne diseases is of great epidemiological significance because of the different implications that their unique transmission characteristic patterns have for veterinary and public health worldwide.

1.1.2 RVF epidemiology and ecology

Rift Valley fever virus (RVFV), a member of the phlebovirus genus, and family Bunyaviridae, is an enveloped virus with a segmented, RNA genome. RVF is a viral disease that primarily affects both domestic and wild animals but is also capable of infecting humans [22, 23]. Major host disease amplifiers are sheep, cattle and goats but the disease also affects camels, buffaloes and other mammalian species [24], causing high mortality, abortion and significant morbidity in domestic livestock [13]. The disease is predominately transmitted through bite of an infected mosquito [11, 25]. However, the majority of human infections results from direct and indirect contact with blood or organs of infected ruminants [26]. The disease manifests itself in humans as a fatal haemorrhagic disease syndrome, severe influenza/malaria-like cases while in livestock it is characterized by the sudden onset of abortion in a large proportion of the herd/flock associated with high neonatal mortality [27].

The virus has been isolated from at least 30 mosquito species in the field [27], biting midges, blackflies and ticks [11, 28, 29], though this does not conclusively implicate them as competent biological vectors [30]. Major vectors can be divided in two groups: 'reservoir/maintenance' vectors which are a certain species of mosquitoes of the genera *Aedes (mcintoshi,vexans, dentatus)* associated with freshly flooded temporary or semi-permanent fresh-water bodies [29, 31, 32] and 'epidemic/amplifying' vectors consisting of *Culex (pipiens,quinquefasciatus,antennatus)* species commonly associated with permanent fresh–water bodies [11, 33].
The disease is endemic in sub-Saharan Africa and it exhibits different virus ecology and transmission patterns in different regions of the continent [3]. In southern

and eastern regions the disease is highly correlated to heavy rainfall and *Aedes* mosquitoes are thought to be the reservoirs between epizootics [1, 14]. However, the same cannot be said for west Africa, where no relationship between epidemics or epizootics and heavy rainfall has been demonstrated [7, 29]. For the purpose of model parametrization we design our models to fit disease patterns observed in the eastern and southern regions with particular focus on East Africa. In this region, RVF epizootics/epidemics have been largely correlated to the occurrence of the warm phase of the El Nino/Southern Oscillation (ENSO) phenomenon [34], associated with subsequent elevation of Indian Ocean temperatures which lead to heavy rainfall and flooding of habitats suitable for the production of immature *Aedes* and *Culex* mosquitoes [35, 36]. *Aedes mcintosh* is thought to be the reservoir of the virus as it has the ability to transmit the pathogen transovarially to offspring [11, 35], leading to virus persistence during dry season/inter-epidemic periods in the endemic cycle [35]. In periods of rainfall activities, transovarially infected adult mosquitoes may emerge in large numbers and transmit RVFV to nearby domestic livestock populations [13]. High viraemia in these animals may then lead to infection of secondary arthropod vector species including various *Culex* species [37], and probably ticks species which are also capable of carrying RVFV [28, 29] which further disperses the virus causing an outbreak.

1.1.3 Disease epidemic and inter-epidemic activities

Studies have shown that the disease has two distinct cycles: the epizootic/epidemic and the enzootic/inter-epidemic also known as endemic. The existence of these two cycles is intrinsically related to virus ecology and abiotic factors. The disease epidemic activities occur at very irregular intervals of up to 15 years in the southern and eastern regions of Africa as well as in the horn of Africa [1, 11, 14]. These activities are highly correlated to heavy rainfall and flooding that stimulate hatching of infected *Aedes* mosquito eggs, resulting in a massive emergence of adult infected *Aedes* mosquitoes. These infected mosquitoes then feed on nearby vulnerable livestock, triggering virus amplification leading to an epizootic. An epizootic/epidemic is mainly driven by the subsequent elevation of various *Culex* mosquito populations, which serve as excellent secondary vectors if immature mosquito habitats remain flooded for a long enough period [36]. Epizootics are known to cause abortion storms with $> 90\%$ mortality in newborns and $10 - 30\%$ in adults [38], stimulating human exposure to viremic livestock blood and tissue which can occur during livestock slaughtering and care triggering outbreaks in humans. The word epidemic refers to the rapid spread of an infectious disease on a large number of people in a given population within a relatively short period of time. When a similar event happens in an ruminant population it is called epizootic. However, throughout this thesis I will use the two terms interchangeably with more frequency on the term epidemic. Disease activities are also observed in both mammalian host and vector populations between epidemics or post epidemics. These are hereby referred to as disease inter-epidemic activities characterized by sporadic cases of livestock infection at low levels during periods of average rainfall.

However, these generally pass undetected clinically, but can be revealed where active serological surveillance is regularly carried out in livestock [39]. Such inter-epidemic activities have been detected without noticeable outbreaks or clinical cases in cattle in Mayotte [40, 41], in sheep and goat in Senegal [42] and Mozambique [43], in cattle, sheep and goats in Tanzania [3, 39] and Kenya [44–46]. It is thought that the virus is maintained in nature through transovarial transmission from the female *Aedes* mosquitoes to their eggs [11, 35], and by occasional amplification cycles in nearby livestock. Understanding mechanisms underlying both disease epidemic and inter-epidemic activities is a prerequisite for developing appropriate tools useful for disease management.

1.1.4 Global Geographical Distribution of RVF

Although a RVF disease-like was first described between 1912 and 1913 at the Naivasha area in Rift Valley province in Kenya [47], its aetiological agent was first isolated and characterized in the 1930s in Kenya [47]. The disease is named after its endemic location in Africa, the Great Rift Valley, which stretches 6,000 miles along the earth's crust from Lebanon to Mozambique through East Africa [48]. Since then the trend of its geographical expansion has increased significantly due to several factors including increased irrigation and dams, climate change, and movement of livestock between countries. Outbreaks have been reported in sub-Saharan, North Africa and outside the Africa continent. In 1930-31 RVF was reported in Kenya and Tanzania followed by epizootics in 1947 in Tanzania; 1950-51 in Kenya and South Africa; 1955-51 in Kenya, Namibia and Zimbabwe; 1956-57 in Kenya, Tanzania and Zimbabwe; 1960-64 in Kenya and Tanzania; 1967-68 in Kenya and Tanzania; 1969-70 in Mozambique and Zimbabwe; 1970-71 in Kenya; 1973-74 in Zambia and Sudan; 1974-75 in South Africa; 1974-76 in Namibia; 1977-78 in Kenya, Tanzania, Zambia, Zimbabwe and Egypt. The 1977 outbreak in Egypt was the first to occur out of sub-Saharan Africa and since then RVFV has been found in Madagascar and smaller islands of the coast of mainland Africa [49]. Then, in 1981 and 1983 in Kenya; 1985 in Zambia; 1987 in Mauritania; 1989-91 in Kenya and Tanzania; 1990-91 in Madagascar; 1997-1998 in Kenya, Tanzania and Somali; 1998-99 in Mauritania, Gambia and South Africa; 2000-01 in Saudi Arabia and Yemen; 2002 in Mauritania and Gambia; 2006-07 in Kenya, Tanzania and Somali; 2007-2008 in Sudan; 2008-2009 in Madagascar and South Africa; 2010 in South Africa, Mauritania, Botswana and Namibia [1, 3, 27, 50–55]. The 2000 and 2001 RVF outbreaks in Saudi Arabia and Yemen marked the first occurrence of the disease out of the Africa continent. This is evidence of the potential of the disease to extend its range to other receptive regions to the north and northeast outside Africa, such as the Tigris/Euphrates Delta zone, which would be receptive for RVFV transmission [27]. Studies suggest that the introduction of the disease into new virgin areas is facilitated by aerial transport of vectors and increased livestock movements [56], which is of great epidemiological concern that the virus will emerge further in non-endemic areas, including the United States and temperate countries [57, 58].

1.2 State of the Art

Disease transmission interactions in a population are very complex so that it is difficult to comprehend the large scale dynamics of a disease spread without the formal structure of a mathematical model [59]. An epidemiological model uses a microscopic description (the role of an infectious individual) to predict the macroscopic behaviour of disease spread through a population. This formalism allows us to predict population-level epidemic dynamics from an individual-level knowledge of epidemiological factors, long-term behaviour from early invasion dynamics, or the impact of vaccination on the spread of infection [21].
In many sciences it is possible to conduct experiments to obtain information and test hypotheses. Experiments with infectious disease spread in either human or domestic livestock populations are often impossible, unethical or expensive. Data are sometimes available from naturally occurring epidemics or from the natural incidence of endemic diseases; however, the data are often incomplete due to under reporting. This lack of reliable data makes accurate parameter estimation difficult so that it may only be possible to estimate a range of values for some parameters [59]. Therefore, mathematical models and computer simulations can be used to perform needed theoretical experiments. Mathematical epidemiological models are often used for prediction and understanding of processes underlying the spread of a certain infection. In this thesis I consider both categories moving from understanding to predictive. Understanding models begin from building simple to more complex models. In this way one can begin to understand all the rich complexities and dynamics that are observed in the real world. Then the understanding gained can help us to develop more sophisticated predictive models and help to gather more relevant epidemiological data [21].
Epidemics/epizootics have been modelled mathematically for over a century. The quantitative foundations of today's development in infectious disease modelling are traced back to early pioneers such as R. Ross 1908-1916, H. Hudson 1927, A. Lotka 1923, Kermack and Mckendrick 1927 and others (for more details see [60] and references therein). From these early models, we obtain the standard categories used to describe an epidemic by means of subgroups of the population known as compartments. The SIS (Susceptible-Infected-Susceptible) model which describes diseases for which there is no acquired immunity; the SIR (Susceptible-Infected-Removed) model which represents diseases with acquired immunity. Further detailed structures can be obtained such as the $SEIR$ or $SLIR$ (Susceptible-Exposed/Latent-Infected-Removed) model with an intermediate step which represents the latent period between exposure and external symptoms and thus can take into account differing degrees of infectiousness which occur during these two stages [61]. It is still possible to divide the Infected compartment into two or more such as infected asymptomatic or symptomatic as well as obtaining further subgroups according to the epidemiology of the disease.
These basic epidemiological models written in the language of classical deterministic models assume that the population being considered is uniform and homogeneously mixing, however, most infectious diseases actually spread in a diverse or dispersed population. In these settings, spatial effects of spread of epidemics, interaction

between individuals, effects of individual behaviour among others are ignored. However, implementation of such simplifying assumptions facilitates the use of analytic techniques to gain background understanding of disease dynamics [59], in the case of non-complex models. On the contrary, rapid growth of the mathematical complexity is observed when systems are used to describe various aspects of disease phenomena in sufficient detail, which may limit their practical use in specific cases. Alternative tools are multi-agent systems [62], that are based on cellular automata [63] or network theory. Extensive literature on multi-agent systems exists, especially in social sciences [64] and ecology [65]. In epidemiology, despite some individual-based models for directly-transmitted diseases [66], multi-agent or individual-based systems have not been used to study vector-borne disease dynamics in spatial contexts [67].

In this thesis I build my models based on two categories: the classical equation-based (deterministic and stochastic) models and the individual-based models (IBM). Unlike for other vector-borne diseases such as malaria, cholera, where extensive literature in mathematical models is available, this is not the case for RVF. Two reasons can be pointed out: (1) RVF has for long been considered a disease of ruminants only, thus it is has been neglected; (2) the mechanisms underlying its spread, re-emergence and maintenance in nature have not been fully understood. The present work builds on previous studies of RVF dynamics. Favier et al. [68] formulated and analysed a pond-level metapopulation model to assess the possibility of RVF endemicity without wild animals providing a permanent virus reservoir, assuming that *Aedes* was the sole source of virus and abundance of mosquitoes was triggered by rainfall. Various theoretical transmission scenarios were explored and it was shown that without livestock migration from outside the system, virus persistence was possible if cattle moved between ponds and if rainfall did not occur at the same time at all ponds. A novel mathematical model in a closed system based on ordinary differential equations, with two mosquito population species *Aedes* and *Culex*, and one population of livestock showed that the virus could persist if there was high contact rate between hosts and mosquito vectors [69]. Another theoretical mathematical model on RVFV dynamic transmission was proposed by Mpeshe et al. [48] which modified the model in [69] by adding human hosts, merging all mosquitoes into one population, and removing mosquito egg compartment and vertical transmission. Results showed that disease prevalence in mosquitoes is sensitive to mosquito death rate, while disease prevalence in livestock and humans is sensitive to livestock and human recruitment rates and that isolation of livestock from humans is a viable preventive strategy during an outbreak [48]. Later Gaff et al. [70] extended their previous model [69] to include several disease control measures in order to study the efficacy of countermeasures to disease transmission parameters. Their results revealed that livestock vaccination and culling offer the greatest benefit in terms of reducing livestock morbidity and mortality. Niu et al. [71] extended the model in [69] to include mitigation strategies by considering the movement of humans, livestock, and mosquitoes between patches, which cause the geographical transfer of the virus to new receptive locations. Their study mainly contributed by providing a methodology for analysing the likelihood of

pathogen establishment should an introduction occur into a new area. Chitnis et al. [5] analysed a RVF model with vertical transmission for *Aedes* mosquitoes as in [69, 70] but removed compartments representing *Culex* mosquitoes. Their model included an asymptomatic class for livestock. Additionally, they extended the model to explicitly include an aquatic juvenile stage and compared versions of the model with and without this juvenile class. They suggested that vertical transmission is an important factor in the size and persistence of RVF epidemics. Xue et al.[72] proposed and analysed a network model with ODE systems at the nodes including both *Aedes* and *Culex* mosquitoes, humans and livestock while focusing on the role of spatial heterogeneity in the spread of a single outbreak. Using the model they were able to reproduce the different starting times of the 2010 outbreak in South Africa. Then, Xue et al. [73] extended their model for much larger scale to investigate possible implication of virus introduction in the US soil, and cattle movement between farms was found to be the major driver of virus expansion. Recently, Mpeshe et al. [74] extended their previous study [48] to include vertical transmission in *Aedes* species and climate-driven parameters.
From the above literature review it is more than obvious that little research has been undertaken on this topic, and there is much room to further improve the models to obtain more insights about the dynamics of the disease. So far, few studies have focussed on exploring mechanisms of RVF virus circulation during inter-epidemic periods if none. Further, models that take into account other disease vector hosts are essential for improving our understanding of virus maintenance in nature between epidemics. The present study intends to build on from previous studies to more detailed models including individual-based models (IBM) to better investigate disease epidemic and inter-epidemic activities. These models include pathogen propagation via movement of livestock and mosquitoes, taking into account individual's variability and interaction with the environment and synchronization of the mosquito life cycle with weather conditions.

1.3 Problem Statement

During RVF outbreaks domestic livestock loss can lead to food shortages, loss of earnings and livelihoods with devastating economic impacts on the already economically challenged vulnerable African communities with low resilience to economic and environmental challenges [1, 11, 14]. The majority of these communities are pastoralist, at least in East Africa and their livelihood mainly depends on livestock production [45, 58]. In East Africa estimates indicate that the 2006/07 RVF outbreak resulted in losses amounting to more than 60 million US$ due to disruption in trade of livestock, including costs of livestock deaths [75], with an estimate of 27,500 human cases [45] and losses amounting to $>$ 610 million Ksh due to domestic livestock losses in Kenya [76].
Currently, two types of vaccines are available for livestock: inactivated whole-virus and live-attenuated Smithburn vaccines [27]. Inactivated vaccines can be applied to ruminants of all ages without causing abortions but they are expensive and repeated doses are required, which makes it difficult to sustain in RVF affected

countries for economic reasons [11]. On the other hand, live-attenuated vaccines are cheap and effective. They confer a lifelong immunity with a single dose [77]. However, they may lead to fetal abnormalities and abortions in pregnant ruminants and there is the safety concern of reversion to virulence [78]. Therefore, alternatives are required in order to minimize the burden posed by the disease during outbreaks.

RVF is known to occur in outbreaks that come in cycles of up to 15 years after heavy rainfall and floods [11]. Climate variability and the occurrence of the El Niño/Southern Oscillation (ENSO) phenomenon lead to heavy rainfall which stimulates massive emergence of disease potential vectors [34], however it remains unclear the exact role of rainfall on the temporal characteristic pattern of disease outbreaks. On the other hand, there is more and more evidence of RVF transmission during the inter-epidemic period [3, 39, 44–46]. However, these generally pass undetected clinically, but can be revealed where active serological surveillance is regularly done in either livestock or human populations [39]. RVF maintenance in nature between epidemics both in the mammalian host and vector populations has not been fully explained. This is partly due to the limited evidence that has been gathered and knowledge of the other factors driving its maintenance in a particular geographical scale. Such factors interact in diverse ways in different geographical regions of Africa or beyond and may play a crucial role in vector population dynamics and disease transmission.

Understanding underlying factors leading to disease epidemic and inter-epidemic activities is central for disease management. What could be the actual role of intensive rainfall and flooding regimes regarding the characteristic pattern of disease outbreaks? Could RVF outbreaks build up from disease inter-epidemic activities? Both climatic and weather conditions increase the number of breeding sites for mosquitoes resulting in an increase in the number of vectors and therefore more intense virus transmission and circulation [79], enhancing risk of vector-borne disease infection. An increase in temperature increases the development rate of each stage of the mosquito, hence reduces time from egg to adult. Hence, rapid emergence of young adults is triggered enhancing risk of disease transmission. What features of the mosquito life cycle affect mosquito population dynamics? Is there any correlation between abundance of mosquitoes and rainfall events? The virus outlives in nature between outbreaks through infected eggs from some female *Aedes* mosquitoes. Is there any correlation between abundance of mosquitoes and RVF incidences during the inter-epidemic period (IEP)? What are the factors during the mosquito life cycle that contribute to disease inter-epidemic activities? What are the necessary levels of vertical transmission to maintain the disease between outbreaks? The present research aims to test the above mentioned hypothesis by means of mathematical models and computer simulation models. These models are to be used to learn many characteristics of disease outbreaks such as the probability, size, and duration time of an epidemic, or the probability for the epidemic to die out. On the other hand understanding mechanisms of disease persistence during inter-epidemic period may help to stop an outbreak at early stages by controlling parameters that are key drivers of the spread of the disease. The developed models

may also be used to explore post-epidemic activities for enhancing the utilization of rapid response measures and observe the impact over time under varying scenarios.

1.4 Research Objectives

The goal of the study is therefore to develop models for analysing and understanding the epidemic and inter-epidemic activities of RVF and use the outcome for improving the disease management strategies.

1.4.1 Specific Objectives

The specific objectives are:

1. To formulate and assess model parameter sensitivity to RVF transmission and prevalence and the impact of vertical infection for the persistence of the disease.
2. To explore the stability of equilibrium points of the RVF model.
3. To explore means of predicting RVF outbreak periods based on the disease inter-epidemic activities.
4. To develop an approach that provides a framework for analysing systems of ecological and inter-epidemiological interactions of RVF drivers.
5. To explore possibilities of adjusting current RVF management strategies to help reduce the disease impact.

1.5 Thesis Contribution

Efforts have been capitalized on formulating and analysing disease mathematical models for both RVF epidemic and inter-epidemic activities. The models include both mammalian and vector hosts. Further, individual-based models that incorporate effects of environment, temperature, rainfall, individual's variability, behaviour and mosquito life cycle have been studied to explore various hypotheses regarding small scale movement of vectors, mosquito life cycle, and effects of climatic conditions in the spread of the disease. The present thesis is a valuable contribution to both the academic community and decision makers. Below major contributions are outlined:

1. Vertical transmission on *Aedes* mosquitoes, which is central to understanding initial disease spread and persistence has been included and thoroughly investigated.

2. The livestock infected class was further divided into two compartments of asymptomatic and symptomatic infected animals for examining their impact in the spread of the disease in both cases of severe and non severe outbreaks.

3. In the deterministic model, effects of seasonality were modelled by implementing an extrinsic forcing function in the oviposition rate for both *Aedes* and *Culex* mosquitoes for determining the actual contribution of rainfall in the temporal characteristic patterns of RVF outbreaks.

4. An explicit expression of the basic reproduction number, R_0 for non and periodic environment considering both vertical and horizontal transmission was computed and assessed for different disease control strategies.

5. Both time invariant and time varying uncertainty and sensitivity analysis were performed for both the measure of the initial spread of the disease, R_0 and the measure of disease prevalence providing new light as to how each model parameter contributes to disease dynamics at every important stage of the epidemic which is central for designing appropriate intervention programs.

6. Stability analyses of the deterministic model were conducted for establishing critical conditions of disease spread and extinction. Bifurcation and chaos analyses were explored for determining fluctuations found in RVF empiric outbreak data, as well as the non deterministic nature of both RVF epidemic and inter-epidemic activities.

7. A model with additional vectors other than mosquitoes was formulated and analysed for determining the possible contribution of ticks in the spread and persistence of RVF.

8. Relationships among disease invasion and extinction probabilities and the basic reproduction numbers are analytically derived from a stochastic host-vector model with vertical transmission. Additionally the theoretical dominant period of disease outbreaks is determined and will be compared with actual prediction when reliable data become available.

9. Novel relationships among temperature, rainfall and abundance of mosquitoes are determined. Furthermore, important stages of the mosquito life cycle in disease spread are identified allowing disease managers to focus their efforts on specific features of the mosquito life cycle.

10. Correlation between abundance of mosquitoes and RVF incidence cases during the inter-epidemic period was determined and contributions of vertical transmission to disease inter-epidemic activities are characterized in detail.

1.6 Methodology and Thesis Outlines

In order to investigate the dynamics underlying both epidemic and inter-epidemic activities of RVF we build models that range from classical approaches to more

recent ones. In the first part we formulate and analyse two mathematical epidemiological models: one based on ordinary deterministic differential equations (ODE) and the other on stochastic processes and simulations. In the second part we formulate and analyse an individual-based model of the mosquito life cycle. The first part consists of four chapters. Chapter 1 provides a general introduction to the thesis. In Chapter 2 which corresponds to specific objective 1 we formulate an ODE model that accounts for one population of livestock (we do not make distinction of whether sheep, cattle or goats), one population of *Aedes* mosquitoes and one population of *Culex* mosquitoes. For *Aedes* we incorporate mechanisms of vertical transmission and for livestock we include mechanisms underlying the development of symptoms in each individual livestock, given that even in scenarios of severe outbreaks some infected livestock presents no symptoms. We use this model to derive an explicit formula for the basic reproduction number, R_0 then we use R_0 to study the relative importance of vertical transmission in the spread and persistence of the disease over a long time period. Furthermore, using techniques of uncertainty and sensitivity analysis we carry out a systematic investigation of the relative importance of every model parameter to the initial spread and prevalence of the disease [80]. In Chapter 3 which is related to the specific objective 2 we use the model developed in Chapter 2 to analytically study the stability behaviour of the steady states of the model and by means of numerical simulations we investigate the attractors structure of the steady states under the influence of external forcing [4]. The external forcing functions are used to mimic the effects of rainfall in the emergence of new cohorts of mosquitoes. Optimal climatic conditions and the presence of mosquitoes have not fully explained the dynamics of both disease epidemic and inter-epidemic activities. Therefore, in Chapter 4 we extend the previous model to include another vector host (a ticks species of genera *Hyalomma truncatum*) that have been implicated in the transmission of the virus. This aims to examine the possible role of additional vectors (for example ticks) in the spread of the disease. This Chapter results from an extension of the specific objectives 1 and 2. In Chapter 5 which corresponds to specific objective 3 we formulate a stochastic host-vector model for investigating the relationships among the invasion probabilities, extinction and basic reproduction numbers. Further, we use the model for predicting the temporal characteristic pattern of disease outbreaks.
In Chapter 6 we develop an individual-based model (IBM) of the mosquito life cycle based on daily temperature and rainfall data. Then we use the model to investigate the correlation between climatic conditions and abundance of mosquitoes, and determine features of the mosquito life cycle that affect the mosquito population dynamics. In Chapter 7 we extend the model developed in Chapter 6 to study spread of the disease during the inter-epidemic period in livestock and assess the relationship between abundance of mosquitoes and RVF incidence cases. The model is also applied to assess different levels of vertical transmission responsible for disease inter-epidemic activities and determine important features of the mosquito life cycle that affect the transmission and persistence of the disease.
In Chapter 8 we conclude the thesis summarising what we have learnt about the different models and methodologies. In addition we summarise several future studies suggested by these investigations.

Chapter 2

Uncertainty and Sensitivity Analysis of a Rift Valley fever Model[1]

2.1 Introduction

Rift Valley fever (RVF) is a vector-borne viral disease caused by RVF virus (RVFV) belonging to the genus *Phlebovirus* of the family Bunyaviridae [22]. The virus infects primarily both wild and domestic livestock, however it is also capable of infecting humans. In ruminants, infection can produce high rates of abortion and significant morbidity and mortality [81]. Livestock losses can lead to food shortages, loss of earnings and livelihoods with devastating economic impacts, particularly in vulnerable African communities with low resilience to economic and environmental challenges [1, 11]. The 2006-07 RVF outbreak in East Africa was the most widespread with total number of deaths of 16,973 in cattle, 20,193 in goats and 12,124 in sheep resulting in economic losses amounting to US$32 million in Kenya alone [76]. The disease is endemic in much of sub-Saharan Africa [9] with significant differences in the ecology and epidemiology of the disease. The disease occurs in two distinct cycles: the enzootic/endemic and the epizootic/epidemic cycles [13]. The enzootic transmission occurs at low levels in nature during periods of average rainfall (low moisture) in which the virus is maintained through vertical transmission from the female *Aedes* mosquito to eggs and through occasional amplification cycles in susceptible livestock [11, 35]. The epizootic cycle appears at irregular intervals, after heavy rainfall and floods (high moisture), which stimulate the hatching of infected *Aedes* mosquito eggs, resulting in a massive emergence of *Aedes* with subsequent elevation of various *Culex* species that serve as the amplifiers of the disease [13, 36].
Vector control in either adult or mosquito larvae and livestock vaccination are

[1]This chapter has been published: S.A. Pedro et al., Uncertainty and sensitivity analysis of a Rift Valley fever model, Applied Mathematics and Computation (2016), http://dx.doi.org/10.1016/j.amc.2016.01.003

among the most effective disease control and public health intervention measures. However, the effectiveness of any intervention program depends mainly in our knowledge of disease transmission, threshold concept in the epidemiology of the disease and disease parameters that govern its spread. The basic reproduction, R_0 is one of the foremost concepts in the epidemiology of the disease [82], which is widely used to quantify the spread of the disease at early stage of the epidemic. This quantity is either derived from data or from mathematical models that describe the dynamics of the disease. Mathematical models consist of parameters and initial conditions for independent and dependent variables. In most cases these parameters are not known with sufficient degree of certainty due to natural variations and error in measurements [83].

Uncertainty and sensitivity analysis of model parameters is very important for quantifying these variations and uncertainties. For example, sensitivity analysis enhances our understanding and guide in developing appropriate measures for disease control. Uncertainty analysis is used to explore the uncertainty in the model output that is generated from uncertainty in input parameters [83] while sensitivity analysis assesses how variations in model outputs can be attributed qualitatively and quantitatively to different input parameters [84]. Although the field of mathematical epidemiology is well established very few models of RVF have been developed and analysed. This is in part due to the fact that the disease for many years was known as a disease of ruminants only. Thus, receiving little attention from various stakeholders. In the recent past few RVF mathematical models have been developed, see [4, 5, 48, 69, 71, 72, 74] and references therein. However, only few studies have performed uncertainty and sensitivity analysis of RVF epidemic models to the parameters and to the endemic equilibrium state [5, 48, 69, 71]. These studies have determined the relative importance of various parameters in RVF transmission and spread characterized by R_0 using sampling-based uncertainty and sensitivity analysis techniques, with exception of Mpeshe et al.[48] who applied sensitivity indices of the endemic equilibrium point to the model parameters. Still, two main questions remain not completely explored: (1) what is the role and contribution of vertical transmission from *Aedes* mosquitoes for both disease epidemic and endemic activities? (2) What is the time contribution of each model parameters to model output variations during an outbreak? The former question is central to our understanding of the relative importance of various input parameters as the disease evolve with time. The same input model parameter may contribute to model output variations in different ways as the model evolves with time. That is, for instance at the beginning of an outbreak the parameter may be positively correlated to the size of the epidemic but at the peak of the outbreak this correlation may inverse [83]. To the best of our knowledge these types of analyses are missing in disease models, particularly to vector-borne disease models such as RVF models.

Therefore, in this paper we use our previous RVF model [4] to systematically study the sensitivity of both the measure of the initial spread of the disease, R_0 and the measure of disease prevalence, represented by the endemic equilibrium state, E^* to both low and high moisture model parameters. The initial spread of the disease depends on the competence of primary vectors, the *Aedes* mosquitoes through vertical transmission [4]. Hence, we start our analysis by investigating the relative

importance of vertical transmission in disease transmission and persistence. Then we proceed with sensitivity analysis of the basic reproduction number, R_0 using two approaches: one based on local derivatives and the other on sampling-based method, that is, Latin hypercube sampling (LHS) on combination with partial rank correlation coefficient (PRCC). Furthermore, we perform uncertainty and sensitivity analysis of some chosen model state variables (Uninfected eggs, U_1, Exposed *Aedes* E_1, Infected *Aedes* I_1, Infected symptomatic host A_2, Infected symptomatic host I_2, Exposed *Culex* E_3 and Infected *Culex* I_3) to model input parameters at a particular time during the course of the outbreak. In addition, we compute the sensitivity indices of the endemic equilibrium state, E^* using local derivatives in order to assess the relative importance of different input parameters to disease prevalence. Finally, in order to assess whether significance of each parameter occurs over an entire time interval during model dynamics, we investigate the rank correlation coefficient (RCCs) for multiple time points and plot them versus time. We show that during endemic cycle (low moisture) vertical transmission drives the persistence of the disease. In addition, a threshold of this rate is required for virus reproduction and subsequent propagation. However, during periods of outbreaks (high moisture) the effect of vertical transmission is significant in the first transmission cycle and may actually reduce the time of the outbreak. Our analysis sheds new light on the relative importance of the most significant input parameter for both disease epidemic and endemic/inter-epidemic activities for both single and multiple time points. Time varying sensitivity analysis provides to our understanding deep insights about how each parameter contributes to disease dynamics at every important stage of the epidemic which is central for designing appropriate intervention strategies.

2.2 RVF Model

The RVF model in [4] consists of a system of nonlinear ordinary differential equations, that describes disease transmission through interaction among *Aedes*, *Culex* mosquitoes and livestock. The *Aedes* mosquito population is divided into 5 compartments: Uninfected eggs P_1, Infected eggs U_1, Susceptible adults S_1, Exposed adults E_1 and Infected adults I_1 and their total population size is given by $N_1 = S_1 + E_1 + I_1$. The *Culex* mosquito population is divided into 4 compartments: Uninfected eggs P_3, Susceptible adults S_3, Exposed adults E_3 and Infected adults I_3 and their total population size is given by $N_3 = S_3 + E_3 + I_3$. The livestock population has 4 compartments: susceptible S_2, Infected asymptomatic A_2, Infected Symptomatic I_2 and Recovered R_2. The total population size is given by $N_2 = S_2 + A_2 + I_2 + R_2$. The set of equations that describe the system is given below (see systems (2.1-2.3)) and the description of parameters and their respective baseline values and ranges are given in Appendix A.

Aedes

$$\begin{aligned}
\dot{P}_1(t) &= b_1(N_1 - q_1 I_1) - \theta_1 P_1, \\
\dot{U}_1(t) &= b_1 q_1 I_1 - \theta_1 U_1, \\
\dot{S}_1(t) &= \theta_1 P_1 - \frac{\sigma_1\sigma_2\beta_{12}}{\sigma_1 N_1 + \sigma_2 N_2} I_2 S_1 - \frac{\sigma_1\sigma_2\tilde{\beta}_{12}}{\sigma_1 N_1 + \sigma_2 N_2} A_2 S_1 - d_1 \frac{S_1 N_1}{K_1}, \\
\dot{E}_1(t) &= \frac{\sigma_1\sigma_2\beta_{12}}{\sigma_1 N_1 + \sigma_2 N_2} I_2 S_1 + \frac{\sigma_1\sigma_2\tilde{\beta}_{12}}{\sigma_1 N_1 + \sigma_2 N_2} A_2 S_1 - \gamma_1 E_1 - d_1 \frac{E_1 N_1}{K_1}, \\
\dot{I}_1(t) &= \gamma_1 E_1 + \theta_1 U_1 - d_1 \frac{I_1 N_1}{K_1},
\end{aligned} \tag{2.1}$$

Livestock

$$\begin{aligned}
\dot{S}_2(t) &= b_2 N_2 - \frac{\sigma_1\sigma_2\beta_{21}}{\sigma_1 N_1 + \sigma_2 N_2} I_1 S_2 - \frac{\sigma_3\sigma_2\beta_{23}}{\sigma_3 N_3 + \sigma_2 N_2} I_3 S_2 - d_2 \frac{S_2 N_2}{K_2}, \\
\dot{A}_2(t) &= (1-\theta_2)\frac{\sigma_1\sigma_2\beta_{21}}{\sigma_1 N_1 + \sigma_2 N_2} I_1 S_2 + (1-\theta_2)\frac{\sigma_3\sigma_2\beta_{23}}{\sigma_3 N_3 + \sigma_2 N_2} I_3 S_2 - \tilde{\varepsilon}_2 A_2 - d_2 \frac{A_2 N_2}{K_2}, \\
\dot{I}_2(t) &= \theta_2 \frac{\sigma_1\sigma_2\beta_{21}}{\sigma_1 N_1 + \sigma_2 N_2} I_1 S_2 + \theta_2 \frac{\sigma_3\sigma_2\beta_{23}}{\sigma_3 N_3 + \sigma_2 N_2} I_3 S_2 - \varepsilon_2 I_2 - d_2 \frac{I_2 N_2}{K_2} - m_2 I_2, \\
\dot{R}_2(t) &= \tilde{\varepsilon}_2 A_2 + \varepsilon_2 I_2 - d_2 \frac{R_2 N_2}{K_2},
\end{aligned} \tag{2.2}$$

Culex

$$\begin{aligned}
\dot{P}_3(t) &= b_3 N_3 - \theta_3 P_3, \\
\dot{S}_3(t) &= \theta_3 P_3 - \frac{\sigma_3\sigma_2\beta_{32}}{\sigma_3 N_3 + \sigma_2 N_2} I_2 S_3 - \frac{\sigma_3\sigma_2\tilde{\beta}_{32}}{\sigma_3 N_3 + \sigma_2 N_2} A_2 S_3 - d_3 \frac{S_3 N_3}{K_3}, \\
\dot{E}_3(t) &= \frac{\sigma_3\sigma_2\beta_{32}}{\sigma_3 N_3 + \sigma_2 N_2} I_2 S_3 + \frac{\sigma_3\sigma_2\tilde{\beta}_{32}}{\sigma_3 N_3 + \sigma_2 N_2} A_2 S_3 - \gamma_3 E_3 - d_3 \frac{E_3 N_3}{K_3}, \\
\dot{I}_3(t) &= \gamma_3 E_3 - d_3 \frac{I_3 N_3}{K_3}.
\end{aligned} \tag{2.3}$$

Note that the natural death rate $d_i \frac{I_i N_i}{K_i}$ is also denoted as μ_i for $i = 1, 2, 3$. Table 2.1 gives description of the state variables and further details regarding the model are given in the next chapter.

Variable	Description
P_1	Number of uninfected *Aedes* mosquito eggs
Q_1	Number of infected *Aedes* mosquito eggs
S_1	Number of susceptible *Aedes* mosquitoes
E_1	Number of exposed *Aedes* mosquitoes
I_1	Number of infected *Aedes* mosquitoes
S_2	Number of susceptible livestock
E_2	Number of exposed livestock
A_2	Number of asymptomatic livestock
I_2	Number of infected livestock
P_3	Number of uninfected *Culex* mosquito eggs
S_3	Number of susceptible *Culex* mosquitoes
E_3	Number of exposed *Culex* mosquitoes
I_3	Number of infected *Culex* mosquitoes

TABLE 2.1: State variables for the model system (3.1-3.3)

2.3 Model Analysis

2.3.1 Basic Reproduction Number, R_0

In host-vector systems R_0 is described as the expected number of secondary infections after one average, complete (host-vector-host or vector-host-vector) transmission cycle [85]. An analytical expression of the basic reproduction, R_0 has been derived in [4] and R_0 for horizontal transmission only is given by

$$R_{0,H} = \sqrt{\frac{(1-\theta_2)(l_3^0)^2\beta_{23}\tilde{\beta}_{32}\gamma_3 N_2^0 N_3^0}{b_3(\tilde{\varepsilon}_2+b_2)(\gamma_3+b_3)} + \frac{(1-\theta_2)(l_1^0)^2\beta_{21}\tilde{\beta}_{12}\gamma_1 N_1^0 N_2^0}{b_1(\tilde{\varepsilon}_2+b_2)(\gamma_1+b_1)} + \frac{\theta_2(l_3^0)^2\beta_{23}\beta_{32}\gamma_3 N_2^0 N_3^0}{b_3(\varepsilon_2+b_2+m_2)(\gamma_3+b_3)} + \frac{\theta_2(l_1^0)^2\beta_{21}\beta_{12}\gamma_1 N_1^0 N_2^0}{b_1(\varepsilon_2+b_2+m_2)(\gamma_1+b_1)}} \tag{2.4}$$

where $l_1^0 = \dfrac{\sigma_1\sigma_2}{\sigma_1 N_1^0 + \sigma_2 N_2^0}$ and $l_3^0 = \dfrac{\sigma_3\sigma_2}{\sigma_3 N_3^0 + \sigma_2 N_2^0}$. When strictly defined as the reproductive rate of the pathogen, R_0 (obtained via the next generation-matrix) for the overall model that accounts for both vertical infection and horizontal transmission is given by:

$$R_0 = \frac{q_1}{2} + \frac{1}{2}\sqrt{q_1^2 + 4R_{0,H}^2}. \tag{2.5}$$

In the absence of vertical transmission, $q_1 = 0$, $R_0 = R_{0,H}$ is the geometric mean of the number of new infections in livestock from *Aedes* and *Culex* infected mosquitoes, and the number of new infections in both species of mosquitoes from an infected ruminant (asymptomatic or symptomatic), in the limiting case that both populations are fully susceptible. Thus, $R_{0,H}$ can be described in four parts, corresponding to the *Aedes*-asymptomatic livestock interaction, *Aedes*-symptomatic

livestock interaction, the *Culex*-asymptomatic livestock interaction and *Culex*-symptomatic livestock interaction. On the other hand, the reproduction number $R_{0,H}$ can be written as follows:

$$R_{0,H} = \sqrt{\frac{(l_3^0)^2\beta_{23}\gamma_3 N_2^0 N_3^0}{b_3(\gamma_3+b_3)}\left[\frac{(1-\theta_2)\tilde{\beta}_{32}}{\tilde{\varepsilon}_2+b_2}+\frac{\theta_2\beta_{32}}{\varepsilon_2+b_2+m_2}\right]+\frac{(l_1^0)^2\beta_{21}\gamma_1 N_1^0 N_2^0}{b_1(\gamma_1+b_1)}\left[\frac{(1-\theta_2)\tilde{\beta}_{12}}{\tilde{\varepsilon}_2+b_2}+\frac{\theta_2\beta_{12}}{\varepsilon_2+b_2+m_2}\right]}. \tag{2.6}$$

2.3.2 Vertical transmission and reproductive numbers

At early stage of an epidemic/epizootic vertical transmission from the female *Aedes* mosquitoes is likely to have a significant impact. An increase in the number of infectious *Aedes* mosquitoes directly affects the number of secondary infections and indirectly increases the transmission from livestock to mosquitoes and back to livestock. The number of secondary infections at initial spread of the disease is usually described by R_0. The basic reproductive number, R_0 is defined as the average number of secondary infections caused by a single infected individual in an otherwise susceptible population during his infectious life period. However, R_0 obtained through the next generation method does not produce the exact expected number of secondary cases in a host-vector disease such as RVF, but rather the geometric mean of the number of secondary infections per generation. Therefore, to carefully determine the relationship between vertical transmission and the reproduction number we apply the approach used in [85] where we define type reproductive numbers as follows: the number of new infected hosts caused by a single infected host, T_1^h and the number of new infected vectors caused by a single infected vector, T_1^v. Since the model accounts for vertical transmission from the female *Aedes* mosquito, R_0 then represents the expected number of secondary infections after a complete average (host-vector-host or vector-host-vector) transmission cycle, but it does not correspond to a specific transmission cycle. Therefore, the type reproductive number that describes the total average number of secondary host infections required to account for vector-vector transmission cycles that occur during both disease cycles is given by

$$T_1^h = \frac{R_{0,H}^2}{1-q_1} \tag{2.7}$$

and the vector type reproductive number is given by

$$T_1^v = q_1 + R_{0,H}^2. \tag{2.8}$$

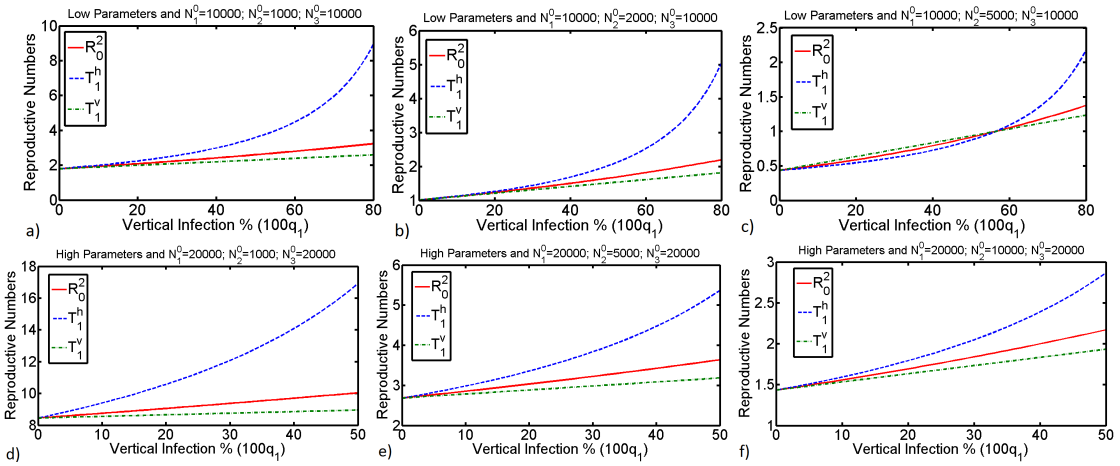

FIGURE 2.1: Relationship between percentage efficiency of vertical transmission with both complete transmission cycle R_0^2 and type reproductive numbers T_1^v and T_1^h. This relationship is depicted for both low moisture parameters (see (a)-(c)) and high moisture parameters (see (d)-(f)) while varying the initial number of livestock N_2^0 and keeping initial number of adult mosquitoes constant N_1^0 and N_3^0. All other parameter values are in Table A.1.

Figure 2.1 describes the behaviour of both complete transmission cycle R_0^2 and type reproductive numbers T_1^v and T_1^h below and above unity for both low and high moisture parameters depending on the percentage efficiency of vertical infection. From (a)-(c) we depict this relationship for low moisture parameters given in Appendix A Table A.1 for different values of initial number of livestock N_2^0 while keeping constant the initial number of adult *Aedes* and *Culex* mosquitoes N_1^0 and N_3^0 respectively. We observe that vertical infection efficiency leads to a linear increase in the basic reproductive number and vector type reproductive number but an exponential increase in the host type reproductive number. *Aedes* eggs, after maturing hatch during the next flooding event, leading to emergence of probably the first generation of vertically infected *Aedes* mosquitoes. Thus, the higher the proportion of vertical infection the higher the quantity of R_0 and T_1^v is, since at the beginning of each rainy season, *Aedes* mosquitoes quickly grow towards the maximum densities. As infected *Aedes* mosquitoes feed on nearby vulnerable livestock, they trigger virus amplification resulting in an exponential increase of T_1^h in the subsequent generations or transmission cycles. This is furthermore enhanced through subsequent elevation of secondary vectors including various *Culex* species that amplify the spread of the disease. In (a) and (b) the trajectories of all reproductive numbers are almost indistinguishable for vertical infection efficiency of up to 20%. A clear divergence begins when vertical infection is around 40%. This suggests that a certain level of vertical transmission efficiency should be met for the initial spread of the disease [4]. Nevertheless, the efficiency of vertical infection is a function of moisture since high moisture leads to massive hatching of mature eggs. This is confirmed by Figures (d)-(f) depicting the relationship between vertical infection efficiency and all reproductive numbers. Here the host type reproductive number quickly accelerates even for vertical infection less than

5%. In (c) an interesting feature is observed. All reproduction numbers lie below unity for vertical infection efficiency below 60% with a substantial divergence when vertical infection is above 60%. The divergence between T_1^h and R_0 reveal the degree to which initial spread of RVF outbreaks depends on vertical infection efficiency. However, if the initial number of livestock, N_2^0 is kept higher we observe a substantial decrease in the magnitude of all reproductive numbers. This suggests that if the ruminants stay together in large herds the effort it takes for each domestic livestock to prevent a mosquito bite (such as switching its tail) is likely to be more effective than if there were in small herds.

Two types of vaccines (live vaccine and inactivated vaccine) can be used to reduce the negative impacts of RVF morbidity and mortality in livestock. However, the current live vaccine cannot be used for prevention because it is not sustainable in current RVF affected countries due to economic limitations [1, 74, 86]. In such conditions, reducing vector population is the most viable disease control measure. R_0 is a quantity that is directly related to the initial spread of an epidemic, heavily used for disease prevention. But, it is also used to guide eradication efforts when a disease is endemic [87]. In this case we define the eradication effort as the percentage reduction in vector population size required to prevent disease transmission and persistence [85]. This means that either the vector or host type reproductive numbers should be kept below the threshold. Thus, using the host type reproductive number, the eradication effort is $100(1 - 1/T_1^h)$. Therefore, the efficiency of vertical infection is linearly related to the eradication effort, as shown in Fig.2.2, and vertical infection at $x\%$ can be responsible for at most $x\%$ of the required eradication effort. Again, we observe that increasing the initial number of livestock, N_2^0 the magnitude of eradication effort required to prevent the spread of the disease reduces dramatically. Note that we have only considered eradication effort for high moisture parameters only. This is due to the fact that the relationship between eradication effort and percentage efficiency of vertical infection for low parameters follows the same behaviour as for parameters for high moisture.

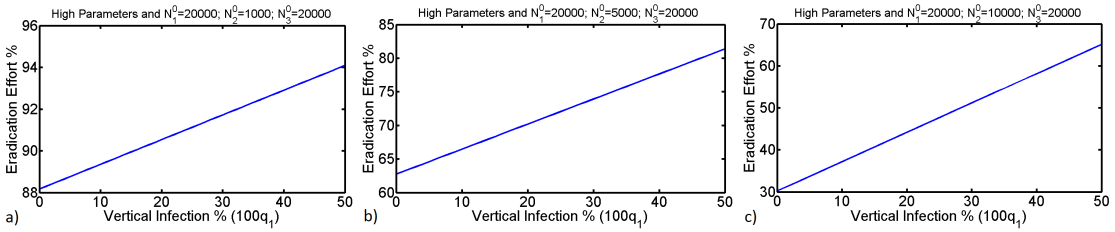

FIGURE 2.2: Percentage of mosquito population that must be removed to reduce the host type reproductive number below unity and eradicate the virus, depending on the efficiency of vertical infection for high moisture parameters and for different values of initial number of livestock N_2^0. The values of all other parameters are given in Table A.1.

2.3.3 Vertical transmission and persistence of RVF

The derivation of R_0 via the next generation method is obtained when the disease-free state is at equilibrium, which makes R_0 very useful to describe initial spread of the disease. Hence, R_0 is not appropriate to describe the potential for long term circulation of the virus, that is, during inter-epidemic periods. Persistence may be affected by seasonal fluctuations, low mosquito-livestock transmission cycles due to low population densities, high levels herd immunity, long viral incubation period or many other factors [4, 5, 85]. Since the disease persists during inter-epidemic periods through transovarial transmission from the female *Aedes* mosquito to eggs, we only focus on the role of vertical transmission by considering a proportion of infected newly born and adult *Aedes* mosquito populations with no transmission between mosquitoes and livestock or vice versa. Therefore, we describe the process through a pair of ordinary differential equations:

$$\begin{aligned} \frac{dU_1}{dt} &= b_1 q_1 I_1 - \theta_1 U_1 \\ \frac{dI_1}{dt} &= \theta_1 U_1 - \mu_1 I_1 \end{aligned} \tag{2.9}$$

where $\mu_1 = \frac{d_1 N_1}{K_1}$.
In the absence of mosquito-livestock transmission, one may expect long term viral extinction. However, this is not the case for RVF disease which is mediated by various vectors and one of them is *Aedes* mosquitoes whose eggs undergo diapause. The system (2.9) can be solved subject to the initial condition of U_1^0 of infected pre-adults and I_1^0 of infected adults. Since part of the solution is multiplied by $\exp(-(\mu_1 + \theta_1 + \phi))$ which makes it decay very rapidly and can be discarded to give a good approximate solution for the total number of infections at time t, $I(t) = U_1(t) + I_1(t)$ is given by:

$$I(t) = \frac{(\phi + \mu_1 + \theta_1)U_1^0 + (\phi + \mu_1 + 2b_1 q_1 + \theta_1)I_1^0}{2\phi} e^{-\frac{(\mu_1 + \theta_1 - \phi)t}{2}} \tag{2.10}$$

where $\phi = \sqrt{(\mu_1 - \theta_1)^2 + 4b_1 q_1 \theta_1}$.
The quantity, $I(t)$ represents a decay process and can be used to determine the half-life, $t_{1/2}$ which is the amount of time required for $I(t)$ to fall to half its value. Thus, the approximated time until the number of infected mosquitoes is reduced by 50% is given by

$$t_{(1/2)} = \frac{2}{\mu_1 + \theta_1 - \phi} ln \left[\frac{(U_1^0 + I_1^0)\phi}{(\phi + \mu_1 + \theta_1)U_1^0 + (\phi + \mu_1 + 2b_1 q_1 + \theta_1)I_1^0} \right] \tag{2.11}$$

and the approximated time until the number of infected mosquitoes is less than unity is:

$$t_e = \frac{2}{\mu_1 + \theta_1 - \phi} ln \left[\frac{2\phi}{(\phi + \mu_1 + \theta_1)U_1^0 + (\phi + \mu_1 + 2b_1 q_1 + \theta_1)I_1^0} \right]. \tag{2.12}$$

Both half-life and total time to extinction increase with vertical infection efficiency see Fig.2.3. The rate at which percentage efficiency of vertical infection extends both half-time and total time to extinction is exponential. For both Figures 2.3(a) and (b) $U_1^0 = I_1^0 = 10$, but half-life does not depend on the initial conditions. However, the approximate time until the number of infected mosquitoes is less than unity increases substantially with increments in the values of initial conditions U_1^0 and I_1^0 (see (b)-(d)). It is worth noting that we have plotted half-time and additional time only for high moisture parameters. This is because we are interested in quantifying these indicators in case of outbreaks activities and not inter-epidemic activities. During inter-epidemic activities the infection may pass undetectable as infection remains asymptomatic or dormant within livestock hosts. Nevertheless, both half-time and additional time to extinction for low moisture parameters follow the same trend as for high moisture parameters but with reduced time.

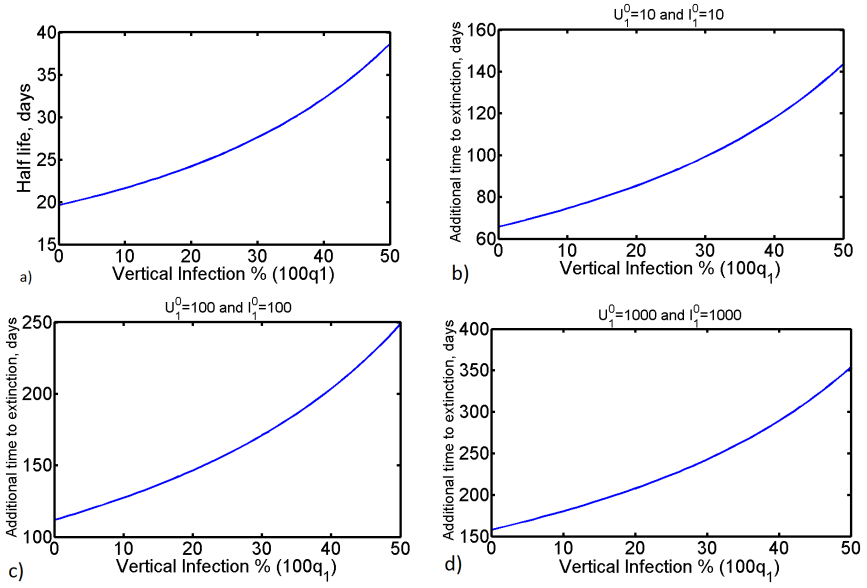

FIGURE 2.3: Time taken for the density of *Aedes* mosquitoes to fall by half and unity depending on the efficiency of vertical transmission if no transmission between mosquito and livestock for high moisture parameters. (b)-(d) approximate time until the number of individuals is less than unity for different initial conditions. All other parameters are given in Table A.1.

2.4 Sensitivity Analysis of R_0

In order to assess the impact of the parameters and decision rules within the model, a sensitivity analysis is performed to determine how sensitive the model is to changes in the parameters value as well as to determine the parameters that have the most influence on the stability/instability of the equilibrium points and on the reproduction number. We also assess the relative importance of different factors responsible for transmission and prevalence of RVF to better determine

how to reduce the livestock mortality and morbidity. Initial disease transmission and endemicity are directly related to R_0. In the following section we compute the sensitivity indices of R_0 based on perturbation of fixed point estimation [88], also known as normalized forward sensitivity index [89].

2.4.1 Sensitivity indices of R_0

Sensitivity indices for the basic reproduction number, R_0 change with the change in input parameter values. Here we study these variations in parameter values in order to explore the relative importance of different drivers responsible for disease transmission. The sensitivity indices for R_0 are given by

$$\Gamma_{\psi}^{R_0} = \frac{\partial R_0}{\partial \psi} \times \frac{\psi}{R_0} \tag{2.13}$$

where ψ represents an arbitrary model parameter. For more details in the derivation of the above formula see [88, 89]. The sensitivity indices of R_0 with respect to all model parameters for both low and high parameter values are shown in Table 2.2. For both low and high parameter values, the sensitivity indices for $q_1, \theta_2, \sigma_1, \sigma_2, \sigma_3$, $\beta_{12}, \beta_{21}, \beta_{23}, \beta_{32}, \tilde{\beta}_{12}, \tilde{\beta}_{32}, \gamma_1, \gamma_3, N_1^0$ and N_3^0 are positive and the remaining are negative. The sign of the sensitivity indices of R_0 suggests a monotonic relationship between R_0 and the parameters. That is, an increase/decrease on parameters increases/decreases R_0, which agrees with the intuitive expectation from the model. For both low and high parameter values the *Aedes* death rate and the number of times an *Aedes* mosquito would bite a host are the most sensitive, followed by the probability of transmission from an infected *Aedes* mosquito to a susceptible host. However, for low parameter values, the initial number of livestock N_2^0, initial number of *Aedes* N_1^0, the recovery rate of the infected symptomatic host and the number of bites a *Culex* mosquito would bite a host are more sensitive than the corresponding high parameter values. For both low and high parameter values in order to have 10% decrease in the value of R_0 it is necessary to increase the *Aedes* deaths by 2.8605% and 0.1095% respectively; decrease σ_1 by 4.1952% and 1.3459% respectively. The explanation for other sensitivity indices is similar.

	Low Parameters $R_0 = 0.8560$		High Parameters $R_0 = 4.8681$	
Parameters	Sensitivity Indices	Corresponding Changes	Sensitivity Indices	Corresponding Changes
b_1	−0.5718	+2.8605	−0.3750	+0.1095
b_2	−0.0051	+6.4607	−0.0004	+1.4925
b_3	−0.2668	+6.1309	−0.1719	+0.2391
q_1	+0.0614	−19.0398	+0.0104	−19.7946
θ_2	+0.1967	−35.6357	+0.1039	−11.8577
σ_1	+0.6962	−4.1952	+0.5037	−1.3459
σ_2	+0.1343	−1652.2703	+0.2551	−152.9760
σ_3	+0.3248	−8.9916	+0.2308	−2.9370
β_{12}	+0.2816	−29.0399	+0.2241	−6.4160
β_{21}	+0.3939	−6.2285	+0.3393	−1.2713
β_{23}	+0.18378	−9.5353	+0.1555	−1.9817
β_{32}	+0.1437	−40.6559	+0.1143	−8.9824
$\tilde{\beta}_{12}$	+0.1123	−31.2130	+0.1152	−5.3493
$\tilde{\beta}_{32}$	+0.0401	−43.6982	+0.0411	−7.4891
γ_1	+0.1779	−11.1646	+0.0357	−9.7770
γ_3	+0.0830	−23.9291	+0.0164	−21.3360
ε_2	−0.3014	+9.6915	−0.1879	2.7328
$\tilde{\varepsilon}_2$	−0.1507	+19.3805	−0.1562	3.2884
m_2	−0.1205	+9.6915	−0.1503	+2.7328
N_1^0	+0.3023	−386470.8209	+0.1644	−249965.7111
N_2^0	−0.4433	+26351.9978	−0.2397	+8570.8127
N_3^0	+0.0263	−828321.1332	+0.0753	−545493.0811

TABLE 2.2: Sensitivity indices of R_0

2.4.2 Uncertainty Analysis of R_0

Many of the parameters in this model, although they have biological interpretations, are either known imprecisely or vary significantly from region to region, taking on a range of values. Therefore, it is necessary to see how the outcome of the model may vary over these ranges of plausible parameter values.
We employed the technique of Latin Hypercube Sampling [83], which belongs to the Monte Carlo class of sampling methods. Latin hypercube sampling technique is a stratified sampling without replacement, where each parameter distribution is divided into N equal probable intervals, which are then sampled. For each input parameter we have assumed a normal distribution across the ranges listed in the second table in Appendix A. We then calculated R_0 as the model output using $n = 5000$ sets of sampled parameters. Averaging R_0 over all parameter sets gives a mean of 1.19 and a median of 1.18.

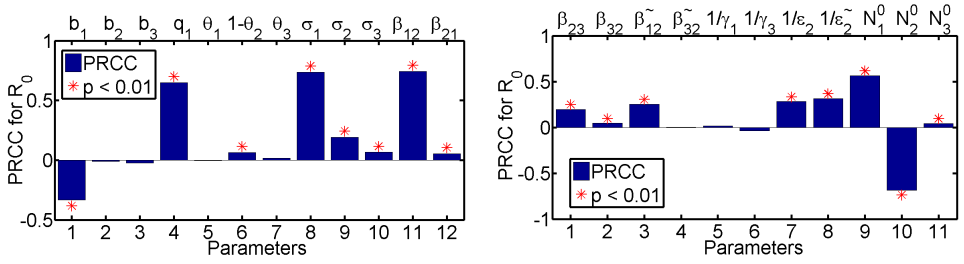

FIGURE 2.4: Significance test of model parameters and PRCC results for R_0 for 5000 simulations. The $(*)$ denotes PRCCs that have P-value < 0.01.

We used the partial rank correlation coefficient (PRCC) to assess the significance of each parameter with respect to R_0. Partial rank correlation characterizes the non-linear but monotonic relationship between outputs and inputs [83] and it has been successfully used to characterize the linear relationship between rank-transformed inputs $X_{ranked}(i)$ and output Y_{ranked} after the linear effects on the output Y_{ranked} of the remaining inputs are discounted [70]. The results are shown in Figure 2.4. The sign of the correlation coefficient indicates the direction of the relationship and the value of the correlation indicates the strength of the relationship between input parameters and model output. The more the p-value is close to zero the more the parameter is significant. The per capita birth rate/death rate b_1, b_2 and b_3 show moderate influence to the model output with increasing per capita death rates decreasing R_0. This relationship is due to the fact that increasing these rates reduces the species lifespan or simply mean that reducing the mosquito densities will help to control the outbreak. Vertical infection q_1 and the probability of transmission from *Aedes* mosquitoes to susceptible livestock β_{21} have positive PRCC values, all above 0.5 indicating high significance to R_0 with direct proportional relationship, that is, an increase in q_1 and β_{21} increases R_0. This results from the fact that vertical infection initiate the transmission with high significance during dry season when infected eggs hatch after rainfall and the first generation of infected female *Aedes* bites livestock for blood meal during their second gonotrophic cycle from which they are able to infect the host, hence, further spreading the virus.
The parameters $1-\theta_2$, β_{23}, β_{12}, β_{32}, $\tilde{\beta}_{12}$, $1/\varepsilon_2$ and $1/\tilde{\varepsilon}_2$ appear to be significant with PRCC positive indicating an increase in R_0 with an increase in the probability of susceptible livestock moving to asymptomatic class, probabilities of virus transmission and the average duration of infection in livestock (symptomatic and asymptomatic). The model output is also highly sensitive to initial total *Aedes* population N_1^0, initial total livestock population N_2^0 and to the number of times an *Aedes* mosquito would bite a host σ_1, with directly proportional increase in R_0, that is only influenced by N_1^0 and σ_1. This relationship results from the that an outbreak at early stage may be dependent on the initial number of vectors, number of bites to a host and initial number of available host. Since in our model the total number of bites on livestock varies with both the livestock and mosquito population sizes, increasing the initial size of host population does not necessarily mean that we will observe an increase in R_0 as shown by the PRCC value for N_2^0. This may be explained by the fact that livestock availability to mosquitoes can be

reduced through human control interventions and by the efforts the host takes to prevent mosquito bites (such as switching its tail) making σ_1 possibly very small.

2.5 Sensitivity Analysis of the Endemic Equilibrium, E^*

Sensitivity analysis of the endemic equilibrium state is used to determine the relative importance of different parameters responsible for equilibrium disease prevalence [88], which is related to the endemic equilibrium state $E^* = (P_1^*, U_1^*, S_1^*, E_1^*, I_1^*, S_2^*, A_2^*, I_2^*, R_2^*, P_3^*, S_3^*, E_3^*, I_3^*)$. However, for our analysis we assume that the equilibrium disease prevalence is related to the following disease states: $U_1^*, E_1^*, I_1^*, A_2^*, I_2^*, E_3^*, I_3^*$. Given the fact that E^* is not expressed explicitly, analytical derivation of the indices is not possible. Therefore, we compute the sensitivity indices numerically using the method developed by Chitnis et al.[89], also applied in [88]. Following the notation in [88], we have replaced the model state variables $(U_1, E_1, I_1, A_2, I_2, E_3, I_3)$ by $(x_1, x_2, x_3, x_4, x_5, x_6, x_7)$, the model parameters $(b_1, d_1, d_2, d_3, q_1, \theta_1, \theta_2, \sigma_1, \sigma_2, \sigma_3, \beta_{12}, \beta_{21}, \beta_{23}, \beta_{32}, \tilde{\beta}_{12}, \tilde{\beta}_{32}, \gamma_1, \gamma_2, \varepsilon_2, \tilde{\varepsilon}_2)$ have been replaced by
$(y_1, y_2, y_3, y_4, y_5, y_6, y_7, y_8, y_9, y_{10}, y_{11}, y_{12}, y_{13}, y_{14}, y_{15}, y_{16}, y_{17}, y_{18}, y_{19}, y_{20}, y_{21})$ and the endemic equilibrium disease state $(U_1^*, E_1^*, I_1^*, A_2^*, I_2^*, E_3^*, I_3^*)$ by $(x_1^*, x_2^*, x_3^*, x_4^*, x_5^*, x_6^*, x_7^*)$. The sensitivity index of the endemic equilibrium disease state, x_i^*, to the parameter, y_j is given by

$$\frac{\partial x_i^*}{\partial y_j} \times \frac{y_j}{x_i^*} \tag{2.14}$$

for $1 \leq i \leq 7$ and $1 \leq j \leq 21$. The numerically computed endemic disease state for low parameter values is given by

$$E^* = (500, 0.4095, 4956, 9.639, 93.5, 66.81, 0.4395, 0.351, 890.6, 500, 4974, 6.238, 53.34) \tag{2.15}$$

and for high parameter values is

$$E^* = (500, 40, 4956, 40, 40, 66.81, 0.005, 0.5, 890.6, 500, 4974, 14, 24.18). \tag{2.16}$$

2.5.1 Sensitivity Indices of E^*

Parameters	U_1^*	E_1^*	I_1^*	A_2^*	I_2^*	E_3^*	I_3^*
b_1	+0.0108	+0.0008	+0.0008	−25.2897	−0.7227	−0.0070	−0.0042
d_1	−0.1763	−0.1998	−0.1763	+6433.9936	+183.8729	+1.7728	+1.0566
d_2	0.0000	0.0000	0.0000	+0.0165	−0.0001	0.0000	0.0000
d_3	+0.3466	+0.3367	+0.3466	+6420.7205	+9.9271	−1.2941	−0.7543
q_1	+0.0108	+0.0008	+0.0008	−25.2897	−0.7227	−0.0070	−0.0042
θ_1	+7.0042	+7.7755	+8.0042	−250367.8884	−7155.1013	−68.9862	−41.1172
θ_2	+0.0001	+0.0001	+0.0001	−109.9836	+0.7489	+0.0001	+0.0001
σ_1	−0.0635	+0.0079	−0.0635	−262.2369	−7.9111	−0.0755	−0.0450
σ_2	−0.0080	−0.0018	−0.0080	−68.8993	−0.7646	+0.0028	−0.0057
σ_3	−0.0291	−0.0283	−0.0291	−531.1488	−0.8931	+0.1076	−0.0207
β_{12}	−0.0681	+0.0091	−0.0681	−293.8141	−8.3967	−0.0810	−0.0483
β_{21}	−0.0006	−0.0006	−0.0006	+10.0632	−0.1655	−0.0008	−0.0005
β_{23}	−0.0003	−0.0003	−0.0003	+4.3452	−0.0714	−0.0003	−0.0002
β_{32}	−0.0313	−0.0304	−0.0313	−579.8804	−0.8966	+0.1169	−0.0222
$\tilde{\beta}_{12}$	−0.0003	+0.0000	−0.0003	−1.2592	−0.0360	−0.0003	−0.0002
$\tilde{\beta}_{32}$	−0.0001	−0.0001	−0.0001	−1.7396	−0.0027	+0.0004	−0.0001
γ_1	+7.7510	+6.5581	+7.7510	−211168.8756	−6034.8582	−58.1854	−34.6796
γ_3	−6.5110	−6.3249	−6.5110	−120624.6443	−186.4978	+24.3123	+15.0696
ε_2	0.0000	0.0000	0.0000	−0.6373	+0.0051	0.0000	0.0000
$\tilde{\varepsilon}_2$	+0.0004	+0.0004	+0.0004	+30.1844	−0.1344	+0.0005	+0.0003
m_2	0.0000	0.0000	0.0000	+2.4148	−0.0108	0.0000	0.0000

TABLE 2.3: Sensitivity indices of E^* to the high parameters.

Intuitively, the sensitivity indices of the endemic equilibrium state indicate that an increase/decrease in disease prevalence leads to a decrease/increase in the equilibrium of the infected symptomatic livestock due to disease-induced death rate m_2 in livestock [48]. Note that these intuitive explanations agree with the signs of the sensitivity indices (see Tables 2.3 and 2.4). For both low and high parameter values for A_2^* and I_2^* the most sensitive parameters are: $d_1, d_3, \sigma_1, \theta_2, \gamma_1, \gamma_3$. This agreement results from the fact that the prevalence of the disease is driven mainly by the dynamics of the vectors.

Parameters	U_1^*	E_1^*	I_1^*	A_2^*	I_2^*	E_3^*	I_3^*
b_1	+7.8391	−0.0046	−0.0007	−1.4086	−4.6158	−0.0571	−0.0094
d_1	+32.1994	+0.6773	+0.1410	+208.0621	+681.7857	+8.4392	+1.3933
d_2	+0.0033	+0.0001	0.0000	−0.0033	+0.0116	+0.0001	0.0000
d_3	+96.9302	+2.9169	+0.4245	+103.5420	+174.6454	−3.7730	−0.5748
q_1	+7.8391	−0.0046	−0.0007	−1.4086	−4.6158	−0.0571	−0.0094
θ_1	−1.2533	−0.0076	−0.0011	−2.3418	−7.6736	−0.0950	−0.0157
θ_2	−0.8320	−0.0250	−0.0036	−24.0414	17.8278	−0.0221	−0.0036
σ_1	−18.3365	−0.1926	−0.0803	−8.6146	−42.1976	−0.4872	−0.0804
σ_2	−1.3460	−0.0169	−0.0059	−0.6855	−3.0531	−0.0285	−0.0059
σ_3	−2.1224	−0.0639	−0.0093	−1.8055	−4.2095	+0.0533	−0.0093
β_{12}	−8.9103	−0.0190	−0.0390	−5.8370	−19.1270	−0.2368	−0.0391
β_{21}	−5.8510	−0.1761	−0.0256	−0.2120	−15.5825	−0.1555	−0.0257
β_{23}	−0.4768	−0.0143	−0.0021	−0.0173	−1.2699	−0.0127	−0.0021
β_{32}	−1.2595	−0.0379	−0.0055	−1.3454	−2.2693	+0.0490	−0.0055
$\tilde{\beta}_{12}$	−4.7815	−0.0102	−0.0209	−3.1323	−10.2641	−0.1271	−0.0210
$\tilde{\beta}_{32}$	−0.5257	−0.0158	−0.0023	−0.5615	−0.9472	+0.0205	−0.0023
γ_1	+19.8838	−0.1100	+0.0871	−33.7844	−110.7061	−1.3703	−0.2262
γ_3	−15.4500	−0.4649	−0.0677	−16.5039	−27.8372	+0.6014	+0.2162
ε_2	+0.1477	+0.0044	+0.0006	−0.6400	+0.9321	+0.0039	+0.0006
$\tilde{\varepsilon}_2$	+0.1477	+0.0044	+0.0006	+0.3490	+0.1066	+0.0039	+0.0006
m_2	+0.0118	+0.0004	+0.0001	+0.0279	−0.0085	+0.0003	+0.0001

TABLE 2.4: Sensitivity indices of E^* to the low parameters.

2.6 Uncertainty and sensitivity analysis of the model dynamics

In this section we aim to determine the uncertainty of various model output state variables $(U_1, E_1, I_1, A_2, I_2, E_3, I_3)$ based on the uncertainty of the input parameters sampled using the Latin hypercube sampling technique described in section 2.4.2. Our model (2.1-2.3) consists of more than 23 parameters, however for this analysis we are considering only 21 parameters. Each parameter is divided into 100 equal probable intervals, used to construct the LHS-matrix which is then used to compute 100 model simulations. Given, this matrix of randomly selected input parameters we can calculate the model output values providing means for determining parameter sensitivity. Marino and colleagues [83] reports that for nonlinear but monotonic relationship between model outputs and model input parameters, sensitivity analysis techniques that work well include Spearman rank correlation coefficient (RCC), partial rank correlation coefficient (PRCC), and standardized rank regression coefficients (SRRC). Although, the PRCC is widely used and is reported to be more powerful tool [90]. For the following sections, instead of the PRCC we make use of the Spearman rank correlation coefficient by assuming that model output state variables monotonically depend on input model parameters. By this approach we may neglect possible statistical dependencies between input variables. Note however that we keep the notation PRCC although the RCC algorithm was used to compute the sensitivity indices. Since our model is formulated to predict disease outbreaks we only consider high rainfall and moderate temperature parameter values to generate the LHS-matrix (see Table A.1 in Appendix A).

2.6.1 Time invariant sensitivity analysis

The model is simulated for 600 days and the 12th day is selected (representing the peak of the outbreak) and the PRCCs and their respective significances are computed for $U_1, E_1, I_1, A_2, I_2, E_3, I_3$ model state variables. RVF outbreaks in a particular location are very short and the peak of the epidemic is usually reached between 10-20 days [4, 48]. Hence, we have selected the 12th day to assess the variation on model output when we are at the peak zone using PRCCs. PRCC provides answers to questions about how the output is affected if we increase (or decrease) a specific parameter [83].
As shown in Figure 2.5 the number of infected eggs U_1 is highly correlated to the *Aedes* death rate d_1, birth rate b_1, infected symptomatic disease-induced death rate m_2 and to the vertical transmission rate q_1. The number of exposed *Aedes* E_1 is highly correlated to the number of bites an *Aedes* mosquito would bite a host σ_1, the number of bites a host would sustain σ_2, probability of transmission from an infected asymptomatic host to susceptible *Aedes* $\tilde{\beta}_{12}$, the probability of transmission from an infected *Aedes* to a susceptible host β_{21} and to m_2. The number of infected *Aedes* I_1 is more sensitive to d_1 and m_2 followed by the probability of transmission from an infected *Culex* to a susceptible host β_{23} and vertical transmission q_1. In general, we observe that reducing the prevalence of the disease in livestock reduces the number of secondary infections in mosquitoes.

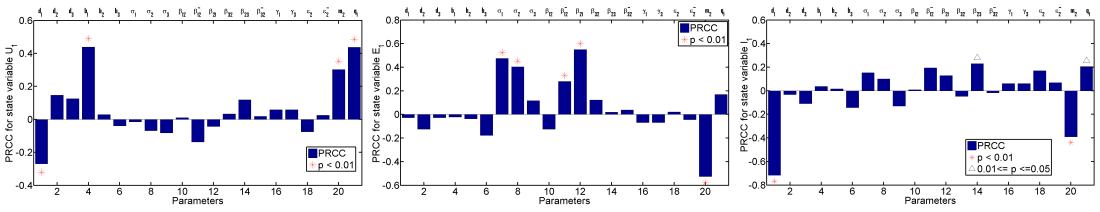

FIGURE 2.5: Presentation of PRCC results for $n = 100$ simulations at time $t = 12$ days. $*$ and $\triangle$ denote PRCCs that are significant with $p < 0.01$ and $0.01 \leq p \leq 0.05$ respectively, for *Aedes* infected eggs U_1, Exposed *Aedes* E_1, and Infected *Aedes* I_1 state variables.

In Figure 2.6 we represent the PRCCs for A_2, I_2, E_3, I_3. The number of infected asymptomatic livestock A_2 is more sensitive to σ_1, σ_2 and β_{21} followed by d_2. However, the number of infected symptomatic livestock I_2 is more sensitive to $\sigma_1, \sigma_2, \beta_{21}$ and to m_2 followed by q_1. These results suggest that reducing $\sigma_1, \sigma_2, \beta_{21}$ and the efficiency of vertical transmission q_1, reduces the prevalence of the disease. This agrees with common knowledge that vector control and intervention in livestock are effective control measures [13]. In addition, our results suggest that if m_2 is taken as removal rate, then livestock isolation can be an additional control measure, as increasing m_2 decreases I_2. The number of exposed *Culex* E_3 is more sensitive to $\sigma_1, \sigma_2, \beta_{21}$ and m_2 followed by the probability of transmission from an infected asymptomatic host to a susceptible *Culex* mosquito $\tilde{\beta}_{32}$. While the number of infected *Culex* I_3 is highly sensitive to the *Culex* death rate d_3.

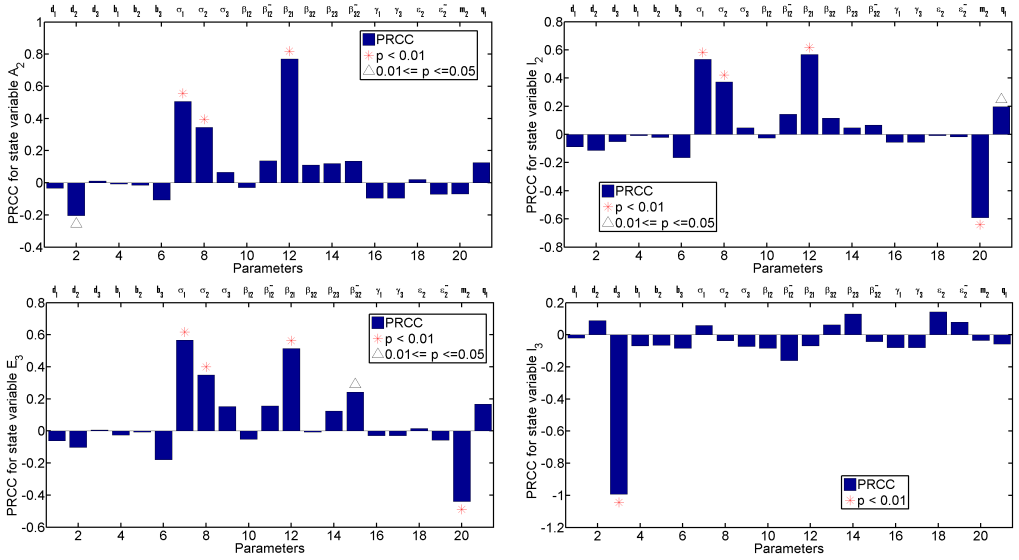

FIGURE 2.6: Presentation of PRCC results for $n = 100$ simulations at time $t = 12$ days. $*$ and $\triangle$ denote PRCCs that are significant with $p < 0.01$ and $0.01 \leq p \leq 0.05$ respectively, for Asymptomatic infected host A_2, Symptomatic infected host I_2, Exposed *Culex* E_3, and Infected *Culex* I_3 state variables.

2.6.2 Time varying sensitivity analysis

Time varying sensitivity indices are calculated over a specified time period and plotted versus time. This is fundamental to assess the significance of model input parameter over a specified time interval during model dynamics [83]. For our analysis we took a time period that goes from day 1 to the 60th day of the outbreak. RVF outbreaks in most cases take less than 60 days in a particular location. This time interval is sufficient to capture all parameter changes due to the natural evolution of the disease. Figure 2.7 (a)-(d) show the PRCCs for U_1 which is highly sensitive to vertical transmission q_1 for the entire interval. It is worth to note that in c) the relationship between U_1 and β_{23} changes sigh between 40-50 days of the outbreak. E_1 is more sensitive to d_1 around the peak of the outbreak and tends to be more sensitive to b_2 after the peak (see Fig.2.7(e)). In (f) E_1 is more sensitive to σ_1 before the 40th day. E_1 is also sensitive to β_{21}, however, the relationship between E_1 and β_{21} changes sigh around the 30th day Fig.2.7(g). Here the effect of β_{21} (probability of disease transmission from an infected *Aedes* mosquito to a susceptible symptomatic ruminant) changes with respect to the number of exposed *Aedes* mosquitoes E_1 over time: it is positively correlated right from the beginning of the outbreak up to the end of its peak, then it becomes negatively correlated as the infection progresses to the steady state. This means that transmission of infection to susceptible livestock is responsible for updating the new generation of infected mosquitoes until the end of the outbreak. A similar phenomenon is also observed in Fig.2.9(c). I_1 is more sensitive to d_1 over the entire interval (see Fig.2.7(i)), to σ_1 and β_{21} during the first 20 days of the outbreak Fig.2.7(j) and (k). I_1 is also sensitive to q_1 as the epidemic progresses over the time period.

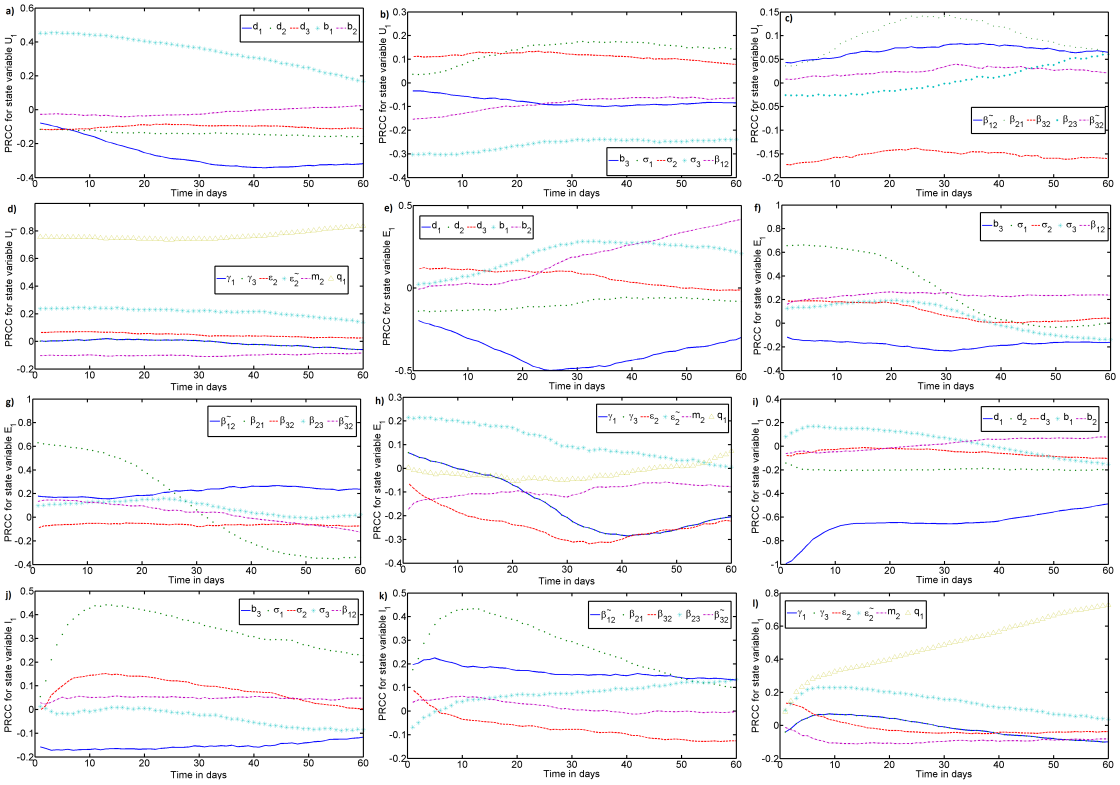

FIGURE 2.7: Description of how the sensitivity of parameters changes as the system dynamic progress. Note that here we have considered the *Aedes* Infected eggs U_1, *Aedes* Exposed E_1 and *Aedes* Infected I_1 state variables.

A_2 is more sensitive to σ_1 and β_{21} Fig.2.8(b) and (c) respectively. However, the relationship between A_2 and σ_1 and β_{21} changes sign after the first 20 days. The effect of parameter σ_1 (number of bites an *Aedes* mosquito would bite a host) changes with respect to the number of infected asymptomatic hosts over time: it is positively correlated right from the beginning of the epidemic up to the end of its peak, then it becomes negatively correlated as the infection progresses to the steady state. This indicates that the number of times an infected *Aedes* mosquito feeds on a host is responsible for spreading the infection; however, as time progresses these infected animals start to recover from the infection. Thus, the number of susceptible and infected livestock reduces while the number of recovered ones increases. This phenomenon has also been observed in Fig.2.8(f) for infected symptomatic ruminants.

Furthermore, A_2 is more sensitive to the asymptomatic host recovery rate $\tilde{\varepsilon}_2$ and changes sign (see Fig.2.8(d)). The effect of the rate of recovery of infected asymptomatic ruminants changes with respect to the number of infected asymptomatic ruminants over time: it is positively correlated (low) at the very beginning of the infection, but few days before the peak it then becomes negatively correlated (strong) until the infection dies out. The negative sign suggest that if we increase ε_2, the number of infected asymptomatic ruminants increases quickly (and vice versa). These results suggest that intervention strategies in asymptomatic ruminants even after the initial spread of the disease are essential for stopping further spread of

the disease.
I_2 is more sensitive to b_2 over the end of the interval Fig.2.8(e). I_2 is also sensitive to σ_1, β_{21} and ε_2 Fig.2.8(f),(g) and (h) respectively. Note that the relationship between I_2 and σ_1 and β_{21} changes sign after the first 20 days.

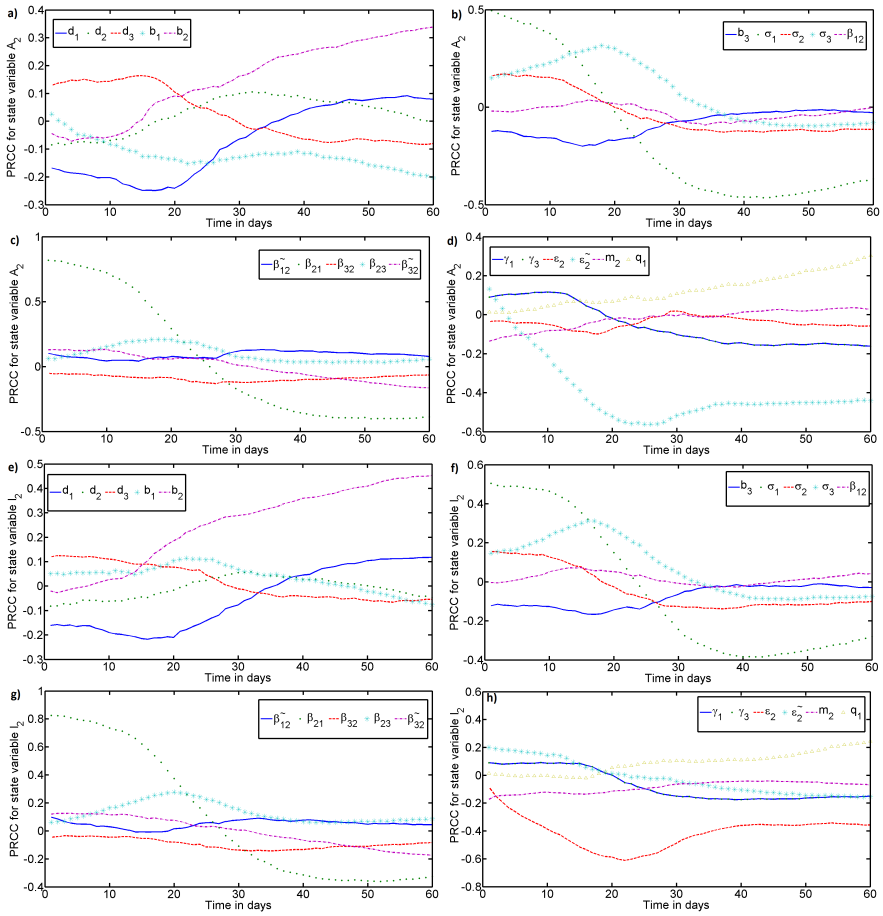

FIGURE 2.8: Description of how the sensitivity of parameters changes as the system dynamic progress. Note that here we have considered the Asymptomatic infected host A_2 and the Symptomatic infected host I_2 state variables.

The number of exposed *Culex* E_3 is more sensitive to σ_1 and β_{21} Fig.2.9(b) and (c) respectively. In both cases σ_1 and β_{21} change sign and E_3 tends to be more sensitive to d_3 towards the end of the time interval (see Fig.2.9(a)). I_3 is more sensitive to d_3 at the beginning and the end of the interval Fig.2.9(e). This is an interesting situation. As the infection progresses to the steady state the parameter birth rate b_2 enhances its correlation (positively) with the number of infected symptomatic livestock I_2. This improvement of the correlation indicates that new born ruminants may be responsible of a second wave for the epidemic if these ruminants are not vaccinated. These insights are fundamental for guiding intervention programs both at the beginning of the infection and after the peak. I_3 is also more sensitive to σ_3 over the entire interval Fig.2.9(f) and more sensitive to β_{21} over the first 30 days.

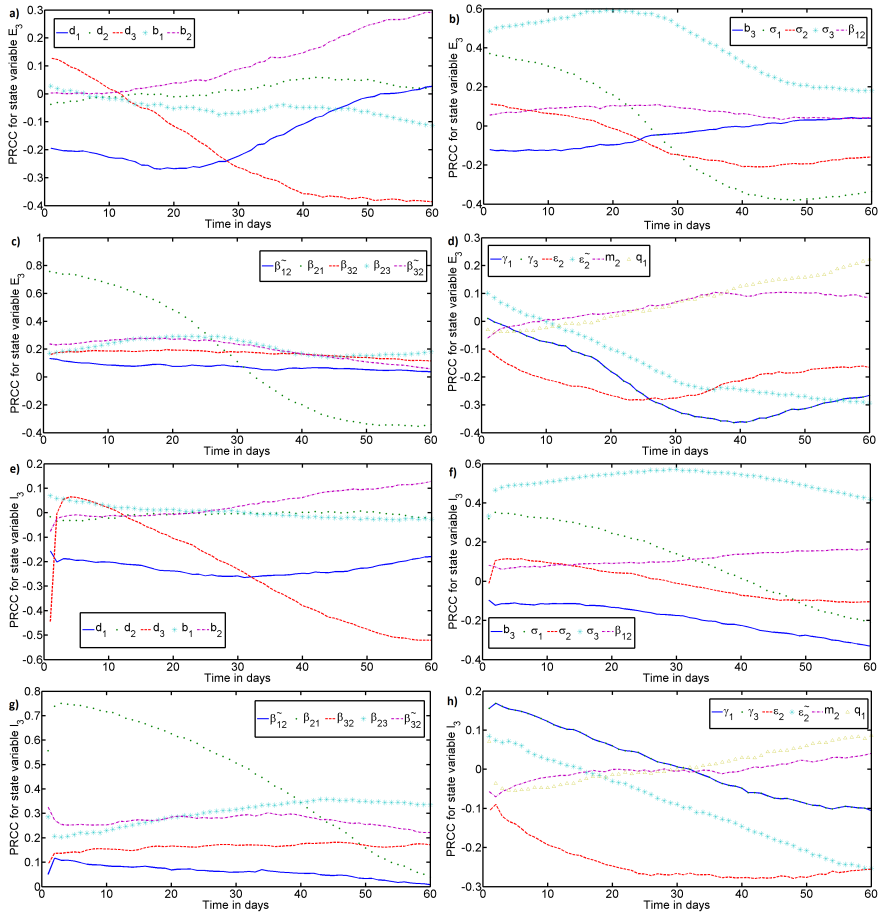

FIGURE 2.9: Description of how the sensitivity of parameters changes as the system dynamic progress. Note that here we have considered the *Culex* Exposed E_3 and *Culex* Infected I_3 state variables.

2.7 Vector abundance during an outbreak

Using model system (2.1-2.3) we investigate the effects of vertical transmission on the abundance of adult mosquitoes in an epidemic situation. Fig.2.10 depicts the time evolution of the number of infected adult *Aedes* mosquitoes for different values of initial number of infected eggs U_1^0. In a) we observe that for $U_1^0 = 999$ the number of infectious adult *Aedes* reaches its maximum around 25 days, while for $U_1^0 = 100$ the number of infectious adult *Aedes* reaches its maximum at around 40 days see Fig.2.10(b). This suggests that: depending on the efficiency of transovarial/vertical transmission RVF outbreak at a particular site is very brief, and the peak is likely to be reached in a span of 30 days; depending on the efficiency of vertical transmission the duration of the outbreak is likely to either be reduced or increased.

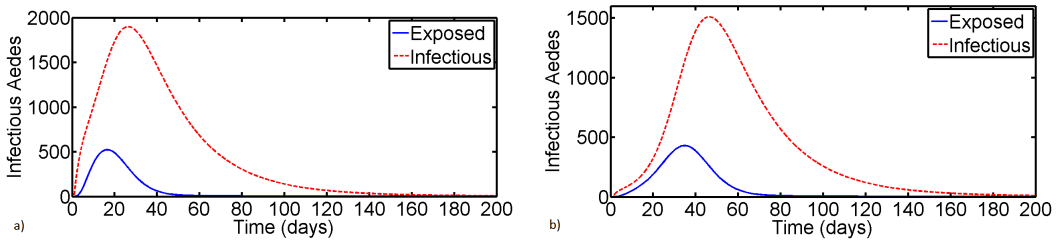

FIGURE 2.10: Simulation of infectious *Aedes* populations with varying initial number of infected eggs. (a) With 999 initial infected eggs and (b) with 100 initial infected eggs. The remaining initial conditions are: $S_1 = 5000, P_1 = 1000, E_1 = 0, I_1 = 1, S_2 = 1000, A_2 = I_2 = R_2 = 0, S_3 = 5000, P_3 = 1000, E_3 = 0$ and $I_3 = 1$. All model parameters (high moisture) are given in Table A.1.

2.8 Conclusions

Using a RVF model developed by Pedro et al.[4] and its analytical expression of the basic reproduction, R_0 we studied the relative importance of vertical transmission to disease spread governed by R_0. Reducing the model system to a system of two ordinary differential equations (U_1, I_1) we investigated the importance of vertical transmission to disease persistence and its relation with the basic reproductive number and type reproductive numbers. Furthermore, by employing techniques based on perturbation of fixed points estimations we determined sensitivity indices of various model outputs to the input parameters. Based on Latin hypercube sampling (LHS) and Partial rank correlation coefficients (PRCCs) and rank correlation coefficients (RCCs) we systematically determined the relative importance of model parameters to the basic reproduction number R_0 and to model state variables for single time and multiple time points. Sampling-based procedures provided a range of values of both R_0 and model state variables in an interval while methods based on perturbation of fixed points estimations or computation of local derivatives provided only a single value of the model output [88]. Thus sampling-based procedures (both time varying and time invariant) provide more information as compared to local derivative techniques.

Using the basic reproductive number, R_0 to assess the importance of vertical infection efficiency, we characterized the relationship predicted by the model output: for low moisture parameters the response was initially very small but strengthened rapidly when the vertical infection efficiency exceeded 20%, highlighting the importance of vertical transmission for initial spread and persistence of the disease during endemic activities. Applying vector type reproductive number, T_1^v we showed that vertical infection of 20% can be responsible for more than 80% of the required effort to eradicate the epidemic. This suggests that reducing the size of mosquito population and mosquito biting rates will help control both the initial spread of the disease and ongoing disease activities during an outbreak. Previous studies have also shown that, if policy-makers wish to decrease the transmission of RVF, keeping the vector populations at the lowest levels is required [4, 5, 48].

In addition, two important features were observed: (1) during epidemic activities vertical transmission accelerated the course of the outbreak as it increased the size of infected vectors and reduced the duration of the outbreak while during endemic activities heavily contributed to disease persistence; (2) an increase in the initial number of livestock N_2^0 substantially reduced the magnitude of all reproductive numbers.

We then used global sensitivity analysis to determine which parameters are most important to disease persistence and epidemicity. The basic reproductive number, R_0 was most sensitive to probability of vertical transmission q_1, probability of transmission from an *Aedes* mosquito to livestock β_{21}, initial density population of *Aedes* mosquitoes N_1^0 and livestock N_2^0 and to the *Aedes* biting rate σ_1. Vertical transmission has potential for initiating virus circulation [26], mosquito biting to spread the infection to nearby susceptible livestock [36]. Thus, understanding the role of each of the above five parameters (q_1, β_{21}, N_1^0, N_2^0 and σ_1) is central for designing effective RVF control strategies.

The sensitivity indices of the endemic equilibrium state variables showed that for both low and high parameter values for A_2^* and I_2^* the most sensitive parameters are: *Aedes* death rate, *Culex* death rate, the number of bites an *Aedes* mosquito would bite a host, the progression rates from exposed to infectious stage for both *Aedes* and *Culex*. This agrees with the fact that the prevalence of the disease is driven mainly by the dynamics of the vectors. Nevertheless, reducing the prevalence of the disease in livestock reduces the number of secondary infections in mosquitoes. On the other hand the RCCs calculated between the values of each of the 21 model parameters and model state variables which was derived from the uncertainty analysis strongly supported previous results obtained through perturbation of fixed point estimations method. Furthermore, time varying sensitivity analysis of model state variables showed an extra potential for exploring parameter space variations and their contribution to model variations during disease evolution. The effect of model input parameters to model output variations does not remain static over time. There are changes that occur as the disease evolve. One of the main objectives of this study was to quantify the attribution of model output variations to input parameters over time. Through this analysis we have identified four key parameters (β_{21}, σ_1, b_2 `and` $\tilde{\varepsilon}_2$) which effect change over time. The results of this analysis are of higher epidemiological significance as they provide experimental epidemiologists and health policy-makers with time specific information on major disease factors. In addition, this opens a new direction into future research [88] which should exhaustively investigate the effects of these parameters both at the initial phase of the epidemic and during the transient phase when the effect of initial conditions have been discarded.

Chapter 3

Stability, bifurcation and chaos analysis of vector-borne disease model with application to Rift Valley fever[1]

3.1 Introduction

Rift Valley fever virus (RVFV), a member of the phlebovirus genus, and family Bunyaviridae which has been isolated from at least 30 mosquito species in the field [27] infects both wild and domestic livestock and humans. The RVF epizootics/epidemics are closely linked to the occurrence of the warm phase of the El Nino/Southern Oscillation (ENSO) phenomenon [34]. In addition, elevated Indian Ocean temperatures lead to heavy rainfall and flooding of habitats suitable for the production of immature *Aedes* mosquitoes that serve as the primary RVF virus (RVFV) vectors in East Africa [35, 36]. Studies have shown that the life cycle of RVFV has distinct endemic and epidemic cycles. During the endemic cycle the virus persists during dry season/inter-epizootic periods through vertical transmission in *Aedes* mosquito eggs [35]. *Aedes* eggs need to be dry for several days before they can mature. After maturing, they hatch during the next flooding event large enough to cover them with water [11, 91]. The eggs have high desiccation resistance and can survive dry conditions in a dormant form for months to years. At the beginning of the rainy season, *Aedes* mosquitoes quickly grow to large numbers before declining due to the need for dry conditions for egg maturation. There can be a second peak in mosquito densities at the end of the rainy season if there is a gap in rainfall for several days [91]. When these mosquitoes lay their eggs in flooded areas (including dambos), transovarially infected adults may emerge and transmit RVFV to nearby domestic livestock, including sheep, goats, cattle, and camels. High viremias in

[1]This chapter has been published: Pedro SA, Abelman S, Ndjomatchoua FT, Sang R, Tonnang HEZ (2014) Stability, Bifurcation and Chaos Analysis of Vector-Borne Disease Model with Application to Rift Valley Fever. PLoS ONE 9(10): e108172. doi:10.1371/journal.pone.0108172

these ruminants may then lead to the infection of secondary arthropod vector species including various *Culex* species [37]. Epizootic/epidemic cycles are driven by the subsequent elevation of various *Culex* mosquito populations, which serve as excellent secondary vectors if immature mosquito habitats remain flooded for a long enough period [36]. Their eggs require water to mature and hatch and the mosquitoes survive the dry season in adult form and during the rainy season, the population of *Culex* mosquitoes reaches a maximum towards the end of the season [5]. The disease is known to occur in outbreaks that come in cycles of up to 15 years in the Eastern Africa region and the Horn of Africa [39].

These variations in climatic factors induce seasonal fluctuations in mosquito population densities. Hence the complexity observed on the dynamics of RVF virus transmission and maintenance. The interplay between the internal nonlinear dynamic of ecological systems and various external factors that affect them, makes understanding of population fluctuation a unique problem [92]. Mathematical models have been developed in order to provide a better understanding of the nature and dynamics of the transmission and persistence of the disease, as well as predict outbreaks and simulate the impact of control strategies [5, 48, 69, 70]. Most of these models considered constant mosquito oviposition rates, ignoring effects of seasonal fluctuations in the mosquito population size. Furthermore, some have ignored the effects of vertical transmission and secondary vectors [48] and some only considered *Aedes* species only [5]. Temperature, rainfall and humidity have great influence in all stages of mosquito development from the emergence and viability of eggs, to the size and longevity of adults [6, 93]. Recently, Mpeshe et al. [74] modified their previous study [48] to include vertical transmission in *Aedes* species and climate-driven parameters. These models provide important insights but do not investigate the stability dynamics and attractors structures of the model when there are external forces in the density of vector populations.

The most common manifestation of external forcing is through seasonality including both naturally (e.g. the occurrence of the warm phase of the El Nino/Southern oscillation phenomenon) and induced (e.g human deforestation or human pollution). Studies for understanding dynamical consequences of regular and stochastic external forcing are still ongoing but poorly understood [94–97]. To the best of our knowledge, no systematic investigation of stability and attractor structures of a realistic RVF model comprising two populations of mosquitoes (*Aedes* and *Culex*) and one livestock host population with two infected classes (asymptomatic and symptomatic) and seasonal variation on mosquito oviposition rates has been carried out.

Based on the model proposed by Gaff et al. [69], we investigate a two vector and one host epidemic model, to capture the dynamical behaviour of both the disease free and endemic equilibria, the effects of seasonality on mosquito oviposition rates (b_1, b_3), parametrized by δ_1, δ_3 and effects of asymptomatic class in livestock (parametrized by $1 - \theta_2$). We prove existence and global stability of both the disease-free and the endemic equilibria in the absence of secondary vectors ($I_3 = 0$), as well as the existence and local stability of both disease free and endemic equilibrium points of the overall model. We then investigate the structures of model attractors through bifurcation analysis, taking as bifurcation parameters δ_1 and δ_3 the strengths of seasonality of mosquito oviposition rates.

The bifurcation diagrams with simultaneous variation of seasonal forcing on the oviposition rates of the two mosquito species reveal the complexity induced by their interactions. The understanding of possible state space scenarios through bifurcation analysis is helpful for understanding RVF epidemiological data with its seasonality aspects. To obtain robust analysis we then compute the largest Lyapunov exponents, Poincaré maps and maxima return maps.
The section methods gives a detailed description of the model and its parameters. In results the model is used to study the dynamic behaviour of the disease stability and bifurcation analysis. Simulations are performed to investigate model dependence on initial condition and attractors structures of the model applying an external forcing on mosquito's oviposition rates.

3.2 RVF epidemic model

Gaff et al.[69] proposed a one host and two vectors population model for RVF with vertical transmission in *Aedes* vectors to study the transmission of RVF and the impact of vertical transmission on the persistence of the disease. Chitnis et al.[5] analysed a RVF model with vertical transmission for *Aedes* mosquitoes and included asymptomatic class for livestock and removed one population of mosquitoes.
The model presented in this paper adopts a similar structure as in Gaff et al.[69]. We introduce an asymptomatic class for livestock [5], because for many species of livestock, RVF virus infection are frequently subclinical [27, 98]. As the main purpose of this study is to study the dynamic behaviour of the disease, influenced by changes on the climate and oscillation on rainfall, we include seasonal variation in the oviposition rates of both *Aedes* and *Culex* mosquitoes.
We divide the livestock population into four classes: susceptible, S_2, asymptomatic, A_2 , infectious, I_2 , and recovered (immune), R_2. Livestock enter the susceptible class through birth (at a constant rate). Birth rates are important because after an outbreak, herd immunity can reach 80% and the proportion of susceptible livestock must be renewed through birth or movement before another outbreak can occur [7]. When an infectious mosquito bites a susceptible animal, there is a finite probability that the animal becomes infected. Since the duration of the latent period in cattle is small relative to their life span, we do not model the exposed stage. Many adult cattle do not exhibit clinical signs apart from abortion of foetuses [11, 27], thus, include an asymptomatic class for infectious livestock that transmit the virus at a lower rate than those with acute clinical symptoms. After being successfully infected by an infectious *Aedes* and/or *Culex* mosquito, livestock move from the susceptible class S_2 to either the infected symptomatic I_2 or asymptomatic A_2 class. After some time, the symptomatic and asymptomatic livestock recover and move to the recovered class, R_2. The recovered livestock have immunity to the disease for life. Cattle leave the population through a per capita natural death rate and through a per capita disease-induced death rate only for symptomatic livestock. The size of the livestock population is given by $N_2 = S_2 + A_2 + I_2 + R_2$.
We divide the *Aedes* and *Culex* mosquitoes population into three classes: susceptible, S_a , exposed, E_a , and infectious, I_a. The subscripts $a = 1$ and $a = 3$ represent

Aedes and *Culex* mosquitoes, respectively. Female mosquitoes (we do not include male mosquitoes in our model because only female mosquitoes bite ruminants for blood meals) enter the susceptible class through birth. The virus enters a susceptible mosquito, S_a , with finite probability, when the mosquito bites an infectious animal and the mosquito moves to the exposed class, E_a. After some period of time, depending on the ambient temperature and humidity [99], the mosquito moves from the exposed class to the infectious class, I_a. To reflect the vertical transmission in the *Aedes* species, compartments for uninfected P_1 and infected U_1 eggs are included. As the *Culex* species cannot transmit RVF vertically, only uninfected eggs P_3 are included. Mosquitoes once infected remain infectious during their lifespan. Mosquitoes leave the population through a per capita natural death rate. The size of each adult mosquito population is $N_1 = S_1 + E_1 + I_1$ for adult *Aedes* mosquitoes and $N_3 = S_3 + E_3 + I_3$ for adult *Culex* mosquitoes. The three populations are modelled with carrying capacity K_1, K_2, K_3, for *Aedes*, livestock and *Culex* respectively. While in [69], the total number of mosquito bites on cattle depends on the number of mosquitoes, in our model, the total number of bites varies with both the cattle and mosquito population sizes. This allows a more realistic modelling of situations where there is a high ratio of mosquitoes to cattle, and where cattle availability to mosquitoes is reduced through control interventions [5].

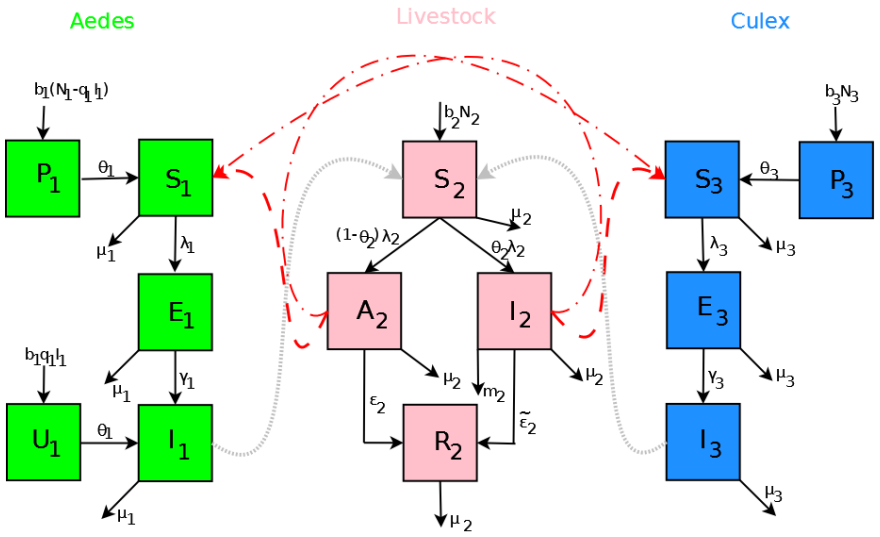

FIGURE 3.1: Flow diagram of RVFV transmission with each species, namely, *Aedes* mosquitoes, *Culex* mosquitoes and livestock (the solid lines represent the transition between compartments and the dash lines represent the transmission between different species).

3.2.1 Mathematical Model

The equations describing the model flowchart 3.1 are given in Chapter 2 (see systems (2.1-2.3)). However, to keep the flow we rewrite them as follows:

Aedes

$$\begin{aligned}
\dot{P}_1(t) &= b_1(N_1 - q_1 I_1) - \theta_1 P_1, \\
\dot{U}_1(t) &= b_1 q_1 I_1 - \theta_1 U_1, \\
\dot{S}_1(t) &= \theta_1 P_1 - \frac{\sigma_1\sigma_2\beta_{12}}{\sigma_1 N_1 + \sigma_2 N_2} I_2 S_1 - \frac{\sigma_1\sigma_2\tilde{\beta}_{12}}{\sigma_1 N_1 + \sigma_2 N_2} A_2 S_1 - d_1 \frac{S_1 N_1}{K_1}, \\
\dot{E}_1(t) &= \frac{\sigma_1\sigma_2\beta_{12}}{\sigma_1 N_1 + \sigma_2 N_2} I_2 S_1 + \frac{\sigma_1\sigma_2\tilde{\beta}_{12}}{\sigma_1 N_1 + \sigma_2 N_2} A_2 S_1 - \gamma_1 E_1 - d_1 \frac{E_1 N_1}{K_1}, \\
\dot{I}_1(t) &= \gamma_1 E_1 + \theta_1 U_1 - d_1 \frac{I_1 N_1}{K_1},
\end{aligned} \tag{3.1}$$

Livestock

$$\begin{aligned}
\dot{S}_2(t) &= b_2 N_2 - \frac{\sigma_1\sigma_2\beta_{21}}{\sigma_1 N_1 + \sigma_2 N_2} I_1 S_2 - \frac{\sigma_3\sigma_2\beta_{23}}{\sigma_3 N_3 + \sigma_2 N_2} I_3 S_2 - d_2 \frac{S_2 N_2}{K_2}, \\
\dot{A}_2(t) &= (1-\theta_2)\frac{\sigma_1\sigma_2\beta_{21}}{\sigma_1 N_1 + \sigma_2 N_2} I_1 S_2 + (1-\theta_2)\frac{\sigma_3\sigma_2\beta_{23}}{\sigma_3 N_3 + \sigma_2 N_2} I_3 S_2 - \tilde{\varepsilon}_2 A_2 - d_2 \frac{A_2 N_2}{K_2}, \\
\dot{I}_2(t) &= \theta_2\frac{\sigma_1\sigma_2\beta_{21}}{\sigma_1 N_1 + \sigma_2 N_2} I_1 S_2 + \theta_2\frac{\sigma_3\sigma_2\beta_{23}}{\sigma_3 N_3 + \sigma_2 N_2} I_3 S_2 - \varepsilon_2 I_2 - d_2 \frac{I_2 N_2}{K_2} - m_2 I_2, \\
\dot{R}_2(t) &= \tilde{\varepsilon}_2 A_2 + \varepsilon_2 I_2 - d_2 \frac{R_2 N_2}{K_2},
\end{aligned} \tag{3.2}$$

Culex

$$\begin{aligned}
\dot{P}_3(t) &= b_3 N_3 - \theta_3 P_3, \\
\dot{S}_3(t) &= \theta_3 P_3 - \frac{\sigma_3\sigma_2\beta_{32}}{\sigma_3 N_3 + \sigma_2 N_2} I_2 S_3 - \frac{\sigma_3\sigma_2\tilde{\beta}_{32}}{\sigma_3 N_3 + \sigma_2 N_2} A_2 S_3 - d_3 \frac{S_3 N_3}{K_3}, \\
\dot{E}_3(t) &= \frac{\sigma_3\sigma_2\beta_{32}}{\sigma_3 N_3 + \sigma_2 N_2} I_2 S_3 + \frac{\sigma_3\sigma_2\tilde{\beta}_{32}}{\sigma_3 N_3 + \sigma_2 N_2} A_2 S_3 - \gamma_3 E_3 - d_3 \frac{E_3 N_3}{K_3}, \\
\dot{I}_3(t) &= \gamma_3 E_3 - d_3 \frac{I_3 N_3}{K_3},
\end{aligned} \tag{3.3}$$

with

$$\begin{aligned}
\tfrac{dN_1}{dt} &= b_1 N_1 - \tfrac{d_1}{K_1}(N_1)^2, \\
\tfrac{dN_2}{dt} &= b_2 N_2 - \tfrac{d_2}{K_2}(N_2)^2 - m_2 I_2, \\
\tfrac{dN_3}{dt} &= b_3 N_3 - \tfrac{d_3}{K_3}(N_3)^2.
\end{aligned} \tag{3.4}$$

Following the approach in [5], σ_a, where $a = 1$ for *Aedes* and $a = 3$ for *Culex* is the rate at which a mosquito would bite livestock (related to the gonotrophic cycle length), and σ_2 is the maximum number of bites that an animal can support per unit time (through physical availability and any intervention measures on livestock taken by humans). Then, $\sigma_a N_a$ is the total number of bites that the mosquitoes would like to achieve per unit time and $\sigma_2 N_2$ is the availability of livestock. Thus, the total number of mosquito-livestock contacts is half the harmonic mean of $\sigma_a N_a$

and $\sigma_2 N_2$,

$$\bar{b} = \bar{b}(N_2, N_a) = \frac{\sigma_a N_a \sigma_2 N_2}{\sigma_a N_a + \sigma_2 N_2} = \frac{\sigma_a \sigma_2}{\sigma_a (N_a/N_2) + \sigma_2} N_a.$$

In addition to having the correct limits at zero and infinity, this form also meets the necessary criteria that $\bar{b} \leq min(\sigma_a N_a, \sigma_2 N_2)$ where $\bar{b}$ is the total number of bites per unit time. The total number of mosquito-livestock contacts depends on the populations of both species. We define $\bar{b}_2 = \bar{b}_2(N_2, N_a) = \bar{b}(N_2, N_a)/N_2$ as the number of bites per livestock per unit time, and $\bar{b}_a = \bar{b}_a(N_2, N_a) = \bar{b}(N_2, N_a)/N_a$ as the number of bites per mosquito per unit time.
We defined the force of infection from mosquitoes to livestock, $\lambda_2^a(t)$, as the product of the number of mosquito bites that one animal has per unit time, b_2, the probability of disease transmission from the mosquito to the animal, β_{2a}, and the probability that the mosquito is infectious, I_a/N_a . We define the force of infection from livestock to mosquitoes, $\lambda_a^2(t)$, as the force of infection from infectious (symptomatic and asymptomatic) livestock. This is expressed as the number of livestock bites one mosquito has per unit time, $\bar{b}_a$; the probability of disease transmission from an infected (asymptomatic) animal to the mosquito, $\beta_{a2}(\tilde{\beta}_{a2})$; and the probability that the animal is infectious, I_2/N_2 (A_2/N_2). Therefore the forces of infection are given by:

$$\begin{aligned}
\lambda_1^2 &= \frac{\sigma_1\sigma_2 N_2}{\sigma_1 N_1 + \sigma_2 N_2}(\beta_{12}\frac{I_2}{N_2} + \tilde{\beta}_{12}\frac{A_2}{N_2}) = \frac{\sigma_1\sigma_2\beta_{12} I_2}{\sigma_1 N_1 + \sigma_2 N_2} + \frac{\sigma_1\sigma_2\tilde{\beta}_{12} A_2}{\sigma_1 N_1 + \sigma_2 N_2},\\
\lambda_2^1 &= \frac{\sigma_1\sigma_2 N_1}{\sigma_1 N_1 + \sigma_2 N_2}\beta_{21}\frac{I_1}{N_1} = \frac{\sigma_1\sigma_2\beta_{21} I_1}{\sigma_1 N_1 + \sigma_2 N_2},\\
\lambda_2^3 &= \frac{\sigma_3\sigma_2 N_3}{\sigma_3 N_3 + \sigma_2 N_2}\beta_{23}\frac{I_3}{N_3} = \frac{\sigma_3\sigma_2\beta_{23} I_3}{\sigma_3 N_3 + \sigma_2 N_2},\\
\lambda_3^2 &= \frac{\sigma_3\sigma_2 N_2}{\sigma_3 N_3 + \sigma_2 N_2}(\beta_{32}\frac{I_2}{N_2} + \tilde{\beta}_{32}\frac{A_2}{N_2}) = \frac{\sigma_3\sigma_2\beta_{32} I_2}{\sigma_3 N_3 + \sigma_2 N_2} + \frac{\sigma_3\sigma_2\tilde{\beta}_{32} A_2}{\sigma_3 N_3 + \sigma_2 N_2},
\end{aligned}$$

The model system (3.1-3.3) is biologically relevant (solutions are positive) in the set

$$\Omega = \Big\{(P_1, U_1, S_1, E_1, I_1, S_2, A_2, I_2, R_2, P_3, S_3, E_3, I_3) \in \mathbb{R}_+^{13} : P_1, U_1, S_1, E_1, I_1, S_2, A_2, I_2,$$
$$R_2, P_3, S_3, E_3, I_3 \geq 0, N_1 \leq \frac{b_1 K_1}{d_1}, N_2 \leq \frac{b_2 K_2}{d_2}, N_3 \leq \frac{b_3 K_3}{d_3}, P_1 + U_1 \leq \frac{b_1 N_1}{\theta_1}, P_3 \leq \frac{b_3 N_3}{\theta_3}\Big\}. \tag{3.5}$$

Lemma 3.1. *The model system (3.1-3.3) is well-posed in Ω which is invariant and attracting.*

Proof. When $S_i = 0$ for $i = 1, 2, 3$ then
$\frac{dS_1}{dt} = \theta_1 P_1$, $\frac{dS_2}{dt} = b_2 N_2$, $\frac{dS_3}{dt} = \theta_3 P_3$ that is $\frac{dS_i}{dt} \geq 0$ for $i = 1, 2, 3$ for $t \geq 0$.
Similarly, when $E_i = 0$, $I_i = 0$, $P_1 = U_1 = P_3 = A_2 = R_2 = 0$ for $i = 1, 2, 3$ we

have $\frac{dE_i}{dt} \geq 0$, $\frac{dI_i}{dt} \geq 0$, $\frac{dP_1}{dt} \geq 0$, $\frac{dU_1}{dt} \geq 0$, $\frac{dP_3}{dt} \geq 0$, $\frac{dA_2}{dt} \geq 0$, $\frac{dI_2}{dt} \geq 0$. If $S_i + E_i + I_i \geq 0$ for $i = 1, 2, 3$ and $S_2 + A_2 + I_2 + R_2 \geq 0$ we have $\frac{dN_i}{dt} = b_i N_i - d_i \frac{N_i^2}{K_i} \Leftrightarrow N_i(t) = \frac{b_i K_i}{d_i + N_i(0)e^{-b_i t}}$ for $i = 1, 3$ and
we show that for $t \to \infty$ $N_i \leq \frac{b_i K_i}{d_i}$ for $i = 1, 3$.
Similarly, if $P_1 + U_1 \geq 0$ we can show that $\dot{P}_1 + \dot{U}_1 \leq \frac{b_1 N_1}{\theta_1}$ and $\dot{P}_3 \leq \frac{b_3 N_3}{\theta_3}$ for $t \geq 0$.
Thus, the solution remain in the feasible region Ω if it starts in this region. □

3.3 Results

3.3.1 Basic Reproduction Number

For epidemiology models, a quantity, R_0 is derived to assess the stability of the disease free equilibrium [69]. R_0 represents the the number of individuals infected by a single infected individual during his or her entire infectious period, in a population which is entirely susceptible [82]. When $R_0 < 1$, if a disease is introduced, there are insufficient new cases per case, and the disease cannot invade the population. When $R_0 > 1$, the disease may become endemic; the greater R_0 is above 1, the less likely stochastic fade out of the disease can occur. To compute this threshold we use the next generation operator approach, as described by Diekmann et al. [100] and van den Driessche and Watmough [101] as well as to describe the conditions for which the disease-free equilibrium points lose stability.
Since the model incorporates both vertical and horizontal transmission, R_0 for the system is the sum of the R_0 values for each mode of transmission determined separately [102],

$$R_0 = R_{0,V} + R_{0,H}.$$

To compute each component of R_0, the model equations in vector form are the difference between the rate of new infection in compartment i, F_i and the rate of transfer between compartment i and all other compartments due to other processes, V_i [101], (see Appendix B). Then, R_0 is given by

$$R_0 = \frac{b_1 q_1}{2\mu_1} + \frac{1}{2}\sqrt{R_{0,V}^2 + 4R_{0,H}^2} \tag{3.6}$$

where $R_{0,V} = \frac{b_1 q_1}{\mu_1}$ and

$$R_{0,H} = \sqrt{\frac{(l_3^0)^2 \beta_{23}\gamma_3 N_2^0 N_3^0}{\mu_3(\gamma_3+\mu_3)}\left[\frac{(1-\theta_2)\tilde{\beta}_{32}}{\tilde{\varepsilon}_2+\mu_2} + \frac{\theta_2\beta_{32}}{\varepsilon_2+m_2+\mu_2}\right] + \frac{(l_1^0)^2\beta_{21}\gamma_1 N_1^0 N_2^0}{\mu_1(\gamma_1+\mu_1)}\left[\frac{(1-\theta_2)\tilde{\beta}_{12}}{\tilde{\varepsilon}_2+\mu_2} + \frac{\theta_2\beta_{12}}{\varepsilon_2+m_2+\mu_2}\right]}. \tag{3.7}$$

3.3.2 Basic Reproduction Number for periodic environment

In periodic environment, the basic reproduction number is the generalization of the R_0 in non periodic environment. It is known as the transmissibility number $\bar{R}_0$, which is defined as the average number of secondary cases arising from the introduction of a single infectious individual into a completely susceptible population at a random time of the year [103]. Thus, $\bar{R}_0$ is defined through the spectral radius of a linear integral operator on a space of periodic functions, given by the integral operator G_j (see Appendix B),

$$G_j = \frac{b_1 q_1}{\mu_1 + 2\pi j i} \bullet \frac{\theta_1}{\theta_1 + 2\pi j i} + \frac{\gamma_1}{\gamma_1 + \mu_1 + 2\pi j i} \bullet \frac{(l_1^0)^2 \beta_{21} S_2^0 S_1^0}{\mu_1 + 2\pi j i} \left[\frac{(1-\theta_2)\tilde{\beta}_{12}}{\tilde{\varepsilon}_2 + \mu_2 + 2\pi j i} + \frac{\theta_2 \beta_{12}}{\varepsilon_2 + m_2 + \mu_2 + 2\pi j i} \right] + \frac{\gamma_3}{\gamma_3 + \mu_3 + 2\pi j i} \bullet \frac{(l_3^0)^2 \beta_{23} S_3^0 S_2^0}{\mu_3 + 2\pi j i} \left[\frac{(1-\theta_2)\tilde{\beta}_{32}}{\tilde{\varepsilon}_2 + \mu_2 + 2\pi j i} + \frac{\theta_2 \beta_{32}}{\varepsilon_2 + m_2 + \mu_2 + 2\pi j i} \right] \tag{3.8}$$

where $i^2 = -1$. As proposed by Bacaer [104], the transmissibility number $\bar{R}_0$ is given by

$$\bar{R}_0 = G_0 + \frac{\delta^2}{2} Re\left(\frac{G_0 G_1}{G_0 - G_1}\right) \tag{3.9}$$

where Re(.) is the real part of (.). G_0 is the basic reproduction number for the non-seasonal model, obtained when $\delta = 0$.

The size of $\bar{R}_0$ is reduced compared to R_0 when oviposition rates are constant, and this makes it slightly difficult for the virus to invade the population with such fluctuations on the transmission rates [104].

From G_0 the following sub-reproduction numbers R_{21}, R_{12}, R_{23}, R_{32} can be obtained:
R_{21} is the number of new infections in livestock from one infected *Aedes* mosquito and is given by

$$R_{21} = \frac{\gamma_1}{\gamma_1 + b_1} \times \frac{\beta_{21} l_1^0 N_2^0}{b_1},$$

representing the product of the probability that the *Aedes* mosquito survives the exposed stage $\frac{\gamma_1}{\gamma_1 + b_1}$, the number of bites on livestock per mosquito $l_1^0 N_2^0$, the probability of transmission per bite β_{21}, and the infectious lifespan of *Aedes* mosquito $1/b_1$.

R_{12} is the number of new infections in *Aedes* mosquitoes from one infected (asymptomatic or symptomatic) animal, and is given by the weighted sum of new infections

resulting from asymptomatic and symptomatic livestock

$$R_{12} = l_1^0 N_1^0 \left(\frac{(1-\theta_2)\tilde{\beta}_{12}}{\tilde{\varepsilon}_2 + b_2} + \frac{\theta_2 \beta_{12}}{\varepsilon_2 + b_2 + m_2} \right).$$

This is the product of the number of bites an animal receives $l_1^0 N_1^0$, the probability of transmission per bite ($\tilde{\beta}_{12}$ for an asymptomatic animal and β_{12} for symptomatic animal), and the duration of the infective period ($\frac{1}{\tilde{\varepsilon}_2+b_2}$ for an asymptomatic animal and $\frac{1}{\varepsilon_2+b_2+m_2}$ for symptomatic animal) weighted by the probability that an animal either becomes asymptomatic or symptomatic upon infection.

R_{23} is the number of new infections in livestock from one infected *Culex* mosquito and is given by

$$R_{23} = \frac{\gamma_3}{\gamma_3 + b_3} \times \frac{\beta_{23} l_3^0 N_2^0}{b_3}.$$

This is the product of the probability that the *Culex* mosquito survives the exposed stage $\frac{\gamma_3}{\gamma_3+b_3}$, the number of bites on livestock per mosquito $l_3^0 N_2^0$, the probability of transmission per bite β_{23}, and the infectious lifespan of *Culex* mosquito $1/b_3$.

R_{32} is the number of new infections in *Culex* mosquitoes from an infected (asymptomatic or symptomatic) animal and is given by the weighted sum of new infections resulting from asymptomatic and symptomatic livestock

$$R_{32} = l_3^0 N_3^0 \left(\frac{(1-\theta_2)\tilde{\beta}_{32}}{\tilde{\varepsilon}_2 + b_2} + \frac{\theta_2 \beta_{32}}{\varepsilon_2 + b_2 + m_2} \right).$$

This is the product of the number of bites one animal receives $l_3^0 N_3^0$, the probability of transmission per bite ($\tilde{\beta}_{32}$ for an asymptomatic animal and β_{32} for symptomatic animal), and the duration of the infective period ($\frac{1}{\tilde{\varepsilon}_2+b_2}$ for an asymptomatic animal and $\frac{1}{\varepsilon_2+b_2+m_2}$ for symptomatic animal) weighted by the probability that an animal either becomes asymptomatic or symptomatic upon infection.
If $q_1 > 0$, R_0 increases because vertical transmission directly increases the number of infectious mosquitoes and indirectly increases the transmission from livestock to mosquitoes and back to livestock.

3.3.3 Stability analysis

The computation of the equilibria for model system (3.1-3.3) yields, respectively: the disease-free equilibrium (DFE),

$$\begin{aligned} X^0 &= (P_1^0, U_1^0, S_1^0, E_1^0, I_1^0, S_2^0, A_2^0, I_2^0, R_2^0, P_3^0, S_3^0, E_3^0, I_3^0) \\ &= (\tfrac{b_1 N_1}{\theta_1}, 0, \tfrac{b_1 K_1}{d_1}, 0, 0, \tfrac{b_2 K_2}{d_2}, 0, 0, 0, \tfrac{b_3 N_3}{\theta_3}, \tfrac{b_3 K_3}{d_3}, 0, 0) \end{aligned} \tag{3.10}$$

and the endemic equilibrium (EE)

$$X^* = (P_1^*, U_1^*, S_1^*, E_1^*, I_1^*, S_2^*, A_2^*, I_2^*, R_2^*, P_3^*, S_3^*, E_3^*, I_3^*)$$

where

$$P_1^* = \frac{b_1N_1 - b_1q_1I_1^*}{\theta_1} \qquad U_1^* = \frac{b_1q_1I_1^*}{\theta_1} \tag{3.11}$$

$$S_1^* = \frac{b_1N_1 - b_1q_1I_1^*}{g_1I_2^* + g_2A_2^* + \mu_1} \qquad E_1^* = \frac{\mu_1 - b_1q_1}{\gamma_1}I_1^* \tag{3.12}$$

$$I_1^* = \frac{g_1I_2^* + g_2A_2^*}{g_1I_2^* + g_2A_2^* + \mu_1} \times \frac{b_1N_1 - b_1q_1I_1^*}{(\gamma_1 + \mu_1)g_7} \tag{3.13}$$

$$S_2^* = \frac{b_2N_2}{g_3I_1^* + g_4I_3^* + \mu_2} \tag{3.14}$$

$$A_2^* = \frac{g_3I_1^* + g_4I_3^*}{g_3I_1^* + g_4I_3^* + \mu_2} \times \frac{1}{g_8} \qquad I_2^* = \frac{g_3I_1^* + g_4I_3^*}{g_3I_1^* + g_4I_3^* + \mu_2} \times \frac{1}{g_9} \tag{3.15}$$

$$R_2^* = \frac{\tilde{\varepsilon}_2A_2^* + \varepsilon_2I_2^*}{\mu_2} \qquad P_3^* = \frac{b_3N_3}{\theta_3} \tag{3.16}$$

$$S_3^* = \frac{b_3N_3}{g_5I_2^* + g_6A_2^* + \mu_3} \qquad E_3^* = \frac{\mu_3}{\gamma_3}I_3^* \tag{3.17}$$

$$I_3^* = \frac{g_5I_2^* + g_6A_2^*}{g_5I_2^* + g_6A_2^* + \mu_3} \times \frac{1}{l_4}, \tag{3.18}$$

$g_1 = \frac{\sigma_1\sigma_2\beta_{12}}{\sigma_1N_1+\sigma_2N_2}$, $g_2 = \frac{\sigma_1\sigma_2\tilde{\beta}_{12}}{\sigma_1N_1+\sigma_2N_2}$, $g_3 = \frac{\sigma_1\sigma_2\beta_{21}}{\sigma_1N_1+\sigma_2N_2}$, $g_4 = \frac{\sigma_3\sigma_2\beta_{23}}{\sigma_3N_3+\sigma_2N_2}$,
$g_5 = \frac{\sigma_3\sigma_2\beta_{32}}{\sigma_3N_3+\sigma_2N_2}$, $g_6 = \frac{\sigma_3\sigma_2\tilde{\beta}_{32}}{\sigma_3N_3+\sigma_2N_2}$, $g_7 = \frac{\mu_1-b_1q_1}{\gamma_1}$, $g_8 = \frac{\tilde{\varepsilon}_2+\mu_2}{(1-\theta_2)b_2N_2}$, $g_9 = \frac{\varepsilon_2+m_2+\mu_2}{\theta_2b_2N_2}$
, $l_4 = \frac{\mu_3(\gamma_3+\mu_3)}{\gamma_3b_3N_3}$, $l_5 = (\gamma_1 + \mu_1)g_7$.
Substituting equations (3.15) into equation (3.13) we obtain

$$b_1N_1g_3l_6I_1^* + b_1N_1g_4l_6I_3^* - \mu_1\mu_2l_5I_1^* = g_3l_7(I_1^*)^2 + g_4l_7I_1^*I_3^* \tag{3.19}$$

where $l_6 = \frac{g_1g_8+g_2g_9}{g_8g_9}$, $l_7 = b_1q_1l_6 + l_5l_6 + \mu_1l_5$.
In solving for the equilibria, we omit the expression containing R_2 because it can be determined when S_2, A_2 and I_2 are known. We then determine analytically the conditions under which these equilibria are stable or unstable. The following result holds without proof to avoid repetition:

Lemma 3.2. *The resulting model is biologically relevant (solutions are positive) in the set*

$$\Omega^1 = \Bigg\{(P_1, U_1, S_1, E_1, I_1, S_2, A_2, I_2, P_3, S_3, E_3, I_3) \in \mathbb{R}_+^{112} : P_1, U_1, S_1, E_1, I_1, S_2, A_2,$$
$$I_2, P_3, S_3, E_3, I_3 \geq 0, N_1 \leq \frac{b_1K_1}{d_1}, N_2 \leq \frac{b_2K_2}{d_2}, N_3 \leq \frac{b_3K_3}{d_3}, P_1+U_1 \leq \frac{b_1N_1}{\theta_1}, P_3 \leq \frac{b_3N_3}{\theta_3}\Bigg\} \tag{3.20}$$

The model system (3.1-3.3) being nonlinear, stability analysis will be carried out via linearisation. The Jacobian matrix of system (3.1-3.3) at an arbitrary equilibrium is

$$J = \begin{pmatrix} -\theta_1 & 0 & 0 & 0 & -b_1q_1 & 0 & 0 & 0 & 0 & 0 & 0 & 0 \\ 0 & -\theta_1 & 0 & 0 & b_1q_1 & 0 & 0 & 0 & 0 & 0 & 0 & \\ \theta_1 & 0 & -a_1-\mu_1 & 0 & 0 & 0 & -a_2 & -a_3 & 0 & 0 & 0 & 0 \\ 0 & 0 & a_1 & -a_{14} & 0 & 0 & a_2 & a_3 & 0 & 0 & 0 & 0 \\ 0 & \theta_1 & 0 & \gamma_1 & -\mu_1 & 0 & 0 & 0 & 0 & 0 & 0 & 0 \\ 0 & 0 & 0 & 0 & -a_4 & -a_5-\mu_2 & 0 & 0 & 0 & 0 & 0 & -a_9 \\ 0 & 0 & 0 & 0 & (1-\theta_2)a_4 & (1-\theta_2)a_5 & -a_6 & 0 & 0 & 0 & 0 & (1-\theta_2)a_9 \\ 0 & 0 & 0 & 0 & \theta_2a_4 & \theta_2a_5 & 0 & -a_7 & 0 & 0 & 0 & \theta_2a_9 \\ 0 & 0 & 0 & 0 & 0 & 0 & 0 & 0 & -\theta_3 & 0 & 0 & 0 \\ 0 & 0 & 0 & 0 & 0 & 0 & -a_{10} & -a_{11} & \theta_3 & -a_{12}-\mu_3 & 0 & 0 \\ 0 & 0 & 0 & 0 & 0 & 0 & a_{10} & a_{11} & 0 & a_{12} & -a_{13} & 0 \\ 0 & 0 & 0 & 0 & 0 & 0 & 0 & 0 & 0 & 0 & \gamma_3 & -\mu_3 \end{pmatrix} \tag{3.21}$$

where $a_1 = g_1I_2 + g_2A_2,\ a_2 = g_2S_1,\ a_3 = g_1S_1,\ a_4 = g_3S_2,\ a_5 = g_3I_1 + g_4I_3,\ a_6 = \tilde{\varepsilon}_2 + \mu_2,\ a_7 = \varepsilon_2 + m_2 + \mu_2,\ a_9 = g_4S_2,\ a_{10} = g_6S_3,\ a_{11} = g_5S_3,\ a_{12} = g_5I_2 + g_6A_2,\ a_{13} = \gamma_3 - \mu_3,\ a_{14} = \gamma_1 + \mu_1$.

Evaluating J at the disease-free equilibrium and using basic properties of matrix algebra, it is evident from the characteristic polynomial of J that the following eigenvalues $\lambda_1 = -\mu_1,\ \lambda_2 = -\theta_1,\ \lambda_3 = -\mu_2,\ \lambda_4 = -\theta_3,\ \lambda_5 = -\mu_3$ have negative real part and the remaining reduced matrix is

$$J_1 = \begin{pmatrix} -\theta_1 & 0 & b_1q_1 & 0 & 0 & 0 & 0 \\ 0 & -(\gamma_1+\mu_1) & 0 & g_2S_1^0 & g_1S_1^0 & 0 & 0 \\ \theta_1 & \gamma_1 & -\mu_1 & 0 & 0 & 0 & 0 \\ 0 & 0 & (1-\theta_2)g_3S_2^0 & -(\tilde{\varepsilon}_2+\mu_2) & 0 & 0 & (1-\theta_2)g_4S_2^0 \\ 0 & 0 & \theta_2g_3S_2^0 & 0 & -(\tilde{\varepsilon}_2+m_2+\mu_2) & 0 & \theta_2g_4S_2^0 \\ 0 & 0 & 0 & g_6S_3^0 & g_5S_3^0 & -(\gamma_3+\mu_3) & 0 \\ 0 & 0 & 0 & 0 & 0 & \gamma_3 & -\mu_3 \end{pmatrix} \tag{3.22}$$

The stability of a disease-free equilibria should be established from the eigenvalues of the reduced Jacobian matrix (3.22). To simplify the computations, we perform the following operations on matrix (3.22): first we add the first row to the third one and take the resultant as the new third row; second we multiply the second row by $\gamma_1/(\gamma_1 + \mu_1)$ and add it to the new third row, then take the resultant as the new third row and at last we multiply the sixth row by $\gamma_3/(\gamma_3 + \mu_3)$ and add it to the last row and maintaining the rest as it is, we obtain the following matrix

$$J_2 = \begin{pmatrix} -\theta_1 & 0 & b_1q_1 & 0 & 0 & 0 & 0 \\ 0 & -(\gamma_1+\mu_1) & 0 & g_2S_1^0 & g_1S_1^0 & 0 & 0 \\ 0 & 0 & b_1q_1-\mu_1 & \frac{\gamma_1g_2S_1^0}{\gamma_1+\mu_1} & \frac{\gamma_1g_1S_1^0}{\gamma_1+\mu_1} & 0 & 0 \\ 0 & 0 & (1-\theta_2)g_3S_2^0 & -(\tilde{\varepsilon}_2+\mu_2) & 0 & 0 & (1-\theta_2)g_4S_2^0 \\ 0 & 0 & \theta_2g_3S_2^0 & 0 & -(\tilde{\varepsilon}_2+m_2+\mu_2) & 0 & \theta_2g_4S_2^0 \\ 0 & 0 & 0 & g_6S_3^0 & g_5S_3^0 & -(\gamma_3+\mu_3) & 0 \\ 0 & 0 & 0 & \frac{\gamma_3g_6S_3^0}{\gamma_3+\mu_3} & \frac{\gamma_3g_5S_3^0}{\gamma_3+\mu_3} & 0 & -\mu_3 \end{pmatrix} \tag{3.23}$$

From the basic properties of matrix algebra, it is evident from the characteristic polynomial of J_2 that the following eigenvalues $\lambda_1 = -\theta_1,\ \lambda_2 = -(\gamma_1+\mu_1)$ and $\lambda_3 = -(\gamma_3 + \mu_3)$ have negative real part and the remaining reduced matrix is

$$\tilde{J}(X^0) = \begin{pmatrix} b_1q_1 - \mu_1 & \frac{\gamma_1g_2S_1^0}{\gamma_1+\mu_1} & \frac{\gamma_1g_1S_1^0}{\gamma_1+\mu_1} & 0 \\ (1-\theta_2)g_3S_2^0 & -(\tilde{\varepsilon}_2+\mu_2) & 0 & (1-\theta_2)g_4S_2^0 \\ \theta_2g_3S_2^0 & 0 & -(\varepsilon_2+m_2+\mu_2) & \theta_2g_4S_2^0 \\ 0 & \frac{\gamma_3g_6S_3^0}{\gamma_3+\mu_3} & \frac{\gamma_3g_5S_3^0}{\gamma_3+\mu_3} & -\mu_3 \end{pmatrix} \tag{3.24}$$

3.3.4 Stability analysis of the model (3.1-3.3) without *Culex* species

In the absence of *Culex* species, $I_3^* = 0$, equation (3.19) can be written as

$$g_3 l_7 (I_1^*)^2 - (b_1 N_1 g_3 l_6 - \mu_1 \mu_2 l_5) I_1^* = 0. \tag{3.25}$$

Equation (3.25) has two possible solutions $I_1^* = 0$ or $I_1^* \neq 0$. The case $I_1^* = 0$ implies an existence of a disease-free equilibria and the case $I_1^* \neq 0$ implies an existence of an endemic equilibria. Let us now derive conditions under which positive endemic equilibria exist. For $I_1^* \neq 0$, we get

$$I_1^* = \frac{b_1 N_1 \gamma_1 g_3 (g_1 \frac{\tilde{\varepsilon}_2+\mu_2}{(1-\theta_2) b_2 N_2} + g_2 \frac{\varepsilon_2+m_2+\mu_2}{\theta_2 b_2 N_2}) - \mu_1 \mu_2 (\gamma_1+\mu_1)(\mu_1 - b_1 q_1) \frac{(\tilde{\varepsilon}_2+\mu_2)(\varepsilon_2+m_2+\mu_2)}{(1-\theta_2)\theta_2 b_2 b_2 N_2 N_2}}{g_3 [b_1 q_1 \gamma_1 (g_1 g_8 + g_2 g_9) + (\gamma_1+\mu_1)(\mu_1 - b_1 q_1)(g_1 g_8 + g_2 g_9) + \mu_1 (\gamma_1+\mu_1)(\mu_1 - b_1 q_1) g_8 g_9]}, \tag{3.26}$$

I_1^* is epidemiologically meaningful, that is, $I_1^* > 0$ if and only if
$b_1 N_1 \gamma_1 g_3 [\theta_2 b_2 N_2 g_1 (\tilde{\varepsilon}_2 + \mu_2) + (1-\theta_2) b_2 N_2 g_2 (\varepsilon_2 + m_2 + \mu_2) > \mu_1 \mu_2 (\gamma_1+\mu_1)(\mu_1 - b_1 q_1)(\tilde{\varepsilon}_2 + \mu_2)(\varepsilon_2 + m_2 + \mu_2)$

which can be written in the form

$$\frac{b_1 b_2}{\mu_1 \mu_2 (1 - \frac{b_1 q_1}{\mu_1})} \times \frac{g_3 \gamma_1 N_2}{\mu_1 (\gamma_1 + \mu_1)} \times \left[\frac{(1-\theta_2) g_2 N_1}{\tilde{\varepsilon}_2 + \mu_2} + \frac{\theta_2 g_1 N_1}{\varepsilon_2 + m_2 + \mu_2} \right] > 1$$

where $R_0^1 = \frac{g_3 \gamma_3 N_2}{\mu_1 (\gamma_1+\mu_1)} \times \left[\frac{(1-\theta_2) g_2 N_1}{\tilde{\varepsilon}_2+\mu_2} + \frac{\theta_2 g_1 N_1}{\varepsilon_2+m_2+\mu_2} \right]$ is the basic reproductive number for the model without *Culex* species and $R_{21} = \dfrac{g_3 \gamma_3 N_2}{\mu_1 (\gamma_1 + \mu_1)}$ represents the number of new infections in livestock from one infected *Aedes* mosquito and $R_{12} = \frac{(1-\theta_2) g_2 N_1}{\tilde{\varepsilon}_2+\mu_2} + \frac{\theta_2 g_1 N_1}{\varepsilon_2+m_2+\mu_2}$ represent the number of new infections in *Aedes* mosquitoes from one infected (asymptomatic or symptomatic) animal and $R_{0,V} = \frac{b_1 q_1}{\mu_1}$ represents the vertical transmission reproductive number. Therefore, $I_1^* > 0$ if and only if $R_{0,V} < 1$ and $R_0^1 > 1$. Thus, the following result holds:

Theorem 3.3. *The RVF model (3.1-3.3) without Culex species has exactly one disease-free equilibrium point (DFE),* $X_1^0 = (P_1^0, U_1^0, S_1^0, E_1^0, I_1^0, S_2^0, A_2^0, I_2^0, R_2^0) = (\frac{b_1 N_1}{\theta_1}, 0, \frac{b_1 K_1}{d_1}, 0, 0, \frac{b_2 K_2}{d_2}, 0, 0, 0)$ *for* $R_0^1 \leq 1$ *and exactly one endemic equilibrium point (EE),* $X_1^* = (P_1^*, U_1^*, S_1^*, E_1^*, I_1^*, S_2^*, A_2^*, I_2^*, R_2^*)$ *whenever* $R_0^1 > 1$.

The result in Theorem 3.3 indicates the impossibility of backward bifurcation in the RVF model system (3.1-3.3) without *Culex* species since it has no endemic equilibrium when $R_0^1 < 1$. This explains that the model (3.1-3.3) without *Culex* species has a globally asymptotically stable disease-free equilibrium whenever $R_0^1 \leq 1$.
In its simplest form, backward bifurcation in epidemic models usually implies the existence of two subcritical endemic equilibria when the basic reproductive number for $R_0^1 < 1$, and a unique supercritical endemic equilibrium for $R_0^1 > 1$ [105]. Thus, a unique positive endemic equilibrium exists only when $R_0^1 > 1$. We note that the

increase in complexity of an epidemic model (by adding more infected classes, for example) can lead to backward bifurcation and even more complicated phenomena associated with endemic equilibria [105]. However, an increase in complexity of the proposed RVF model does not appear to give rise to more complex behaviour with regard to endemic equilibria.

3.3.4.1 Local stability of DFE, X_1^0

In the absence of secondary vector (*Culex* species) that serve as RVF outbreak amplifiers the Jacobian matrix $\tilde{J}(X^0)$ in (3.24) reduces to

$$J(X_1^0) = \begin{pmatrix} b_1q_1 - \mu_1 & \frac{\gamma_1 g_2 S_1^0}{\gamma_1+\mu_1} & \frac{\gamma_1 g_1 S_1^0}{\gamma_1+\mu_1} \\ (1-\theta_2)g_3 S_2^0 & -(\tilde{\varepsilon}_2+\mu_2) & 0 \\ \theta_2 g_3 S_2^0 & 0 & -(\varepsilon_2+m_2+\mu_2) \end{pmatrix} \tag{3.27}$$

The characteristic equation corresponding to the above Jacobian matrix is

$$\lambda^3 + A\lambda^2 + B\lambda + C = 0 \tag{3.28}$$

where $A = \varepsilon_2 + m_2 + \mu_2 + \tilde{\varepsilon}_2 + \mu_2 + \mu_1(1 - \frac{b_1q_1}{\mu_1})$, $B = -\theta_2 g_3 S_2^0 \frac{\gamma_1 g_1 S_1^0}{\gamma_1+\mu_1} - (1-\theta_2)g_3 S_2^0 \frac{\gamma_1 g_2 S_1^0}{\gamma_1+\mu_1} + (\varepsilon_2+m_2+\mu_2)(\tilde{\varepsilon}_2+\mu_2) + (\varepsilon_2+m_2+\mu_2)(\mu_1 - b_1q_1) + (\tilde{\varepsilon}_2+\mu_2)(\mu_1 + b_1q_1)$, $C = -\theta_2 g_3 S_2^0 \frac{\gamma_1 g_1 S_1^0}{\gamma_1+\mu_1}(\tilde{\varepsilon}_2+\mu_2) - (1-\theta_2)g_3 S_2^0 \frac{\gamma_1 g_2 S_1^0}{\gamma_1+\mu_1}(\varepsilon_2+m_2+\mu_2) + (\tilde{\varepsilon}_2+\mu_2)(\varepsilon_2+m_2+\mu_2)(\mu_1 - b_1q_1)$.

Here $A > 0$ for $\frac{b_1q_1}{\mu_1} < 1$, $B > 0 \wedge C > 0$ for $\frac{b_1q_1}{\mu_1} < 1 \wedge R_0^1 < 1$. Thus the equation (3.28) has no root which is positive or zero (Descartes'rule of sign). The equation (3.28) will only have negative roots or complex roots with negative real part if $AB - C > 0$ (according to Routh-Hurwitz criteria), that is, $\frac{b_1q_1}{\mu_1} < 1 \wedge R_0^1 < 1$. Thus, the system (3.1-3.3) without *Culex* species is stable about the interior equilibrium X_1^0 and the following result holds:

Theorem 3.4. *For $R_0^1 < 1$ the model system (3.1-3.3) without Culex mosquitoes has a unique DFE point which is locally asymptotically stable in Ω^1.*

3.3.4.2 Global asymptotic stability of DFE, X_1^0

To ensure that the disease elimination is independent of the initial sizes of the populations, we need to show that the disease-free equilibrium X_1^* is globally asymptotically stable (GAS). This is established using the approach proposed in Castillo-Chavez et al.[106]. There are two conditions that if met guarantee the global asymptotic stability of the disease-free state. First, system (3.1-3.3) without *Culex* mosquitoes must be written in the form:

$$\begin{aligned} \tfrac{dX}{dt} &= F(x, Z), \\ \tfrac{dZ}{dt} &= G(X, Z),\ G(x, 0) = 0 \end{aligned} \tag{3.29}$$

where $X \in R^m$ denotes (its components) the number of uninfected individuals and $Z \in R^n$ denotes (its components) the number of infected individuals including latent and infectious. $U^0 = (x^0, 0)$ denotes the disease-free equilibrium of this system.
(H1) For $\frac{dX}{dt} = F(X,0)$, X^0 is globally asymptotic stable
(H2) $G(X,Z) = AZ - \widehat{G}(X,Z)$, $\widehat{G}(X,Z) \geq 0$ for $(X,Z) \in \Omega^1$
where $A = D_Z G(X^0, 0)$ (see [100] for more details) is an M-matrix (the off diagonal elements of A are nonnegative) and Ω^1 is the region where the model makes biological sense.
If the system (3.29) satisfies the above two conditions then the following Theorem holds.

Theorem 3.5. *The fixed point $U^0 = (x^0, 0)$ is globally asymptotic stable equilibrium of system (3.29) provided that $R_0^1 < 1$ (locally asymptotic stable) and that assumptions (H1) and (H2) are satisfied.*

Proof. Rewriting the model system (3.1-3.3) without *Culex* mosquitoes in the form of equation (3.29) then $X = (P_1, S_1, S_2, R_2)$, $Z = (U_1, E_1, I_1, A_2, I_2)^T$ and $F(X,0) = (b_1N_1 - \theta_1 P_1, \theta_1 P_1 - \mu_1 S_1, b_2 N_2 - \mu_2 S_2, 0)$, then

$$A = D_Z G(X^0, 0) = \begin{pmatrix} -\theta_1 & 0 & b_1 q_1 & 0 & 0 \\ 0 & -(\gamma_1+\mu_1) & 0 & \frac{\sigma_1\sigma_2\tilde{\beta}_{12}}{\sigma_1 N_1+\sigma_2 N_2} S_1^0 & \frac{\sigma_1\sigma_2\beta_{12}}{\sigma_1 N_1+\sigma_2 N_2} S_1^0 \\ \theta_1 & \gamma_1 & -\mu_1 & 0 & 0 \\ 0 & 0 & (1-\theta_2)\frac{\sigma_1\sigma_2\beta_{21}}{\sigma_1 N_1+\sigma_2 N_2} S_2^0 & -(\tilde{\varepsilon}_2+\mu_2) & 0 \\ 0 & 0 & \theta_2 \frac{\sigma_1\sigma_2\beta_{21}}{\sigma_1 N_1+\sigma_2 N_2} S_2^0 & 0 & -(\varepsilon_2+m_2+\mu_2) \end{pmatrix} \tag{3.30}$$

and $\widehat{G}(X,Z) = AZ - G(X,Z) =$

$$= \begin{pmatrix} -\theta_1 & 0 & b_1 q_1 & 0 & 0 \\ 0 & -(\gamma_1+\mu_1) & 0 & \frac{\sigma_1\sigma_2\tilde{\beta}_{12}}{\sigma_1 N_1+\sigma_2 N_2} S_1^0 & \frac{\sigma_1\sigma_2\beta_{12}}{\sigma_1 N_1+\sigma_2 N_2} S_1^0 \\ \theta_1 & \gamma_1 & -\mu_1 & 0 & 0 \\ 0 & 0 & (1-\theta_2)\frac{\sigma_1\sigma_2\beta_{21}}{\sigma_1 N_1+\sigma_2 N_2} S_2^0 & -(\tilde{\varepsilon}_2+\mu_2) & 0 \\ 0 & 0 & \theta_2 \frac{\sigma_1\sigma_2\beta_{21}}{\sigma_1 N_1+\sigma_2 N_2} S_2^0 & 0 & -(\varepsilon_2+m_2+\mu_2) \end{pmatrix} \begin{pmatrix} U_1 \\ E_1 \\ I_1 \\ A_2 \\ I_2 \end{pmatrix} -$$

$$- \begin{pmatrix} b_1 q_1 I_1 - \theta_1 U_1 \\ \frac{\sigma_1\sigma_2\beta_{12}}{\sigma_1 N_1+\sigma_2 N_2} S_1 I_2 + \frac{\sigma_1\sigma_2\tilde{\beta}_{12}}{\sigma_1 N_1+\sigma_2 N_2} S_1 A_2 - (\gamma_1+\mu_1) E_1 \\ \gamma_1 E_1 + \theta_1 U_1 - \mu_1 I_1 \\ (1-\theta_2)\frac{\sigma_1\sigma_2\beta_{21}}{\sigma_1 N_1+\sigma_2 N_2} S_2 I_1 - (\tilde{\varepsilon}_2+\mu_2) A_2 \\ \theta_2 \frac{\sigma_1\sigma_2\beta_{21}}{\sigma_1 N_1+\sigma_2 N_2} S_2 I_1 - (\varepsilon_2+m_2+\mu_2) I_2 \end{pmatrix} = \begin{pmatrix} 0 \\ \frac{\sigma_1\sigma_2}{\sigma_1 N_1+\sigma_2 N_2}(\beta_{12} I_2 + \tilde{\beta}_{12} A_2)(S_1^0 - S_1) \\ 0 \\ (1-\theta_2)\frac{\sigma_1\sigma_2\beta_{21}}{\sigma_1 N_1+\sigma_2 N_2}(S_2^0 - S_2) \\ \theta_2 \frac{\sigma_1\sigma_2\beta_{21}}{\sigma_1 N_1+\sigma_2 N_2}(S_2^0 - S_2) \end{pmatrix}$$

Since $0 \leq S_1 \leq K_1$ and $0 \leq S_2 \leq K_2$ it is clear that $\widehat{G}(X,Z) \geq 0$. Then $X^0 = (b_1N_1 - \theta_1 P_1, \theta_1 P_1 - \mu_1 S_1, b_2 N_2 - \mu_2 S_2, 0)$ is globally asymptotic stable equilibrium of $\frac{dX}{dt} = F(X,0)$. Hence, by the above Theorem, U^0 which represents the disease-free equilibrium X_1^0 is globally asymptotic stable. □

3.3.4.3 Global asymptotic stability of EE, X_1^*

Since the DFE is locally stable when $R_0^1 < 1$ (this will suggest local stability of the EE for the reverse condition [101]), we only investigate the global stability of the endemic equilibrium.

Theorem 3.6. *For $R_0^1 > 1$, the model system (3.1-3.3) without Culex mosquitoes has unique positive EE point X_1^*, such that*
$\frac{E_1^*}{E_1} \leq \frac{F_1^* S_1^* E_1}{F_1 S_1 E_1^*} \leq 1$ *for* $0 < E_1 < E_1^*$,
$\frac{S_2^*}{S_2} \geq \frac{I_1^* S_2^*}{I_1 S_2} \geq 1$ *for* $0 < S_2 < S_2^* \ \wedge \ 0 < I_1 < I_1^*$ *and*
$\frac{S_1^*}{S_1} \leq \frac{P_1 S_1^* G_1^*}{P_1^* S_1 G_1} \leq 1$ *for* $0 < S_1^* < S_1 \ \wedge \ 0 < P_1 < P_1^*$
Then, X_1^* is globally asymptotic stable in $\mathring{\Omega}^1 \subset \Omega^1$.

Proof. Global stability of the EE is explored via the construction of a suitable Lyapunov function. Let us consider the following function:

$$\begin{aligned} V(P_1, U_1, S_1, E_1, I_1, S_2, A_2, I_2) \quad &= e_1(P_1 - P_1^* \ln P_1) + e_2(U_1 - U_1^* \ln U_1) + e_3(S_1 - S_1^* \ln S_1) \\ &+ e_4(E_1 - E_1^* \ln E_1) + e_5(I_1 - I_1^* \ln I_1) + e_6(S_2 - S_2^* \ln S_2) \\ &+ e_7(A_2 - A_2^* \ln A_2) + e_8(I_2 - I_2^* \ln I_2), \end{aligned} \tag{3.31}$$

where $e_i > 0$ for $i = 1, 2, \cdots, 8$ with $e_7 = \frac{1}{I_1^* S_2^*}$, $e_8 = \frac{1-\theta_2}{\theta_2} \frac{1}{I_1^* S_2^*}$. e_2 and e_5 are chosen very small such $e_2 X_1^* < \delta$, $e_5 X_1^* < \delta$ for $\delta \in (0, 1)$. V (> 0 in $\mathring{\Omega}^1$) is a Lyapunov function (Korobeinikov [107]). The time derivative of V is

$$\begin{aligned} \dot{V} \quad &= e_1(1 - \tfrac{P_1^*}{P_1})\dot{P}_1 + e_2(1 - \tfrac{U_1^*}{U_1})\dot{U}_1 + e_3(1 - \tfrac{S_1^*}{S_1})\dot{S}_1 + e_4(1 - \tfrac{E_1^*}{E_1})\dot{E}_1 + e_5(1 - \tfrac{I_1^*}{I_1})\dot{I}_1 \\ &+ e_6(1 - \tfrac{S_2^*}{S_2})\dot{S}_2 + e_7(1 - \tfrac{A_2^*}{A_2})\dot{A}_2 + e_8(1 - \tfrac{I_2^*}{I_2})\dot{I}_2 \\ &= e_1(1 - \tfrac{P_1^*}{P_1})\left[b_1(N_1 - q_1 I_1) - \theta_1 P_1\right] + e_2(1 - \tfrac{U_1^*}{U_1})\left[b_1 q_1 I_1 - \theta_1 U_1\right] + e_3(1 - \tfrac{S_1^*}{S_1}) \\ &\left[\theta_1 P_1 - g_1 I_2 S_1 - g_2 A_2 S_1 - \mu_1 S_1\right] + e_4(1 - \tfrac{E_1^*}{E_1})\left[g_1 I_2 S_1 + g_2 A_2 S_1 - (\gamma_1 + \mu_1) E_1\right] \\ &+ e_5(1 - \tfrac{I_1^*}{I_1})\left[\gamma_1 E_1 + \theta_1 U_1 - \mu_1 I_1\right] + e_6(1 - \tfrac{S_2^*}{S_2})(b_2 N_2 - g_3 I_1 S_2 - \mu_2 S_2) \\ &+ e_7(1 - \tfrac{A_2^*}{A_2})\left[(1 - \theta_2) g_3 I_1 S_2 - (\tilde{\varepsilon}_2 + \mu_2) A_2\right] + e_8(1 - \tfrac{I_2^*}{I_2})\left[\theta_2 g_3 I_1 S_2 - (\varepsilon_2 + m_2 + \mu_2) I_2\right]. \end{aligned} \tag{3.32}$$

At X_1^*, we have $b_1 N_1 = b_1 q_1 I_1^* + \theta_1 P_1^*$, $b_1 q_1 = \frac{\theta_1 U_1^*}{I_1^*}$, $\theta_1 = \frac{g_1 I_2^* S_1^* + g_2 A_2^* S_1^* + \mu_1 S_1^*}{P_1^*}$, $\gamma_1 + \mu_1 = \frac{g_1 I_2^* S_1^* + g_2 A_2^* S_1^*}{E_1^*}$,
$\mu_1 = \frac{\gamma_1 E_1^* + \theta_1 U_1^*}{I_1^*}$, $b_2 N_2 = g_3 I_1^* S_2^* + \mu_2 S_2^*$, $\tilde{\varepsilon}_2 + \mu_2 = \frac{(1-\theta_2) g_3 I_1^* S_2^*}{A_2^*}$, $\varepsilon_2 + m_2 + \mu_2 = \frac{\theta_2 g_3 I_1^* S_2^*}{I_2^*}$.

Let $F_1 = g_1 I_2 + g_2 A_2$, $F_1^* = g_1 I_2^* + g_2 A_2^*$, $G_1 = g_1 I_2 + g_2 A_2 + \mu_1$, $G_1^* = g_1 I_2^* + g_2 A_2^* + \mu_1$, $H_1 = \gamma_1 E_1 + \theta_1 U_1$,
$H_1^* = \gamma_1 E_1^* + \theta_1 U_1^*$. Then, $\dot{V}$ can now be written as

$$\begin{aligned}\dot{V} &= e_1(1-\tfrac{P_1^*}{P_1})(b_1q_1I_1^*+\theta_1P_1^*-b_1q_1I_1-\theta_1P_1)+e_2(1-\tfrac{U_1^*}{U_1})(\tfrac{\theta_1U_1^*}{I_1^*}-\theta_1U_1)\\ &+e_3(1-\tfrac{S_1^*}{S_1})(\tfrac{P_1G_1^*S_1^*}{P_1^*}-G_1S_1)+e_4(1-\tfrac{E_1^*}{E_1})(F_1S_1-\tfrac{F_1^*S_1^*E_1}{E_1^*})+e_5(1-\tfrac{I_1^*}{I_1})(H_1-\tfrac{H_1^*I_1}{I_1^*})\\ &+e_6(1-\tfrac{S_2^*}{S_2})\left[(g_3I_1^*+\mu_2)S_2^*-(g_3I_1+\mu_2)S_2\right]+e_7(1-\tfrac{A_2^*}{A_2})\left[(1-\theta_2)g_3I_1S_2-\tfrac{(1-\theta_2)g_3I_1^*S_2^*A_2}{A_2^*}\right]\\ &+e_8(1-\tfrac{I_2^*}{I_2})\left[\theta_2g_3I_1S_2-\tfrac{\theta_2g_3I_1^*S_2^*I_2}{I_2^*}\right].\end{aligned} \tag{3.33}$$

Further simplification yields

$$\dot{V} = -e_1(1-\tfrac{P_1^*}{P_1})^2\theta_1P_1-e_6(1-\tfrac{S_2^*}{S_2})^2\mu_2S_2+F(P_1,U_1,S_1,E_1,I_1,S_2,A_2,I_2) \tag{3.34}$$

where

$$\begin{aligned}F &= e_1b_1q_1(1-\tfrac{P_1^*}{P_1})(\tfrac{I_1^*}{I_1}-1)I_1+e_2\theta_2(1-\tfrac{U_1^*}{U_1})(\tfrac{U_1^*I_1}{U_1I_1^*}-1)U_1+e_3(1-\tfrac{S_1^*}{S_1})(\tfrac{P_1S_1^*G_1^*}{P_1^*S_1G_1}-1)S_1G_1\\ &+e_4(1-\tfrac{E_1^*}{E_1})(1-\tfrac{F_1^*S_1^*E_1}{F_1S_1E_1^*})S_1F_1+e_5(1-\tfrac{I_1^*}{I_1})(1-\tfrac{H_1^*I_1}{H_1I_1^*})H_1+e_6g_3(1-\tfrac{S_2^*}{S_2})(\tfrac{I_1^*S_2^*}{I_1S_2}-1)I_1S_2\\ &+e_7(1-\theta_2)g_3(1-\tfrac{A_2^*}{A_2})(1-\tfrac{I_1^*S_2^*A_2}{I_1S_2A_2^*})I_1S_2+e_8\theta_2g_3(1-\tfrac{I_2^*}{I_2})(1-\tfrac{I_1^*S_2^*I_2}{I_1S_2I_2^*})I_1S_2.\end{aligned} \tag{3.35}$$

Recalling that $U_1^*=\frac{b_1q_1}{\theta_1}I_1^*$, $e_7=\frac{1}{I_1^*S_2^*}$ and $e_8=\frac{1-\theta_2}{\theta_2}\frac{1}{I_1^*S_2^*}$ we obtain,

$$e_2\theta_2(1-\frac{U_1^*}{U_1})(\frac{U_1^*I_1}{U_1I_1^*}-1)U_1=e_2\theta_2U_1^*(1-\frac{U_1}{U_1^*}-\frac{U_1^*I_1}{U_1I_1^*})+e_2\theta_2\frac{b_1q_1}{\theta_1}I_1, \tag{3.36}$$

$$e_5(1-\frac{I_1^*}{I_1})(1-\frac{H_1^*I_1}{H_1I_1^*})H_1=e_5H_1(1-\frac{I_1^*}{I_1}-\frac{H_1^*I_1}{H_1I_1^*})+e_5H_1^*, \tag{3.37}$$

and $e_7(1-\theta_2)g_3(1-\frac{A_2^*}{A_2})(1-\frac{I_1^*S_2^*A_2}{I_1S_2A_2^*})I_1S_2+e_8\theta_2g_3(1-\frac{I_2^*}{I_2})(1-\frac{I_1^*S_2^*I_2}{I_1S_2I_2^*})I_1S_2=$
$(1-\theta_2)g_3\frac{I_1S_2}{I_1^*S_2^*}(2-\frac{A_2^*}{A_2}-\frac{I_1^*S_2^*A_2}{I_1S_2A_2^*}-\frac{I_2^*}{I_2}-\frac{I_1^*S_2^*I_2}{I_1S_2I_2^*})+2(1-\theta_2)g_3$.

By theorems hypothesis,

$$\begin{aligned}e_1b_1q_1(1-\frac{P_1^*}{P_1})(\frac{I_1^*}{I_1}-1)I_1\le 0,\\ e_3(1-\frac{S_1^*}{S_1})(\frac{P_1S_1^*G_1^*}{P_1^*S_1G_1}-1)S_1G_1\le 0,\\ e_4(1-\frac{E_1^*}{E_1})(1-\frac{F_1^*S_1^*E_1}{F_1S_1E_1^*})S_1F_1,\\ e_6g_3(1-\frac{S_2^*}{S_2})(\frac{I_1^*S_2^*}{I_1S_2}-1)I_1S_2\le 0,\end{aligned}$$

where strict equalities holds only when,
$P_1=P_1^*,\ I_1=I_1^*,\ S_1=S_1^*,\ E_1=E_1^*$ and $S_2=S_2^*$.

Furthermore,

$$\begin{aligned}\frac{U_1}{U_1^*}+\frac{U_1^*I_1}{U_1I_1^*}&\geq 2,\\ \frac{I_1^*}{I_1}+\frac{H_1^*I_1}{H_1I_1^*}&\geq 2,\\ \frac{A_2^*}{A_2}+\frac{I_1^*S_2^*A_2}{I_1S_2A_2^*}+\frac{I_2^*}{I_2}+\frac{I_1^*S_2^*I_2}{I_1S_2I_2^*}&\geq 4,\end{aligned}$$

for all $I_1,\ S_2,\ A_2,\ I_2 \geq 0$, because the arithmetic mean is greater than or equal to the geometric mean. Thus, $F \leq 0$ for $P_1, U_1, S_1, E_1, I_1, S_2, A_2, I_2 > 0$. Hence, $\dot{V} \leq 0$ for all $P_1, U_1, S_1, E_1, I_1, S_2, A_2, I_2 > 0$ and is equal to zero for $P_1 = P_1^*,\ U_1 = U_1^*,\ S_1 = S_1^*, E_1 = E_1^*, I_1 = I_1^*, S_2 = S_2^*, A_2 = A_2^*, I_2 = I_2^*$ and X_1^* is the only equilibrium state of the system on this plane. Therefore, the largest compact invariant set in $\mathring{\Omega}^1$ such that $\dot{V} \leq 0$ is the singleton X_1^* which is the endemic equilibrium point. LaSalle's invariant principle [108] guarantees that X_1^* is globally asymptotically stable (GAS) in $\mathring{\Omega}^1$, the interior of Ω^1. □

3.3.5 Stability analysis of the overall model (3.1-3.3)

The overall model system (3.1-3.3) describes the epidemiological and ecological complexity involved on RVF dynamics. Theorem 2 in van den Driesche and Watmough [101] states that the local stability of the disease-free equilibrium of the model can be determined by its basic reproduction number, R_0. However, in host-vector models where multiple transmission cycle are observed to occur as in the case of our model (vertical transmission, host to *Aedes* infection, *Aedes* to host infection, host to *Culex* infection and *Culex* to host infection) the basic reproductive number obtained via next-generation method does not give the number of host infected by a single host if there an intermediate vector, but rather the geometric mean of the number of infections per generation [87]. Therefore, in our case the local stability of the disease -free equilibrium, X^0, (3.10) of the model is established through the Routh-Hurtwitz criteria [109, 110], and the following result holds:

Theorem 3.7. *The model system (3.1-3.3) always has the disease-free equilibrium* X^0. *If* $\frac{b_1q_1}{\mu_1} < 1 \wedge R_0^1 < 1 \ \wedge \ R_0^3 < 1 \ \wedge \ R_0 < 1$, *the disease-free equilibrium is locally asymptotically stable in* Ω^1.

Proof. To prove the stability of the equilibrium point X^0 we use the Jacobian matrix (3.24) of the linearised system, which yield the following characteristic polynomial:

$$x^4 + n_1x^3 + n_2x^2 + n_3x + n_4 = 0 \tag{3.38}$$

where $n_1 = \mu_3 + \tilde{\varepsilon}_2 + \mu_2 + \varepsilon_2 + m_2 + \mu_2 + \mu_1 - b_1q_1$,
$n_2 = \mu_3(\tilde{\varepsilon}_2 + \mu_2)(1 - c_1) + \mu_3(\varepsilon_2 + m_2 + \mu_2)(1 - c_2) + (\mu_1 - b_1q_1)(\tilde{\varepsilon}_2 + \mu_2)(1 - c_3) +$
$(\mu_1 - b_1q_1)(\varepsilon_2 + m_2 + \mu_2)(1 - c_4) + \mu_3(\mu_1 - b_1q_1) + (\tilde{\varepsilon}_2 + \mu_2)(\varepsilon_2 + m_2 + \mu_2)$,
$n_3 = (\mu_1 - b_1q_1)(\tilde{\varepsilon}_2 + \mu_2)(\varepsilon_2 + m_2 + \mu_2)(1 - R_0^1) + \mu_3(\tilde{\varepsilon}_2 + \mu_2)(\varepsilon_2 + m_2 + \mu_2)(1 - R_0^3) +$

$\mu_3(\mu_1 - b_1q_1)(\tilde{\varepsilon}_2 + \mu_2)[1 - (c_1 + c_3)] + \mu_3(\mu_1 - b_1q_1)(\varepsilon_2 + m_2 + \mu_2)[1 - (c_2 + c_4)]$, $n_4 = \mu_3(\mu_1 - b_1q_1)(\tilde{\varepsilon}_2 + \mu_2)(\varepsilon_2 + m_2 + \mu_2)[1 - (c_1 + c_2 + c_3 + c_4)] = \mu_3(\mu_1 - b_1q_1)(\tilde{\varepsilon}_2 + \mu_2)(\varepsilon_2 + m_2 + \mu_2)(1 - R_0)$,

with $c_1 = \frac{(1-\theta_2)\gamma_3 g_4 g_6 S_2^0 S_3^0}{\mu_3(\gamma_3+\mu_3)(\tilde{\varepsilon}_2+\mu_2)}$, $c_2 = \frac{\theta_2\gamma_3 g_4 g_5 S_2^0 S_3^0}{\mu_3(\gamma_3+\mu_3)(\varepsilon_2+m_2+\mu_2)}$, $c_3 = \frac{(1-\theta_2)\gamma_1 g_1 g_3 S_1^0 S_2^0}{(\mu_1-b_1q_1)(\tilde{\varepsilon}_2+\mu_2)}$,
$c_4 = \frac{\theta_2\gamma_1 g_1 g_3 S_1^0 S_2^0}{(\mu_1-b_1q_1)(\varepsilon_2+m_2+\mu_2)}$, *and*
$$R_0^3 = c_1 + c_2 = \frac{\gamma_3 g_4 S_2}{\mu_3(\gamma_3+\mu_3)}\left[\frac{(1-\theta_2)g_6 S_3^0}{\tilde{\varepsilon}_2+\mu_2} + \frac{\theta_2 g_5 S_3^0}{\varepsilon_2+m_2+\mu_2}\right].$$

Thus, $n_1 > 0$ for $\frac{b_1q_1}{\mu_1} < 1$, $n_2 > 0$ for $\frac{b_1q_1}{\mu_1} < 1 \wedge c_1 < 1$, $c_2 < 1$, $c_3 < 1$, $c_4 < 1$, $n_3 > 0$ for $\frac{b_1q_1}{\mu_1} < 1 \ \wedge \ c_1 + c_3 < 1 \ c_2 + c_4 < 1$ and $n_4 > 0$ for $R_0^1 < 1 \ \wedge \ R_0^3 < 1 \ \wedge \ R_0 < 1$. Thus the equation (3.38) has no root which is positive or zero (Descartes'rule of sign). Therefore equation (3.38) will only have negative roots or complex roots with negative real part if $n_3(n_2n_1 - n_3) - n_1^2 n_4 > 0$ (according to Routh-Hurwitz criteria), that is, $\frac{b_1q_1}{\mu_1} < 1 \wedge R_0^1 < 1 \ \wedge \ R_0^3 < 1 \ \wedge \ R_0 < 1$. Thus, the system (3.1-3.3) is locally asymptotically stable about the boundary equilibrium X^0. □

3.3.5.1 Existence and uniqueness of endemic equilibrium, X^*

The existence of the endemic equilibrium in Ω^1, is determined by equation (3.19). Taking $A = g_3l_7$, $B = g_4l_7$, $C = b_1N_1g_3l_6$, $D = \mu_1\mu_2l_5$ and $E = b_1N_1g_4l_6$, equation (3.19) can be written as

$$A(I_1^*)^2 + (BI_3^* + D - C)I_1^* + EI_3^* = 0. \tag{3.39}$$

Solving equation (3.39) for $\{I_1^*, I_3^*\}$ we get $\{I_1^* > 0, \ I_3^* = -\frac{I_1^*(AI_1^*+D-C)}{I_1^*B-E}\}$ which gives $\{I_1^* > 0, \ I_3^* = \frac{g_3\gamma_1 b_2 I_1^*(aR_0^1-1-g_3l_7I_1^*)}{g_4[g_3\gamma_1b_2l_7I_1^*-\mu_1(\gamma_1+\mu_1)R_0^1]}\}$, with $a = \frac{b_1b_2}{\mu_2(\mu_1-b_1q_1)}$. The existence of positive I_3^* is given by the following inequalities: $\frac{E}{B} < I_1^* < \frac{C-D}{A} \vee \frac{C-D}{A} < I_1^* < \frac{E}{B}$. Since $\frac{E}{B} = \frac{b_1N_1g_4l_6}{g_4l_7} = \frac{b_1N_1l_6}{l_7}$ and $\frac{C-D}{A} = \frac{b_1N_1g_3l_6-\mu_1\mu_2l_5}{g_3l_7} = \frac{b_1N_1l_6}{l_7} - \frac{\mu_1\mu_2l_5}{g_3l_7}$, we get that the meaningful inequality is $\frac{C-D}{A} < I_1^* < \frac{E}{B}$, thus $\frac{aR_0^1-1}{g_3l_7} < I_1^* < \frac{\mu_1(\gamma_1+\mu_1)R_0^1}{g_3\gamma_1b_2l_7}$.
Since $I_1^* > 0$, then $C - D$ should be positive. $C - D$ is the expression on the numerator of equation (3.26), which was verified to be positive whenever $R_0^1 > 1$ and $\frac{b_1q_1}{\mu_1} < 1$. This gives the threshold for the endemic persistence. Therefore the following result holds:

Theorem 3.8. *The RVF model (3.1-3.3) has a unique endemic equilibrium point* X^* *whenever* $R_0^1 > 1$ *and* $\frac{aR_0^1-1}{g_3l_7} < I_1^* < \frac{\mu_1(\gamma_1+\mu_1)R_0^1}{g_3\gamma_1b_2l_7}$.

The result in Theorem (3.8) indicates that depending on vertical transmission efficiency, if the *Aedes* basic reproduction number $R_0^1 > 1$ and I_1^* satisfy the inequality $\frac{aR_0^1-1}{g_3l_7} < I_1^* < \frac{\mu_1(\gamma_1+\mu_1)R_0^1}{g_3\gamma_1b_2l_7}$, it is sufficient to cause an outbreak, since secondary vectors (*Culex* species) co-exist and serve as disease amplifiers. Figure 3.2 shows the region where I_3^* is strictly positive when varying both I_1^* and R_0^1.

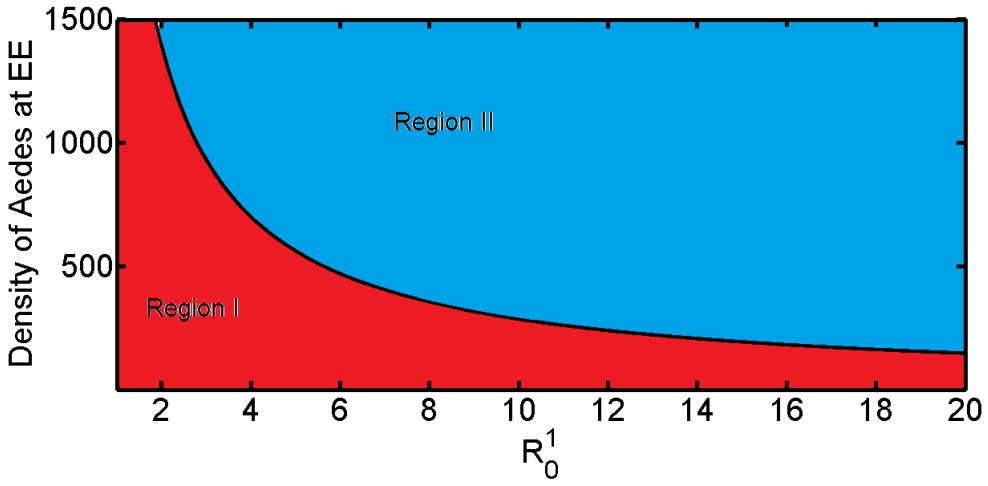

FIGURE 3.2: Base on equation (3.39), we represent the condition for existence of infected *Culex* mosquitoes at the endemic equilibrium (EE) state. The existence of infected *Culex* is impossible in region I. In region II both *Aedes* and *Culex* coexist. The border black line represents the threshold of coexistence, which is exactly $I_3^* = 100$.

That is, in region II both infected *Aedes* and *Culex* co-exist while in region I only infected *Aedes* exist. This confirm the analytical results obtained above. The existence of infected *Culex* at endemic equilibrium depend on the existence infected *Aedes* and initial spread of the disease R_0^1. Thus, *Aedes* species has the potential to initiate the epidemic through transovarial transmission and the potential to sustain low levels of the disease during post epidemic periods.

3.3.6 Bifurcation and chaos investigation on the RVF model

To provide some numerical evidence for the qualitative dynamic behaviour of the model (3.1-3.3), time series with both transient and permanent regimes, phase portraits, Poincaré maps, bifurcation diagrams, Lyapunov exponents to assess model sensitive dependence on initial conditions and return maps are used to illustrate the above analytical results and for determining new dynamics as the parameters vary. We start by introducing a simple case of seasonality on time dependent birth rates of mosquito populations (*Aedes* and *Culex*):

$$b_1(t) = b_1\left(1 + \delta_1 \sin\left(\frac{2\pi t}{T}\right)\right), \quad b_3(t) = b_3\left(1 + \delta_3 \sin\left(\frac{2\pi t}{T}\right)\right) \tag{3.40}$$

where b_1 and b_3 are the baseline parameters of the birth rate of *Aedes* and *Culex* mosquitoes respectively, $T = 1$ year, δ_1 and δ_3 are the external forcing amplitudes for the two species of mosquitoes respectively, which represent the strength of seasonality that controls the magnitude of the fluctuations. When $\delta_1 = \delta_3 \equiv 0$, the model reduces to a non-seasonal model.
When there is no external forcing (i.e. $\delta_1 = \delta_3 = 0$) the system possesses two

types of equilibria: disease free and endemic equilibria. When the magnitude of the external forcing parameters $\delta_1,\ \delta_3$ is sufficiently small, $\delta_1,\ \delta_3 \in (0,1)$ the system responds with oscillations of the same annual period as external forces (see Figs.3.3(a) and (b)). However with larger values (for instance $\delta_1 = 70,\ \delta_3 = 1.1$) the system shows other modes of oscillations Fig.3.3(c),(d) with period 5 as confirmed by Poicaré maps Fig.3.4. In all this section, the system is integrated numerically with the fifth order Runge-Kutta algorithm [111]. The initials conditions and other values are $P_1(0) = 1000$, $U_1(0) = 999$, $E_1(0) = 0$, $I_1(0) = 1$, $S_2(0) = 1000$, $A_2(0) = 0$, $I_2(0) = 0$, $R_2(0) = 0$, $P_3(0) = 1000$, $S_3(0) = 5000$, $E_3(0) = 0$, $I_3(0) = 0$, $K_1 = 10000$, $K_2 = 2000$ and $K_3 = 10000$. The parameter values are shown in Table A.2 in Appendix A.

3.3.6.1 Time series simulations

Figure 3.3 depicts the time evolution of the sum of infectious *Aedes* and *Culex* mosquitoes $I_1 + I_3$ and sum of infectious asymptomatic and symptomatic livestock for different values of $\delta_1 = 0.6,\ \delta_3 = 0.6$; $\delta_1 = 70,\ \delta_3 = 1.1$ and $\delta_1 = 24.7,\ \delta_3 = 1.1$. In (a) the number of infectious mosquitoes oscillates yearly reaching the same maximum. In (c) the quantity $I_1 + I_3$ also oscillates with first peak of above 500 around the second year. In (c) we notice a long lasting peak of about 500 infectious mosquitoes in the interval 18-25 months, which is likely to cause an inter-epidemic outbreak. Fig.3.3(b) shows a constant low oscillation, high peaks around second and fifth year in (d) and high peaks around second and fourth year in (f). Note that the internal figures describes the permanent regime which represent the dynamics where the system is expected to adapt to the external forcing.

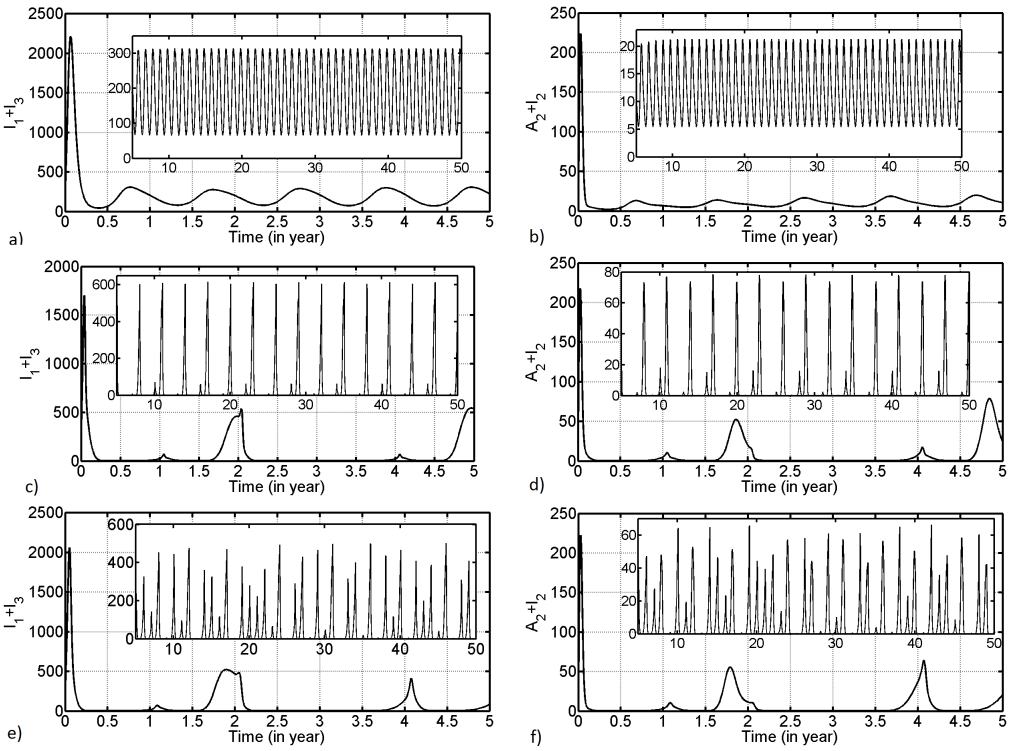

FIGURE 3.3: We display the time series of $(I_1 + I_3)$ left and $(A_2 + I_2)$ right. Parameters used for (a) and (b) are $\delta_1 = 0.6$, $\delta_3 = 0.6$, for (c) and (d) are $\delta_1 = 70$, $\delta_3 = 1.1$, finally for (e) and (f) are $\delta_1 = 24.7$, $\delta_3 = 1.1$. Figure (d) and (f) shows a linear increase in livestock seroprevalence during post-epidemic which comes in cycles of 5 to 7 years approximately.

The time series for $\delta_1, \delta_3 \in (0, 1)$, also shows that the total of infected vectors $I_1 + I_3$ and infected livestock $A_2 + I_2$ stay quite away from zero, avoiding the chance of extinction in stochastic system with reasonable size (see Fig.3.3(a) and (b)). This is due to the fact that for $\delta_1, \delta_3 \in (0, 1)$ vector oviposition continues throughout the year, albeit at lower rates during unfavourable seasons. This is not the case of East African region, where we have two rain seasons (long and short) and a dry season, where under this former we expect stochastic extinction during some intervals of inter-epidemic periods.
In the region $\delta_1 > 1, \delta_2 > 1$ Fig.3.3(c)-(f), we observe fluctuations in the total number of infected from reasonable small peaks (describing RVF post-epidemic activities) to very low values, which in this case drive almost surely the system to extinction.

3.3.6.2 Phase portrait diagrams and Poincaré maps

Instead of studying the entire complicated trajectories, important information is encoded in the phase plane. This approach allow us to analyse geometrically the total dynamics of the system. Varying δ_1, δ_3 the state space plots show a rich

dynamical behaviour with bifurcations from limit cycles, multi-periodic oscillation to completely irregular behaviour which is usually the fingerprint of chaos (see Fig.3.4).

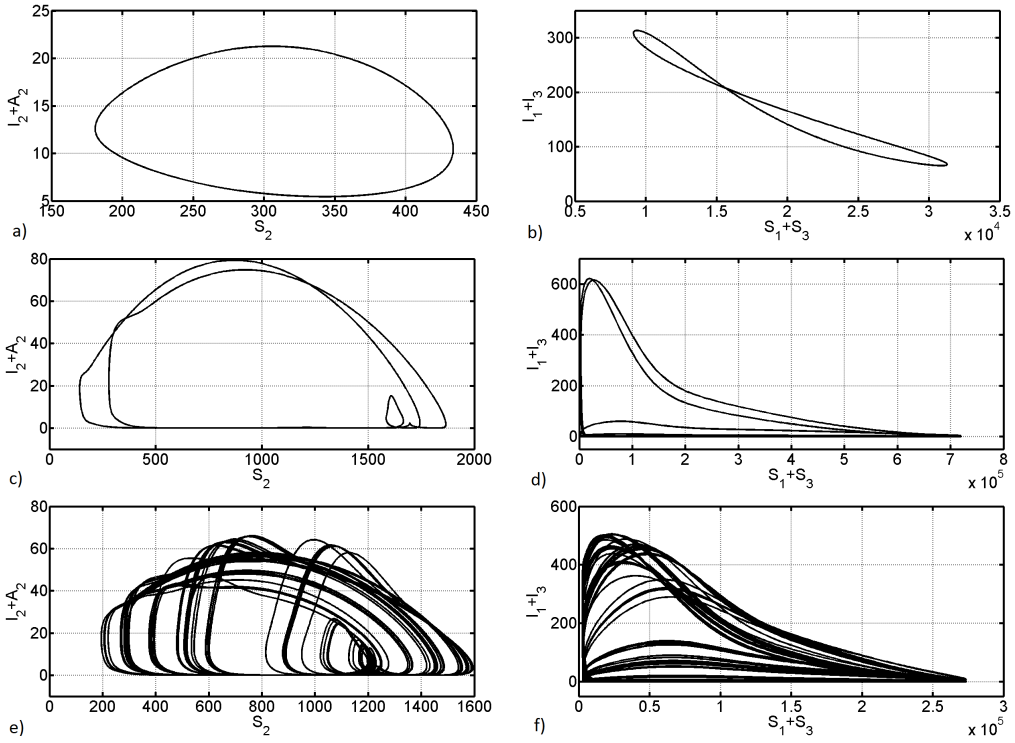

FIGURE 3.4: Phase portrait with couple $(I_2 + A_2, S_2)$ on the left and $(I_1 + I_3, S_1 + S_3)$ on the right. In (a) and (b), $\delta_1 = 0.6$, $\delta_3 = 0.6$, the system is attracted by a limit cycle. In (c) and (d), $\delta_1 = 70$, $\delta_3 = 1.1$, the system is multi-periodic. And in (e) and (f), $\delta_1 = 24.7$, $\delta_3 = 1.1$, the systems behave with higher multi periodicity.

Poincaré map is a useful tool for analysing the dynamics of a nonlinear system. It allows good insight for global dynamics of the system by displaying the types of attractors of the system [112]. The successive iterations of the map are defined as:

$$P : \Sigma \to \Sigma$$
$$\Sigma = \left\{ \mathbf{X} | t = 0, \frac{2\pi}{\Omega}, \frac{4\pi}{\Omega}, \frac{8\pi}{\Omega}, \dots \right\} \in \mathbb{R}^{13} \tag{3.41}$$

The attractor is generated by sampling the system stroboscopically at time corresponding to the multiple of the period $T = 2\pi/\Omega$. We have used $100,000$ points and a period of one year. Figures 3.5(a) and (b) with ($\delta_1 = 0.6$, $\delta_3 = 0.6$) show that the system is attracted by a limit cycle, because of the presence of a single dot. In this case the system is periodic. In (c) and (d) with ($\delta_1 = 70$, $\delta_3 = 1.1$) we notice a presence of a few dots, thus, the system is multi-periodic and in (e) and

(f) with ($\delta_1 = 24.7$, $\delta_3 = 1.1$) we notice a strange attractor which is usually a sign of a chaotic system.

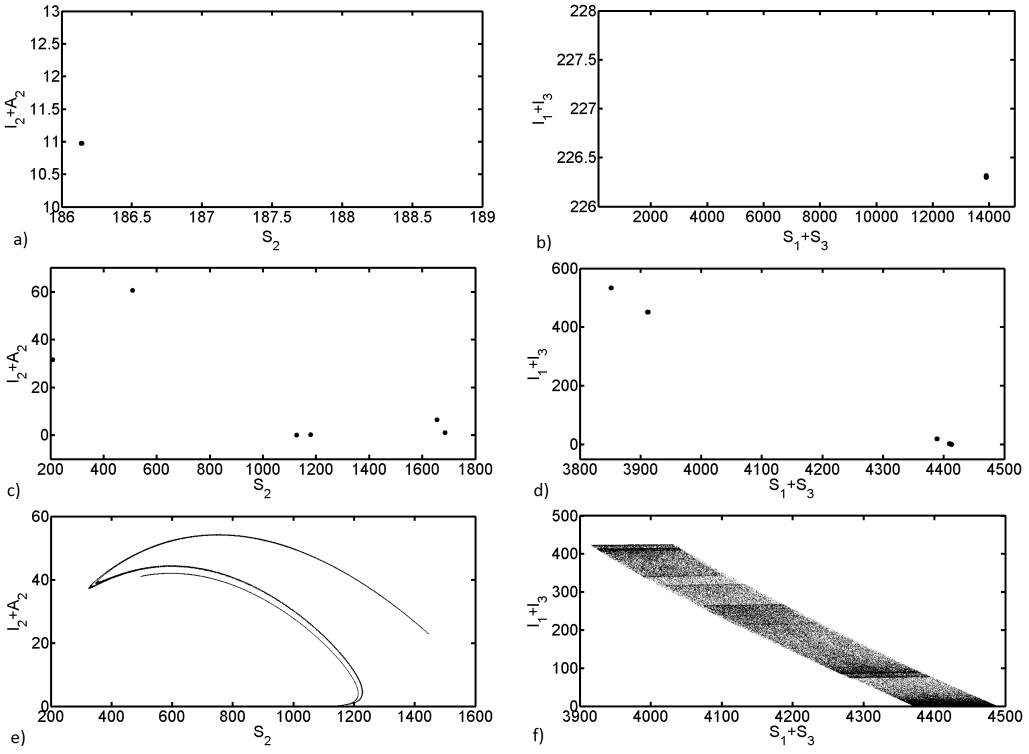

FIGURE 3.5: Poincaré maps with couple $(I_2 + A_2, S_2)$ on the left and $(I_1 + I_3, S_1 + S_3)$ on the right. In (a) and (b), $\delta_1 = 0.6$, $\delta_3 = 0.6$, in (c) and (d), $\delta_1 = 70$, $\delta_3 = 1.1$ and in (e) and (f), $\delta_1 = 24.7$, $\delta_3 = 1.1$.

3.3.6.3 Maxima return maps of $I_1 + I_3$, $A_2 + I_2$ for state phase plots

We have investigated maxima return maps in order to get supplementary classification of different dynamics for parameters δ_1 and δ_3. For a time selected as t_{max}, at which $I_1 + I_3$ and $A_2 + I_2$ have a local maximum, we have plotted the number of infected mosquitoes and livestock respectively at time t_{max} and at the next local maximum $t_{returnmax}$. Figures 3.6(a) and (b) show that all consecutive maxima coincide with themselves as shown by a single dot. In (c) and (d), we notice that consecutive maxima are few and different as a sign of irregularity, and in (e) and (f), we observe that a dot rarely comes back to the same point. The fingerprint of chaotic attractor is clearly visible with the maxima return maps analysis.

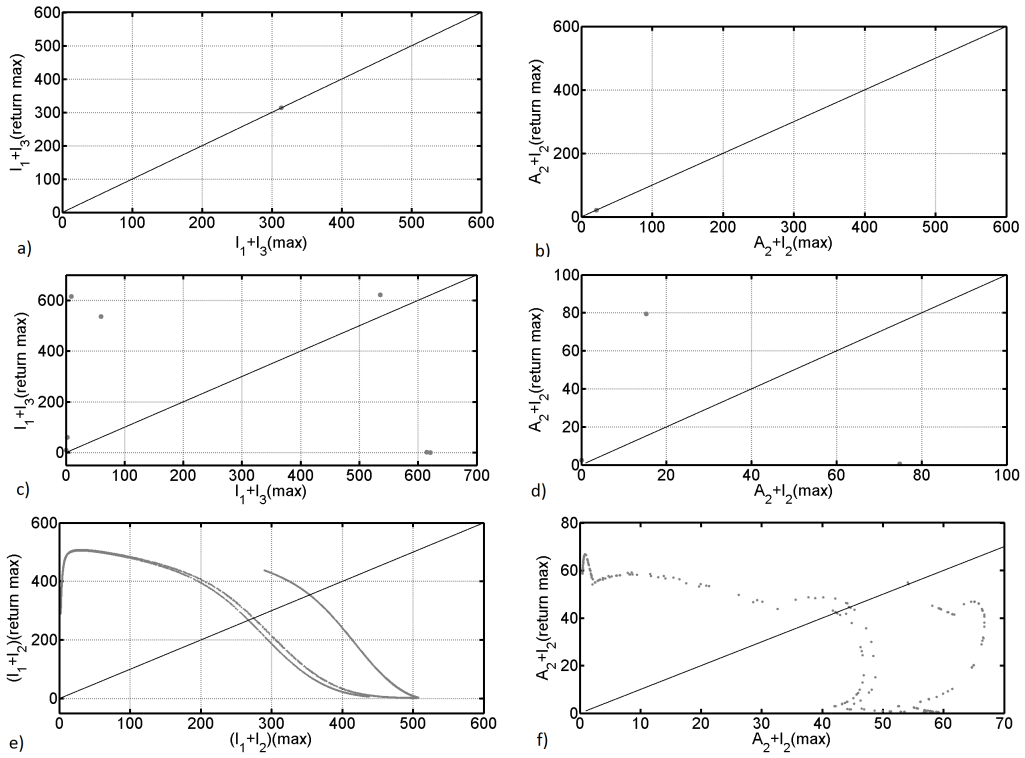

FIGURE 3.6: We display the maxima return map of $I_1 + I_3$ and $A_2 + I_2$ with (a)-(b) $\delta_1 = 0.6$, $\delta_3 = 0.6$, (c)-(d) $\delta_1 = 70$, $\delta_3 = 1.1$ and (e)-(f) $\delta_1 = 24.7$, $\delta_3 = 1.1$. The blanc line represents the first bisectrix of the plane.

3.3.6.4 Lyapunov exponents and bifurcation diagrams

The largest Lyapunov Exponent (LE) is quantitatively characterized by the average rate of separation of infinitesimally close trajectories in the phase space for a dynamic system. It can be used to determine how sensitive a dynamical system is to initial conditions [113]. In general for a N-dimensional dynamical system described by a set of equations $\frac{dX^i}{dt} = F^i(\mathbf{X}, t)$, the LEs are defined by [114]:

$$\lambda_i = \lim_{t\to\infty} \lim_{\delta X_0^i \to 0} \frac{1}{t} \ln \left(\frac{\| \delta X_t^i \|}{\| \delta X_0^i \|} \right), \tag{3.42}$$

where λ_i is the i^{th} LE and $\| \delta X_t^i \|$ is the distance between the trajectories of the i^{th} component of the vector field F at time t. Recall that exponential divergence in the phase space is given by the LEs. If the largest LE is less than or equal to zero, then the system may be regarded as periodic or quasi-periodic. Otherwise, the largest LE is positive the system may have an irregular or chaotic behaviour. Another important fact to be mentioned is that negative LE does not, in general, indicate stability, and that positive largest LE does not, in general indicate chaos [115, 116].

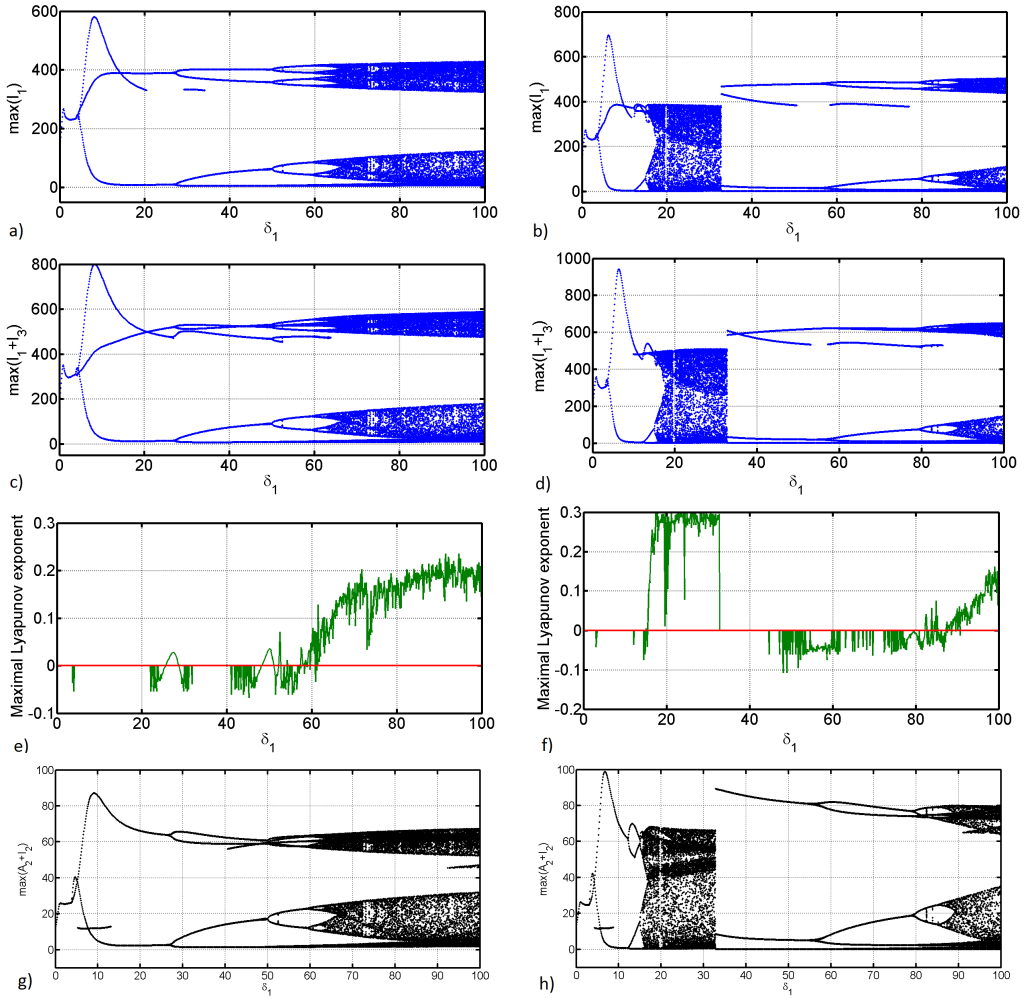

FIGURE 3.7: In (a) and (b), bifurcation diagram for the local maximal quantities of I_1 by varying the parameter δ_1 and fixing δ_3=0.6(a) and δ_3=1.1(b). In (c) and (d), bifurcation diagram for the local maximal quantities of $I_1 + I_3$ by varying the parameter δ_1 and fixing δ_3=0.1(c) and δ_3=1.1(d). In (e) and (f), we have computed the largest LE for δ_3=0.6(e) and δ_3=1.1(f) and in (g) and (h), bifurcation diagram for the local maximal quantities of $A_2 + I_2$ by varying the parameter δ_1, and fixing δ_3=0.6(h) and $\delta_3 = 1.1$(f).

In Figs.3.7(a)-(d) we have computed the bifurcation diagrams with respect to δ_1, the external forcing amplitude on the response of the RVF model. Figures (e) and (f) show the maximal LE after infinitesimal perturbation of 10^{-10} in the initial conditions. In Fig.3.7 (e), the maximal LE is positive for $\delta_1 \gtrsim 60$ and around 50 and 25. In Fig.3.7(f), the maximal LE is positive for $15 \lesssim \delta_1 \lesssim 34$ and for $\delta_1 \gtrsim 85$. Figure 3.7 shows the bifurcation diagrams of the local maxima of infectious mosquitoes and livestock undergoing forward forking bifurcation from period-1 to period-6 oscillatory type behaviour. In Fig.3.7(a), local maxima extrema I_1 of infectious *Aedes* species undergo irregular behaviour for $\delta_1 \gtrsim 65$, which is the fingerprint of chaos. Fig.3.7(b) shows irregular behaviour for $15 \lesssim \delta_1 \lesssim 34$ and $\delta_1 \gtrsim 85$, with large number of periods. In Figs.3.7 (c) and (d), we observe almost the same

qualitative behaviour with the same parameters, but with notable difference in the value of the local maxima of the overall infectious mosquitoes fuelled by the elevation of several secondary vectors which serve as disease amplifiers. When $\delta_3 = 1.1$ the local extrema $A_2 + I_2$ undergoes irregular behaviour for $15 \lesssim \delta_1 \lesssim 34$ and $\delta_1 \gtrsim 85$, with large number of periods Fig.3.7(h).
We observe from Fig.3.7(e) that for a fixed $\delta_3 = 0.1$ and varying δ_1 $(0 \leq \delta_1 \lesssim 62)$ the largest Lyapunov exponent is fairly negative indicating stable limit cycles and multi-periodicity with some shift to positive values as the system bifurcates through period doubling routes to chaos. Above $\delta_1 = 62$ a positive Lyapunov exponent clearly moves away from zero, indicating deterministically chaotic attractors. For a fixed $\delta_3 = 1.1$ and varying δ_1 Fig.3.7(f) the largest Lyaponov exponent fairly confirms the behaviour seen through bifurcation diagrams with positive values on the chaotic regions.

3.3.6.5 Interaction between *Culex* and *Aedes* oviposition rates

In the preceding section we have fixed the value of δ_3, while investigating the bifurcation behaviour when δ_1 is varying. In Fig.3.8 we have computed the maximal LE when those two parameters are varying. For $20 \lesssim \delta_1, \delta_3 \lesssim 100$, the maximal LE is negative, then the system is sensitive to initial conditions. For low values of δ_3 and $18 \lesssim \delta_1, \delta_3 \lesssim 45$, the maximal LE is positive. Another remarkable fact is observed when δ_1 is around 10 no matter the value of δ_3, the maximal LE will be positive. This shows us that the impact of the birth rate of *Aedes* is predominant in leading irregular behaviour in our system, confirming that *Aedes* are indeed the RVF primary vectors.

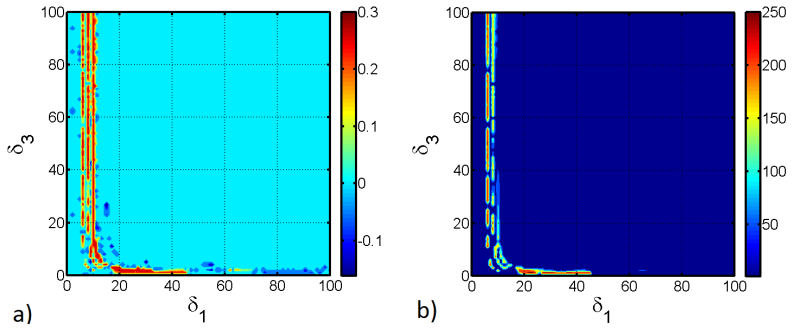

FIGURE 3.8: In (a) we display the maximal LE function of δ_1 and δ_3. The colorbar shows the value of the maximal LE. In (b) we display the number of points in the Poincaré map (the colorbar) according to the set of parameters (δ_1, δ_3).

Both maximal Lyapunov exponent functions of δ_1 and δ_3 and the Poincaré map of the set (δ_1, δ_3) Fig.3.8 around $\delta_1 = 10$ agree with each other, confirming the analytical results obtained in Theorem 3.8.
Recall that in certain *Aedes* species of the subgenera *Neomelaniconion* and *Aedimorphus*, the female mosquitoes transmit RVF virus vertically to their eggs [35].

When these mosquitoes lay their eggs in flooded areas, transovarially infected adults may emerge and transmit RVF virus to nearby domestic livestock which may then lead to the infection of secondary arthropod vectors species including various *Culex* [117]. Thus, there is an initial quantity of primary infected vectors required to trigger an outbreak. Fig.3.8 shows that if the control magnitude of fluctuations in *Aedes* oviposition rate is around 10, and the number of newly transovarially infected mosquitoes is amplified by nearby domestic livestock, then, the number of infectious (both host and vector) will be sufficiently enough to cause subsequent elevation of secondary vectors, including *Culex* species, and consequently trigger an outbreak.

3.4 Discussion and Conclusion

The proposed model accounts for the population dynamics of both livestock and mosquitoes (*Aedes* and *Culex*) and seasonal changes in weather that heavily affects the vector population size. Mosquito density varies over seasons, and the contact rates and vector oviposition rates vary dynamically based upon both host and vector densities since female mosquitoes need blood for oviposition. Qualitative analysis of the model showed that there exists a domain where the model is epidemiologically and mathematically well-posed. We then analysed the existence and stability of both disease free and endemic equilibria.
Dynamical analysis shows that when $R_0 < 1$, then the disease dies out and when $R_0 > 1$ the disease become endemic. A suitably constructed Lypunov function is used to determine the global stability of the endemic equilibrium of the model without *Culex* species and the existence of the endemic equilibrium of the overall model is seen to exist whenever $\frac{aR_0^1-1}{g_3 l_7} < I_1^* < \frac{\mu_1(\gamma_1+\mu_1)R_0^1}{g_3\gamma_1 b_2 l_7}$, meaning that the co-existence of the infectious host, *Aedes* and *Culex* mosquitoes is subject to the number of infected *Aedes* mosquitoes.
We have used visualisation techniques to study the behaviour of RVF epidemic model under external forcing in the mosquito oviposition rates. The bifurcation diagrams show the emergence with an increase in external forcing parameters δ_1, δ_3 of Hopf and pitchfork modes of bifurcation. That they have much larger amplification of infection levels that can take place if the system is encouraged to switch to multi-periodic mode. In transition, further amplification can occur if the multi-periodic mode becomes unstable and the system moves into chaotic state before finding an alternative stable periodic mode (e.g. Fig.3.7).
On the bifurcation diagrams the highest maximum number of infectious *Aedes* mosquitoes is only observed for values of δ_1 ($\delta_1 < 10$) with different values of δ_3, meaning that for the disease to trigger an inter-epidemic a certain number of infectious *Aedes* mosquitoes is necessary. This confirm the analytical results obtain in section 3.3.5, as well as results obtained in [5] which showed that when mosquito populations follow seasonal patterns with large amplitudes, vertical transmission could play a significant role in long-term persistence of a pathogen. Another important conclusion is that even with a low maximum number of infectious individuals, the bifurcation diagrams show that if for fixed $\delta_3 = 1.1$ and varying δ_1 the system

becomes chaotic in the interval $15 \lesssim \delta_1 \lesssim 35$, meaning that unpredictable and possibly uncontrolled low levels of inter-epidemic activities may occur, leading to higher morbidity in livestock. Hence observed fluctuations in RVF outbreak data and non deterministic nature of RVF inter-epidemic activities could now be better understood considering fluctuations on both rain season and dry season as significant factor.

A sero-survey study done in livestock approximately four years after the 2006/07 RVF outbreak in Tanzania, showed a linear increase in seroprevalence in the post-epidemic annual cohorts implying a constant exposure and presence of active foci transmission [39]. Figure 3.3 (d) and (f) demonstrate this behaviour which is shown to come in cycles of 5 to 7 years approximately, as well as fluctuations in the total number of infected from reasonable small peaks (describing RVF post-epidemic activities) to very low values. During these periods of low troughs for the total number of infected, the virus survive through vertical transmission in *Aedes* species and among wild animals as reservoirs [58]. Note that, this recurrent low level RVF virus activity during inter-epidemic periods, in East African region in particular, infects $1-3\%$ of livestock herds annually [118]. Generally, these infections pass undetected where there is no regular active surveillance in the livestock and human populations [39]. This suggests that RVF outbreaks partly result from build up RVF inter-epidemic activities for it has been observed that optimum climatic conditions (temperature and rainfall) only and presence of mosquitoes have not completely explained the RVF outbreaks [26].

Simulation of the interaction between the two populations densities of *Aedes* and *Culex* by varying the magnitudes of external forcing δ_1 and δ_3 of the oviposition rates b_1 and b_3 have opened a new window of research about the potential of *Aedes* species for initiating RVF outbreaks and sustaining low endemic levels of the disease during inter-epidemic periods. This result concurs with the Chitnis et al. [5] suggestion that vertical transmission is required for inter-epidemic persistence.

One of the main objectives of this study was to investigate the possibility of prediction of RVF outbreaks with the aim to control RVF incidence. We have shown that seasonality may induce irregular behaviour on the disease dynamics. It has been shown that the interaction between oviposition rates of *Aedes* and *Culex* mosquitoes makes prediction more complex. In fact it is naturally expected higher irregularity in the higher seasonality forcing. However, our proposed model has shown that the complexity occurs even for a relatively low level of the magnitude of seasonal forces. We have also found that seasonal *Aedes* birth rate is most likely to generate uncontrollable behaviour than *Culex* seasonal birth rate. The epidemiological significance of this study is the higher uncertainty in outbreak prediction of RVF by a simple theoretical mathematical model including seasonal influence in mosquito populations. Also the model including external seasonal forcing on mosquito oviposition rates shows ability to mimic the linear increase in livestock seroprevalence as found in [39], with first post-epidemic peak around the second year, a following peak larger than the previous one around the fifth year Fig.3.3(d) and (f). Currently, two types of RVF vaccine for livestock exist: a live vaccine and inactivated vaccine. However, the current live vaccine can not be used for prevention and prevention using the inactivated vaccine is almost impossible to sustain in RVF affected countries for economic reasons [1, 74, 86]. Then, the

possible alternative of controlling RVF transmission remains in keeping the vector population at the lowest levels. Therefore we argue that locations that may serve as RVF virus reservoirs should be eliminated or kept under control to prevent multi-periodic outbreaks and consequent chains of infections. We also recommend a systematic surveillance in the livestock or human population in order to monitor inter-epidemic RVF activities.

This study is not exhaustive and can be extend to include humans not just as dead ends [48] but also as disease amplifiers since it has been demonstrated that humans have potential to transmit the virus, particularly to *Aedes* mosquito species [119]. Also, including ticks on the model may help to explain and gain more insights on the understanding of disease dynamics and enhance control strategies, since ticks have been reported to play a role on disease transmission [26]. For mathematical convenience and tractability of the model, we made several assumptions, thus our results are driven by the model formulation and structure. A step toward a more quantitative and qualitative study is viable by relaxing some of the assumptions made and incorporating more epidemiological features of the disease as well as the use of a double periodic function and inclusion of stochasticity in order to capture the dynamic of the two rainfall seasons in East Africa (long and short rainy seasons), where the disease is likely to be more predominant. Further studies are needed to enhance the understanding of RVF epidemic and inter-epidemic activities in order to provide further insights in assessing the current and future control strategies.

Chapter 4

The role of *Hyalomma Truncatum* on the dynamics of Rift Valley fever. Insights from a mathematical epidemic model[1]

4.1 Introduction

Tick-borne diseases in livestock have a significant economic impact in particular in the sub-Saharan region where Rift Valley fever (RVF) prevalence is endemic [7, 8]. Ticks are vectors of a number of both human and ruminant diseases including Lyme disease, colorado tick fever, Rocky Mountain spotter fever, African tick bite fever, bovine anaplasmosis and tick paralysis, just to mention a few. Virus isolation and laboratory investigations have implicated ticks in the transmission of RVF [7, 11, 28, 29]. Ticks attach to the skin of humans and ruminants and feed on blood causing direct loss through sucking blood [26], limiting livestock production and improvement [120].

In this chapter, we propose a model that investigates the possible implications of ticks in the transmission of RVF [26, 28] and the resulting epidemiological consequences in efforts for controlling RVF epidemics. We adapt previous RVF transmission models [4, 69] to include ticks compartments. *Hyalomma truncatum* is both a two-host and three-host tick depending on the hosts species [121]. This means that it must feed on two different hosts as larva and adult or three different hosts as larva, nymph and adult respectively [120]. Therefore, we include in our model attached and detached compartments and combine both immature stages and adults in one compartment to keep the model tractable.

[1]This chapter has been published: S. A. Pedro et al. The role of *Hyalomma Truncatum* on the dynamics of Rift Valley fever. Insights from a mathematical epidemic model. Acta Biotheor. 64(3) 2016. DOI 10.1007/s10441-016-9285-0

The chapter is set out as follows. In sections 4.1.1 and 4.1.2 we describe the epidemiology of the disease and its important features as well as the biology of ticks and their possible involvement in RVF transmission. In addition, we discuss previous work and contribution in the sphere of understanding disease transmission and persistence. Section 4.2 follows with model formulation, including the definition of a domain where the model is mathematically and epidemiologically well posed. In Section 4.3, we derive an explicit formula for the basic reproductive number, R_0, an important critical condition for quantifying initial disease invasion, then we prove the existence and global stability of the disease-free equilibrium. In Section 4.4 we simulate the system to understand various underlying RVF dynamics and possible contribution of ticks to the disease spread and persistence. Finally in Section 4.5, we explore global sensitivity analysis followed by local sensitivity analysis of the model output with respect to input parameters.

4.1.1 RVF epidemiology mechanism

Rift Valley fever virus (RVFV), a member of the phlebovirus genus, and family Bunyaviridae, is an enveloped virus with a segmented, RNA genome. RVF is a viral disease that primarily affects both domestic and wild animals but is also capable of infecting humans [22, 23]. Major host disease amplifiers are sheep, cattle and goats but the disease also affects camels, buffaloes and other mammalian species [24], causing high mortality, abortion and significant morbidity in domestic livestock [13]. The virus has been isolated from at least 30 mosquito species in the field [27], biting midges, blackflies and ticks [11, 28, 29]. However, major vectors are certain species of mosquitoes, most commonly of the genera *Aedes*, *Culex*, *Eretmopodites* and *Mansonia* among others [29, 122]. For further details about the epidemiology and ecology of the disease see Section 3.1 in Chapter 3.

4.1.2 Ticks and their possible role on the transmission of RVF

Hlyalomma truncatum is a tick species of the family Ixodidae, widely distributed within the African tropical geographical region [123], which is found throughout the entire geographic range of RVFV [28]. Ticks require blood meals to survive at each of their four life stages: egg, larvae, nymph and adult. Their hosts include humans, mammals, birds, reptiles and amphibians. However, most ticks have a variant of mammalian hosts at each stage of their life and disease transmission occurs through the process of feeding. As pointed out in the introduction, *Hyalomma truncatum* is both a two-host and three-host tick depending on the hosts species [121]. Thus, a susceptible larvae, nymph or adult may acquire the disease when feeding on an infected host, drop off and switch to another host while in the same stage, and infect that host. Alternatively, susceptible larvae or nymph may acquire the disease by feeding from an infected host then transmit the disease in a later stage to the new susceptible host [120]. The present research study is motivated by

a review undertaken by Nchu and Rand [26] on possible implications of *Hyalomma truncatum* on the dynamics of RVF outbreaks and it aims to hypothetically evaluate this phenomenon by means of mathematical modelling. This research builds on important features that underline the biology and the ecology of ticks in particular in Sub-Saharan Africa where RVF is endemic. The features are as follows:

1. Wild animals including rodents and livestock (sheep, cattle and goats) are the same hosts for both ticks and mosquitoes that transmit RVF [11, 124]. In addition, immature stages of ticks prefer feeding on hares and rodents, extending the range of feeding hosts [26].

2. Ticks can be transported over long distances on their vertebrate hosts, hence serving as possible hosts for RVFV [28, 29].

3. Ticks are widely distributed in the entire geographic range of RVFV.

4. Ticks can often survive for long time between blood meals [125] and the virus can persist in ticks for their whole lifespan [126]. Thus, long life for ticks means a long time of persistence for the virus increasing the chances of contact between ticks and hosts [26].

5. When feeding on blood, a tick excretes substances in its saliva which have several effects. One is to modulate the hosts immune system. Viruses can benefit from this mechanism, helping it to infect co-feeding ticks on the same hosts vertebrate [127].

6. Ticks cause direct loss through sucking blood [26], reducing host production and increasing host vulnerability to diseases.

7. Mosquito population peaks generally coincide with availability of pastures for domestic livestock and abundance of adult *H. truncatum* ticks [26].

Putting together the above ticks, mosquito and host's epidemiological and ecological features we hypothesize that ticks may be contributing to RVF spreading and endemicity. In spite of all these inherent complexities, mathematical models can provide some very useful informative indicators regarding the potential contribution of ticks in the transmission of RVF. Disease outbreaks in livestock in a particular site are very brief [58] and the peak is likely to pass undetected or under-reported. This may be due to interruption in the rainy events or the duration of the rain in a particular site as well as to ruminant incubation period which is very short [11], and the resulting acquired immunity. In livestock the peak is likely to occur after the second or third week after the onset of the epidemic while in humans it is likely to occur between the fourth and sixth week after the first human case [13, 58, 128, 129]. RVF modelling studies have also suggested that arthropods other than *Aedes* and *Culex* species may be contributing to RVF transmission by accelerating the cause of the outbreak [4]. Thus, this study aims to assess factors leading to this accelerated exponential phase of RVF outbreaks. [26] suggested that in addition to mosquitoes, optimum climatic conditions, international trade of livestock and livestock products,

ticks could be implicated in the spread of RVF. This would affect the dynamics of the disease, including the number of infected host, host extrinsic incubation period and size of the epidemic. In recent years RVF disease models have been developed for addressing a variety of questions related to disease transmission, maintenance and propagation across geographical regions [4, 5, 48, 69–72, 74]. However, none of these models has included ticks compartments in order to access the possible implications of these blood feeding arthropods in the spread and endemicity of RVF. Characterization of tick host preference at different life stages by means of attached and detached compartments makes this modelling framework unique for investigating how the above ecological tick features could affect the transmission and maintenance of the disease. To explain this, we extend previous deterministic epidemic models with two modes of disease transmission: horizontal (host-vector) transmission and vertical transmission from a female *Aedes* to its eggs to include compartments of ticks according to their questing and feeding behaviour. Then, we thoroughly investigate the system analytical and numerically and show that certain model parameters are relevant to the start of an outbreak, exponential phase of an outbreak, the prevalence of RVFV and the epidemic size of an outbreak. Some conclusions may also apply to other vector-borne diseases in which ticks are thought to participate in transmission of the pathogen as additional or secondary vectors. Our analysis provides general qualitative insights on the importance of the time ticks spend attached to a particular host and their host life cycle preference. These results suggest that it is possible to diminish the impact of ticks in the transmission of RVF by either inhibiting ticks to attach to a host or by enhancing the immunity of the host to avoid passage of the infection when a tick feeds on the host.

4.2 RVF Model Development

Three vector species, *Aedes, Culex* mosquitoes and ticks and one host livestock population (not necessarily cattle, sheep or goat) are considered in the model to investigate the role of ticks on RVF disease dynamics. Female infectious *Aedes* mosquitoes not only transmit RVFV to susceptible livestock, but also to their own eggs [35, 69]. *Culex* mosquitoes and ticks acquire RVFV during blood meals on an infected ruminant and then amplify the transmission while feeding on other susceptible ruminants. The animal host, *Aedes* and *Culex* compartments follow the same structure as in [4] while the ticks sub-model follows the structure proposed in [130] and successfully applied by [120, 131], which is according to the questing and feeding behaviour of ticks.

In livestock, the majority of animals do not manifest clinical signs even in regions with severe RVF outbreaks [58]. However, for tractability, in this model we do not include an asymptomatic class. Thus, the density of animal population is divided into three classes according to the following epidemiological status: susceptible, S_2, infectious, I_2, and recovered (immune), R_2. Further details on disease progression

among compartments for the mosquitoes-livestock sub-model are given in Chapter 3 Section 3.2. Ticks have unique life histories that create epidemics which differ from other vector-borne diseases. Depending on the host species *Hyalomma truncatum* has both two-host and three-host life cycles [121]. Meaning that they may need to attach to two or three hosts during their developmental stages for a blood meal at least once at the stages of larvae, nymph and or adult [120]. We assume no transovarial transmission, meaning that no disease transmission from mother to eggs. Thus, ticks become infected when feeding on infectious livestock. As a result only the nymph and adult are able to transmit the infection when feeding on a susceptible ruminant.

The structure of the tick sub-model follows the model framework of [120]. In this framework, we assume that the population of ticks interacts with a population of hosts where both tick and hosts may be infected or uninfected. For mathematical tractability, we combine the larvae, nymphs and adults into one compartment. However, we make distinction between attached and detached ticks such that adult female ticks lay their eggs after detaching. The oviposition rate is proportional to the number of newly attached ticks, $A(t) = S_a(t) + I_a(t)$ as we do not keep track of the time a tick stays attached or matures [120]. After birth they join the susceptible detached compartment, $S_d(t)$ and ticks die only while detached from the host at rate d_t. Both uninfected and infected ticks reproduce or lay eggs after having detached from the host upon successful feeding or by rejection mechanisms by the host or by human intervention. Ticks prefer feeding in some special areas of the host, making it difficult for an extra tick to attach where one is already attached [120]. Thus, we postulate that ticks attach with a constant rate depending on host density and ticks already attached. This rate is a decreasing function of the total number of attached ticks $A(t)$ and an increasing function of the host population N_2, and it is defined to be $\alpha N_2/(1 + A(t))$. The constant is set equal to unity such that if the number of attached ticks is zero then the overall attachment rate of ticks will be αN_2. On the other hand detaching ticks will increase with increasing number of tick-susceptible livestock grazing in a given area. Thus, instead of a constant detachment rate we set it as a linear function of N_2, namely δN_2. The size of the animal host population may be reduced due to the disease-induced mortality reducing the interaction between hosts and vectors. Therefore, for the tick-submodel we assume that the rate at which new cases are produced in both ticks and livestock follows the density dependent transmission mechanism and both hosts and ticks are treated as separate populations but interacting species as in a prey-predator system [120, 131]. The above RVF transmission process is summarized by a schematic representation of the flow of individuals between epidemiological classes (see Fig. 4.1).

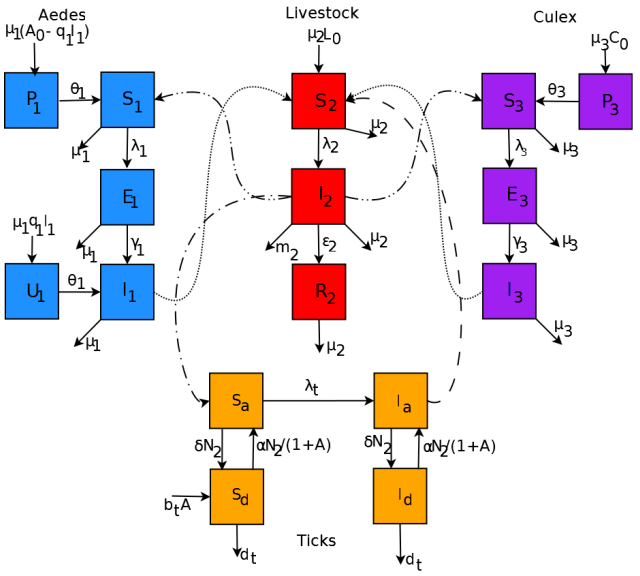

FIGURE 4.1: Flow diagram of RVFV transmission with each species, namely, *Aedes* mosquitoes, *Culex* mosquitoes, ticks and livestock (the solid lines represent the transition between compartments and the dashed lines represent the transmission between different interacting species).

4.2.1 Mathematical model of RVF transmission with three vectors

Here we develop the mathematical representation of the RVF transmission processes by making use of ordinary differential equations. Consider livestock population settled in regions close to mosquito habitats, particularly species of genus *Aedes*. When it rains mosquito eggs hatch and transovarially infected eggs emerge and transmit RVFV to nearby domestic livestock [13]. High circulation of the virus in these ruminants may then lead to infection of secondary arthropod vectors including various *Culex* species [3, 37], and probably some ticks species, enough to trigger an outbreak. The mosquito-host and vice-versa disease transmission depends on both the vector and host population sizes [5]. The flow diagram in Fig. 4.1 with state variables described in Table 4.1 and parameters interpreted in Table 4.2 satisfy the following system of ordinary differential equations:

Aedes

$$\begin{aligned}
\dot{P}_1(t) &= \mu_1(A_0 - q_1 I_1) - \theta_1 P_1, \\
\dot{U}_1(t) &= \mu_1 q_1 I_1 - \theta_1 U_1, \\
\dot{S}_1(t) &= \theta_1 P_1 - \frac{\sigma_1\sigma_2\beta_{12}}{\sigma_1 N_1 + \sigma_2 N_2} I_2 S_1 - \mu_1 S_1, \\
\dot{E}_1(t) &= \frac{\sigma_1\sigma_2\beta_{12}}{\sigma_1 N_1 + \sigma_2 N_2} I_2 S_1 - \gamma_1 E_1 - \mu_1 E_1, \\
\dot{I}_1(t) &= \gamma_1 E_1 + \theta_1 U_1 - \mu_1 I_1,
\end{aligned} \tag{4.1}$$

Livestock

$$\begin{aligned}
\dot{S}_2(t) &= \mu_2 L_0 - \frac{\sigma_1\sigma_2\beta_{21}}{\sigma_1 N_1 + \sigma_2 N_2} I_1 S_2 - \frac{\sigma_3\sigma_2\beta_{23}}{\sigma_3 N_3 + \sigma_2 N_2} I_3 S_2 - \beta_{2t} I_a S_2 - \mu_2 S_2, \\
\dot{I}_2(t) &= \frac{\sigma_1\sigma_2\beta_{21}}{\sigma_1 N_1 + \sigma_2 N_2} I_1 S_2 + \frac{\sigma_3\sigma_2\beta_{23}}{\sigma_3 N_3 + \sigma_2 N_2} I_3 S_2 + \beta_{2t} I_a S_2 - \varepsilon_2 I_2 - \mu_2 I_2 - m_2 I_2, \\
\dot{R}_2(t) &= \varepsilon_2 I_2 - \mu_2 R_2,
\end{aligned} \tag{4.2}$$

Culex

$$\begin{aligned}
\dot{P}_3(t) &= \mu_3 C_0 - \theta_3 P_3, \\
\dot{S}_3(t) &= \theta_3 P_3 - \frac{\sigma_3\sigma_2\beta_{32}}{\sigma_3 N_3 + \sigma_2 N_2} I_2 S_3 - \mu_3 S_3, \\
\dot{E}_3(t) &= \frac{\sigma_3\sigma_2\beta_{32}}{\sigma_3 N_3 + \sigma_2 N_2} I_2 S_3 - \gamma_3 E_3 - \mu_3 E_3, \\
\dot{I}_3(t) &= \gamma_3 E_3 - \mu_3 I_3,
\end{aligned} \tag{4.3}$$

Ticks

$$\begin{aligned}
\dot{S}_a(t) &= \frac{\alpha N_2 S_d}{1 + S_a + I_a} - \beta_{t2} I_2 S_a - \delta N_2 S_a, \\
\dot{S}_d(t) &= b_t(S_a + I_a) - \frac{\alpha N_2 S_d}{1 + S_a + I_a} + \delta N_2 S_a - d_t S_d, \\
\dot{I}_a(t) &= \beta_{t2} I_2 S_a + \frac{\alpha N_2 I_d}{1 + S_a + I_a} - \delta N_2 I_a, \\
\dot{I}_d(t) &= \delta N_2 I_a - \frac{\alpha N_2 I_d}{1 + S_a + I_a} - d_t I_d.
\end{aligned} \tag{4.4}$$

Variables	Description of the model (4.1-4.4) variables
S_a	Number of attached susceptible ticks
S_d	Number of detached susceptible ticks
I_a	Number of attached infected ticks
I_d	Number of detached infected ticks

TABLE 4.1: Description of state variables of the RVF model. Other state variables are described in Table 2.1 in Chapter 3.

For *Aedes*-Livestock-*Culex* RVF horizontal transmission we assume that the total number of bites varies with both the livestock and mosquito population sizes (for more details see [5]). While for the tick-livestock RVF horizontal transmission we assume that the livestock and ticks separate populations that interact in a similar manner as in a prey-predator system [120], such that the number of newly infected ticks is proportional to infected livestock and the number of newly infected

livestock is proportional to attached infected ticks [131]. Therefore, the forces of infections are given by:

$$\begin{aligned}
\lambda_1 = \lambda_{12} &= \frac{\sigma_1\sigma_2 N_2}{\sigma_1 N_1 + \sigma_2 N_2}\beta_{12}\frac{I_2}{N_2} = \frac{\sigma_1\sigma_2\beta_{12} I_2}{\sigma_1 N_1 + \sigma_2 N_2},\\
\lambda_2 = \lambda_{21} + \lambda_{23} + \lambda_{2t} &= \frac{\sigma_1\sigma_2\beta_{21} I_1}{\sigma_1 N_1 + \sigma_2 N_2} + \frac{\sigma_3\sigma_2\beta_{23} I_3}{\sigma_3 N_3 + \sigma_2 N_2} + \beta_{2t} I_a,\\
\lambda_3 = \lambda_{32} &= \frac{\sigma_3\sigma_2 N_2}{\sigma_3 N_3 + \sigma_2 N_2}\beta_{32}\frac{I_2}{N_2} = \frac{\sigma_3\sigma_2\beta_{32} I_2}{\sigma_3 N_3 + \sigma_2 N_2},\\
\lambda_4 = \lambda_{t2} &= \beta_{t2} I_2.
\end{aligned} \tag{4.5}$$

Parameters	**RVF model (4.1-4.4) parameters and their dimensions**
b_t/d_t	Tick birth/death rate, Days^{-1}
β_{t2}	Transmission rate of infection from livestock to ticks, Days^{-1}
β_{2t}	Transmission rate of infection ticks to livestock, Days^{-1}
δ	Detachment rate, Days^{-1}
α	Attachment rate, Days^{-1}
L_0	Stable livestock population in the absence of the disease, dimensionless
A_0	Stable *Aedes* mosquito population, dimensionless
C_0	Stable *Culex* mosquito population, dimensionless

TABLE 4.2: Parameters of the RVF model. Other model parameters are described in Table A.2 in Appendix A.

To establish the positivity and feasibility of solutions of the model system (4.1-4.4) we discuss two invariant sub-systems as follows:

I. A sub-system of uninfected livestock, attached and detached ticks such that:

$$\begin{aligned}
\dot{S}_2(t) &= \mu_2 L_0 - \mu_2 S_2,\\
\dot{S}_a(t) &= \frac{\alpha N_2 S_d}{1 + S_a} - \delta N_2 S_a,\\
\dot{S}_d(t) &= b_t S_a - \frac{\alpha N_2 S_d}{1 + S_a} + \delta N_2 S_a - d_t S_d.
\end{aligned} \tag{4.6}$$

In the absence of the disease $S_2 = L_0$, thus the livestock population is at equilibrium. Now we can investigate the remaining two equations of sub-system (4.6) describing the dynamics of ticks as in [120]. Clearly there is one free-tick equilibrium $(S_a, S_d) = (0, 0)$, however, we are interested on the non-trivial one. Adding the last two equations of (4.6) and equating the sum to zero we obtain:

$$S_a = \frac{d_t}{b_t} S_d. \tag{4.7}$$

Then after substituting equation (4.7) into the last equation of (4.6) gives

$$S_d = \frac{\alpha b_t^2 - \delta b_t d_t}{\delta d_t^2}, \tag{4.8}$$

such that the quantities S_a and S_d are only positive if and only if

$$\frac{\alpha b_t}{\delta d_t} > 1. \tag{4.9}$$

Clearly the equilibrium $(S_a, S_d) = (0, 0)$ is unstable if equation (4.9) holds. The trace of the Jacobian matrix for the (S_a, S_d) system is negative. Thus, by the negative criteria of Bendixon, periodic orbits do not exist which implies that every trajectory goes to a stationary point [120, 132].

II. Now we consider a system made of livestock, *Aedes* and *Culex* mosquitoes only. However, when no confusion arises we establish the positivity of solutions of this sub-system together with the tick sub-system to avoid repetition.

Hence, we reorganize the system (4.1-4.4) and write it in matrix form as

$$\frac{dX}{dt} = M(x)X + F \tag{4.10}$$

where $X = (P_1, U_1, S_1, E_1, I_1, S_2, I_2, R_2, P_3, S_3, E_3, I_3, S_a, S_d, I_a, I_d)$. $M(x)$ is a 16 by 16 matrix and F is a column matrix. Substituting $I_1 = N_1 - S_1 - E_1$ we have $\dot{P}_1(t) = \mu_1 A_0(1-q_1) + \mu_1 q_1 A_0 S_1 + \mu_1 q_1 A_0 E_1 - \theta_1 P_1$. Thus

$$M(x) = \begin{pmatrix} M_1(x) & 0 & 0 & 0 \\ 0 & M_2(x) & 0 & 0 \\ 0 & 0 & M_3(x) & 0 \\ 0 & 0 & 0 & M_4(x) \end{pmatrix}, \tag{4.11}$$

where

$$M_1 = \begin{pmatrix} -\theta_1 & 0 & \mu_1 q_1 A_0 & \mu_1 q_1 A_0 & 0 \\ 0 & -\theta_1 & 0 & 0 & \mu_1 q_1 \frac{A_0}{N_1} \\ \theta_1 & 0 & -g_1 I_2 - \mu_1 & 0 & 0 \\ 0 & 0 & g_1 I_2 & -(\gamma_1 + \mu_1) & 0 \\ 0 & \theta_1 & 0 & \gamma_1 & -\mu_1 \end{pmatrix}, M_2 = \begin{pmatrix} -g_3 I_1 - g_4 I_3 - \beta_{2t} I_A - \mu_2 & 0 & 0 \\ g_3 I_1 + g_4 I_3 + \beta_{2t} I_A & -(\varepsilon_2 + m_2 + \mu_2) & 0 \\ 0 & \varepsilon_2 & -\mu_2 \end{pmatrix}, \tag{4.12}$$

$$M_3 = \begin{pmatrix} -\theta_3 & 0 & 0 & 0 \\ \theta_3 & -g_5 I_2 - \mu_3 & 0 & 0 \\ 0 & g_5 I_2 & -(\gamma_3 + \mu_3) & 0 \\ 0 & 0 & \gamma_3 & -\mu_3 \end{pmatrix}, M_4 = \begin{pmatrix} -b_{t2} I_2 - \delta N_2 & \frac{\alpha N_2}{1+S_a+I_a} & 0 & 0 \\ b_t + \delta N_2 & -\frac{\alpha N_2}{1+S_a+I_a} & b_t & 0 \\ \beta_{t2} I_2 & 0 & -\delta N_2 - d_t & \frac{\alpha N_2}{1+S_a+I_a} \\ 0 & 0 & \delta N_2 & -\frac{\alpha N_2}{1+S_a+I_a} - d_t \end{pmatrix} \tag{4.13}$$

and $F = (\mu_1 A_0(1-q_1), 0, 0, 0, 0, \mu_2 L_0, 0, 0, \mu_3 C_0, 0, 0, 0, 0, 0, 0, 0)^T$.
Combining all matrices together, $M(x)$ is a Metzler matrix, i.e. a matrix such that off diagonal terms are non-negative, for all $\mathbb{R}_+^{16}$. F is non-negative given the fact that $1 - q_1 \geq 0$ and F is Lipschitz continuous. Thus, system (4.10) is positively

invariant in $\mathbb{R}^{16}_{+}$. Then, the feasible region for the model system is the set

$$\Phi = \left\{ (P_1, U_1, S_1, E_1, I_1, S_2, I_2, R_2, P_3, S_3, E_3, I_3, S_a, S_d, I_a, I_d) \geq 0 \in \mathbb{R}^{16}_{+} \right\}. \quad (4.14)$$

The solution remains in the feasible region Φ if it starts in this region. Hence, the system is epidemiologically and mathematically well posed and it is sufficient to study the dynamics of the model in Φ.

4.3 Model Analysis and Results

4.3.1 Existence and stability of equilibrium points

We analyse model system (4.1-4.4) to obtain equilibrium points of the system and their stability. Let
$X(P_1^*, U_1^*, S_1^*, E_1^*, I_1^*, S_2^*, I_2^*, R_2^*, P_3^*, S_3^*, E_3^*, I_3^*, S_a^*, S_d^*, I_a^*, I_d^*)$ be an arbitrary equilibrium point of system (4.1-4.4). At the equilibrium point, we have

$$P_1' = U_1' = S_1' = E_1' = I_1' = S_2' = I_2' = R_2' = P_3' = S_3' = E_3' = I_3' = S_a' = S_d' = I_a' = I_d' = 0. \quad (4.15)$$

4.3.1.1 Disease-free equilibrium (DFE), X^0

In the absence of the disease, that is, $U_1^0 = E_1^0 = I_1^0 = I_2^0 = E_3^0 = I_3^0 = I_a^0 = I_d^0 = 0$, model system (4.1-4.4) has an equilibrium point called the disease-free equilibrium, X^0. When solving for the equilibria equation (4.15) for the tick sub-model we obtain

$$\{S_d^0, S_a^0\} = \{0, 0\} \text{ or } \left\{ \frac{(b_t\alpha - \delta d_t)b_t}{d_t^2\delta}, \frac{b_t\alpha - \delta d_t}{\delta d_t} \right\}. \quad (4.16)$$

The later is biologically significant whenever $b_t\alpha > d_t\delta$. At equilibrium the birth is equal to the death rate, hence the inequality $b_t\alpha > d_t\delta$ can be written as $\alpha > \delta \Leftrightarrow \frac{\alpha}{\delta} > 1$. $1/\delta$ refers to the time ticks spend attached to the host and α/δ is the rate that gives rise to the number of newly attached ticks. This shows that we have two possible disease-free equilibria: one when we do not have a tick population at all, that is a system without ticks; another one with the presence of ticks. Since we are interested in studying the role of ticks in the spread of RVF among livestock, we consider $S_d^0 > 0$ and $S_a^0 > 0$. Therefore the disease-free equilibrium of the system is given by

$$\begin{aligned} X^0 &= (P_1^0, 0, S_1^0, 0, 0, S_2^0, 0, 0, P_3^0, S_3^0, 0, 0, S_a^0, S_d^0, 0, 0) \\ &= \left(\tfrac{\mu_1 A_0}{\theta_1}, 0, A_0, 0, 0, L_0, 0, 0, \tfrac{\mu_3 C_0}{\theta_3}, C_0, 0, 0, \tfrac{b_t\alpha - \delta d_t}{\delta d_t}, \tfrac{(b_t\alpha - \delta d_t)b_t}{d_t^2\delta}, 0, 0 \right). \end{aligned} \quad (4.17)$$

In order to establish the linear stability of the model equilibria states, we employ the next generation matrix approach of [101]. A reproduction number obtained in this way determines the local stability of the disease-free equilibrium for $R_0 < 1$ and instability for $R_0 > 1$. Its definition follows the notation in [101] as done in previous chapters and for details on the derivation of the matrices F and V see Appendix C Section C.1.

Hence, the basic reproduction number, R_0 is the largest eigenvalue of the spectral radius of FV^{-1} and is given by

$$R_0 = \frac{1}{2}R_{0,V} + \frac{1}{2}\sqrt{R_{0,V}^2 + 4R_{0,H}^2}, \tag{4.18}$$

where

$$R_{0,V} = \frac{\mu_1 q_1}{\mu_1} \tag{4.19}$$

and

$$R_{0,H} = \sqrt{\frac{\gamma_1}{\gamma_1+\mu_1}\frac{g_3 S_2^0}{\mu_1} \times \frac{g_1 S_1^0}{\varepsilon_2+m_2+\mu_2} + \frac{\gamma_3}{\gamma_3+\mu_3}\frac{g_4 S_2^0}{\mu_3} \times \frac{g_5 S_3^0}{\varepsilon_2+m_2+\mu_2} + \left(\frac{\beta_{2t} S_2^0 \alpha}{d_t(1+S_a^0)\delta} + \frac{\beta_{2t} S_2^0}{\delta N_2}\right)\frac{\beta_{t2} S_a^0}{\varepsilon_2+m_2+\mu_2}}, \tag{4.20}$$

where $g_1 = \frac{\sigma_1\sigma_2\beta_{12}}{\sigma_1 A_0+\sigma_2 L_0}$, $g_3 = \frac{\sigma_1\sigma_2\beta_{21}}{\sigma_1 A_0+\sigma_2 L_0}$, $g_4 = \frac{\sigma_3\sigma_2\beta_{23}}{\sigma_3 C_0+\sigma_2 L_0}$ and $g_5 = \frac{\sigma_3\sigma_2\beta_{32}}{\sigma_3 C_0+\sigma_2 L_0}$.
In the absence of vertical transmission, $q_1 = 0$, R_0 is the geometric mean of the number of new infections in livestock from infected *Aedes*, *Culex* mosquitoes and ticks, and the number of new infections in both mosquitoes and ticks from an infected ruminant in the limiting case that both livestock and vector populations are fully susceptible.

4.3.1.2 Biological interpretation of R_0

From the expression for $R_{0,H}$ we obtain the following sub-reproduction numbers:

$$\bar{R}_0^1 = \frac{\gamma_1}{\gamma_1+\mu_1}\frac{g_3 S_2^0}{\mu_1} \times \frac{g_1 S_1^0}{\varepsilon_2+m_2+\mu_2}$$

is the basic reproduction number for the model without vertical transmission, *Culex* mosquitoes and ticks;

$$R_0^3 = \frac{\gamma_3}{\gamma_3+\mu_3}\frac{g_4 S_2^0}{\mu_3} \times \frac{g_5 S_3^0}{\varepsilon_2+m_2+\mu_2}$$

is the basic reproduction number for the model without *Aedes* mosquitoes and ticks, and

$$R_0^t = \left(\frac{\beta_{2t} S_2^0 \alpha}{d_t(1+S_a^0)\delta} + \frac{\beta_{2t} S_2^0}{\delta L_0}\right)\frac{\beta_{t2} S_a^0}{\varepsilon_2+m_2+\mu_2}$$

is the basic reproduction number for the model without *Aedes* and *Culex* mosquitoes. $\bar{R}_0^1$ is the product of $R_{21} \times R_{12}$, where R_{21} is the number of new infections in livestock from one infected *Aedes* mosquito and is given by

$$R_{21} = \frac{\gamma_1}{\gamma_1 + \mu_1} \times \frac{g_3 S_2^0}{\mu_1} = \frac{\gamma_1}{\gamma_1 + \mu_1} \times \frac{\sigma_1 \sigma_2 \beta_{21} S_2^0}{\sigma_1 A_0 + \sigma_2 L_0} \times \frac{1}{\mu_1},$$

representing the product of the probability that an *Aedes* mosquito survives the exposed stage $\frac{\gamma_1}{\gamma_1+\mu_1}$, the number of bites on livestock per mosquito $\frac{\sigma_1\sigma_2}{\sigma_1 A_0+\sigma_2 L_0} S_2^0$, the probability of transmission per bite β_{21}, and the infectious lifespan of an *Aedes* mosquito $1/\mu_1$. R_{12} is the number of new infections in *Aedes* mosquitoes from one infected ruminant, and is given by

$$R_{12} = \frac{g_1 S_1^0}{\varepsilon_2 + m_2 + \mu_2} = \frac{\sigma_1 \sigma_2 \beta_{12} S_1^0}{\sigma_1 A_0 + \sigma_2 L_0} \times \frac{1}{\varepsilon_2 + m_2 + \mu_2},$$

which describe the product of the number of bites a ruminant receives $\frac{\sigma_1\sigma_2}{\sigma_1 A_0+\sigma_2 L_0} S_1^0$, the probability of transmission per bite β_{12} from an infected animal and the duration of the infective period $\frac{1}{\varepsilon_2+m_2+\mu_2}$ for a ruminant.
R_0^3 is the product of $R_{23} \times R_{32}$, where R_{23} is the number of new infections in livestock from one infected *Culex* mosquito and is given by

$$R_{23} = \frac{\gamma_3}{\gamma_3 + \mu_3} \times \frac{g_4 S_2^0}{\mu_3} = \frac{\gamma_3}{\gamma_3 + \mu_3} \times \frac{\sigma_3 \sigma_2 \beta_{23} S_2^0}{\sigma_3 C_0 + \sigma_2 L_0} \times \frac{1}{\mu_3},$$

which is the product of the probability that a *Culex* mosquito survives the exposed stage $\frac{\gamma_3}{\gamma_3+\mu_3}$, the number of bites on livestock per mosquito $\frac{\sigma_3\sigma_2}{\sigma_3 C_0+\sigma_2 L_0} S_2^0$, the probability of transmission per bite β_{23}, and the infectious lifespan of a *Culex* mosquito $1/\mu_3$. R_{32} is the number of new infections in *Culex* mosquitoes from an infected livestock and is given by

$$R_{32} = \frac{g_5 S_3^0}{\varepsilon_2 + m_2 + \mu_2} = \frac{\sigma_3 \sigma_2 \beta_{32} S_3^0}{\sigma_3 L_0 + \sigma_2 L_0} \times \frac{1}{\varepsilon_2 + m_2 + \mu_2}.$$

This is the product of number of bites one ruminant receives $\frac{\sigma_3\sigma_2}{\sigma_3 C_0+\sigma_2 L_0} S_3^0$, the probability of transmission per bite β_{32} an infected ruminant and the duration of the infective period $\frac{1}{\varepsilon_2+m_2+\mu_2}$ for a ruminant. R_0^t is the product of $R_{2t} \times R_{t2}$, where R_{2t} is the number of new infections in livestock from one infected attached tick and is given by

$$R_{2t} = \frac{\beta_{2t} \alpha S_2^0}{d_t(1 + S_a^0)} + \frac{\beta_{2t}}{\delta},$$

which is the product of the probability of transmission β_{2t} from an infectious tick, number of ticks attached to the host $\frac{\alpha S_2^0}{1+S_a^0}$, and the infectious lifespan of ticks $1/d_t$ together with new infections β_{2t}/δ during the attached period. R_{t2} represents the number of new infections in ticks from one infected ruminant and is given by

$$R_{t2} = \frac{\beta_{t2} S_a^0}{\varepsilon_2 + m_2 + \mu_2},$$

which is the product of the probability of transmission β_{t2} from an infected ruminant to attached susceptible ticks, number of susceptible ticks S_a^0 and the livestock infective period $1/(\varepsilon_2 + m_2 + \mu_2)$.
The square root in the expression for R_0 comes from the 'two generations' required for an infected vector or host to reproduce itself.
If $q_1 > 0$, R_0 increases because vertical transmission directly increases the number of infectious mosquitoes and indirectly increases the transmission from livestock to mosquitoes and back to livestock. Therefore, from [101] (Theorem 2), the following result holds;

Lemma 4.1. *The disease-free equilibrium X^0, of the RVF model with ticks, given by (4.1-4.4) is locally asymptotically stable if $R_0 < 1$, and unstable if $R_0 > 1$.*

Note that, applying Theorem 2 in [101] we state that for $R_0 > 1$ there exists an endemic equilibrium (EE), a solution where the disease persists in the community. However, we will not be investigating the stability of the EE for the following reasons: the model is too complex to analytically derive expressions for the EE, and it will be a daunting task to analyse its stability. This will be considered in a subsequent study that will extend the model and then employ techniques of numerical simulations.

4.3.1.3 Global asymptotic stability of DFE, X^0

Following the approach and results obtained by [133] and successfully applied in [134] and using the properties of DFE, we write the system (4.1-4.4) in the following form

$$\begin{aligned} \dot{x}_S &= A_1(x)(x_S - x_{DFE,S}) + A_{12}(x)x_I \\ \dot{x}_I &= A_2(x)x_I \end{aligned} \tag{4.21}$$

where x_S is the vector representing disease-free compartments (susceptible and immune individuals) and the vector x_I represents the state of infected compartments (exposed and infectious individuals). Hence, we have $x_S = (P_1, S_1, S_2, R_2, P_3, S_3, S_a, S_d)^T$, $x_I = (U_1, E_1, I_1, I_2, E_3, I_3, I_a, I_d)^T$ and $x_{DFE,S} = (P_1^0, S_1^0, S_2^0, R_2^0, P_3^0, S_3^0, S_a^0, S_d^0)^T$.
Then we rewrite some equations of system (4.1-4.4) as follows:

$$\dot{P}_1(t) = -\theta_1(P_1 - P_1^0) - \mu_1 q_1 A_0 \frac{I_1}{N_1}, \tag{4.22}$$

$$\dot{S}_1(t) = \theta_1(P_1 - P_1^0) - g_1 I_2 S_1 - \mu_1(S_1 - S_1^0), \tag{4.23}$$

$$\dot{S}_2(t) = -\mu_2(S_2 - S_2^0) - g_3 I_1 S_2 - g_4 I_3 S_2 - \beta_{2t} I_a S_2, \tag{4.24}$$

$$\dot{P}_3(t) = -\theta_3(P_3 - P_3^0), \tag{4.25}$$

$$\dot{S}_3(t) = \theta_3(P_3 - P_3^0) - g_5 I_2 S_3 - \mu_3(S_3 - S_3^0), \tag{4.26}$$

$$\dot{S}_a(t) = \frac{\alpha N_2 S_d}{1 + S_a + I_a} - (\beta_{t2} I_2 + \delta N_2)(S_a - S_a^0) - (\beta_{t2} I_2 + \delta N_2) S_a^0, \tag{4.27}$$

$$\dot{S}_d(t) = b_t(S_a + I_a) + \delta N_2 S_a - \left(\frac{\alpha N_2}{1 + S_a + I_a} + d_t\right)(S_d - S_d^0) - \left(\frac{\alpha N_2}{1 + S_a + I_a} + d_t\right) S_d^0. \tag{4.28}$$

Thus, we obtain the following matrices for $A_1(x), A_{12}(x)$ and $A_2(x)$

$$A_1(x) = \begin{pmatrix} -\theta_1 & 0 & 0 & 0 & 0 & 0 & 0 & 0 \\ \theta_1 & -\mu_1 & 0 & 0 & 0 & 0 & 0 & 0 \\ 0 & 0 & -\mu_2 & 0 & 0 & 0 & 0 & 0 \\ 0 & 0 & 0 & -\mu_2 & 0 & 0 & 0 & 0 \\ 0 & 0 & 0 & 0 & -\theta_3 & 0 & 0 & 0 \\ 0 & 0 & 0 & 0 & \theta_3 & -\mu_3 & 0 & 0 \\ 0 & 0 & 0 & 0 & 0 & 0 & -(\beta_{t2}I_2+\delta N_2) & \frac{\alpha N_2}{1+S_a^0} \\ 0 & 0 & 0 & 0 & 0 & 0 & \delta N_2 & -(\frac{\alpha N_2}{1+S_a^0}+d_t) \end{pmatrix} \tag{4.29}$$

$$A_{12}(x) = \begin{pmatrix} 0 & 0 & -\mu_1 q_1 A_0 \frac{I_1}{N_1} & 0 & 0 & 0 & 0 & 0 \\ 0 & 0 & 0 & -g_1 S_1 & 0 & 0 & 0 & 0 \\ 0 & 0 & -g_3 S_2 & 0 & 0 & -g_4 S_2 & -\beta_{2t} S_2 & 0 \\ 0 & 0 & 0 & \varepsilon_2 & 0 & 0 & 0 & 0 \\ 0 & 0 & 0 & 0 & 0 & 0 & 0 & 0 \\ 0 & 0 & 0 & -g_3 S_3 & 0 & 0 & 0 & 0 \\ 0 & 0 & 0 & -\beta_{t2} S_a^0 & 0 & 0 & -\frac{\alpha N_2 S_d}{(1+S_a+I_a)^2} & \frac{\alpha N_2}{1+S_a+I_a} \\ 0 & 0 & 0 & 0 & 0 & 0 & b_t - \frac{\alpha N_2 S_d}{(1+S_a+I_a)^2} & 0 \end{pmatrix} \tag{4.30}$$

and

$$A_2(x) = \begin{pmatrix} -\theta_1 & 0 & \mu_1 q_1 A_0 \frac{I_1}{N_1} & 0 & 0 & 0 & 0 & 0 \\ 0 & -(\gamma_1+\mu_1) & 0 & g_1 S_1 & 0 & 0 & 0 & 0 \\ \theta_1 & \gamma_1 & -\mu_1 & 0 & 0 & 0 & 0 & 0 \\ 0 & 0 & g_3 S_2 & -(\varepsilon_2+m_2+\mu_2) & 0 & g_4 S_2 & \beta_{2t} S_2 & 0 \\ 0 & 0 & 0 & g_5 S_3 & -(\gamma_3+\mu_3) & 0 & 0 & 0 \\ 0 & 0 & 0 & 0 & \gamma_3 & -\mu_3 & 0 & 0 \\ 0 & 0 & 0 & \beta_{t2} S_a & 0 & 0 & -(\frac{\alpha N_2 I_d}{(1+S_a+I_a)^2}+\delta N_2) & \frac{\alpha N_2}{1+S_a+I_a} \\ 0 & 0 & 0 & 0 & 0 & 0 & \frac{\alpha N_2 I_d}{(1+S_a+I_a)^2}+\delta N_2 & -(\frac{\alpha N_2}{1+S_a+I_a}+d_t) \end{pmatrix}. \tag{4.31}$$

Both $A_1(x)$ and $A_2(x)$ are Metzler matrices and the eigenvalues of matrix $A_1(x)$ are real and negative. Thus, the system
$\dot{x}_S = A_1(x)(x_S - x_{DFE,S})$ is globally asymptotically stable (GAS) at $x_{DFE,S}$. In order to proceed with the investigation of the GAS of the disease-free equilibrium, X^0 we base our results on the Theorem in [133], which was successfully applied in [134].

Theorem 4.2. *Let $\Phi \subset \mathcal{U} = \mathbb{R}^8_+ \times \mathbb{R}^8_+$. The system (4.21) is of class C^1, defined on $\mathcal{U}$ if*

1. *$\mathcal{U}$ is positively invariant relative to (4.21),*
2. *The system $\dot{x}_S = A_1(x)(x_S - x_{DFE,S})$ is GAS at $x_{DFE,S}$,*
3. *For any $x \in \Phi$, matrix $A_2(x)$ is Metzler irreducible,*
4. *There exists a matrix $\bar{A}_2$, which is an upper bound of the set $\mathcal{M} = \{A_2(x) \in \mathcal{M}_8(\mathbb{R}) | x \in \bar{\Phi}\}$, with the property that if $\bar{A}_2 \in \mathcal{M}$, for any $\bar{x} \in \bar{\Phi}$, such that $A_2(\bar{x}) = \bar{A}_2$, then $\bar{x} \in \mathcal{R}^8 \times \{0\}$,*
5. *The stability modulus of $\bar{A}_2, \alpha(\bar{A}_2) = max_{\lambda \in S_p(A_2)} Re\,(\lambda)$, satisfies $\alpha(\bar{A}_2) \leq 0$.*

Then the DFE is GAS in $\bar{\Phi}$

Proof. The proof of the theorem requires verification of its underlying assumptions: it is obvious that condition (1-3) are satisfied. In particular for all $x \in \Phi$, $A_2(x)$ is irreducible if and only if $(I + |A_2(x)|)^7 > 0$. An upper bound of the set of matrices $\mathcal{M}$, which is the matrix $\bar{A}_2$ is given by matrix $A_2(\bar{x})$, where $\bar{x} = (\bar{P}_1, \bar{S}_1, \bar{S}_2, 0, \bar{P}_3, \bar{S}_3, \bar{S}_a, \bar{S}_d, 0, 0, 0, 0, 0, 0, 0, 0) \in \mathbb{R}^8 \times \{0\}$. Similarly matrix $\bar{A}_2$ is irreducible. Recall that the Perron-Frobenius theorem for an irreducible matrix states that one of the matrix eigenvalues is positive and greater than or equal to all others, that is, the dominant eigenvalue. Thus, matrix A_2 is exactly the matrix used to compute the basic reproductive number, i.e., the dominant eigenvalue. For more details or proof in general settings see [133]. □

Conditions (1-4) are now verified. The proof of the last condition is based on the following Lemma in [133], also successfully applied in [134].

Lemma 4.3. *Let H be a square Metzler matrix written in block form $H = \left(\begin{smallmatrix} A & B \\ C & D \end{smallmatrix}\right)$, with A and D squares matrices. H is Metzler stable if and only if matrices A and $D - CA^{-1}B$ are Metzler stable.*

Thus, matrix $A_2(x)$ can be written in the following block form:

$$A = \begin{pmatrix} -\theta_1 & 0 & \mu_1 q_1 A_0 \frac{I_1}{N_1} & 0 \\ 0 & -(\gamma_1+\mu_1) & 0 & g_1 S_1 \\ \theta_1 & \gamma_1 & -\mu_1 & 0 \\ 0 & 0 & g_3 S_2 & -(\varepsilon_2+m_2+\mu_2) \end{pmatrix}, B = \begin{pmatrix} 0 & 0 & 0 & 0 \\ 0 & 0 & 0 & 0 \\ 0 & 0 & 0 & 0 \\ 0 & g_4 S_2 & \beta_{2t} S_2 & 0 \end{pmatrix},$$

$$C = \begin{pmatrix} 0 & 0 & 0 & g_4 S_2 \\ 0 & 0 & 0 & 0 \\ 0 & 0 & 0 & \beta_{t2} S_a \\ 0 & 0 & 0 & 0 \end{pmatrix}, D = \begin{pmatrix} -(\gamma_3+\mu_3) & 0 & 0 & 0 \\ \gamma_3 & -\mu_3 & 0 & 0 \\ 0 & 0 & -(\frac{\alpha N_2 I_d}{(1+S_a+I_a)^2}+\delta N_2) & \frac{\alpha N_2}{1+S_a+I_a} \\ 0 & 0 & \frac{\alpha N_2 I_d}{(1+S_a+I_a)^2}+\delta N_2 & -(\frac{\alpha N_2}{1+S_a+I_a}+d_t) \end{pmatrix}.$$

A is a stable Metzler matrix and

$$D - CA^{-1}B = \begin{pmatrix} -(\gamma_3+\mu_3) & \frac{(\mu_1-\mu_1 q_1)(\gamma_1+\mu_1) g_5 \bar{S}_3 g_4 \bar{S}_2}{1-R_0^1} & \frac{(\mu_1-\mu_1 q_1)(\gamma_1+\mu_1) g_5 \bar{S}_3 \beta_{2t} \bar{S}_2}{1-R_0^1} & 0 \\ 0 & -\mu_3 & 0 & 0 \\ 0 & \frac{(\mu_1-\mu_1 q_1)(\gamma_1+\mu_1) \beta_{t2} \bar{S}_a g_4 \bar{S}_2}{1-R_0^1} & -\delta N_2 + \frac{(\mu_1-\mu_1 q_1)(\gamma_1+\mu_1) \beta_{t2} \bar{S}_a \beta_{2t} \bar{S}_2}{1-R_0^1} & 0 \\ 0 & 0 & \delta N_2 & -\frac{\delta N_2}{1+\bar{S}_a} - d_t \end{pmatrix}$$

is a stable Metzler matrix if $\frac{\beta_{2t}\bar{S}_2}{\delta N_2} \frac{\beta_{t2}\bar{S}_a}{\varepsilon_2+m_2+\mu_2} < \frac{1-R_0^1}{(\mu_1-\mu_1 q_1)(\gamma_1+\mu_1)(\varepsilon_2+m_2+\mu_2)}$ (see Appendix C Section C.2). It is worth noting that at disease-free equilibrium $N_1 = A_0$. Finally, from Theorem 4.2 and Lemma 4.3, we deduce the following:

Theorem 4.4. *If $b_t \alpha > d_t \delta$, then the disease-free equilibrium of the system (4.1-4.4),*
$(P_1^0, 0, S_1^0, 0, 0, S_2^0, 0, 0, P_3^0, S_3^0, 0, 0, S_a^0, S_d^0, 0, 0)$ exists and is globally asymptotically stable if $R_0^1 < 1$ and $\frac{\beta_{2t}\bar{S}_2}{\delta N_2} \frac{\beta_{t2}\bar{S}_a}{\varepsilon_2+m_2+\mu_2} < \frac{1-R_0^1}{(\mu_1-\mu_1 q_1)(\gamma_1+\mu_1)(\varepsilon_2+m_2+\mu_2)}$.

The above result is epidemiologically relevant, because it shows that even though disease vectors such as *Culex* and *H. truncatum* and others, may play a significant

role on amplifying the disease, the initial spread of RVF outbreaks depends on the competence of the *Aedes* species. From Theorem 4.4 we observe that $R_{0,V}$ should be kept below unity. This is an indication that if at any time, through appropriate interventions (e.g. destruction of breading sites, herd vaccination, etc), we are able to lower R_0^1 below unity and R_0^t below its critical value, then the disease will die out. From $R_0^1 = \frac{1}{\mu_1 - \mu_1 q_1}\bar{R}_0^1$, which depends on both *Aedes* mosquitoes vertical and horizontal transmission, the inequality, $\mu_1 q_1 < \mu_1$, shows that vertical infection efficiency should be kept below the threshold, which can be accomplished by destroying possible locations that may allow *Aedes* eggs to dessicate. $\bar{R}_0^1 < 1$ shows that horizontal transmission can be controlled for instance through herd immunization. Another important relation is $\frac{\beta_{t2}\bar{S}_2}{\delta N_2}\frac{\beta_{2t}\bar{S}_a}{\varepsilon_2+m_2+\mu_2} < \frac{1-R_0^1}{(\mu_1-\mu_1 q_1)(\gamma_1+\mu_1)(\varepsilon_2+m_2+\mu_2)}$, the left hand side is related to R_0^t describing the host-ticks interactions while the right side describes the *Aedes* ability to intermediate disease invasion. From this we learn that if herd immunity is not attained and ticks are capable of transmitting the disease, host-ticks interactions may serve as disease reservoirs or possibly disease amplifiers. Therefore, we argue that if ticks are capable of carrying and transmitting RVFV, ticks may play an important role in the spread of the disease and may also be more responsible for RVF inter-epidemic activities.

4.4 Numerical Simulation

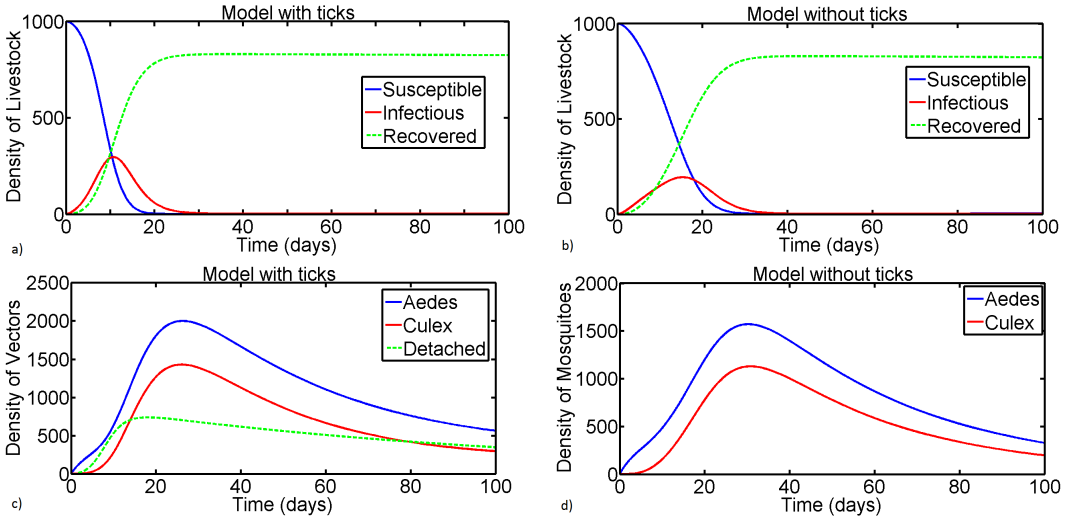

FIGURE 4.2: Time series plot of both mammalian and vector populations against time of a model with and without ticks. The initial conditions are $S_1 = 5000, P_1 = 1000, U_1 = 400, E_1 = 0, I_1 = 1, S_2 = 1000, I_2 = 1, R_2 = 0, S_3 = 5000, P_3 = 1000, E_3 = 0$ and $I_3 = 1, S_a = 1000, S_d = 0, I_a = I_d = 1$.

To explore the behaviour of RVF when introduced into a naive population taking into account ticks as RVF competent vectors, we conducted numerical simulations of an isolated system (i.e. no immigration or emigration). The model uses a daily time

step and high rainfall and moderate temperature (wet season) parameter values see Table C.1. Figure 4.2.(a) depicts the time series plot of susceptible, infectious and recovered livestock for a model with ticks while (b) shows the dynamics of disease transmission in livestock within a model without ticks. The epidemic is very brief lasting for only 20 and 30 days and reaching its peak at about 10 and 15 days for a model with and without ticks respectively. This results indicate that ticks not only increase the size of an epidemic but also accelerate it and reduce its duration. Data about cases of infected livestock are very difficult to compile for several reasons: (1) RVF cases are not clinically specific and laboratory confirmation is necessary; (2) virus isolation techniques are costly and time consuming, and require high biocontainment level facilities [11]; (3) RVF outbreaks occur in rural areas with low accessibility to various needed services and during this period most of the areas are flooded and cannot be accessed by road. However, information about human cases is available although it is not representative as it only captures clinical cases reported in some district level hospitals [58]. Human cases appear about one month after infection in livestock and they reach a peak between the fourth and sixth week after the onset of the epidemic [13, 58, 128, 129]. Figs.4.2(c) and (d) depict the time series plot of infectious *Aedes*, *Culex* mosquitoes and infectious detached ticks for a model with and without ticks respectively. Their population densities reach their peak at approximately 25 and 30 days respectively. This results suggest that by time mosquito population reaches its peak the peak of the disease in the mammalian host is already passed, meaning that the presence of mosquitoes may not be appropriate for timing the peak of the outbreak, highlighting the necessity of continuous surveillance and communications with communities in endemic areas as has been pointed out by empirical studies [13, 39, 58].

4.5 Sensitivity Analysis

To assess the impact of the parameters and decision rules within the model, uncertainty in input parameters and their sensitivity analysis are performed to determine how sensitive the model is to changes/shifts in the values of the parameters [84, 135]. Many of the parameters in disease epidemiological models can be found in the literature, not necessarily as constants but as approximate values or intervals. These intervals describe the range of values a parameter may assume with the evolution of the disease [88]. In order to measure the sensitivity of the model, two different approaches are considered. One is based on perturbation of the model parameters, useful for determining the impact of local changes, while the other is based on uncertainty in the model parameter estimation, which allows for determining the impact of global changes [84].

4.5.1 Global sensitivity analysis

Here, we employed the Latin Hypercube Sampling (LHS) technique, which belongs to the Monte Carlo class of sampling methods [136]. LHS technique is a stratified

sampling without replacement, where each parameter distribution is divided in N equal probable intervals, which are then sampled [83]. For each input parameter we assumed uniform distribution [69] across the range listed in Table **??** (see Appendix C Section C.3). We calculated R_0 using $N = 1000$ sets of sampled parameters as the model output. In the LHS scheme, all model parameters are independent and varied simultaneously such that the Partial Rank Correlation Coefficient (PRCC) is used to evaluate statistical relationships [83, 84], in order to assess the significance of each parameter with respect to R_0. PRCC indicates the qualitative relationship, in particular the degree of monotonicity between specific input parameter and model output [83] and it has been successfully applied in other epidemic models [69, 88]. The results are shown in Figure 4.3. The PRCCs for the parameters $b_2, q_1, \alpha, \beta_{t2}, \beta_{2t}, \beta_{12}, \beta_{21}, \beta_{23}, \beta_{32}, 1/\varepsilon_2, S_a^0, S_1^0, S_2^0, \sigma_1, \sigma_2, \sigma_3$ are all positive indicating an increase in R_0 with an increase in livestock birth/death rates, *Aedes* vertical transmission, ticks attachment, probabilities of transmission, mosquito incubation periods, length of infection in livestock, initial number of susceptible ticks, *Aedes*, *Culex* and mammalian host populations, number of times a mosquito would bite host and number of bites a host can sustain respectively.
It is expected that at an early stage of an epidemic in a system without ticks, RVF outbreaks may be highly influenced by numerous factors including: the initial number of susceptible *Aedes* mosquitoes; competence of *Aedes* mosquitoes in transmitting the disease transovarially and the initial number of available susceptible hosts and mosquito death rates [5, 48, 69]. However, we observe that in the presence of ticks ($b_t\alpha > d_t\delta$) the situation changes. The ticks attachment rate α, probability of transmission from ticks to host β_{2t} and from host to ticks β_{t2}, length of infection in livestock, ticks detachment rate δ and ticks death rate have greater impact on R_0. This shows that if ticks are capable of transmitting RVF, they may be playing a major role in RVF outbreaks and endemicity. Ticks spend long periods feeding on the host, disease-bearing ticks may survive long periods of dessication and an infected fully fed female *H. truncatum* tick can continue to harbour RVFV post oviposition [28] enhancing virus circulation and maintenance. As observed in our model analysis, the RVF tick-system only exists if the number of ticks that attach to a host is greater than those that detach. This emphasizes that the time ticks spend attached to a particular host is a critical factor in the dynamics of the disease. Therefore, this calls for more attention to research with strength to establish the role that *H. truncatum*, other ticks and biting insects play in the transmission of RVFV in nature.

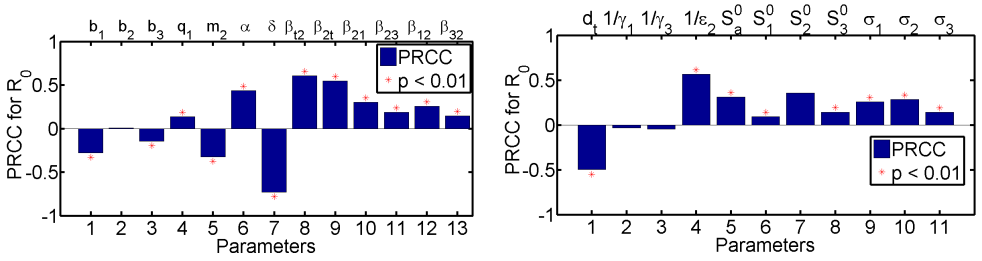

FIGURE 4.3: PRCC results and $(*)$ denotes PRCCs that have P-value < 0.01.

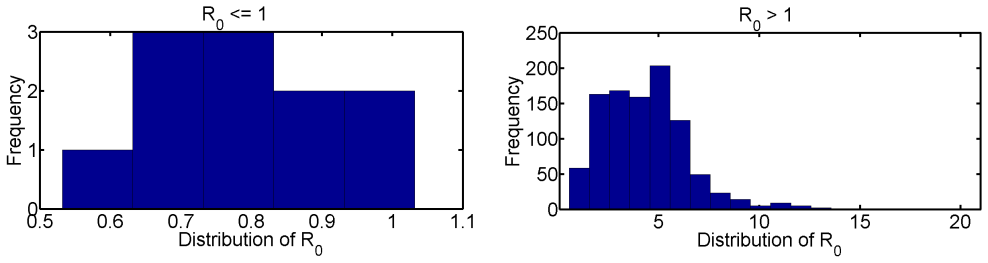

FIGURE 4.4: Distribution of the basic reproductive number, R_0 from a pool of 1000 sets of model parameters for $R_0 <= 1$ and for $R_0 > 1$.

In addition to the PRCCs results we show the distribution of R_0 when it is less and above unity see Fig.4.4. Very few parameter combinations would yield $R_0 < 1$ as the disease is intermediated by more than one disease vector. In this situation it is generally possible to have the overall R_0 greater than unity even if either the vector or host reproductive number is less than unity [137]. Averaging R_0 when it is above unit over all parameter sets gives a mean of 4.8497 and it ranges between 0.5822 and 26.5939.
Moreover, varying *Aedes* mosquito biting preference parameter, σ_1 and ticks attachment frequency, α in the host, results in significant changes in the values of the basic reproductive number, R_0. This is shown in Fig.4.6 (left) in which we note that higher efficacy of σ_1 and α result in higher probability of occurrence of RVF outbreaks as expected. Given that the vectorial capacity of the vector is a critical component of its ability to transmit the infection [138]. Hence, an increase in the parameter σ_1 results in an exponential increase in the basic reproduction number. Another important observation is that a minimum of $\delta = 0.3$ is necessary to keep R_0 around the average value, highlighting the role of ticks questing behaviour. In addition, analysis of the parameter σ_1, suggests that *Aedes* vertical transmission efficiency may play a significant role at an early stage of the epidemic, which eventually leads to a rapid spread of the disease as witnessed by Fig.4.2.

4.5.2 Local sensitivity analysis

Using uncertainty and Partial Rank Correlation Coefficient (PRCC) analysis we were able to identify which parameters are important in contributing to variability in the outcome of the basic reproductive number. However, in order to reduce disease mortality and morbidity in livestock, focus should be oriented to disease prevalence [48, 88]. Therefore, in this section we use localized sensitivity analysis to determine the relative importance of some chosen parameters with respect to the state variable I_2. Many parameters are directly related to disease prevalence, but for our analysis we focus on parameters related to the time ticks spend attached to a host and the number of times an *Aedes* mosquito would bite a host. These parameters are: σ_1, α and δ. We simulate the system at a fixed value of the parameter then plot I_2 versus the entire range of values that the parameter assumes along the evolution of the disease. The dynamical behaviour of disease prevalence

in livestock, I_2 along the range of these parameters is depicted in Fig.4.5. Clearly, Fig.4.5 shows the zone where changes should be made for an input parameter to determine the desired value of a predictor parameter.

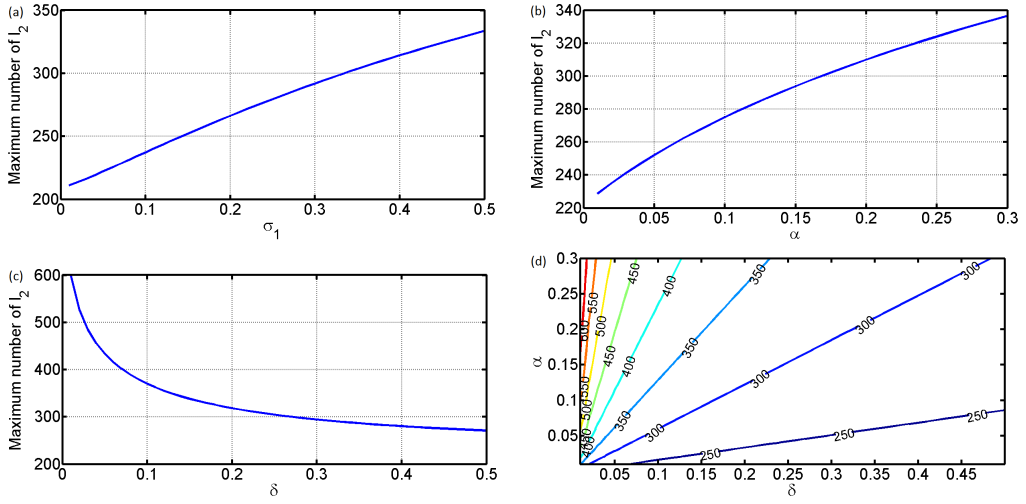

FIGURE 4.5: Simulation of the system where maximum number of infected livestock I_2 is selected at each point of the ranges of the number of bites an *Aedes* mosquito would bite a ruminant σ_1, ticks attachment rate α and the ticks detachment rate δ. (a)-(c) illustrate the changes in the local maximums of the state variable (I_2) with respect to model parameters σ_1, α and δ. (d) shows the contour plot of max(I_2) in the (δ, α) plane.

The maximum density of infected livestock increases with any increment in the number of bites an *Aedes* mosquito would bite a host and with the rate at which ticks attach to a host (see Figs.4.5(a) and (b)); however, it decreases exponentially with an increase in the rate at which ticks detach from a host (Fig.4.5(c)). In Fig.4.5(d) we observe that even at very low values of ticks attachment rate, the maximum number of infected hosts will rise to very high values. This suggests that any amount of time ticks spend on the host represents a high risk factor in the transmission of RVF. In addition we observe that there should be a balance between the attachment and the detachment rates for the disease to persist.
Furthermore, we compute sensitivity indices for some chosen parameters previously identified to contribute to the basic reproductive number variability. Thus we derive an analytical expression for each R_0 sensitivity index based on the concept of the normalized sensitivity index [5, 88], given by

$$\Upsilon_{\psi}^{R_0} = \frac{\partial R_0}{\partial \psi} \frac{\psi}{R_0}$$

for any parameter ψ.

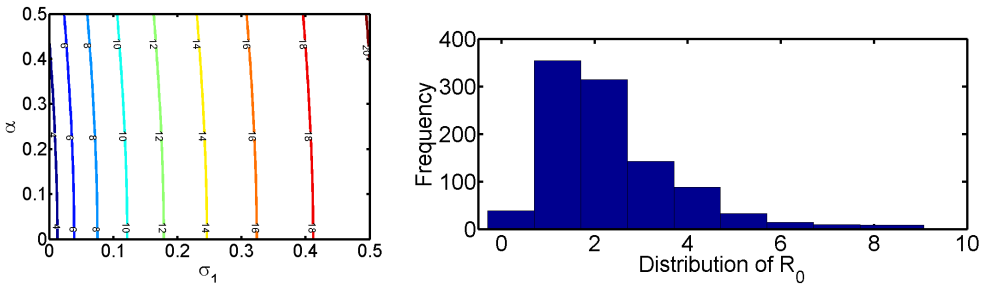

FIGURE 4.6: Left: This shows R_0 as a function of the number of times an *Aedes* mosquito would bite a ruminant, σ_1 and the ticks attachment rate, α. The curves are contours in the (σ_1, α) plane along which R_0 at early stage of disease following an introduction of a single infectious livestock or vector (mosquito or tick), is constant. Right: Distribution of R_0 of the model without ticks from a pool of 1000 sets of model parameters.

The sensitivity index results (see Figure 4.7 (left)) agree strongly with the above uncertainty analysis. Increasing transmission rates of infection from livestock to ticks β_{t2} and from ticks to livestock β_{2t}, and initial number of susceptible livestock, S_2^0, increases the basic reproductive number, R_0. While decreasing livestock recovery and disease-induced death rates as well as ticks death rate increase R_0. The former results from the fact that ticks may die before transmitting the infection, thereby reducing R_0.

4.5.3 Comparison of mean values of R_0

In order to quantify the extent at which ticks may be contributing in the transmission and spread of RVF, we review the overall mean of the basic reproductive number, R_0 obtained from different studies which did not include additional vectors such as ticks. Figure 4.6 (right) represents the distribution of R_0 derived from our model without ticks. Fig.4.7 (right) is a table describing the review of R_0 from previous studies, which did not include ticks in their models. From these studies we observe that R_0 varies from 1.19 to 3.5 on average while our model with ticks predicts $R_0 = 4.8497$ on average. However, it is worth noting that some of the studies mentioned in the table used a different approach to compute the expression of R_0, by taking the sum of R_0 from vertical transmission and R_0 from horizontal transmission [69, 71]. These differences on the computation of R_0 imply different values of R_0 but do not influence the trend we observe in this comparison of different values of R_0. From these comparisons it appears that ticks may have a significant contribution in the dynamics of the disease. Further, R_0 computed in the basis of the next-generation matrix for vector-borne disease such as RVF does reflect the actual average number of secondary infections but rather the geometric mean [87]. This leads to low values of R_0 as this method estimates R_0 at each generation regardless of whether the generation is of mammalian host or vector. Consider that at the first generation or infection event, a single *Aedes* infects two ruminants, each of whom subsequently infect two *Aedes*, two *Culex* and two

ruminants, then, a single infected *Aedes* will result in four *Aedes*, four *Culex* and four ruminants. This leads to an exponential increase of R_0, resulting in a rapid spread of the virus if the target host is vulnerable to the disease, resulting in the so-called exponential phase of the outbreak [21, 137].

	Parameter	Sensitivity index
1	β_{2t}	+0.4696
2	β_{t2}	+0.4696
3	S_2^0	+0.4319
4	d_t	−0.4557
5	ε_2	−0.3528
6	m_2	−0.1411

R_0 in previous study	Mean
Our model without ticks	2.3555
Our model with ticks	4.8497
Gaff et al.[69]	1.19
Chitnis et at.[5]	1.539
Mpeshe et al.[48]	2.64675
Niu et al.[71]	1.19
Mpeshe et al.[74]	3.5006

FIGURE 4.7: Left: Sensitivity indices of the model outcome R_0 with respect to some model parameters. Right: Mean values of R_0 in previous models without ticks.

4.6 Discussion and Conclusion

To the best of our knowledge this is the first time, compartments representing epidemiological states of ticks are included in models of the evolution of RVF epizootics. Using a mathematical epidemiological model via a system of nonlinear ordinary differential equations we have formulated and analysed a RVF model that includes ticks as disease vectors other than *Aedes* and *Culex* mosquitoes. Based on the basic reproductive number, R_0 Theorems in [101], analytical results establish that when $R_0 < 1$, the disease-free equilibrium (DFE) is locally asymptotically stable while for $R_0 > 1$ the endemic equilibrium (EE) is locally asymptotically stable. This is a very important result in epidemiology if one seeks to control vector-borne diseases via the control of the vector population, which remains an alternative of RVF control strategies [4, 58, 74]. The above results suggest that Rift valley fever virus (RVFV) is endemic if $R_0 > 1$ and and more likely remains at a very low level after an outbreak or between outbreaks. These findings are in line with empirical studies in many endemic areas which have shown that 1-3 % of domesticated livestock are being infected with RVFV in endemic areas during the inter-epidemic period [39, 42, 118]. In addition to the overall model basic reproduction number R_0 other epidemiological thresholds have been derived and interpreted. An example of this is the number of new infections resulting from an introduction of an *Aedes* mosquito, R_0^1 in the absence of *Culex* and ticks. The derivation of such type reproductive numbers is of great epidemiological significance since it is possible for the disease to persist even if the overall R_0 is greater than unity as long as either the vector or host type reproductive number is beyond unity [137]. Global stability of the DFE was determined following the approach and results obtained by [133]. The results showed that although host-ticks interactions may serve as disease reservoirs or disease amplifiers, the values of R_0^1 should be

kept under unity if disease post epizootics activities are to be controlled. R_0^1 encompasses two important informations: *Aedes* vertical transmission efficiency and their competence for initial spread and endemicity of the disease. This results from the fact that newly emerged transovarially infected mosquitoes will then infect nearby vulnerable ruminants leading to persistence of the virus during the endemic cycle [13, 35]. However, for this transmission cycle to take place after large outbreaks resulting in sporadic disease activities in ruminants new pools of susceptible livestock should be recruited into the population [77], given that after the outbreak surviving ruminants may still be immune to the disease [11]. These conclusions suggest that to prevent these low level transmission cycles appropriate control interventions (for instance destruction of mosquito breading sites and herd vaccination of newly recruited livestock) or integrated vector control programs [58] should be employed. However, herd vaccination is almost impossible to sustain in RVF affected countries for economic reasons [11, 74, 139]. Therefore, affordable and effective integrated control interventions need to be developed in support of those vulnerable African communities with low resilience to economic and environmental challenges [1, 11, 14].

Global and local sensitivity analysis of R_0 have been carried out to determine the relative importance of each parameter in the disease transmission and prevalence. Through PRCCs analysis we found that R_0 increases with an increase in the following model parameters, $b_2, q_1, \alpha, \beta_{t2}, \beta_{2t}, \beta_{12}, \beta_{21}, \beta_{23}, \beta_{32}, 1/\varepsilon_2, S_a^0, S_1^0, S_2^0, \sigma_1, \sigma_2, \sigma_3$. The fact that an increase in livestock birth rate b_2 implies an increase in the magnitude of R_0 indicates that this parameter may be an important predictor for determining the total size of livestock population and the prevalence of RVFV after an outbreak. This result further confirms our findings through global stability analysis of the DFE highlighting the relative importance of recruitment of new susceptible livestock after an outbreak and a study by [77] have arrived to a similar conclusion. Moreover, results of sensitivity analysis have indicated that ticks attachment and detachment rates α and δ, probability of transmission from ticks to host β_{2t} and from host to ticks β_{t2}, length of infection in livestock and ticks death rate d_t have a greater impact on R_0. Recall that R_0 is a measure of initial disease transmission. Hence, decreasing the time and the proportion of ticks that attach to a host and reducing host-ticks interactions, disease transmission probabilities reduce the magnitude of R_0. The parameters α and δ are related to ticks questing behaviour while the parameters β_{2t} and β_{t2} correspond to ticks feeding behaviour. Therefore, these results highlight the role that ticks questing and feeding behaviour play in the transmission of the virus. These findings are in good agreement with empirical studies indicating that ticks spend long periods feeding on the host, disease-bearing ticks may survive long periods of desiccation and an infected fully fed female *H. Truncatum* tick can continue to harbour RVF virus post-oviposition [28]. Another important result is that increasing ticks death rate d_t substantially decreases R_0. Hence, control strategies aiming to reduce the tick population may help reduce the disease burden. Although our assumption of constant tick death rate suggests that control of ticks implies eliminating their population, [140] discuss several scenarios of optimal application of tick-killing

treatment in controlling risk of tick-borne diseases without completely eliminating their population. Despite that little is known about what mainly regulates tick populations in the field, several studies demonstrate that host's immune status strongly affects tick survival and fecundity [131]. This deserves, on itself, further investigation for determining specific features that regulates ticks population that can then be targeted for disease management. Additionally, controlling the lifespan and biting rates of the vectors will help control both the initial spread of disease and ongoing infections, hence, reduce disease prevalence during an outbreak and after. These results are in agreement with findings from other theoretical studies [5, 48, 69, 77], which have highlighted the relative importance of both RVF related death and natural deaths.

[58] discussed several RVF vector control programs and strategies with different applications such as interrupting epidemic cycles, preventing emergence of new cohorts of infected vectors and much more. Ticks questing and feeding behaviour is a critical component of the vector's ability to transmit diseases. Therefore, control strategies targeting these features would be of great epidemiological significance. In addition, other studies [140] have suggested that use of pesticides (acaricides) to control tick population would enhance the effort made by hosts to avoid ticks attaching. Moreover, results from sensitivity analysis have suggested that decreasing the length of infection in hosts and decreasing the number of susceptible hosts significantly reduces R_0. Contours curves of the maximum of I_2 in the (δ, α) plane suggested that even at very minimum values of the attachment rate, α we obtain high values of $\max(I_2)$ if the detachment rate is very small, which is equivalent to long periods of time ticks spend attached to the host. This result further confirm the epidemiological implications of the time ticks spend attached to a host as highlighted by empirical studies [26, 28].
Using the model parameter ranges to capture the entire history of disease evolution and running 1000 stochastic simulations, we computed the mean value of R_0 which was found to exceed 4.5. This result is far beyond findings from other epidemic models without ticks [5, 48, 69, 71], including our own model. These results stem from the fact that ticks not only increase the size of an epidemic but also accelerate the exponential phase of the outbreak. This calls for attention in designing preventive measures to curtail and stop the epidemic in the event of an outbreak [48]. Surveillance studies [39, 58] have highlighted that effective and continuous surveillance in livestock is a critical factor in detecting and responding to both RVF outbreaks and inter-epidemic activities. These results are important for controlling transient epidemics which are likely to take off even when $R_0 < 1$ [5, 137]. This is important in preventing the virus eventually building up from disease inter-epidemic activities and halt any future outbreak [4, 39], as a result of vertical transmission efficiency which was found to linearly increase R_0. These results further confirm our findings through analytical analysis of the global asymptotic stability of the DFE, which indicated that the global stability of this equilibrium can only be attained if the *Aedes* mosquito reproductive number, R_0^1 with vertical transmission is kept under unity. This is the first time that global stability of the DFE of a complex realistic RVF model is thoroughly analysed by

means of analytical methods. This analysis has enabled us to obtain useful qualitative insights about the necessary conditions for long-term stability of the DFE which have shown dependence between tick-host interactions thresholds and *Aedes* mosquito reproductive number. This highlights the role of vertical transmission in some female *Aedes* mosquitoes and mammalian hosts in sustaining low levels of disease activities between outbreaks as virus reservoirs. However, the reservoirs and means of inter-epizootic maintenance are still subjects of further investigations.

Entomological studies have suggested that biting insects other than *Aedes* and *Culex* mosquitoes are also involved in the transmission of RVF [7, 11, 29]. In this chapter we have formulated a deterministic model of RVF transmission which accounts for ticks as additional RVF potential vectors. The ticks species taken as an example in this model have been indicated to be potential vectors of RVFV [11, 28, 29]. Similar to [26, 124, 141] and other theoretical studies investigating the hypothetical introduction of RVF in temperate countries [73, 142, 143], this study does not by any means aim to demonstrate that ticks are actually involved in the spread of RVF in endemic areas. Rather, we aimed by means of an epidemic model to yield qualitative information for enhancing our understanding in the case when ticks are assumed to be potential vectors of disease transmission. The analyses of this model have provided critical insights on the mechanisms underlying the possible role of ticks in the transmission of RVF. This was possible by structuring the ticks population following their questing and feeding behaviour which is a critical component of their ability to transmit and further disperse the virus [131]. Our results indicate that ticks not only increase the size of an epidemic but also accelerate it and reduce its duration. These results implicate ticks as one of the contributors to the exponential phase of the outbreak.

The results of all model analysis presented in this chapter should be interpreted as qualitative and relative, as opposed to quantitative, until future data, obtained by further interdisciplinary research studies focusing on RVF molecular epidemiology and tick chemical ecology, can be used to parametrize, calibrate and validate the model. Nevertheless, the current model framework and analysis enables us to gain valuable insights regarding the epidemiology of the disease and its implications and the model remains an important step towards the theoretical study of the role of ticks on the dynamics of RVF. The value of the present research study is not limited to only providing qualitative understanding of the systems underlying processes but it is also useful in pointing out relevant model parameters that require further attention from experimental ecologists and modellers. Such estimates would be of great importance for parametrizing more refined predictive models which would yield specific informative indicators useful for improving disease control strategies [77, 120], by providing effective guidance to public health policy makers. Furthermore, this model framework can be of great use to theoretical ecologists and epidemiologists working on vector-borne diseases in which ticks are secondary vectors or additional potential vectors.

Chapter 5

Predicting Rift Valley fever Outbreaks from Inter-Epidemic Activities. Insights from a Stochastic host-vector Model [1]

5.1 Introduction

Rift Valley fever (RVF) is an emerging zoonotic disease characterized by fluctuating disease outbreaks that occur at irregular intervals throughout Sub-Saharan Africa [1, 14]. Such outbreaks are driven by changes in climatic conditions and, between outbreaks, disease activities are known to be maintained through vertical transmission on *Aedes* mosquitoes [11, 33]. This characteristic temporal pattern of disease outbreaks adds an additional complication towards efforts for understanding and predicting occurrence of outbreaks. Findings from a pioneering empirical study in Tanzania on the subject of disease temporal and spatial patterns [3] suggest that continuous endemicity of Rift Valley fever virus (RVFV) may lead to periodic disease outbreaks. Similar observations have also been reported in Kenya [1] and South Africa [2, 144]. Although correlation between RVF outbreaks and the warm phase of El Niño/Southern Oscillation (ENSO) phenomena which lead to abnormal rainfall has been reported [34], there have been instances where no outbreaks were recorded following seasons of exceptionally above normal rainfall [3]. This suggests that while rainfall might be the major determinant factor for the onset and switch-off of an outbreak, it is likely to not be the only factor responsible for this temporal characteristic pattern of disease outbreaks. The present research study aims to investigate factors underlying the characteristic temporal patterns of RVF outbreaks and to make predictions of the periodicity of these outbreaks.

[1] This chapter has been submitted to: PLOS Neglected Tropical Diseases

Over the past decades mathematical models have been used to translate assumptions concerning transmission and spread of RVF at population level. From the pioneer RVF models by Favier et al. [68] and Gaff et al. [69], several models have been formulated and analysed using deterministic compartmental modelling approach [4, 5, 48, 70–72, 74, 77, 142]. Although these models have potential for examining factors underlying dynamics of the disease, they fail to capture observed fluctuations on the occurrence of RVF outbreaks. Nevertheless, extending these models to include seasonality yielded rich dynamics including chaotic behaviour [4]. In this situation such dynamics are attributed to climatic variations disregarding the fact that interaction between the deterministic dynamics and demographic stochasticity is central for explaining realistic disease patterns [145]. Deterministic models are typically assumed to be reasonable approximations for infinitely large homogeneous populations, and arise from the analysis of mean field stochastic models, such that if one considers finite populations which is the case of livestock, stochastic interactions even within a well-mixed system may introduce new phenomena [146]. Therefore, it is more likely that these characteristic disease temporal patterns can be captured by fully stochastic models [146, 147], which are known to show large oscillations caused by the stochasticity exciting the system's natural frequency [148, 149]. Stochastic effects are known to show major impacts whenever the prevalence of infection in either the host or vector population, or both are low and can be highly significant during the period immediately after the introduction of infection into a population [150].

In this study we formulate a full host-vector stochastic model which takes into account mechanisms of vertical transmission on the vector population. Our aim is to examine the impact of stochastic effects and virus endemicity on the invasion and persistence of the disease. Stochastic effects can also lead to disease extinction during endemic settings [151]. To investigate these situations we employ branching process theory [152–154], which has been successfully applied in vector-borne epidemic models (for more details see [150, 155]). Here we extend the analysis presented in [150] to include vertical transmission while implementing infection rates that depend on both host and vector populations. Our objective is to examine the impacts of mosquito biting behaviour and host efforts to avoid the biting on the invasion and persistence of the disease. Although stochasticity can cause large departures from equilibrium, potentially allowing the number of infectives to fall to low levels [150], it could act passively to kick the system between different deterministic states [156], as well as interacting with the non-linearity to excite the transients [147], leading to either periodic or non-periodic oscillations. Using power spectra analysis we investigate the periodicity of fluctuations of RVF outbreaks as was undertaken for avian influenza in [146]. This is accomplished by formulating the model as a master equation which is then studied using van Kampen's system size expansion [157], to provide a prediction for the dominant period of disease oscillations. Since the macroscopic dynamics can then be viewed as a sum of a deterministic and a stochastic part, this approach provides a unique opportunity to investigate the effects of stochasticity on disease endemicity and outbreaks. This approach has been successfully applied while investigating the effects of stochastic

amplification [149, 158] and seasonal forcing [147, 159, 160] on disease outbreaks in particular in childhood diseases and more recently on avian influenza [146]. This analysis provides prediction of the dominant period of disease fluctuations depending on the efficiency of vertical transmission. The results highlight the role of continuous RVFV endemicity driven by vertical transmission on mosquitoes, on the periodicity of disease outbreaks which agree with findings from empirical studies [1–3]. Therefore, it is reasonable to argue that it could be possible to reduce the frequency and intensity of RVF outbreaks by controlling transovarial transmission.

5.2 RVF stochastic host-vector model with vertical transmission

To analytically investigate temporal dynamics of a RVF model by means of stochastic processes we formulate a simple but realistic stochastic host-vector model that captures all important features of RVF dynamics. The present study does not use primary data (medical records or public records), rather during model development we calibrate the model towards temporal characteristic patterns of RVF epidemic and inter-epidemic activities observed in East Africa and Southern Africa. In particular, the data used reflect patterns observed in Kenya, Tanzania and South Africa (see [1–3, 39, 45] and references therein). A description of all model parameters and their respective values, ranges and sources is given in Table 5.1.

We investigate both disease epidemic and inter-epidemic activities in a livestock population where the transmission of the infection is intermediated by *Aedes* mosquitoes only. Thus, neglecting the presence of *Culex* species which are known to be the secondary vectors of the disease as in [5]. *Aedes* mosquitoes are responsible for both initial spread and persistence of the disease since the female can transmit the virus transovarially to her eggs [11, 33]. The mosquito sub-model is an *SI* type model, that is, with only two compartments: susceptible and infectious. This way we ignore the exposed class and mosquitoes once infected remain infected for life. The livestock sub-model is an *SIR* type model, that is, susceptible, infectious and recovered.

Mammalian hosts enter the susceptible class through birth at a constant rate, μ_2. When an infectious *Aedes* mosquito bites a susceptible ruminant, there is a finite probability, β_{21} that the ruminant becomes infected. Once a ruminant is successfully infected by an infected vector, it moves from susceptible class S_2 to infectious class I_2. After some time, the infectious ruminant either recovers at rate ϵ_2 and moves to recovered class, R_2 or dies naturally at per capita rate of μ_2. Female *Aedes* mosquitoes (we do not include male mosquitoes in our model because only female mosquitoes bite livestock for blood meals) enter the susceptible class through birth at rate, b_1. The term birth for mosquitoes accounts for and is proportional to the egg-laying rate; and survival of larvae [5]. Since most density-dependent survival of mosquitoes occurs in the larvae stage, we assume a constant emergence rate that is not affected by the number of eggs laid; that is, all emergence of new

adult mosquitoes is limited by the availability of breeding sites [5]. Susceptible vectors, S_1 are infected when they bite an infected ruminant with probability β_{12} and depending on the ambient temperature and humidity [99] the mosquitoes move from S_1 to the infectious class, I_1. To reflect the vertical transmission in *Aedes* mosquitoes a proportion of infected, q_1 newly hatched mosquitoes joins class I_1. Mosquitoes leave the population through a per capita natural death rate, μ_1.

Parameter	Description	Units	Baseline	Range	Reference
$1/\mu_1$	Mosquito life span	Days	20	10-30	[5, 57]
$1/\mu_2$	Livestock life span	Days	2190	360-3600	[69]
q_1	Probability of vertical transmission		0.1	0-1	[161]
α_1	Number of times a mosquito would bite a host	Days^{-1}	0.33	0.1-0.5	[5, 91]
α_2	Number of bites a host can sustain	Days^{-1}	19	0.1-50	[5]
α	Biting rate	Days^{-1}	0.71	0.1-0.8	[162]
β_{21}	Probability of successful infection in livestock		0.21	0.001-0.54	[5, 11, 99]
β_{12}	Probability of successful infection in mosquitoes		0.51	0.3-0.9	[5, 11, 99]
$1/\epsilon_2$	Infectious duration in livestock	Days	4	1-7	[5, 91, 163, 164]
m_0	The ratio female mosquitoes to hosts		1.5	0-5	[165]

TABLE 5.1: The parameters for the RVF model for high rainfall and moderate temperature (wet season) for model in Table 5.2 with values, range and references. Note that all parameter units are days. The parameter α_1 is a function of the mosquito's gonotrophic cycle (the amount of time a mosquito requires to produce eggs) and its preference for livestock blood, while α_2 is a function of the ruminant's exposed surface area, the efforts it takes to prevent mosquito bites (such as swishing its tail), and any vector control interventions in place to kill mosquitoes encountering cows or prevent bites [5].

Although births and deaths are intrinsically distinct events, we assume, for simplicity, that the vector birth and death rates have the same values, which means that the total population size $N_1 = S_1 + I_1$ is kept constant. A key feature of the model is that the rate at which new infections occur in both host and vector is proportional to both host and vector population. That is, the total number of bites varies with both the host and vector population sizes. This allows more realistic modelling of situations where there is a high ratio of mosquitoes to livestock and where livestock availability to mosquitoes is reduced through control intervention as well as the efforts a host takes to prevent mosquito bites (such as swishing its tail) [4, 5]. Thus, the force of new infections in livestock is $\lambda_{21} = \frac{\alpha_1\alpha_2\beta_{21}I_1}{\alpha_1 N_1+\alpha_2 N_2}$ and the force of new infections in mosquitoes is $\lambda_{12} = \frac{\alpha_1\alpha_2\beta_{12}I_2}{\alpha_1 N_1+\alpha_2 N_2}$, where α_1 is the number of times one *Aedes* mosquito would bite a host per day, if livestock were freely available (for details on their derivation see Appendix D section D.1). This is a function of the mosquitoes gonotrophic cycle (the amount of time a mosquito requires to produce eggs) and its preference for livestock blood. α_2 is the maximum number of mosquito bites a host can sustain per day. This is a function of the hosts exposed surface area, the efforts it takes to prevent mosquito bites (such as swishing its tail), and any vector control interventions in place to kill mosquitoes encountering hosts or preventing bites [5]. This formalism allow us to evaluate how mosquito biting behaviour and vertical transmission in *Aedes* female mosquitoes impact both the probabilities of disease invasion and extinction and disease fluctuations. The

former is accomplished by employing branching process theory which is central for determining critical epidemic behavioural thresholds [150], and for the later we used system-size expansion technique [166] and Fourier analysis. However, a standard incidence function used in mosquito transmitted diseases usually assumes that mosquitoes bite a particular host at a constant rate irrespective of the number of available hosts. Therefore, for very large N_2 the above forces of infection can be approximated by the following standard incidence functions $\lambda'_{21} = \beta_{21}\alpha m_0 \frac{I_1}{N_1}$ and $\lambda'_{12} = \beta_{12}\alpha \frac{I_2}{N_2}$ as the model forces of infections. In this case α is the mosquito biting rate, such that α/N_2 is the rate at which a particular host is bitten by a particular mosquito, $m_0 = N_1/N_2$ is the ratio female mosquitoes to hosts and β_{21} and β_{12} are the probabilities of successful transmission per bite [21, 167], for more details see Appendix D section D.1. All the transitions of the host and the vector associated with their corresponding rates are illustrated graphically in Fig5.1.

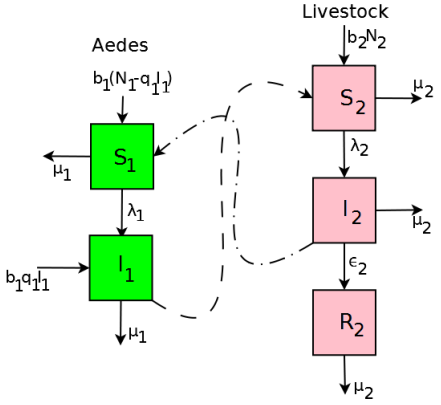

FIGURE 5.1: Flow diagram of RVF model with both vertical and horizontal transmission. Susceptible livestock, S_2, acquire infection and move to compartment I_2 when they are bitten by an *Aedes* infectious mosquito I_1. They then recover with a constant per capita recovery rate to enter the recovered compartment, R_2, class. Susceptible mosquito vectors, S_1, become infected when they bite infectious livestock and progress to class I_1. The solid lines represent the transition between compartments and the dashed lines represent the transmission between different species.

Setting the livestock population size to remain constant, we can omit the equation containing R_2, since it can be obtained when S_2 and I_2 are known. Therefore, the basic ingredients of our new model framework are susceptible livestock S_2, infected livestock I_2 and infected *Aedes* mosquitoes I_1. Unlike in deterministic models the numbers in these classes are no longer treated as continuous varying quantities [150], but instead as integers since individual-based stochastic models consider movements of individuals between classes to be discrete [168]. To be precise, these transitions are assumed to take place in a small time interval $(t, t+\Delta t)$ with inflows and outflows of magnitude unity. If we denote the numbers in each class as s_2, i_2 and i_1 respectively, the general state of the system is then written as $\sigma = (s_2, i_2, i_1)$. Thus, $T(\sigma'|\sigma)$ represents the transition probability per unit time from state σ to

the state σ'. Note that we characterize the events taking place in the system into three distinct groups:

1. Infection

$$\begin{aligned} T(s_2-1, i_2+1, i_1|s_2, i_2, i_1) &= \beta_{21}\alpha' m_0 \tfrac{i_1}{N_1} s_2, \\ T(s_2, i_2, i_1+1|s_2, i_2, i_1) &= \beta_{12}\alpha' \tfrac{i_2}{N_2}(N_1 - i_1), \end{aligned} \tag{5.1}$$

2. Birth/Death

$$\begin{aligned} T(s_2+1, i_2, i_1|s_2, i_2, i_1) &= \mu_2 N_2, \\ T(s_2-1, i_2, i_1|s_2, i_2, i_1) &= \mu_2 s_2, \\ T(s_2, i_2, i_1-1|s_2, i_2, i_1) &= \mu_1 i_1. \end{aligned} \tag{5.2}$$

3. Recovery

$$T(s_2, i_2-1, i_1|s_2, i_2, i_1) = (\epsilon_2 + \mu_2) i_2. \tag{5.3}$$

where $\alpha' = \frac{\alpha_1\alpha_2}{\alpha_1 m_0 + \alpha_2}$ for general forces of infections λ_{21} and λ_{12}, and $\alpha' = \alpha$ for standard forces of infections λ'_{21} and λ'_{12}.

For better illustration we summarize all of the processes taking place in the system and their corresponding rates and probabilities of occurrence in Table 5.2. Note that these rates are the conditional instantaneous stochastic rates of individuals entering or leaving each compartment at time t and also depend on the sizes of each compartment.

Event	**Transition**	**Rates of occurrence**	**Probability in** $[t, t+dt]$
Birth of uninfected *Aedes*	$S_1 \to S_1 + 1$	$\mu_1(N_1 - q_1 I_1)$	$\mu_1(N_1 - q_1 I_1)dt$
Infected *Aedes birth*	$I_1 \to I_1 + 1$	$b_1 q_1 I_1$	$b_1 q_1 I_1 dt$
Infection of susceptible *Aedes* from infectious host	$S_1 \to S_1 - 1,\ I_1 \to I_1 + 1$	$\beta_{12}\alpha' \frac{I_2}{N_2} S_1$	$\beta_{12}\alpha' \frac{I_2}{N_2} S_1 dt$
Death of susceptible *Aedes*	$S_1 \to S_1 - 1$	$\mu_1 S_1$	$\mu_1 S_1 dt$
Death of infectious *Aedes*	$I_1 \to I_1 - 1$	$\mu_1 I_1$	$\mu_1 I_1 dt$
Birth of susceptible host	$S_2 \to S_2 + 1$	$\mu_2 S_2$	$\mu_2 S_2 dt$
Infection of susceptible host from infectious *Aedes*	$S_2 \to S_2 - 1,\ I_2 \to I_2 + 1$	$\beta_{21}\alpha' m_0 \frac{I_1}{N_1} S_2$	$\beta_{21}\alpha' m_0 \frac{I_1}{N_1} S_2 dt$
Infectious host recovery	$I_2 \to I_2 - 1,\ R_2 \to R_2 + 1$	$\epsilon_2 I_2$	$\epsilon_2 I_2 dt$
Death of susceptible host	$S_2 \to S_2 - 1$	$\mu_2 S_2$	$\mu_2 S_2 dt$
Death of infectious host	$I_2 \to I_2 - 1$	$(m_2 + \mu_2) I_2$	$(m_2 + \mu_2) I_2 dt$
Death of recovered host	$R_2 \to R_2 - 1$	$\mu_2 R_2$	$\mu_2 R_2 dt$

TABLE 5.2: Stochastic model for vector-host disease system. The parameter $m_0 = N_1/N_2$ is the ratio mosquitoes to hosts, and $\alpha' = \frac{\alpha_1 \alpha_2}{\alpha_1 m_0 + \alpha_2}$ is for general forces of infections λ_{21} and λ_{12}, and $\alpha' = \alpha$ is for standard forces of infections λ'_{21} and λ'_{12}.

Using the probabilities in Table 5.2, we can now construct the master equation in its general form [149, 157, 169], describing temporal evolution of the probability distribution of determining the system in state σ at time t.

$$\frac{dP(\sigma;t)}{dt} = \sum_{\sigma' \neq \sigma} T(\sigma|\sigma')P(\sigma';t) - \sum_{\sigma' \neq \sigma} T(\sigma'|\sigma)P(\sigma;t), \tag{5.4}$$

where $\sigma = (s_2, i_2, i_1)$ represents the state of the system, $P(\sigma, t)$ is the probability of the system in the state σ at time t. This can also be referred to as the forward Fokker-Planck (or forward Kolmogorov) equation, which is a differential equation for the probability density function $P(\sigma, t)$ of determining the system in σ at time t and it cannot be solved exactly. An alternative analytical approach can be the derivation of the moments of the distribution of the state σ. However, for the purpose of our study we analyse the master equation using van Kampen's system-size expansion [157], see Section 5.3.2. In the following sections we determine both the probabilities of a major outbreak and extinction after introduction of a single or few infectives into a population that is otherwise susceptible.

5.3 Methods and Model Analysis

5.3.1 Estimating the probability of a major outbreak

In any disease model, a question of fundamental interest is to determine conditions under which a disease if introduced into a community with no immunity will develop into a large outbreak, and if it does, conditions under which the disease may become endemic. For this purpose, a key threshold parameter called the basic reproduction number, R_0 is derived and analysed usually in deterministic epidemic models. This epidemic threshold is such that for $R_0 < 1$ each infected individual will produce less than one infected case and the probable result is that the disease will die out.

On the contrary, if $R_0 > 1$ each individual will produce more than one case and eventually the infection will invade the population. However, in the stochastic models, invasion of an infection into a susceptible population is not guaranteed by having $R_0 > 1$: stochastic extinction can occur during the period immediately following introduction, when there are few infective individuals [150]. Thus, rather than the major outbreak that would be expected based on the behaviour of the deterministic model, only a minor outbreak might occur. During this early stage after the introduction of the pathogen, little depletion of susceptibles will have occurred and so probabilities of major outbreaks can be derived using the linear model that arises by assuming that the populations are entirely susceptible [170–172]. Thus, in the resulting model, the number of infectives can be approximated through a multi-type linear birth-death process [170]. In a multi-type branching process, individuals in the population are categorised into a finite number of types and each individual behaves independently [150]. An individual of a given type can produce offspring of possibly all types and individuals of the same type have the same offspring distribution [173, 174]. In our model the disease is spread via two modes of infection transmission: vertical and horizontal. Thus, an infectious mosquito produces an infected ruminant, and a proportion q_1 of infectious mosquitoes produce infectives of the same type while an infected ruminant produces an infected mosquito. Therefore, by assuming that secondary infections arise independently and at a constant rate over the infectious period of each infective, then the distribution of secondary infections follow geometric distributions [150], with means R_0^{11}, R_0^{21} and R_0^{12} for mosquito-to-mosquito, mosquito-to-animal and animal-to-mosquito transmission respectively (for more details see subsection D.2.2 of Appendix D).
In this settings, for horizontal transmission the probability generating functions (PGF) for the joint distribution of the dynamic variables when a single infected mosquito was introduced at time 0 can be obtained and it is given by

$$G_i(s) = E[\prod_{j=1}^{2} s_j^{X_{ij}}]. \tag{5.5}$$

For vertical transmission the PGF is simply G_1^2 [175]. Note that $\{X_{ij}, i, j = 1, 2\}$ is the number of infectives of type j produced by an infective of type i. $G(s)$ is the probability generating function of the distribution of secondary infections and equation (5.5) can be solved to find the extinction probability if there is initially one infective individual present. Extinction in the linear model is most likely to occur early in the process, so this corresponds to the occurrence of minor outbreaks in the nonlinear model, whereas non-extinction in the linear model corresponds to a major outbreak in the nonlinear model [150]. Equation (5.5) can be expanded to obtain the following formula [150],

$$G_i(s_1, s_2) = \sum_{k_1,k_2} s_1^{k_1} s_2^{k_2} P(X_{i1} = k_1, X_{i2} = k_2) = \frac{1}{1 + \sum_{j=1}^{2} R_{ji}(1 - s_j)} \tag{5.6}$$

where i is equal to 1 or 2. An infective livestock only directly give rise to secondary infections in the vector population. Thus, we have that $P(X_{21} = j, X_{22} = k)$ is equal to $P(X_{21} = j)$ when $k = 0$ and zero otherwise. Consequently the generating function $G_2(s_1, s_2)$ is a function of s_1 alone,

$$G_2(s_1, s_2) = \frac{1}{1 + R_{12}(1 - s_1)}. \tag{5.7}$$

However, when effects of vertical transmission are included, infective mosquitoes not only give rise to secondary infections in the livestock population but also to secondary infection in the mosquito population through transmission from mother to eggs. Therefore, the generating function $G_1(s_1, s_2)$ is a function of s_1 and s_2,

$$G_1(s_1, s_2) = \frac{1}{1 + R_{11}(1 - s_1) + R_{21}(1 - s_2)}. \tag{5.8}$$

Extinction probabilities can be calculated by solving the pair of equations, $G_1(G_2(s_1)) = s_1$ and $G_2(G_1(s_1, s_2)) = s_2$ resulting from composition of functions in equations (5.7) and (5.8). The pair $(s_1, s_2) = (1, 1)$ is always a solution. If $R_0 \leq 1$ it is the only solution, whereas for $R_0 > 1$ there is another solution with both s_1 and s_2 being less than unity [153], where $R_0 = \frac{q_1}{2} + \frac{1}{2}\sqrt{q_1^2 + 4R_{12}R_{21}}$ with $R_{12} = \frac{1}{\epsilon_2+m_2+\mu_2}\frac{\alpha_1\alpha_2\beta_{12}}{\alpha_1 N_1+\alpha_2 N_2}S_1^0$ being the number of new infections in *Aedes* mosquitoes generated by single infected ruminant and $R_{21} = \frac{\alpha_1\alpha_2\beta_{21}}{\alpha_1 N_1+\alpha_2 N_2}S_2^0\frac{1}{\mu_1}$ the number of new infections in livestock generated by single infected *Aedes* mosquito.

5.3.2 System size expansion of the stochastic host-vector model

So far we have formulated a fully stochastic host-vector model with both horizontal and vertical transmission, under well-mixed conditions and constructed the master equation (5.4). To analyse the model we apply two methods: one is to simulate the system using the Gillespie algorithm [176], which gives the exact realization of temporal disease evolution. The other is analytical and consists of performing van

Kampen's system-size expansion [149, 157] of the master equation, which allows for quantitative prediction of the power spectrum of the time fluctuations of each of the system variables, and, therefore, of the dominant period of disease outbreaks [146]. Full details of van Kampen's system size expansion are discussed in Section D.3 of Appendix D. This method allows us to derive analytical approximate solutions which involves making the following substitutions,

$$\begin{aligned} s_2 &= N_2\phi_1 + \sqrt{N_2}x_1, \\ i_2 &= N_2\phi_2 + \sqrt{N_2}x_2, \\ i_1 &= N_1\psi + \sqrt{N_1}x_3, \end{aligned}$$

where ϕ_1, ϕ_2, ψ are fractions of the susceptible livestock, the infected livestock and infected *Aedes* mosquitoes respectively, with $x_l (l = 1, 2, 3)$ describing the stochastic corrections to the variables s_2, i_2, i_1. This expands the master equation in powers of $N_1^{-1/2}$ and $N_2^{-1/2}$, such that the probability distribution $P(s_2, i_2, i_1; t)$ is now written in terms of the new variables x_1, x_2, x_3 as follows:

$$\frac{dP}{dt} = \frac{\partial \Pi}{\partial t} - \sqrt{N_2}\frac{d\phi_1}{dt}\frac{\partial \Pi}{\partial x_1} - \sqrt{N_2}\frac{d\phi_2}{dt}\frac{\partial \Pi}{\partial x_2} - \sqrt{N_1}\frac{d\psi}{dt}\frac{\partial \Pi}{\partial x_3}. \tag{5.9}$$

Then, by introducing step operators and expanding them in $N_2^{-1/2}$ and $N_1^{-1/2}$ we obtain

$$\begin{aligned} &\frac{dP}{dt} = \\ &\Big\{[(1 + \tfrac{1}{\sqrt{N_2}}\tfrac{\partial}{\partial x_1} + \tfrac{1}{2N_2}\tfrac{\partial^2}{\partial x_1^2})(1 - \tfrac{1}{\sqrt{N_2}}\tfrac{\partial}{\partial x_2} + \tfrac{1}{2N_2}\tfrac{\partial^2}{\partial x_2^2}) - 1]\beta_{21}\alpha' m_0 i_1 s_2 + (-\tfrac{1}{\sqrt{N_1}}\tfrac{\partial}{\partial x_3} + \tfrac{1}{2N_1}\tfrac{\partial^2}{\partial x_3^2}) \\ &[\beta_{12}\alpha' i_2(N_1 - i_1) + \mu_1 q_1 i_1] + (-\tfrac{1}{\sqrt{N_2}}\tfrac{\partial}{\partial x_1} + \tfrac{1}{2N_2}\tfrac{\partial^2}{\partial x_1^2})\mu_2 N_2 + (\tfrac{1}{\sqrt{N_2}}\tfrac{\partial}{\partial x_1} + \tfrac{1}{2N_2}\tfrac{\partial^2}{\partial x_1^2})\mu_2 s_2 \\ &+(\tfrac{1}{\sqrt{N_2}}\tfrac{\partial}{\partial x_2} + \tfrac{1}{2N_2}\tfrac{\partial^2}{\partial x_2^2})(\epsilon_2 + \mu_2)i_2 + (\tfrac{1}{\sqrt{N_1}}\tfrac{\partial}{\partial x_3} + \tfrac{1}{2N_1}\tfrac{\partial^2}{\partial x_3^2})\mu_1 i_1\Big\}\Pi(x_1, x_2, x_3; t). \end{aligned} \tag{5.10}$$

Then, by drawing a comparison with equation (5.9) order by order yields the macroscopic equations such that at leading order we obtain the following set of deterministic equations, describing the mean behaviour, which scale with the system size N_1 for vectors and N_2 for hosts,

$$\begin{aligned} \tfrac{d\phi_1}{dt} &= -\beta_{21}\alpha' m_0 \psi\phi_1 + \mu_2(1 - \phi_1), \\ \tfrac{d\phi_2}{dt} &= \beta_{21}\alpha' m_0 \psi\phi_1 - (\epsilon_2 + \mu_2)\phi_2, \\ \tfrac{d\psi}{dt} &= \beta_{12}\alpha'\phi_2(1 - \psi) + \mu_1 q_1 \psi - \mu_1\psi. \end{aligned} \tag{5.11}$$

When integrating the above deterministic equations (5.11) with respect to t we obtain trajectories of the mean behaviour which show damped oscillations tending to a fixed point see Fig.5.2. This is eventually the expected long-term behaviour for realistic parameter values for host-vector models. This further confirms the results of system stability analysis (see subsection D.3 of Appendix D).

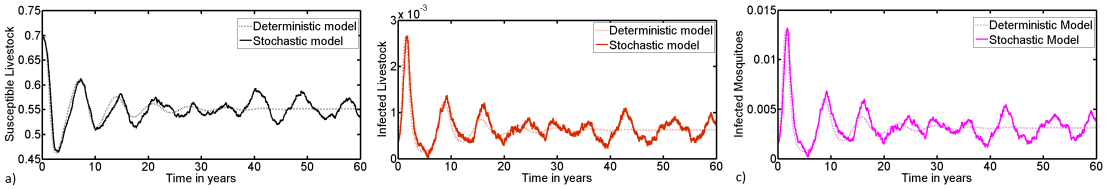

FIGURE 5.2: Realization of the RVF host-vector stochastic model and its deterministic counterpart. The trajectories of the deterministic counterpart are generated by integrating the mean field equations (5.11). The values of the parameters in years are as follows: $q_1 = 0.05, \mu_1 = (1/16) * 360, \mu_2 = 1/10, \beta_{12} = 0.170, \beta_{21} = 0.116, \epsilon_2 = (1/4) * 360, \alpha' = \alpha = 256, m_0 = 1.5$ and their description and sources is given in Table 5.1. This gives $R_0 = 1.0066$.

Results of qualitative analysis of the system show that the above system has a trivial fixed point, named the disease-free equilibrium E^0:

$$\phi_1^0, \quad \phi_2^0, \quad \psi^0,$$

and a unique non-trivial fixed point named the endemic equilibrium E^*:

$$\phi_1^* = \frac{a + \mu_2 R_0}{(a + \mu_2) R_0}, \quad \phi_2^* = \frac{\mu_1 \mu_2 (1 - q_1)(R_0 - 1)}{b(a + \mu_2)}, \quad \psi^* = \frac{\mu_1 \mu_2 g (1 - q_1)(R_0 - 1)}{a(b\mu_2 + \mu_1 g(1 - q_1))},$$

where $a = \beta_{21} \alpha' m_0, \quad b = \beta_{12} \alpha', \quad g = \epsilon_2 + \mu_2$ and $R_0 = \frac{1}{1-q_1} \frac{\beta_{21} \alpha' m_0}{\mu_1} \frac{\beta_{12} \alpha'}{\epsilon_2 + \mu_2}$ is the basic reproductive number and the later equilibrium exists and is stable whenever $R_0 > 1$.

5.3.3 Periodicity of the stochastic host-vector model

A fundamental question is whether the existence of a stable fixed point in the deterministic system generates oscillations and multi-year periodicity in the corresponding stochastic system [149]. In order to investigate this and describe the stochastic fluctuations of the system by an analytical method, we introduce step operators which allow us to express the master equation (5.4) in a more compact form which further facilitates the expansion of the system. Details are given in Section D.3.1 of Appendix D, where it is shown that the resulting master equation can be written in a power series of $N_1^{-1/2}$ and $N_2^{-1/2}$ and the step operators in terms of the fluctuation variables x_1, x_2 and x_3. Then, at next-to-leading order of the newly formed master equation (D.29) we obtain a linear Fokker-Planck equation for the fluctuation variables $x_l (l = 1, 2, 3)$,

$$\frac{\partial \Pi}{\partial t} = - \sum_{k,l=1}^{3} A_{kl} \frac{\partial (x_l \Pi)}{\partial x_k} + \frac{1}{2} \sum_{k,l=1}^{3} B_{kl} \frac{\partial^2 \Pi}{\partial x_k \partial x_l}. \tag{5.12}$$

This is equivalent to a set of Langevin equations [157] for the stochastic corrections to the deterministic equations (5.11) having the form

$$\frac{dx_k}{dt} = \sum_{l=1}^{3} A_{kl}x_l + \xi_k(t), \quad (k,l = 1,2,3), \tag{5.13}$$

where $\xi_k(t)(k = 1,2,3)$ is Gaussian white noise with zero mean and a cross-correlation function given by $\langle \xi_k(t)\xi_l(t')\rangle = B_{kl}\delta(t-t')$. Note that system (5.13) combines both the deterministic and stochastic contributions. Given that we are interested in evaluating fluctuations of the system trajectories around the non-trivial fixed point of the deterministic system, we evaluate the entries of the Jacobian matrix A_{kl} and B_{kl} of the noise covariance matrix at this stable fixed point. Explicit expressions for these two matrices are given in subsection D.3.1 of Appendix D.

The Langevin equations (5.13) describe temporal evolution of the normalized fluctuations of variables around the equilibrium state. By Fourier transformation of these equations, we are able to analytically calculate the power spectral densities (PSD) that correspond to the normalized fluctuations, independent of community size N. By taking the Fourier transform of equation (5.13), we transform them into a linear system of algebraic equations, which can be solved. After taking averages, in the three expected power spectra of the fluctuations of susceptible livestock, infected livestock and infected *Aedes* mosquitoes around the deterministic stationary values we obtain:

$$\begin{aligned} P_{S_2}(\omega) &= \langle|\tilde{x}_1(\omega)|^2\rangle = \frac{B_{11}\omega^4+\Gamma_{S_2}\omega^2+\chi_{S_2}}{|\mathcal{D}(\omega)|^2}, \\ P_{I_2}(\omega) &= \langle|\tilde{x}_2(\omega)|^2\rangle = \frac{B_{22}\omega^4+\Gamma_{I_2}\omega^2+\chi_{I_2}}{|\mathcal{D}(\omega)|^2}, \\ P_{I_1}(\omega) &= \langle|\tilde{x}_3(\omega)|^2\rangle = \frac{B_{33}\omega^4+\Gamma_{I_1}\omega^2+\chi_{I_1}}{|\mathcal{D}(\omega)|^2}, \end{aligned} \tag{5.14}$$

The complete derivation of these $PSDs$ and detailed descriptions about the way the functions χ_i, B_{kl}, Γ_k and $\mathcal{D}(\omega)$ depend on model parameters are discussed in Subsection D.3.2 of Appendix D.

5.4 Model Simulations and Results

5.4.1 Probability of a major outbreak in the absence of vertical transmission

In the absence of vertical transmission, that is, $R_{11} = 0$ the solutions of the equations $G_1(s_1,s_2) = s_1$ and $G_2(s_1,s_2) = s_2$ are provided in [150] and for the case of introduction of a single infectious vector, it is reproduced here as follows:

To obtain the extinction probability requires determining the smallest non-negative

root of

$$s_1 = \frac{1}{1 + R_{21}[1 - \frac{1}{1+R_{12}(1-s_1)}]}, \tag{5.15}$$

which is obviously given by

$$\frac{1 + R_{12}}{R_{12}(R_{21} + 1)}. \tag{5.16}$$

Note that this is smaller than 1 if and only if the product $R_{12}R_{21} = R_{0,H}$ is greater than 1. Consequently, when $R_{0,H} \leq 1$, the relevant solution is 1 and so a major outbreak can never happen [150, 171]. For $R_{0,H} > 1$, both the probability of extinction and of a major outbreak, are found by swapping the roles of R_{12} and R_{21} in the preceding elaboration.

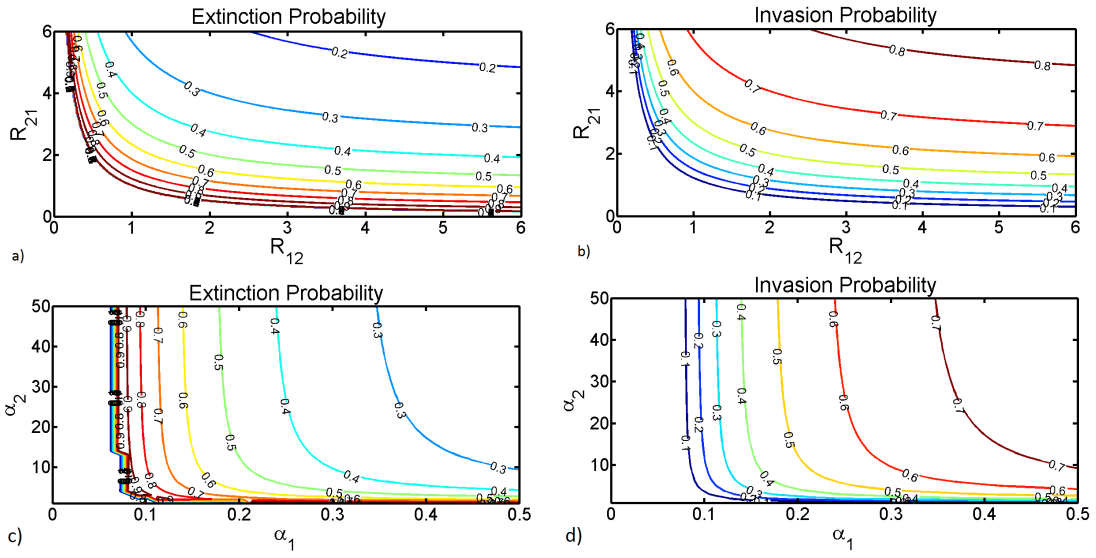

FIGURE 5.3: Solution of Eq.(5.15) when the product $R_{12} \times R_{21}$ is greater than unity. The curves in (a) and (b) are contours in the plane (R_{12}, R_{21}), along which the probabilities of extinction and invasion respectively, after an introduction of a single vector is constant. In (c) and (d) we plot probabilities of extinction and invasion respectively, when varying parameters α_1 and α_2. The values of the remaining parameters in days are as follows: $q_1 = 0.01, \mu_1 = 1/30, \mu_2 = 0.00046, \beta_{12} = 0.676, \beta_{21} = 0.28, \epsilon_2 = 0.25$.

Lloyd et al.[150] concluded that the asymmetry observed within the relationship between either probability of extinction or invasion with the reproductive numbers may stem from the disparity between the sizes of the host and vector populations. To further investigate this phenomenon we compute the probability of extinction and invasion while varying the biting ability of the vector when host ability to avoid a mosquito bite is taken into account. This is accomplished by varying the parameters α_1 (number of bites that a mosquito would bite a host) and α_2 (number of bites a host would sustain) when plotting the extinction and invasion probabilities. This is possible since in our approach we generalized the mosquito

biting rates so that they can be applied to wider ranges of population sizes. Instead of letting the total number of mosquito bites on livestock depend on the number of mosquitoes as in [150], we set the total number of bites to vary with both the livestock and mosquito population sizes. Results from Fig.5.3 (d) further rephrase the roots of the observed asymmetry highlighting that although the high ratio of mosquitoes to livestock is a major factor, any form of intervention to reduce livestock availability to mosquitoes can lead to such disparity. And disease extinction is only possible if the ratio mosquito to livestock is kept at a very low level resulting in values of α_1 less than 0.1 see Fig.5.3 (c). This explains why when environmental conditions are satisfied, that is, during rainy seasons disease outbreaks are expected as a result of the presence of massive numbers of potential vectors. However, without virus reservoirs in either host or vector population or virus introduction from the outside even in the presence of optimal climatic conditions, disease activities are almost impossible. Therefore, in the following section we examine the relationships of disease persistence, extinction and spread when effects of vertical transmission efficiency are taken into consideration.

5.4.2 Probability of a major outbreak in the presence of vertical transmission

In the presence of vertical transmission, determining the probability of extinction requires solving equations (5.7) and (5.8) when $R_{11} \neq 0$. In this regard, the extinction probability following the introduction of a single infectious mosquito is given by the smallest non-negative root [171] of

$$s_1 = \frac{1}{1 + R_{11}(1 - s_1) + R_{21}[1 - \frac{1}{1+R_{12}(1-s_1)}]}. \tag{5.17}$$

After rearranging the above equation we obtain

$$R_{11}R_{12}(1 - s_1)^2 s_1 + (R_{11} + R_{12} + R_{12}R_{21})(1 - s_1)s_1 - R_{12}(1 - s_1) + s_1 - 1 = 0, \tag{5.18}$$

which is a cubic polynomial in s_1. Note that for $R_{11} = 0$ this equation reduces to quadratic equation (5.15). It is evident that $s_1 = 1$ is a solution to equation (5.18) and the remaining solutions are found by solving the quadratic equation

$$R_{11}R_{12}s_1^2 - (R_{11} + R_{12} + R_{11}R_{12} + R_{12}R_{21})s_1 + R_{12} + 1 = 0. \tag{5.19}$$

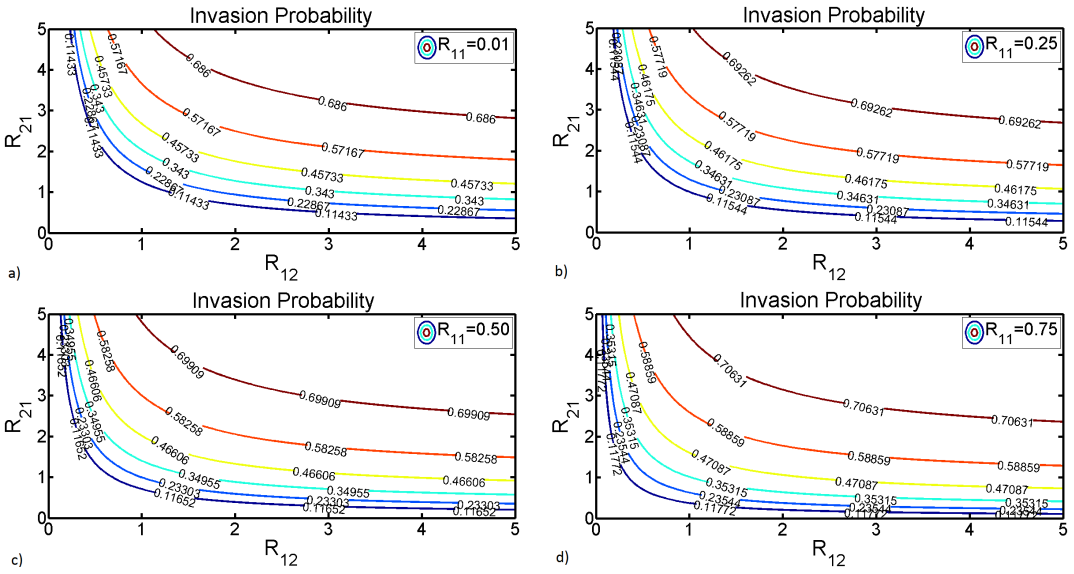

FIGURE 5.4: The curves represent contours in the plane (R_{12}, R_{21}), with varying vertical transmission efficiency, along which the probability of invasion after an introduction of a single vector is constant. These probabilities are obtained from the solutions of equation (5.19).

Studies have shown that in the absence of vertical transmission in mosquitoes RVFV dies out when $R_0 < 1$ and becomes endemic when $R_0 > 1$. However, in the presence of vertical transmission the disease may persist even for $R_0 < 1$ [4, 5, 77]. This situation stems from the fact that in host-vector systems, R_0 results from a complete cycle of host-vector-host or vector-host-vector transmission and does not reflect the average number of secondary infections of a specific population type [85]. For instance, $R_0 = 0.75$ may result from a product of host reproductive number $R_{12} = 5$ and vector reproductive number $R_{21} = 0.15$. Nevertheless, in each generation, the number of host infections is proportional to the number of infected mosquitoes, and decreases proportionally to the vertical infection efficiency. However, if the host reproductive number is high it is likely to boost up new vector infections in future generations. Figure 5.4 shows the dependency of probability of disease invasion on R_{12}, R_{21} and vertical transmission efficiency R_{11}. The invasion probability increases linearly with increments on vertical transmission efficiency with significant impact when the proportion of vertical infection efficiency exceeds 20%. Other studies have found that it is only from this level of vertical transmission efficiency that time of viral persistence is observed [80, 85]. Another interesting relationship is that as the invasion probability increases with vertical infection efficiency the horizontal transmission $R_0 = R_{12} \times R_{21}$ tends to decrease highlighting an asymmetric relationship with R_{12} and R_{21} as highlighted in the previous section.

5.4.3 Temporal patterns of Rift Valley fever in Sub-Saharan Africa

RVF is known to be endemic in Sub-Saharan Africa [9] with some differences in temporal patterns characterized by long periods with no outbreaks in eastern and southern regions of the continent [3]. However, a closer look at temporal patterns of disease outbreaks in Tanzania and Kenya (East Africa) and South Africa (Southern Africa) shows existence of some possible differences in the temporal characteristic patterns of disease outbreaks. Figure 5.5 depicts temporal characteristic patterns of disease outbreaks from 1930 to 2007 in Tanzania [3], from 1951 to 2007 in Kenya [1] and from 1950 to 2011 in South Africa [2]. The prevalence shown for Kenya and South Africa is artificial, it is only for representation purposes since real information regarding prevalence of the disease at each year is not available. Although data regarding reported cases for each outbreak exist [3], it is not complete. Data for the years 1960, 1963 and 1968 is missing. The plots in Fig.5.5 are based on data reported in [1] for Kenya, in [2] for South Africa and in [3] for Tanzania. According to Pienaar and Thompson [2] during this period South Africa experienced only three major outbreaks (1950-1951, 1974-1976 and 2010-2011) and the remaining are considered smaller or isolated outbreaks. Interestingly the 1974 outbreak lasted for 3 consecutive years, a situation which can be compared to the 1960 outbreak that occurred in Kenya which continued until 1964 [1]. From the time series Fig.5.5 (b) we observe that after each major outbreak including the outbreak in 1985-1986 in South Africa there are subsequent outbreaks occurring nearly each year. According to findings by Murithi et al.[1] during the period 1950-2007 only 11 large scale outbreaks were recorded with an average inter-epizootic period of 3.6 years (range 1-7 years). However, for Tanzania an average inter-epizootic period of 7.9 years (range 3-17 years) is reported [3]. These disease post-epidemic activities in ruminants are known to occur without clinical cases and can only be detected where active surveillance is carried out[39, 46]. Could it be that these differences in temporal patterns are results of a deficit of surveillance system to cover all remote regions that are vulnerable to the disease or are due to differences in the ecology of the vector? This question takes us to another question which is the driving force of this study. Could it be possible that smaller or sporadic RVF outbreaks occur every year after major outbreaks without noticeable outbreaks or clinical cases due lack of active surveillance? Could the prevalence of these outbreaks show multi-year periodicity? If disease prevalence data could be available we would apply techniques of wavelet analysis which performs a time-scale decomposition of a time signal to estimate spectral characteristics of the signal as a function of time [146, 177].

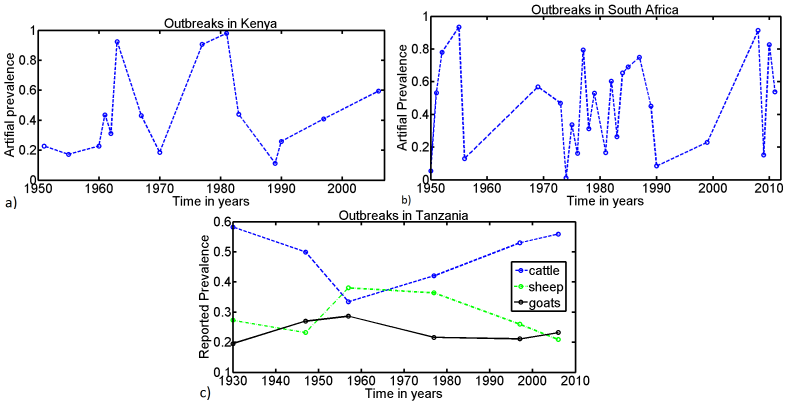

FIGURE 5.5: Temporal history of RVF outbreaks in some countries of Sub-Saharan Africa. In (a) and (b) the circles represent years of outbreaks occurrence in Kenya and South Africa [1, 2] and the prevalence indicated in the figure is not real, it is just for representation only since data on prevalence is not available. In (c) the circles represent the prevalence of disease outbreaks in Tanzania [3].

This would allow us to predict the dominant period of outbreak fluctuations when varying some model parameters in particular, vertical transmission which is known to be the driving force behind the continuous disease endemicity in these regions [3]. Since reliable information is not available, in the following section we theoretically estimate the power spectra of disease oscillations taking into account effects of demographic stochasticity and vertical transmission.

5.4.4 Effects of stochasticity and vertical transmission on disease outbreaks

Figure 5.6 depicts the power spectrum density (PSD) for fluctuations of the total number of susceptible livestock, infected livestock and infected mosquitoes as derived in equations (5.14).

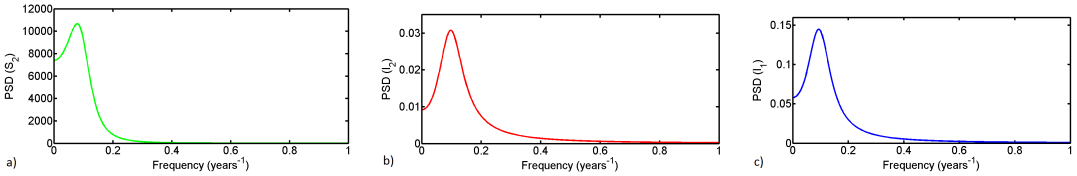

FIGURE 5.6: Theoretical prediction of the power spectrum density (PSD) (Eq.5.14) for fluctutions of the total number of susceptible livestock, infected livestock and infected mosquitoes. Values of the parameters in years are as follows: $q_1 = 0.05, \mu_1 = (1/16) * 360, \mu_2 = 1/10, \beta_{12} = 0.170, \beta_{21} = 0.116, \epsilon_2 = (1/4) * 360, \alpha' = \alpha = 256, m_0 = 1.5$ and their description and sources are given in Table 5.1.

Our derivation of exact expressions for the power spectrum of the stochastic variables around the endemic equilibrium, see (Eq.5.14) gives additional benefits. Using the expression for the power spectrum density (PSD) for variable I_2 we examine how changes in female *Aedes* vertical transmission efficiency affects the periodicity of RVF outbreaks. In Fig.5.7 (a) we observe that an increase in vertical transmission efficiency causes a significant increase in the frequency of disease outbreaks. To better illustrate this phenomenon, we show that for vertical transmission of $q_1 = 0.05$ the dominant period of disease outbreaks is about 10 years while for $q_1 = 0.5$ the dominant period is about 1 year. These results suggest that with low efficiency of vertical transmission there is a high probability of disease extinction after a major outbreak, followed by a long period without outbreaks. This stems from the fact that the mosquito life cycle is relatively short and vertically acquired infections are multiplicatively diluted with every generation such that the virus is rapidly lost unless there is regular amplification in the host population. This could be only possible if renewal of susceptible livestock would happen with high frequency. Since the PSD formula (5.14) describes components of the deterministic model we can examine effects of the nature of the basic reproduction number R_0 on outbreaks periodicity. If R_0 is less than or equal to unity, with a high probability the disease outbreak is relatively small. This is the reason why most studies would rather concentrate on the complementary case. However, our analysis (see Fig.5.7(b) and Fig.5.7(c)) shows that the most important and interesting case is where R_0 is near unity. We see that as R_0 moves away from unity the PSD surface becomes flatter, indicating that more frequencies are involved in the stochastic fluctuations. This simply means that when increasing R_0, the dominant period decreases (the dominant frequency increases), however for larger values ($R_0 > 2$) the PSD becomes totally flat. In this region 'coherence resonance', that is, a phenomenon in which random fluctuations sustain nearly periodic oscillations around the deterministic endemic equilibrium is lost and becomes white noise. Furthermore, we examine the PSD surface for nearly extreme values of vertical transmission efficiency $q_1 = 0.05$ and $q_1 = 0.5$. For larger values of vertical transmission the frequency of system fluctuation tends to increase, resulting in continuous endemicity of the disease as has been observed in some of the endemic regions [3]. While for small values of vertical infections the frequency of outbreaks is significantly reduced.

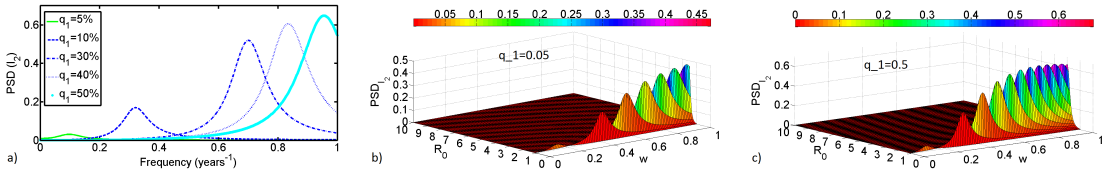

FIGURE 5.7: Power Spectra Density (PSD) for the variable I_2 (Eq.5.14). a) Effects of vertical transmission efficiency on the PSD. Three-dimensional representation of the PSD when varying R_0 and the frequency for $q_1 = 0.05$ and $q_5 = 0.5$ in b) and c) respectively. Model parameter values used are as follows: $\beta_{12} = 0.170, \beta_{21} = 0.116, \epsilon_2 = (1/4) * 360, \alpha' = \alpha = 256, \mu_2 = 1/10, m_0 = 1.5, \mu_1 = (1/16) * 360$. This gives $R_0 = 1.0066$.

5.5 Discussion and Conclusion

We have explored the use of analytical tools to measure and examine effects of demographic stochasticity in host-vector models with two routes of transmissions. Host-vector models are designed to explain the dynamics of diseases in which transmission of the pathogen is mediated by a vector. For our study case which is Rift Valley fever (RVF), the vector is a mosquito of genus *Aedes* with special ability of transmitting the virus to its offspring transovarially. In disease dynamics, this leads to two modes of transmission: horizontal and vertical. The analytical tools applied are: branching process theory to examine the impact of stochastic effects on the invasion and persistence of RVF infection when vertical transmission is taken into account and van Kampen's method to investigate effects of mosquito vertical transmission on the characteristic temporal patterns of multi-year periodic disease outbreaks. As found in Lloyd et al.[150], results obtained using branching process methodology highlighted that the existing asymmetry relationship between the disease transmission potentials from hosts to vectors and from vectors to hosts can have significant epidemiological impacts. This stems from the fact that the disease invasion probability starting from a single infective host and the invasion probability starting from a single infective vector can differ significantly, even though the overall basic reproductive number of the infection is the same in both cases [150]. This asymmetry can lead to a situation where the overall basic reproduction number is greater than unity while either the vector or host reproductive number is less than unity, resulting in dramatic implications for disease control efforts. To further investigate the impacts of this asymmetry relationship in disease control strategies we computed the invasion and extinction probabilities when varying the mosquito biting ability α_1 and the host ability to avoid mosquito bites α_2. Our findings suggest that although the ratio of mosquitoes to livestock is a major factor, any form of intervention to reduce livestock availability to mosquitoes can lead to such disparity.

Previous studies have shown that in the absence of vertical transmission in mosquitoes RVFV dies out when $R_0 < 1$ and becomes endemic when $R_0 > 1$. However, in the presence of vertical transmission the disease may persist even for $R_0 < 1$ [4, 5, 77]. To investigate this phenomenon we computed the invasion and extinction probabilities while varying the intensity or efficiency of vertical transmission. Our results suggested that invasion probability increases linearly with increments on vertical transmission efficiency with significant impact when the proportion of vertical infection efficiency exceeded 20% as found in other studies of vector-borne diseases [80, 85]. Adams and Boots [85] found that vertical infection could only be important in dengue ecology, if the efficiency in nature is substantially greater than that found in empirical studies. On the contrary, vertically acquired infections are multiplicatively diluted at every mosquito life-cycle generation, such that, the virus is rapidly lost unless there is regular amplification in the host population. However, regular amplification of the virus in the host population is not certain for several factors. Recovered ruminants from RVF infection are immune for several days if not months [178], and vaccinated livestock may produce a high level of neutralizing antibodies, making them protected against subsequent RVF viral infections [179].

However, how long do these neutralizing antibodies persist and other immune responses such as innate, humoral and cell mediated are not known with good degrees of certainty and require further investigation [11]. Another, interesting factor is the viraemic phase whose intensity and duration may vary according to the inoculated dose, the virus strain and the degree of natural susceptibility of the infected ruminant [11]. Results from experimental studies have indicated that depending on the host's innate susceptibility or resistance the infection may be classified as: severe acute lethal infection, delayed onset of complications or mild to asymptomatic infection [180–182]. Low level asymptomatic circulation and host re-introduction from external reservoir populations are also likely to be important factors [4, 5, 85]. Chamchod et al.[77] concluded that re-introduction of susceptible livestock from external sources (either through movement or buying) may lead to a certain probability of some subsequent outbreaks if the renewal takes place every year. Certainly in such a situation if vertical transmission is very low we are likely to observe long intervals with no outbreaks just like the situation in Tanzania (see Fig.5.5(a)); while for high values of vertical transmission we are likely to observe frequent waves of disease outbreaks just like in South Africa Fig.5.5(b). In summary, our results reveal that higher values of vertical transmission or vertical infection efficiency increase the frequency of disease outbreaks and highlight the importance of the interplay between horizontal and vertical transmission [4, 5, 69, 77] in the spread of the disease.

A study of temporal and spatial patterns of RVF in Tanzania [3] concluded that only continuous activity of virus circulation could lead to the observed characteristic temporal pattern of disease outbreaks in Sub-Saharan Africa. Our results in Fig.5.4 further indicated that although invasion probability increases with vertical infection efficiency, the horizontal transmission reproductive number tends to decrease, highlighting an asymmetric relationship between the host and vector reproductive numbers. This further highlights the role of vertical transmission efficiency in inducing complex behaviours in the dynamics of RVF outbreaks. Such complex dynamics may partially be explained from the fact that effects of vertical infection are further compounded by effects of the diapause phenomena in *Aedes* mosquitoes.

Previous RVF modelling studies [4, 5, 77] have relied on the use of seasonal type functions in order to explain periodicity or subsequent waves of RVF outbreaks in endemic regions as well as characterizing the nature of the resulting oscillations when mosquito population varies according to seasons or climatic conditions [4]. This is the standard paradigm in the framework of deterministic models [146], where seasonal and/ or climatic extrinsic forcing and intrinsic host-pathogen dynamics are both used in order to understand the nature of different types of disease oscillations and system's attractor structures [183]. However, more recently, it has become clear that the interaction between the deterministic dynamics and demographic stochasticity is fundamental to understand realistic patterns of disease outbreaks [145]. To the best of our knowledge this is the first time a non seasonal full stochastic host-vector model is used to explain the temporal characteristic

pattern of disease multi-year periodicity depending on vertical transmission efficiency. This was accomplished by performing van Kampen [166] system size expansion, which allows us to derive an approximate analytical solution of the model. This method enables us to further view the population-level dynamics as being composed of a deterministic part and a stochastic part, where the spectrum of stochastic fluctuations is intimately related to the stability of the deterministic level dynamics [147]. Through power spectra analysis we were able to calculate the power spectrum of the stochastic fluctuations analytically and by comparison with simulations we can gain general insights into mechanisms underlying the peaks. Our analysis predicts complex fluctuations with a dominant period of 1 to 10 years for acceptable parameter values, which essentially depends on the efficiency of vertical transmission. These findings are in good agreement with observations, which indicate that in endemic areas RVFV is known to circulate continuously and outbreaks occur at irregular intervals of up to 15 years [1, 184], or 10-15 or even 3-7 years [1, 51]. Note however, that these periods of disease outbreaks are not known with exact details due to lack of appropriate infrastructure and active disease surveillance.

Although, we do not reproduce the exact known patterns of RVF outbreaks fluctuations, we provide a simpler and plausible explanation, showing that the interplay between the stochastic component and vertical transmission is central to understanding the erratic patterns of disease outbreaks characterized by a dominant period of 1 to 10 years. Our results indicated that an increase in the vertical transmission efficiency increases the frequency of disease outbreaks, hence reducing the periodicity of outbreaks to nearly a dominant period of one year. This further confirms our findings through branching process theory as discussed above. When vertical infection efficiency is higher RVFV is likely to circulate every year with virus amplification at every rainfall season leading to yearly sporadic cases of disease outbreaks. This situation can be compared with the observation of disease outbreaks in South Africa as shown in Fig.5.5(b). According to a review by Pienaar and Thompson [2] since the first outbreak in 1950, South Africa has experienced only three major outbreaks (1950-1951, 1974-1976 and 2010-2011), with sporadic or isolated outbreaks in between. Two interesting temporal patterns can be discussed: (1) the post-epidemic disease activities or disease activities between two major outbreaks are of one year cycle; (2) the second major outbreak lasted for three consecutive years. Could it be that the efficiency of vertical transmission in South Africa is relatively higher, sustaining continuous endemicity patterns? Our analysis provides a simple but one of the most relevant explanations for this situation. An increase in vertical transmission efficiency leads to low frequency of disease outbreaks of nearly one year cycle which is in good agreement with findings from empirical studies [2, 144]. The epidemic continued through the winter, spilling over into the next rainfall season. It is believed that such spillover was possible due to warm temperatures and wet conditions during winter, which are conductive for reproduction of mosquitoes maintaining infection through winter. However, other dynamical factors such as susceptible livestock recruitment (or movement), mosquito seasonal abundance and livestock immune responses could play a role on fluctuations of RVF

outbreaks [4, 5, 77]. Perhaps a combination of these factors was responsible for the 1974-1976 and 1960-1964 outbreaks in South Africa and Kenya respectively, which lasted for at least three consecutive years [1, 2]. Such 'long-lasting' consecutive outbreaks are not common and their underlying factors are not yet fully understood.

On the other hand, our model predicts that for low levels of vertical transmission the frequency of outbreaks becomes very low resulting in a dominant period of disease outbreaks of nearly 10 years. These findings suggest that when efficiency of vertical transmission is very low the virus may require a long period of time to build up and eventually trigger an initial phase of the outbreak. This is a reasonable explanation for why there have been instances with no records of outbreaks following seasons of exceptionally above normal rainfall. This is likely to be the situation in East Africa, for example Tanzania (see Fig.5.5(a)). The outbreaks occur at irregular intervals followed by long periods (inter-epidemic period) without records of disease outbreaks, however, RVFV activities have been detected but with no clinical signs in the mammalian host [39, 45, 46]. During this inter-epidemic period (IEP) the virus exists but it fails to further amplify within the host during every wet season. Our explanation is that since the mosquito life cycle is very short, if there is no regular amplification of the virus in the mammalian host population, vertically acquired infections can be rapidly lost. Low virus activities result in lower immunity in the host population and create conditions for large outbreaks whenever the virus may have sufficiently built up. In summary, for low vertical infection efficiency we expect long intervals without outbreaks.

For a long time entomological studies have highlighted the relationship between abnormal rainfall and RVF outbreaks [1, 13, 34, 185]. However, optimum climatic conditions and the presence of mosquitoes have not completely explained the epidemiology of RVF outbreaks [26]. For instance, abundant rainfall, which normally correlates with increased number of mosquitoes in East Africa, was not often associated with RVF outbreaks in West Africa [11], and even in East Africa there have been instances where no outbreaks were recorded following seasons of exceptionally above normal rainfall [3]. These observations suggest that while rainfall might be the major determinant factor for the onset and switch-off of an outbreak [3], it is likely to not be the only factor responsible for the characteristic pattern of disease outbreaks. Other factors such as causal association between local environmental factors, livestock density and movement, encroachment of mosquitoes into new areas and livestock immune responses could be responsible for the observed characteristic pattern of disease outbreaks [3]. However, in this study we maintain the focus on the role of vertical transmission and chance event on the oscillation of disease outbreaks and endemicity as we expect our results to be valid even when the above factors have been taken into account. Nevertheless, effects of livestock immune responses and livestock re-introduction or movement deserve their own further investigation.

Chapter 6

An Individual-based Model of Rift Valley fever Mosquito Life Cycle for Predicting Abundance of Mosquitoes

6.1 Introduction

Rift Valley fever is a mosquito-borne zoonotic disease causing fear in the majority of most vulnerable communities in many regions of the African continent [1, 11, 14]. The majority of these communities are pastoralist, at least in East Africa and their livelihood mainly depends on livestock production [45, 58]. In East Africa it is estimated that the recent RVF outbreak in 2006/07 resulted in losses amounting to more than 60 million US$ due to disruption in trade of domestic livestock, including costs of livestock deaths [75], with an estimate of 27,500 human cases [45]. Disease outbreaks (epidemic activities) are correlated with heavy rainfall and excessive flooding, in particular in East, South and horn of Africa [1, 14, 34]. These events cause a massive emergence of *Aedes* mosquitoes [117], which trigger the initial spread of the infection through vertically infected mosquitoes. Then, they are succeeded by *Culex* species, which if infected when feeding on viraemic livestock further disperse the virus [3].

Both climatic and weather conditions increase the number of breeding sites for mosquitoes resulting in an increase in the number of vectors and therefore more intense virus transmission and circulation [79], enhancing risk of vector-borne disease infection. The two vectors species involved in the transmission of RVF breed in fresh water [11]. The *Aedes (mcintoshi,vexans, dentatus)* species, usually called floodwater mosquitoes are associated with freshly flooded temporary water-bodies [31, 186], while *Culex (pipiens,quinquefasciatus,antennatus)* are associated with more permanent fresh water-bodies [11, 33]. Female *Aedes* lay their eggs in the

wet soil surrounding the pools. Once the embryonic development is completed, eggs may either enter a period of diapause (withstanding up to four years of drought) [187, 188] or hatch producing first stage larvae, when flooding and temperature at the breeding sites are suitable [187, 189]. On the other hand, *Culex* females lay their eggs on the water surface [189]. Therefore, fluctuations of these vector populations are strongly correlated with the flooding regimes of the breeding sites and atmospheric temperature which govern their development [189]. This is also a function of both the flooded area and water permanence during the time required for the mosquito to complete its preimaginal development [190]. The extension of the flooded area is directly related to rainfall volume and inversely related to the time elapsed since the last rain event, owing to evaporation and/or infiltration [191]. An increase in temperature increases the development rate of each stage of the mosquito, hence reducing its time from egg to adult. Therefore, a rapid emergence of young adults is triggered, which leads to abundance of mosquitoes during favourable seasons. In spite of all these inherent complexities, modelling has proven to be a very useful approach for handling complex systems and for years it has impacted both our understanding of vector ecology and disease management. Complex systems are often formulated and analysed on the basis of simulation models, with particular emphasis on agent-based or individual-based models thanks to recent advances in computer technology (in both hardware and software). Individual-based models (IBM) compared to equation-based models, offer certain unique features which include the ability to incorporate individual variability of agents and to investigate macroscale properties by integrating microscale interactions [192]. Several simulation models have been developed to investigate correlation between weather conditions and abundance of mosquitoes. The majority of these models have dealt with mosquitoes involved in the transmission of: malaria infections (for more details see [193–195] and references therein); dengue and/or chikungunya viruses [196–199]; West Nile viruses [200] and also RVFV [79]. However, most of these models either include effects of rainfall or temperature alone with little effects on individual's variability. In this chapter we present an individual-based model (IBM) of RVF mosquito life cycle following the framework proposed in [65]. This modelling framework presents several benefits as it provides modellers with complete guidance while in model development, analysis and application [201]. This approach has been successfully adopted by several researchers while addressing a variety of research questions [65, 202–204]. Our model builds upon daily rainfall and temperature data sets which govern the development of mosquitoes. The model simulates the population of all stages of *Aedes* and *Culex* mosquito life cycle. This includes all important features of both mosquito life cycle such as: oviposition, egg maturation, diapause, developmental stages (egg, larva instar 1 to 4, pupa and adult), development and mortality in all different stages, aquatic habitats, host seeking, engorgement and oviposition site seeking, adults age-dependent mortality and flight behaviour. Transition in all aquatic/immature stages (egg, larva and pupa) is modelled using the concept of degree days [205, 206]. Mosquitoes are exothermic organisms and their development mainly depends on environmental temperature. Therefore, their physiological time can be approximated by heat accumulation in units measured in degree days [207–209]. Our objectives are to correlate abundance of mosquitoes with weather conditions for predicting temporal

patterns of mosquito population dynamics. Our efforts will be capitalized on answering the following questions: (1) Is there any synchronization between rainfall and abundance of mosquitoes? (2) What features of the mosquito life cycle affect the mosquito population dynamics? The weather data (precipitation and temperature) used to investigate the performance of the model were collected from a weather station in Ijara district of Kenya from 2009 to 2010. This model differs with other related models in many important ways:

1. The mosquito species involved here are floodwater and not indoor. Thus, their breeding habitats only depend on rainfall [186, 189]. The time it takes while the water persists in these habitats is inversely related to air temperature [191]. Thus, we include the effects of evaporation by assuming that water persists for about 20 to 40 days [210, 211].

2. Hatching of mature eggs (those with embryonic development completed) depends on the amount of precipitation accumulated in the larval habitat [187, 189]. The minimum level of water required for egg hatching and development of all aquatic stages is assumed to be 16 *mm* [212].

3. We implement diapause in both mosquito species to ensure long-term survival of the vectors. *Aedes* survive unfavourable seasons through dessication of the eggs, while *Culex* survive on the adult stage [189].

4. In addition to temperature and rainfall dependent mortality, we include the effects of drought or long periods of dessication in the survival of immature stages [213].

5. Survival of both *Aedes* and *Culex* adults is age dependent [214].

6. The mosquito dispersal behaviour used for host blood-meal seeking is of type oriented [189, 215] and it depends on the distance to the host within vision radius [189].

A model with all the above features built into the framework of IBM is an unique tool for: predicting both short and long-term patterns of RVF mosquito population and investigating how both temperature and rainfall contribute to the intra- and inter-annual variations observed in the dynamics of adult mosquitoes. Analysis of the model provides general insights and valuable informative indicators of mosquitoes life cycle stages such as gonotrophic cycle, longevity of adults, number of eggs laid by each adult and adults flight behaviour that could be targeted for vector control. Additionally, this type of model offers an excellent opportunity for investigating a broad range of vector related biological questions and the model is extendible to include to fit several application such as disease transmission, disease management among others.

6.1.1 Study site and data collection

Ijara is one of the semiarid districts of North Eastern Kenya with low erratic rainfall but prone to flooding in times of heavy persistent rainfall [46]. The majority of its inhabitants are nomadic pastoralists and over 90% of the population depends on livestock for daily nourishment and as a source of income [45]. Sangailu is its main town and it is located 1°19′0″ S and 40°44′0″ E, with temperatures ranging between 15°C and 38°C, bimodal rainfall ranging between 700 and 1000 mm per annum, average relative humidity of 68 mm and altitude range of 0 to 90 m above sea level [45]. We focus in this area for two reasons: (1) availability of weather data; (2) availability of detailed studies about occurrence of RVF disease activities during the inter-epidemic period which we would like to focus on in subsequent studies. Both temperature and precipitation were recorded daily.

6.2 The Model

The model was developed using Netlogo 5.2 software (http://ccl.northwestern.edu/netlogo/.) [216], combined with R extension (RNetlogo) for model analysis [217, 218] and Matlab was used for graphical outputs. The model description follows the ODD (Overview, Design concepts, Details) protocol for describing individual- and agent-based models [219]. A complete schematic representation outlining all processes and algorithms of the RVF mosquito life cycle model which consists of both aquatic and terrestial (adult) mosquitoes is shown in Figure 6.1. A summary of all model input parameters included within the simulation model is given in Table 6.2.

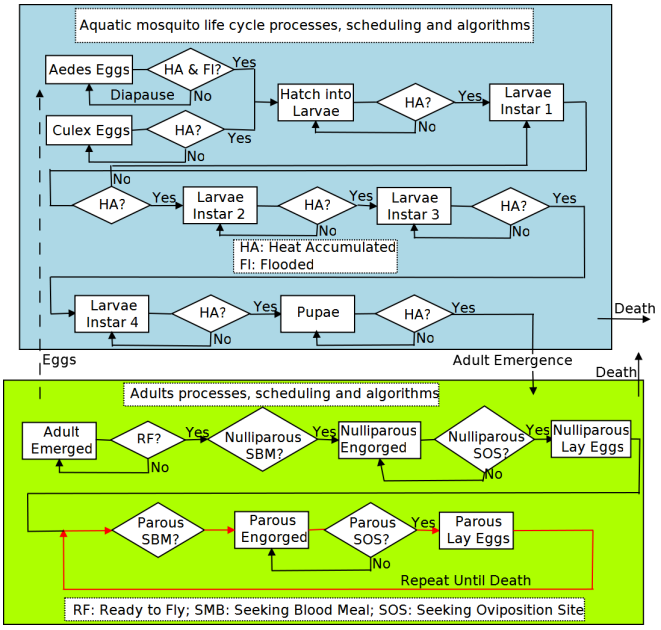

FIGURE 6.1: Outline of model processes and scheduling of the sub-models algorithms. The rectangular boxes represent the process (a state) of a given entity while the rhombus represents a decision point. Details on the decision processes are discussed in Section 6.2.7.

6.2.1 Purpose

This model aims to predict the temporal abundance of RVF mosquitoes based on the synchronization and de-synchronization between a mosquito's life cycle and both temperature and rainfall patterns.

6.2.2 Entities, State Variables and Scales

We have five groups of entities in the model: aquatic mosquitoes (eggs, larvae and pupae), terrestrial mosquitoes (adult mosquitoes), livestock, mosquito habitats (water-bodies and edges of water-bodies) and the model environment. Note that we have two types of mosquito species, *Aedes* and *Culex*, hence we have ten entities, also referred to as breeds in the Netlogo terminology: Aedes-Eggs, Aedes-Larvae, Aedes-Pupae, Aedes-Adult, Culex-Eggs, Culex-Larvae, Culex-Pupae, Culex-Adult, Livestock and Habitats. Transitions from one stage to another of the mosquito life cycle is modelled using the concept of degree days. Degree-days (DD) are used to compute the total amount of heat required, between the lower and upper temperature thresholds, for a poikilothermic organism to develop from one stage to another in its life cycle [207–209]. Aquatic stages of both mosquito species with exception of *Aedes* eggs breed in fresh temporary water and the minimum accumulated rainfall required to initiate the first cohort of mosquitoes is 16 *mm* in each breeding site [212]; for more details (see Table 6.1). These two mosquito species

differ only in terms of egg adaptation, adult adaptation, oviposition behaviour and identification of oviposition site [189]. *Aedes* eggs are laid in damp soil (here called edges of water-bodies) singly and they have one static variable for their location (edge of the water-body) and other dynamic variables such as: accumulated-DD for embryonic development to be compared with the minimum accumulated-DD required for embryonic development, a counter of time it takes for eggs to mature and diapause. *Culex* eggs have the same state variables with exception of diapause and their habitat which is the water-body.
Both *Aedes* and *Culex* larvae and pupae develop in water, thus, they have one static variable for their location (water-body). The larvae go through four intermediate developmental stages: instar 1, instar 2, instar 3 and instar 4. They have the following dynamic variables: accumulated-DD to develop from one stage to another to be compared to the minimum accumulated-DD required to complete the development at each stage. Once the stage of pupae has been completed they become adults and the adults consist of immature adults, blood-seeking and engorged. Adult mosquitoes emerge from the water and begin flying a short time after they have dried out and their body parts have hardened. This period in the model sense takes 1 or 2 days as it also accounts for the mating period [189]. After a successful blood meal the time elapsed to the next blood feeding activity is a function of the mosquito's gonotrophic cycle. Livestock only have one static state variable, which is their location since in this model they are just a source of blood for the mosquitoes.

The model does not use real geographic space, but instead represents the environment as a two-dimensional space of 10201 m^2 grid with 20 m x 20 m grid squares corresponding to an area of 2 km x 2 km. A scale of 20 m x 20 m grids (patches in the Netlogo language) was chosen, since a mosquito can identify a host from a distance of $> 20m$ [189]. Hence, mosquito host-seeking behaviour is approximated at this scale. In this environment we then define water-bodies and water-body edges representing larval habitats. Water-bodies are patches representing pools that are intermittently flooded depending on rainy regimes and water-body edges are patches surrounding water-bodies representing damp soil for *Aedes* adults to lay their eggs. Each water-body has a state variable the 'daily water level' and the 'water-body depth' which varies between 16 mm and 100 mm. The surface area of each water-body is set identical since it does not affect flooding regimes of the water-bodies. The model is set so that one time step in the model represents one day and it is run for almost two years from 15 January 2009 to 15 October 2010.

	Minimum Accumulated Degree Days for Development	
Stages	**Value**	**References**
Aedes Eggs	90	[220]
Aedes Instar 1	20	[6]
Aedes Instar 2	17	[6]
Aedes Instar 3	18	[6]
Aedes Instar 4	35	[6]
Aedes Pupae	25	[6]
Aedes Instar 1 to Pupae	90	[6]
Culex Eggs	30	[189]
Culex Instar 1	20	[6]
Culex Instar 2	17	[6]
Culex Instar 3	22	[6]
Culex Instar 4	44	[6]
Culex Pupae	34	[6]
Culex Instar 1 to Pupae	100	[6]
Base Temperature	10	[6, 189]

TABLE 6.1: Minimum accumulated Degree-Days and water levels required for development of each stage of the aquatic mosquito life cycle.

6.2.3 Process Overview and Scheduling

This model simulates complete RVF mosquito (*Aedes* and *Culex* spp.) life cycle stages for predicting patterns of mosquito abundance. Time is modelled in discrete time steps where each time step corresponds to a one day of activities. A time step of one day was chosen because important features of mosquito life cycle can be captured with daily units of measurements and observations [6, 189, 199]. Within each time step in the mosquito life cycle model, each entity will go through its developmental stages, while first checking survivability followed by its underlying life cycle activities. At each time step mosquito habitats update the level of accumulated water as temperature and rainfall update their values. A detailed description of all model processes is given in Section 6.2.7.

6.2.4 Design Concepts

6.2.4.1 Basic Principles

Construction of the mosquito life cycle model and its underlying design concepts follows the framework of Pattern Oriented Modelling (POM) [65, 201, 202], in combination with experimental data. This approach has been successfully used in other mosquito population predictive models [195, 199]. The dynamics of mosquito life cycle basically are driven by interactions between temperature and precipitation. Temperature directly influences the rate of mosquito development and population increase. Precipitation is the main factor that triggers the hatching of *Aedes* eggs [187, 189] and is responsible for creating breeding sites for both *Aedes* and *Culex* since these are outdoor species and they breed in temporary shallow fresh water-bodies [186, 189]. However, rainfall may reduce survival of aquatic mosquitoes

through flushing effects [221], hence, reducing abundance of adult population [222]. In addition, extended periods of dessication, that is, lack of precipitation, affects survival of aquatic mosquitoes while survival of adults is age-dependent.

6.2.4.2 Emergence

Both rainfall and temperature affect different stages of the mosquito life cycle leading to appearance and development of new cohorts of adult mosquitoes showing seasonal patterns.

6.2.4.3 Adaptation

The eggs of *Aedes* mosquitoes have a specific adaptive behaviour. They need water to hatch, so if there is no rain they will go diapause (dormant) until when they are flooded enough to hatch [187]. This adaptive behaviour ensures survival during dry season. They accomplish this, within our model, by measuring the daily water level in the water-body. When the level is above the minimum required for hatching they hatch otherwise they go diapause. Within variability to water-flow in the water-body both *Aedes* and *Culex* eggs have another sophisticated adaptive behaviour referred to as "hatching in instalments", that is, not all eggs hatch uniformly [189]. We implement this as follows: if the daily water level and that of the 6 following days is above the minimum required for the eggs to hatch with a given probability depending on daily precipitation. Otherwise, either 50% or 25% of eggs may hatch according to the level of the four consecutive days and one day respectively. This adaptive behaviour also ensures long-term survival of the species in situations of dry spells which may interrupt complete development of the mosquito [189]. *Culex* adults adapt their longevity according to the length of the dry period. The longer the dry period, the higher their survival, hence their longevity. This ensures their survival during periods in which they cannot reproduce [189]. This is accomplished by computing their survival probability based on age-dependent function [214, 223] coupled with dependence on the number of consecutive days with no rain.

6.2.4.4 Fitness

Diapause allows *Aedes* to survive long periods of dry season and long-term survival. *Culex* take advantage of wet season to reproduce massively and use an age-dependent survival probability function coupled with dependence on the number of consecutive days with no rain in order to ensure long-term survival of the species [189].

6.2.4.5 Sensing

Aquatic mosquitoes sense the daily temperature, total precipitation and daily water level of the breeding site for their daily decision-making processes by "reading"

temperature and precipitation each day. Adult mosquitoes are assumed to know distances to all livestock locations within their search radius.

6.2.4.6 Interaction

The interaction between aquatic *Aedes* and aquatic *Culex* takes place when they share a common breeding site, but this does not affect the dynamics of abundance of mosquitoes since we do not implement density dependent mechanisms. Both adults interact while feeding from the same mammalian host.

6.2.4.7 Stochasticity

Both survival and development of both aquatic mosquitoes are simulated as stochastic events with probabilities that are deterministic functions of both temperature, rainfall and duration of drought days. This is to account for other factors leading to death or development of the mosquito or incomplete knowledge with respect to factors leading to these events. Blood feeding is modelled as stochastic process in which proximity to a host is a factor. Gonotrophic time, that is, the time an adult mosquito waits until the next blood feeding is drawn from a normal distribution with a mean of eight days [213] and a standard deviation of a quarter of the mean. This is to ensure that other factors leading to variability in the gonotrophic cycle are captured and incorporated in the model.

6.2.5 Initialization

In order to be able to perform simulations, a model environment of 10201 m^2 grid with 20 m x 20 m grid squares is set. Then water-bodies and water-body edges are created and distributed over the world with different depths ranging from 16 mm to 100 mm. Both aquatic and terrestrial (only *Aedes* eggs and *Culex* adults) and livestock breeders are created when the model is initialized; the total number of each is specified via parameters: initial-number-aedes-eggs, initial-number-aedes-adult, initial-number-culex-adult and initial-number-livestock. Note that these quantities represent only female mosquitoes since only females bite for blood meal. *Aedes* eggs are initialized and distributed uniformly in water-body edges while both *Aedes* and *Culex* adults are initialized and distributed uniformly over the entire world. Note that *Culex* eggs are not initialized since they only breed in water. A complete description of all model parameters is given in Table 6.2.

Agent/Individual	Parameter	Baseline Value	Range	Units	References
Aedes & Culex adults	Gonotrophic time	8	4 - 12	Days	[138, 213]
	Aedes number of eggs	59	50 - 150	-	[195]
	Culex number of eggs	60	50 - 200	-	Estimated
	Resting time after emergence	-	1 - 3	Days	[189]
	Resting time after oviposition	-	1 -3	Days	[189]
	Search radius	60	20 -	Meters	[189]
	Successful blood feeding	0.8	0.5 - 1	-	Estimated
Livestock	No parameter	-	-	-	-
Water-bodies	Evaporation rate	0.1	0.05 - 0.20	$Days^{-1}$	[210, 211]

TABLE 6.2: Model input parameters: calibrated and non-calibrated.

6.2.6 Input Data

Rainfall and temperature daily time series data are used for quantifying the development, hatching of eggs, survival of aquatic mosquitoes (egg, larvae and pupae), water level of water-bodies and moisture index.

6.2.7 Submodels

Regarding traits taking place on the phenology model, many have been modelled using logistic functions. Logistic curve is a sigmoid curve named after Pierre Verhulst [224], and well known for studying species population growth. These curves have been successfully used in other studies of mosquito population dynamics [6, 74, 212, 213, 220].

6.2.7.1 *Aedes* and *Culex* eggs mortality

For both *Aedes* and *Culex* species the survival of eggs depends on both temperature and rainfall. However, in addition, survival of *Culex* is also affected by long periods of dessication [213]. This daily survival probability is assumed to depend independently on temperature, precipitation/rainfall and droughts [74]. For *Aedes* eggs it is given by

$$\rho(T, P) = \rho(T)\rho(P), \tag{6.1}$$

while for *Culex* eggs it is

$$\rho(T, P, D) = \rho(T)\rho(P)\rho(D), \tag{6.2}$$

where $\rho(T)$ is the daily survival probability of eggs due to temperature effect T; $\rho(P)$ is the daily survival probability of eggs due to precipitation effect P; and $\rho(D)$ is the daily survival probability of eggs due to desiccation effect D.

Daily survival probability of eggs due to temperature effect $\rho(T)$

Bayoh et al.[220] using the data of *Aedes* mosquitoes, obtained a nonlinear model that best describes the development time of eggs,

$$D_a(T) = 0.02 \times \left[a + \frac{b}{1 + (T/c)^d} \right], \tag{6.3}$$

where $D_a(T)$ is the development time (in days) at temperature $T(^\circ C)$ for *Aedes* eggs. The parameters are $a = 48.549$,
$b = 970.200$, $c = 12.096$ and $d = 4.839$. Hence, we obtain the following temperature-dependent survival probability for both immature and mature *Aedes* eggs,

$$\rho(T) = \frac{1}{1 + 5e^{-5.7(1/D_a(T))}}. \tag{6.4}$$

Using patterns of *Culex* eggs development time given in [189], we modify equation (6.3) to read $D_c(T) = D_a(T)/0.02$ with the parameters set to be $a = 1$, $b = 12$, $c = 12.096$ and $d = 4.839$. Therefore, the temperature-dependent survival probability for *Culex* eggs is,

$$\rho(T) = \frac{1}{1 + 5e^{-5.7(1/D_c(T))}}. \tag{6.5}$$

Daily survival probability of eggs due to precipitation effect $\rho(P)$
Precipitation or rainfall is important in creating breeding sites for mosquitoes and it can cause massive hatching of eggs. But excessive rainfall may increase mortality of immature stages due to flushing effect [221, 222]. Since rainfall has two effects, that is, positive and negative effect, we use the idea from [225] and assume the daily survival probability of both *Aedes* and *Culex* immature and mature eggs due to precipitation effect to be

$$\rho(P) = e^{(-(\texttt{daily-water-level}-30)^2)/1500}. \tag{6.6}$$

Daily survival probability of immature eggs due to dessication effect $\rho(D)$
Extended periods of drought, make immature development sensitive to the lack of precipitation such that eggs may dry before embryonic development is completed [187]. Following the approach in [213], we model the effect of droughts on immature *Culex* according to the number of consecutive days of drought dt as follows:

$$\rho(D) = \frac{e^{-\omega dt}}{c + e^{-\omega dt}} \tag{6.7}$$

where ω is a shape parameter controlling the sensitivity of ρ to dt and c is a constant that assures that at small values of dt, ρ is close to 1. Once the survival probability has been computed, the next step is to check for their death. The death of eggs is simply a stochastic function of their survival probability. A uniform random number between zero and one is drawn, and if it greater than the survival probability then the eggs die.

6.2.7.2 *Aedes* and *Culex* aquatic mosquitoes development

RVF mosquitoes are exothermic or poikilothermic, that is, they cannot regulate their body temperature [189]. Therefore, their development is somewhat completely temperature-dependent. In this case, using heat accumulation procedures we can estimate their development time [205, 206]. These approximations of physiological time are often expressed in units called degree-days [207–209]. Degree-days are the accumulated product of time and temperature above a particular developmental threshold and below a maximum threshold for an organism to develop. The lower developmental threshold for an organism is the temperature at which development is not possible [189]. The upper developmental threshold is hardly known, but estimates thresholds from which development starts decreasing [6]. We assume that the lower threshold is 10°C and the upper threshold is 35°C [6, 189, 220]. The development of all aquatic stages follows the steps below:

a) Degree-days
One degree-day is one day (24 hours) with the temperature one degree above the lower developmental threshold. There are several methods for calculating degree-days. Here we use the method based on averages:

$$DD = max\{0, \frac{T_{max} + T_{min}}{2} - T_{base}\}. \tag{6.8}$$

Here DD is the degree-days accumulated for the day, T_{max} is the maximum temperature for that day, T_{min} is the minimum temperature for that day, and T_{base} is the lower developmental threshold (10) [6, 189].

b) Accumulated degree-days
This is the literal accumulation of daily Degree-days.

c) Evaluate accumulated degree-days
If accumulated DD is greater than or equal to the minimum accumulated heat required for development at each stage (egg, instar 1, instar 2, instar 3, instar 4 or pupa), then a probability of transition is computed and if satisfied transition occurs. Description of required accumulated degree-days for development at each aquatic stage can be found in Table 6.1.

6.2.7.3 *Aedes* and *Culex* eggs transition probability

When the minimum accumulated degree-days required for development at each stage has been satisfied, a transition probability is calculated. The transition probability relative to the embryonic development of eggs is computed based on their development rate. The embryonic development of *Aedes* eggs usually takes a significantly longer time compared with that of *Culex* species. Larvae of *Aedes* are ready to hatch in 4-8 days after egg oviposition when the eggs are kept between 20°C to 25°C while at a temperature of 30°C, the *Culex* larvae hatch 1 day after the eggs have been laid [189]. Thus, the transition probability for *Aedes* and *Culex* eggs is given by equations (6.4) and (6.5) respectively.

6.2.7.4 *Aedes* and *Culex* eggs hatching

When eggs are matured, the next step is hatching. However, *Aedes* eggs need to be flooded enough to hatch, while *Culex* eggs are laid on the water surface [189]. Therefore, the number of newly hatched eggs will depend on the amount of rain accumulated. However, within variability to water-flow in the water-body both *Aedes* and *Culex* eggs have another sophisticated adaptive behaviour referred to as "hatching in instalments", that is, not all eggs hatch uniformly [189]. This mainly ensures their long-term survival even in the presence of dry spells. Below we outline the steps involved:

a) Accumulated total precipitation
This is the accumulated amount of rainfall up to the current day when evaporation effects have been taken into account.

b) Compute moisture index
Here we compute the current water level and that of the following 4 and 6 days. Note that the current water level is given by the parameter 'daily water level' (see sub-section 6.2.7.17 for its derivation).

c) Evaluate moisture index
Here we check if the current water level and that of the following 6 days is greater than or equal to 16 mm (the minimum amount of water for egg hatching). If this condition is satisfied, then the probability of egg hatching given by equation (6.9) is computed and evaluated. Otherwise, either 50% or 25% of eggs may hatch according to the level of the four consecutive days or one day respectively.

d) Compute probability of egg hatching
This probability is given by

$$\rho_h(P) = \frac{1}{1 + e^{-0.09 \times \texttt{daily-water-level}}}. \tag{6.9}$$

e) Decide to hatch
This is simply a stochastic function of the probability of hatching. A uniform random number between zero and one is drawn, and if it less than the probability of hatching, eggs are hatched into larvae instar 1. Otherwise *Aedes* egg will go diapause while *Culex* eggs will die.

6.2.7.5 *Aedes* eggs diapause

During periods of droughts *Aedes* eggs go diapause if already matured or embryonic development is completed. They can stay dormant in the ground from days up to four years [187].

6.2.7.6 *Aedes* and *Culex*: larvae and pupae mortality

After hatching, the emerged larvae and pupae feed on organic particulate matter in the water, such as algae and other microscopic organisms [189]. The larval and pupal stage of both *Aedes* and *Culex* are spent at the water's surface, and their daily survival probability is assumed to depend independently on temperature, precipitation/rainfall and droughts [74], and it is given by equation (6.2).

Daily survival probability of larvae and pupae due to temperature effect $\rho(T)$

Rueda et al.[6] used data of both *Aedes* and *Culex* mosquitoes to fit the Sharpe & DeMichele nonlinear model of temperature-dependent poikilothermic processes, obtained the following development rate:

$$r(K) = \frac{RH025\frac{K}{298.15}exp\{\frac{HA}{1.987}(\frac{1}{298.15} - \frac{1}{K})\}}{1 + exp\{\frac{HH}{1.987}(\frac{1}{TH} - \frac{1}{K})\}}, \tag{6.10}$$

where $r(K)$ is the median development rate (days^{-1}) at temperature K(°Kelvin) =° $C + 273.15$. RH025, HA, TH, and HH are parameters estimated and given in Table 6.4 [6]. Using this development rate formula we give temperature-dependent survival probabilities for instar 1, instar 2, instar 3, instar 4 and pupa. These survival probabilities are given by logistic curves of the type

$$\rho_1(T) = \frac{1}{1 + a \times e^{-b \times r(K)}} \tag{6.11}$$

where $r(K)$ is the development rate in days^{-1} and parameter values of a and b for each larval stage are given in table 6.3.

Larval stage survival probability	**a**	**b**
"aedes instar1 survival probability"	10	-6.3
"culex instar1 survival probability"	60	-6.5
"aedes instar2 survival probability"	10	-5.7
"culex instar2 survival probability"	60	-5.3
"aedes instar3 survival probability"	3.1	-4.1
"culex instar3 survival probability"	55	-7.4
"aedes instar4 survival probability"	2.6	-6.9
"culex instar4 survival probability"	8	-9.8
"aedes pupae survival probability"	270	-14
"culex pupae survival probability"	270	-14
"aedes instar1 to instar4 survival probability"	2.6	-18.7
"culex instar1 to instar4 survival probability"	10	-25.8

TABLE 6.3: Parameter values of the larval stages survival probabilities. The last two lines refer to the comulative development from egg hatching to instar 4.

Daily survival probability of larvae and pupae due to precipitation effect $\rho(P)$
This probability is given by

$$\rho(P) = e^{-(\texttt{daily-water-level}-15)^2/100}, \tag{6.12}$$

for 'daily water level' less than or equal to 17 *mm* while for above this threshold the survival probability is uniform and above 0.7. This is intended to capture the fact that above the minimum water level survival of larval stages is high [212].

Daily survival probability of larvae and pupae due to dessication effect $\rho(P)$
Note that this is only applied for *Culex* species and it is given by equation (6.7) in sub section 6.2.7.1. After we have calculated the survival probability $\rho(T, P, D)$ we check for death. The death of both *Aedes* and *Culex* larvae and pupae is simply a stochastic function of their survival probability. A uniform random number between zero and one is drawn, and if it is greater than the survival probability then they die.

Life stage	RH025	HA	TH	HH
		Aedes		
Instar 1	0.68007	28,033.83	304.33	72,404.07
Instar 2	1.24508	36,400.55	301.78	81,383.14
Instar 3	1.06144	41,192.69	301.29	60,832.62
Instar 4	0.57065	34,455.89	301.44	45,543.49
Instar 1 to 4	0.20429	36,072.78	301.56	59,147.51
Pupa	0.74423	19,246.42	302.68	5,954.35
		Culex		
Instar 1	1.23439	27,534.92	301.00	37,071.82
Instar 2	1.42950	28,219.93	301.37	39,340.77
Instar 3	0.94308	20,767.22	304.00	36,213.96
Instar 4	0.31230	12,629.46	308.31	140,281.42
Instar 1 to 4	0.21554	24,689.00	301.82	37,270.21
Pupa	0.55490	15,648.63	306.60	43,983.41

TABLE 6.4: Here we reproduce Table 3 in [6] describing parameter estimates for the Sharpe & DeMichele model, see equation 6.10.

6.2.7.7 *Aedes* and *Culex* larvae and pupae transition probability

When the minimum accumulated degree-days required for development at each stage has been satisfied, a transition probability is calculated. The transition probabilities relative to the development at each stage of larvae and pupae are computed based on their respective development rates (see equation (6.10)) and are given by corresponding temperature-dependent survival probabilities.

6.2.7.8 Adult *Aedes* and *Culex* resting time after emergence

After emergence, adults increase their haemolymph pressure which causes legs and wings to stretch [189]. This process allows their body to dry and harden before they can fly and it takes 1 to 2 days [226]. Hence, this is modelled by a discrete random number uniformly distributed between 1 and 2 inclusive.

6.2.7.9 Adult mortality

The daily survival probability of adults is age-dependent and it is described by a Gompertz model [214, 223] with a corresponding hazard function given by $\lambda(x) = ae^{bx}$, such that

$$S(x) = e^{-\int_0^x \lambda(s)ds}, \tag{6.13}$$

where $S(x)$ is the survival function and x represents age of the mosquito and parameters $a = 0.0005$ `and` $b = 0.079$ for *Aedes*. Once an adult emerges a counter (variable representing age) is created and updated daily. Given that *Culex* species survive a dry season in adult form, this survival probability is modified to include effects of droughts on parameter a. For *Culex* adults
$a = 0.001 \times$ `number of dry days` such that the parameter 'number of dry days' has a default value of 1.
The baseline mortality rate a can be written as a function of its degree of mortality deceleration c, such that

$$a = \frac{c}{10000} \texttt{ for } \textit{Aedes} \texttt{ and } a = \frac{c}{1000 \times \texttt{number of dry days}} \texttt{ for } \textit{Culex}, \tag{6.14}$$

with a baseline value of $c = 5$ for *Aedes* and $c = 1$ for *Culex*.

6.2.7.10 Adult *Aedes* and *Culex* search for host

Both *Aedes* and *Culex* adults use odour of carbon dioxide emanating from a host (livestock) to identify their feeding host. They orient their flight pattern upwind to follow air currents containing a filamentous plume of carbon dioxide [189]. As they get closer, odours of other components especially lactic acid emitted from the skin surface, allow them to find and identify a host [189, 227] at a distance of above 20 meters [189]. Given that the factors affecting flight patterns would be difficult to predict in a model we use flight distance range to model this based on its oriented dispersal behaviour [189, 215]. We assume that adult mosquitoes are able to evaluate and identify a host within a distance between patch midpoints less than or equal to the parameter 'search radius'. This parameter has a standard value of 60 m. This is implemented as follows: check if within the radius determined by the parameter 'search radius' there is a host; if yes go to the host within the minimum distance. Otherwise repeat the search to a maximum of three times. This corresponds to the assumption that per day an adult mosquito flies up to

500 m [189]. If no host is found even after moving approximately 200 m the adult stops the search until the next day.

6.2.7.11 Adult *Aedes* and *Culex* blood feeding

Blood and its protein ingredients are essential for egg-production [189]. Blood feeding takes place once a female adult mosquito has found a host, that is, sharing the same patch with the domestic livestock. Then a uniform random number between zero and one is drawn, and if it is less than the parameter 'successful blood feeding', then the mosquito has successfully acquired a blood meal enough for egg maturation such that it becomes engorged and will only take another blood meal after egg oviposition.

6.2.7.12 Adult *Aedes* and *Culex* blood digestion

After a successful blood meal the female requires 2 to 4 days for digesting the blood before egg oviposition [189]. This is the number of days a female adult mosquito stays engorged. Therefore, it is defined as gonotrophic time minus the time a female adult mosquito would rest after egg oviposition. This later may take 1 to 2 days (for more details see 6.2.7.16).

6.2.7.13 Adult *Aedes* and *Culex* Oviposition site

Aedes females lay their eggs on damp soil (water-body edges) with a high degree of soil moisture which protects the sensitive of eggs from drying-out during embryogenesis [187], while *Culex* females lay their eggs on the water surface (water-body). However, factors determining their choice of this breeding site are still unknown [189]. But cues such as water quality, incidence of light, existing eggs, available food, temperature, water depth, presence of competitors and local vegetation are decisive factors in selecting a favourable breeding site [189, 228]. For simplicity, we model this behaviour as a function of the distance to the nearest water-body and its depth. The more the depth is higher than 16 mm the better for *Culex* as it is likely that when flooded the water will persist longer, while *Aedes* prefer those with depth close to 16 mm. The adults move at steps of 50 m and check above condition on a visual radius of 50 m and if these conditions are not met they repeat the search for four times such that per model time step they move for about 200 m which is the limit. If the conditions are met adult *Aedes* lay eggs on the edges of the water-body, while *Culex* lay eggs on the water-body. If no suitable oviposition site is found, the adult stops moving until the following day. Note that in addition to the above conditions *Culex* females are supposed to check whether the minimum water level is satisfied. However, given that precipitation is uniformly distributed within the environment this condition is irrelevant while searching for a suitable oviposition site.

6.2.7.14 Adult *Aedes* and *Culex* egg laying

Once an oviposition site has been selected, then it is time to lay eggs. Rainfall is known to alter the abundance and types of aquatic habitats available to the mosquito for egg oviposition and subsequent development of immature stages [200]. Female adults lay eggs depending on the moisture index. High moisture index correlates with high egg laying rate [200]. To model the daily egg laying probability we follow the steps below:

a) Check moisture index: Moisture Index is given by the daily-water-level see subsection 6.2.7.17. For *Culex* species the daily-water-level should be greater than or equal to 16 mm which is the minimum water level required for larval development since these species lay their eggs on the water surface.

b) Compute the probability of laying eggs: This probability is a function of the moisture index and it is given as follow:

$$b(P) = e^{-(\texttt{daily-water-level}-40)^2/3800}. \tag{6.15}$$

c) Calculate the number of eggs to be laid: The number of eggs laid by each adult is drawn from a normal distribution with average controlled by the parameter 'average number eggs' with a standard deviation of a quarter of the 'average number eggs'. However, the number of eggs laid by an *Aedes* adult should fall between 50 and 150 while for *Culex* it should be between 50 and 200 eggs.

d) Decide to lay eggs.
This is simply a stochastic function of the probability of laying eggs. A uniform random number between zero and one is drawn, and if it is less than the probability of laying eggs, then eggs are laid.

6.2.7.15 Adult *Aedes* and *Culex* resting time after oviposition

After egg oviposition, adults require 1 to 2 days for resting before they can look for another blood meal[226]. Hence, this is modelled by a discrete random number uniformly distributed between 1 and 2 inclusive.

6.2.7.16 Adult *Aedes* and *Culex* gonotrophic time

RVF female mosquitoes are blood sucking insects. However, blood is mainly used for egg production such that eggs are laid each time a successful blood meal has been taken [189, 229]. This is known as gonotrophic cycle and it can be repeated several times throughout the lifespan of the mosquito [230]. Hence, gonotrophic cycle duration may then be defined as the time interval between two consecutive blood-meals (or the time interval between two consecutive acts of egg-laying) [138].

Although very difficult to measure the gonotrophic cycle duration, it has been observed that both *Aedes* and *Culex* females require 6-8 days to complete this cycle: 1-2 days searching for a blood meal, 2-4 days digesting the blood meal, 1-2 days searching for an oviposition site, 1 day to oviposit and, two additional days recovering and searching for a new host [189, 213]. Therefore, in this study the duration of gonotrophic cycle is drawn from normal distribution with $mean = 8$ and standard deviation equal to a quarter of the mean with boundaries at 6 and twice the mean.

6.2.7.17 Daily water level

Combined effects of both rain and temperature are major determinants of the quantity and permanence of temporary water bodies [212]. The variable 'daily water level' of the water-bodies increases with an increase of rainfall and decreases with increments on temperature. Thus, 'daily water level' is equal to the accumulated total precipitation minus evaporation rate times accumulated total precipitation. Evaporation rate is a function of several factors including temperature, rainfall and soil type. However, we implicitly model these effects by assuming that water persists for about 20 to 40 days [210, 211]. Therefore, evaporation rate (E_0), is set by the parameter 'evaporation rate' and should be between zero and 20%.

6.2.8 Model predictions and observations

The mosquito life cycle features are the cores of a predictive model of mosquito abundance. Construction and parametrization of the model follows "model cycling" with a pattern oriented modelling (POM) approach [65, 201, 202], in combination with results from experimental studies [6, 189, 220]. Parametrization is the main process that differentiates one model from another [21] such that adequate model parametrization makes the model yield quality information useful for vector and diseases management. Although several models characterizing important features of RVF mosquito life cycle exist, the majority of them have been calibrated using laboratory data [6, 220] which generally do not capture the entire spectrum of the dynamics of these mosquitoes in field conditions [214]. Furthermore, features such as number of eggs each adult lays after a successful blood meal, survival of adults and gonotrophic cycle are very complicated to determine either in laboratory or field conditions [6]. Using the POM approach we compared patterns of behaviour from our model with selected performance criteria that are geared towards aspects of a predictive model that is able to capture seasonal variations observed in RVF mosquito population dynamics by incorporating important features of mosquitoes life cycle in a model that runs under daily real data sets of temperature and rainfall. The most determinant factors of the mosquito life cycle used for model performance criteria are number of eggs laid per successful blood meal, eggs hatching in instalments, survival of adults, gonotrophic time and diapause during unfavourable seasons. *Aedes* survive dry season in the form of eggs which are able to withstand long periods of dessication [187], while *Culex* survive this unfavourable season in the

adult stage [189]. Gonotrophic time and number of eggs laid per successful blood meal were drawn from normal distribution each time after a successful blood meal. Gonotrophic time can also be determined when information such as parity and survival probability of adults is known [138, 231]. However, after several attempts this approach did not yield the desired results and made the simulation very slow as at each model time step we had to keep track of female adults that were either parous or nulliparous. Drawing these values from a normal distribution we were able to determine optimum values that satisfied selected performance criteria. The timing of larval hatching to coincide with the presence of ideal developmental conditions, is a prerequisite for successful development of RVF mosquitoes as they breed in temporary water bodies which mainly depend on rainfall. These mosquitoes have developed a very sophisticated adaptation behaviour to ensure that the brood will not dry out due to rapid changes in water levels by allowing eggs to hatch in instalments [189]. Using a simple rule for computing the probability of eggs hatching depending on the moisture index of up to six days allowing eggs to hatch in three options of less than 40%, between 40% and 70% and above 70%, we were able to capture expected trends observed in the field. Another two important features are survival of adults and diapause mechanisms. We modelled survival of adults to depend on the age using a logistic function of Gompertz type. Age-dependent mortality of adult mosquito has been confirmed to best describe mortality in the field [214, 232]. By incorporating effects of drought in this survival function we were able to model the effects of diapuase for *Culex* and reproduce observed intra- and inter-annual variation in the population dynamics of mosquitoes.

Besides, we also found patterns that we did not expect in our simulation model but that have been observed in the dynamics of RVF mosquito populations. Periods of greater mosquito abundances coincide with those of heavy rainfall [34, 42, 117] and the maximum number of *Culex* is attained a couple of months after that of *Aedes* [79]. By implementing the above assumptions regarding the inclusion of important features of RVF mosquito life cycle such as number of eggs laid per successful blood meal, eggs hatching in instalments, survival of adults, gonotrophic time and diapause we were able to reproduce peaks of *Aedes* abundance of mosquitoes coinciding with elevation on precipitation and those of *Culex* two months later on average. Furthermore, our model predicts appearance of the first cohort of adult *Aedes* and *Culex* 6 and 27 days respectively after enough first rain for larval development see Fig.6.3.

6.2.9 Effects of stochasticity and model parametrization

Before proceeding into proper model analysis it is important to assess the effects of stochasticity in our model. Variables of most of the processes underlying our model are represented by stochastic processes. For instance, the gonotrophic time, the number of eggs laid by each adult mosquito are drawn from normal distributions. To do this we run 200 replicates and we estimate the average results and their variability around this average. Then the average results were compared

with our performance criterion based on seasonal variations in the abundance of mosquito adult populations. This approach then enabled us to determine reasonable parameter values that make the model reproduce the desired patterns. This process is known as model parametrization or model calibration. Parametrization is the main process that differentiates one model from another [21] such that detailed useful informative indicators can be generated. Note however, that this process does not quantify the uncertainty of the model but only the effects of stochasticity in the model [201]. Figure 6.3 shows how robust our model is with the chosen set of parameters to stochasticity as the trajectories clearly show the same patterns. This was further confirmed by estimating the distribution of the appearance of the first cohort of adults (see Fig.6.3) which was found to be in good agreement with observations [29].

6.3 Model Analysis

We used our model to address the following questions: (1) Is there any correlation between rainfall and abundance of mosquitoes? (2) What features of the mosquito life cycle affects mosquito population dynamics? These questions were addressed by: inspecting the correlation between the intra- and inter-annual variation of both temperature and rainfall with periods of greater mosquito abundances; computing the distribution of appearance of first cohort of both *Aedes* and *Culex* adults; investigating how variations on the mosquito life cycle features contribute to variations in adult mosquito abundances by evaluating the output for different parameter values.

6.4 Results and Discussion

6.4.1 Effects of temperature and rainfall

We used real daily temperature and rainfall data from the Ijara district for the period between 15.01.2009 and 15.10.2010. Temperature in this region shows little variation with a daily average minimum of 15°C and maximum of 38°C throughout the entire period. Peaks are observed during the months of March and April and low temperatures are registered in the months of June, August and September. However, the same cannot be expected for rainfall which shows substantial variations with a daily minimum of zero and maximum of 70.8 mm throughout this entire period. Temperature influences every aspect of the mosquito life cycle since temperature affects both development and mortality of all larval stages (see equations (6.3) and (6.10)). Increasing the value of accumulated degree-days required for transition from one stage to another linearly increases the developmental time, but the overall relationship between temperature and development rate of immature stages is nonlinear [220]. These fluctuations on temperature significantly induce variations in the development of immature stages

and emergence of adults. However, temperature was not responsible for creating the intra- and inter-annual variation on abundance of adults. This was mainly driven by variations on rainfall regimes. Rainfall affects dynamics of the mosquito population in two aspects: creates suitable breeding sites for immature stages and influences their survival. A daily water level of 16 *mm* was set as the minimum amount of water required to keep water-bodies suitable for immature stages development. However, periods of drought would reduce their survival and *Culex* appeared to be more sensitive to drought compared to *Aedes*. This phenomenon may result from the fact that during unfavourable seasons *Aedes* go diapause in the form of egg and the adult is able to continue laying eggs even if the water-bodies are not flooded [189], while *Culex* adults can only lay eggs if water-bodies are flooded [187, 189]. Therefore, successful development of new cohorts of both *Aedes* and *Culex* is dependent on two main factors: temperature and rainfall.

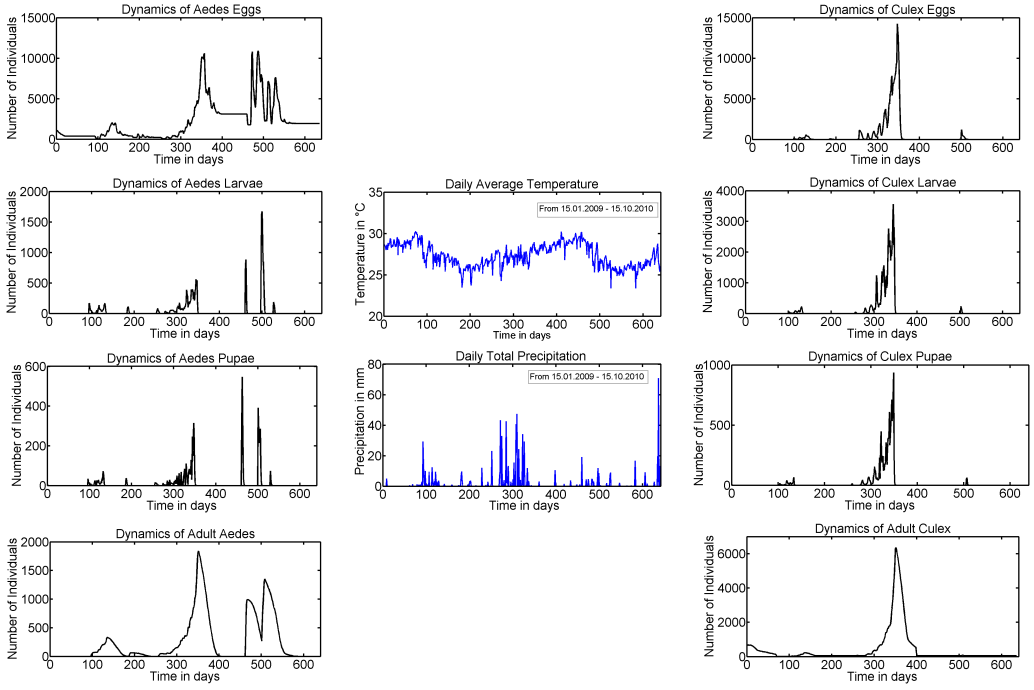

FIGURE 6.2: A one time simulation model output under baseline parameter settings. Left we represent the dynamics of *Aedes* mosquito life cycle; center is the weather data and at the right is the dynamics of the *Culex* mosquito life cycle.

6.4.2 Abundance of adult *Aedes* and *Culex*

In this simulation, the result produced gives daily temporal dynamics of the population of each stage (egg, larva, pupa and adult) based on real daily data sets of temperature and rainfall (see Fig. 6.2). This one time simulation output is ideal for understanding and investigating how both temperature and rainfall affect the development of the brood from egg to adult and appearance of new cohorts

of mosquitoes. It appears that seasonal variations on mosquito abundances are driven by seasonal changes in temperature and rainfall, as expected. However, rainfall demonstrates to be the major driver of the observed trends. Abundance of adult *Aedes* is observed throughout all the rainy events with large numbers of mosquitoes being observed during the long rainy season. In addition, considerable peaks of *Aedes* abundance appear during a relatively dry period following a rainfall event. This concurs with findings by other studies [79, 212, 213] and may be explained by the joint eclosion of large quantities of eggs accumulated during the dry period. However, *Culex* adults are only abundant during long rainy season. This results from the fact that during short rains their population is heavily affected by the occurrence of dry spells which result in death of many of immature stages before completing their life cycle. Additionally, the number of eggs each adult lays per blood meal and the gonotrophic time heavily affect the abundance of these mosquitoes. However, an increase in these parameters does not change the trend of the abundance of the adults; hence for this reason we keep standard values such that the average number of eggs laid per blood meal by an *Aedes* is 59 while for *Culex* it is 60 with equal average gonotrophic time of 8 days (for more details see Section 6.4.4). Note, however that as pointed out in Section 6.2.8 we do not aim to simulate the actual number of abundance of these broods, but rather we aim to reproduce the patterns observed in field trials for investigating various features of the mosquito life cycle underlying emergence of these patterns. While exploring the population dynamics of abundance of mosquito populations it is of great importance to investigate the periods of appearance of the first cohorts of adults after a rainy event. Figure 6.3 shows the distribution of appearance of the first cohort of both *Aedes* and *Culex* adults to be approximately 6 and 27 days respectively. *Aedes* rapidly disappear with the decrease in the amount of water in the water-bodies, while *Culex* tend to increase at the end of the rainy season. Similar results were obtained by Fontenille et al.[29] while studying vectors of RVFV.

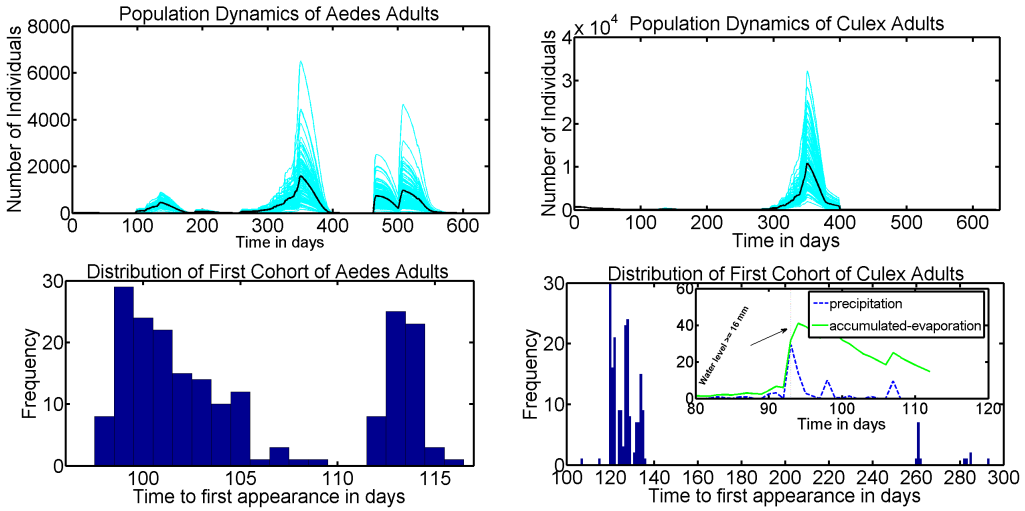

FIGURE 6.3: Top: Population dynamics of *Aedes* and *Culex* adult mosquitoes. The dark line represents the average of 200 replicates. Bottom: Distribution of appearance of the first cohorts of both *Aedes* and *Culex* adults.

6.4.3 Effects of gonotrophic time

The duration of the gonotrophic cycle constitutes a major determinant of the vectorial capacity of a mosquito vector [138] as it determines how many times a female mosquito would bite its host for blood meal. Shorter lengths of gonotrophic cycle not only contribute to the number of bites but also to the reproduction behaviour of the female. Hence, shorter lengths of gonotrophic cycle may imply rapid reproduction of the population increasing the abundance of adults. However, sensitivity analysis of this parameter further expand its relationship with mosquito abundance suggesting that their relationship might not be exactly linear (see Fig. 6.4). Indeed increasing the length of this parameter decreases the abundances of mosquitoes but also shorter durations seems to decrease the population of adult mosquitoes. A length of 8 days happens to be the optimal duration of the gonotrophic cycle. This result may stem from the fact that 8 days is the minimum length of time required to accommodate the time for resting after egg oviposition, time for blood digestion, time for searching for a host and for searching for the oviposition site [213].

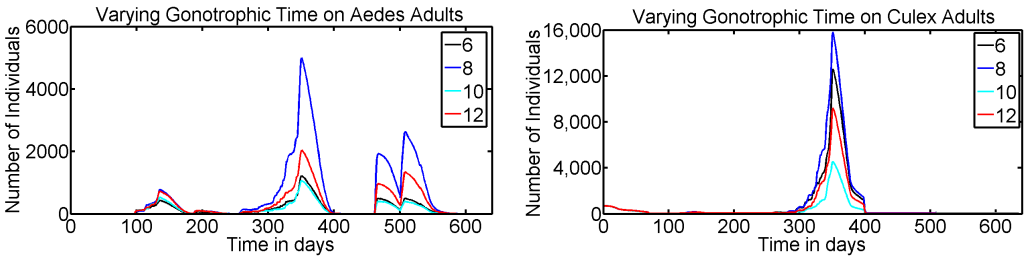

FIGURE 6.4: Population dynamics of *Aedes* and *Culex* adult mosquitoes with varying the length of the gonotrophic cycle.

6.4.4 Effects of the number of eggs laid

Fig. 6.5 shows results of the effects of varying the number of eggs laid by each female *Aedes* and *Culex* adult per blood meal. Similarly to the length of the gonotrophic cycle, the number of eggs laid per blood meal directly correlates to the abundance of adults. We observe that even with possible occurrence of dry spells, if the amount of eggs laid by each female adult per blood meal is large enough, some will be able to survive and complete their development cycle. Besides, large densities of adults contribute to fitness mechanism such that a large proportion of them will survive to the next generation. For *Aedes* (see Fig. 6.5 (left)) we obtain that an increase in the number of eggs implies an increase in the abundance of adults for the chosen parameter values even if other factors remain the same. However, an interesting feature is observed for *Culex* species (see Fig.6.5 (center)). For parameter values less than 85 an increase in the number of eggs results in an increase in the abundance of adults, but for values greater than 85 we obtain a negative correlation. This result suggests that for given biotic and abiotic conditions there exists an optimal level of the number of eggs to be laid since we do not implement density dependent functions in this model. To further verify these results we rerun the model while varying the number of eggs around the value 85 (see Fig.6.5 (right)). This result may also be explained by the fact that eggs inherent adaptability behaviour in which eggs laid at the same time do not hatch uniformly but in instalments [189]. This adaptive behaviour is common within mosquitoes that develop in temporary bodies of water and it is used to ensure their long-term survival. It was implemented based on the moisture index derived according to the 'daily water level' of subsequent days up to six days (for more details see Section 6.2.7.4).

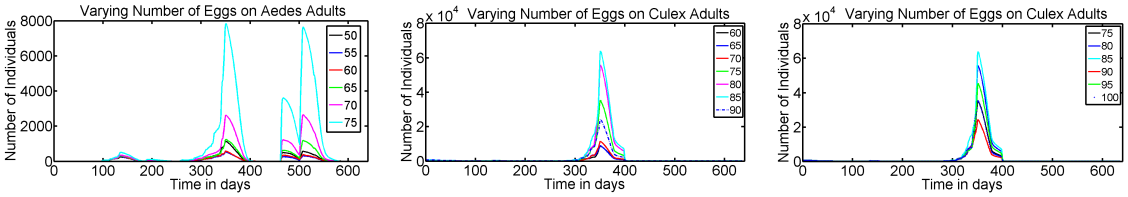

FIGURE 6.5: Effects of varying the number of eggs laid by each female adult *Aedes* and *Culex* mosquito.

6.4.5 Effects of mosquito's age-dependence mortality

The survival of adult female mosquitoes is a critical component of their ability to reproduce and transmit diseases. Increased survival allows the vector to produce more offspring, to increase the chances of them becoming infected, to disperse over greater distances, to survive long enough to become infectious, and then to deliver more infective bites during the remainder of their lifetime [214]. Using age-dependent survival probability we have examined how longevity of adult mosquitoes affects the dynamics of population abundance. The impacts of this parameter on disease transmission will be investigated in future studies that will attempt to assess effects of mosquito life cycle features to the spread of the disease. The survival probability function takes the form of a logistic function (Gompertz model) [223] such that mortality increases exponentially with age [233]. One parameter heavily influences the survival probability function and it is linked to the degree of mortality deceleration, c (for more details see equation (6.14) in Section 6.2.7.9). Varying this factor from 1 to 20 we investigated the effects of adult mosquito's longevity on mosquito population dynamics. For *Aedes*, increases in this factor reduces the mortality of adults, hence increasing their reproduction capacity (see Fig.6.6 (left)). However, if we decrease this parameter from its baseline value 5 to 1 we substantially increase the abundance of adult *Aedes* mosquitoes. These results follow from the fact that reducing the degree of mortality deceleration increases the baseline mortality rate and vice versa such that when the degree of mortality deceleration is very small the longevity of the mosquito is expanded. This allows mosquitoes to survive longer, hence enhancing their reproducibility. However, the effect of the longevity of adult *Culex* in relation to their abundance is not completely linear rather it is nonlinear (see Fig.6.6 (right)). This nonlinearity results from the interplay between degree of mortality deceleration and their adaptive behaviour for surviving during dry spells. For more details see equation (6.14) in Section 6.2.7.9, which gives the relation of the baseline mortality rate with respect to degree of mortality deceleration and effects of droughts.

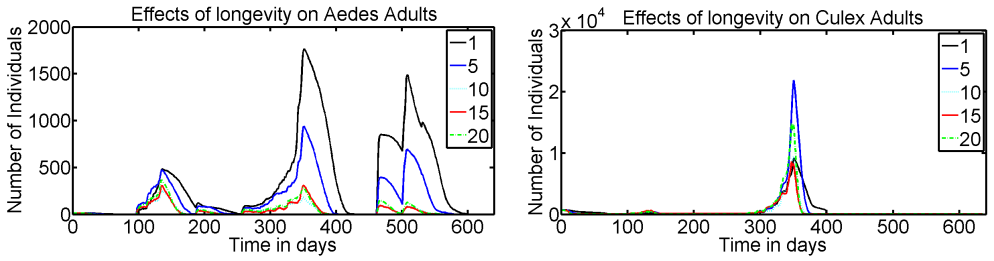

FIGURE 6.6: Here we vary the degree of adult mosquito's deceleration parameter for analysing the effect of age-depence on the abundance of both *Aedes* and *Culex* mosquitoes.

6.4.6 Effects of evaporation rate on mosquito larval habitats

Combined effects of both rain and temperature are major determinants of the quantity and permanence of temporary water bodies [212]. Temperature affects the evaporation velocity and water permanence in the pools. Nevertheless, a combination of less abundant rainfalls with low temperatures, may produce water-saturation of the soils, thus maintaining relatively stable flooding levels [212]. Stable flooding level highly contributes to complete development of immature stages implying an increase in the abundance of adults. Thus, in order to capture different effects of both temperature and rainfall on the evaporation phenomenon, we define this parameter as a daily rate (see Section 6.2.7.17 for more details). This parameter varies between zero and 20% and it indicates daily reduction of the amount of accumulated precipitation due to evaporation effects. Ten percent is the baseline value meaning that water persists in the water-bodies for about ten days. Figure 6.7 depicts the effects of this parameter in abundance of adult *Aedes* and *Culex* mosquitoes by setting the evaporation rate to be 0.066, 0.083 and 0.1 which correspond to 15, 12 and 10 days respectively of water persistence. The more the water persists the higher the abundance of mosquitoes. This is explained by the fact that availability of water is a determinant factor of successful mosquito reproductivity. Larval habitat studies [210, 211], have suggested that these larval habitats (temporary water-bodies) persist for about 20 to 40 days if rain is the main source of water. However, according to our model performance criteria a minimum of 10 days and a maximum of 15 days were chosen, such that the minimum was used as baseline value. There have been several attempts for developing formulas that give evaporation rates. Most of the existing ones can be grouped into two categories: empirical and physical [234]. Either empirical or physical have some limitation with inherent difficulties in either making empirical connections between climate and evaporation for different realities or gathering sufficient information for feeding all variables required in physical formulas such as those of the Penman equation. Linacre [234] further developed this formula reducing it from four input variables to only include temperature accompanied by two other parameters; elevation and latitude of the location. However, this formula

is more suitable for stagnant water such as a lake and in addition it presents differences between measurements of about 1.7 *mm* per day for a day resolution. Therefore, in order to overcome this complication we estimate the evaporation rate based on the knowledge regarding the time the water persists in temporary water-bodies with rain being the main source. This approximation appears to be more reasonable as witnessed by our model predictions and results in various features of the model.

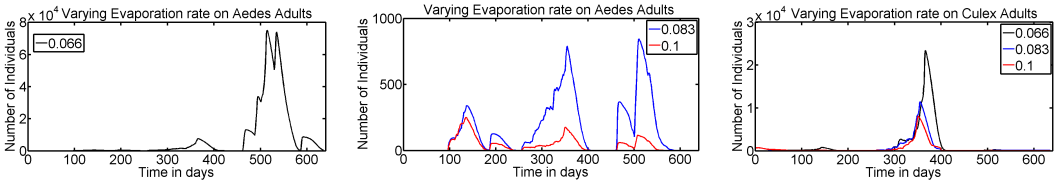

FIGURE 6.7: Determining the effects of evaporation rate of mosquito larval habitats on the abundance of *Aedes* and *Culex*. The evaporation rate is an indicator of the time the water persists in the water-bodies where 0.066, 0.083 0.1 correspond to 15, 12 and 10 days respectively.

An interesting phenomenon can be observed from Fig.6.7(left) which indicates that when the length of water persistence is increased an abundance of adults is likely to increase even when daily total precipitation is low. Such substantial increase in the abundance of adults during periods of low precipitation result from the fact that during this period temperatures are high which facilitates rapid development of broods, hence their efficient reproductivity. This result mainly highlights that to better capture the effects of water persistence on mosquito population dynamics, evaporation should be temperature dependent.

6.4.7 Effects of diapause and mosquito flight behaviour

Environmental fluctuations form a critical component of an ecosystem's ability to sustain a broad range of living species. This may consist of temperature fluctuations, varying degrees of moisture in the air and soil, varying day length, seasonal variations and varying flooding regimes. Mosquitoes need to be able to adapt to such environmental fluctuations in order to survive unfavourable seasons and this phenomenon is called diapause [187]. This complex adaptive behaviour allows mosquitoes to distinguish between favourable developmental conditions in one season, and unfavourable conditions in the other [189]. The *Aedes* survive during unfavourable conditions through diapause in their eggs, which can stay dormant in moisture soil for at least several days up to 4 years [187]. *Culex* species go diapause in the adult stage when conditions are not favourable [189], which mainly depends on flooding regimes. Since both species breed in fresh temporary water we implement this phenomena according to variations in flooding regimes by reading the 'daily water level' parameter. This is the back bone of the mechanism that ensures long-term survival of the species (see Fig.6.2). This can be further

justified from lack of stochastic extinction even within repeated simulations (see Fig.6.3 (top)). Mosquito species involved in this study require blood meal to allow oogenesis to be completed. Successful blood feeding depends on the ability of a mosquito to search for a host which is a critical component of the mosquito's flight behaviour. Primarily, the location of the host is based on olfactory, visual and thermal stimuli [189]. This behaviour can either be non-oriented dispersal which enhances the likelihood of the female coming into contact with stimuli derived from a potential host or oriented meaning it results from contact with host stimuli in which the strengths of the stimuli are increased as the mosquito and host come closer to each other or attraction to a suitable candidate host, once the female has identified it in her immediate vicinity [189, 215].

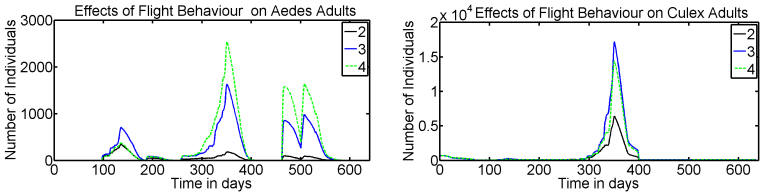

FIGURE 6.8: Effects of mosquito's flight dispersal behaviour by varying its vision range on mosquito population dynamics.

In this model we have implemented the oriented dispersal behaviour where the success of finding a host is a function of the distance to that host according to the mosquito's vision which is at least 20 m [189]. Figure 6.8 shows the effects of varying the parameter 'mosquito vision' on the mosquito population dynamics by setting this parameter to 2, 3 and 5 corresponding to 40, 60 and 80 meters respectively based on the scale of the model environment. The results indicate that the ability of a mosquito to search and identify a host for sucking blood is critical for the mosquito's reproduction capacity, which directly influences the abundance of the species. These results similarly may have influence on the prevalence of the disease given that ability to find a host and take blood meal is directly correlated to the vector's vectorial capacity. Therefore, mosquito's flight behaviour is of great epidemiological significance and interventions may target this feature if one wishes to control the disease through vector control.

6.4.8 Effects of varying water-body depths

Apart from vector and ruminants movements the spatial distribution of RVF can be attributed to the influence of landscape factors on the locations of aquatic habitats of the vector mosquito larvae. Such spatial distribution of the larval habitats has for long been known to partially determine the spatial distribution of the adult mosquitoes in many landscapes [235, 236]. Thus, investigating factors that affect the spatial distribution of larval habitats is central to our understanding of spatial determinants of disease transmission. We examine such situations by simply

varying the depth of water-bodies randomly distributed in our environment given that the daily total precipitation is uniformly distributed over the entire landscape. These differences on the size of water-body depths will simply create differences in larval habitat's flooding regimes. Such that some will be flooded before others based on the fact that a larval habitat is said to be flooded if the 'daily water level' is greater than or equal to 16 *mm*. Note that this setting is not meant to capture the spatial distribution of adults but rather effects of spatial distribution of the larval habitats in the abundance of adults and it is only implemented for *Aedes* species as their eggs are laid in damp soil and only hatch if flooded. In our model the variability of water-body depths is achieved by setting the variable 'water-body depth' to assume random values uniformly distributed between two limits such that the upper limit is always less than or equal to the overall maximum of the variable 'daily water level'.

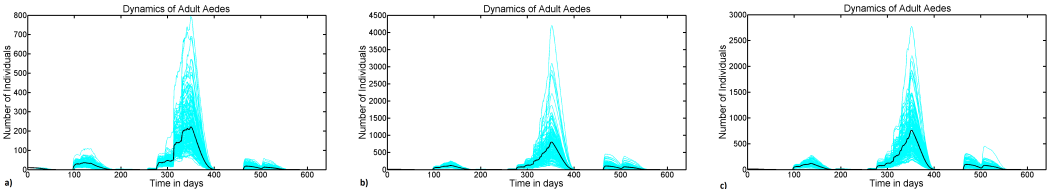

FIGURE 6.9: Effects of water-body depth variability on mosquito population dynamics.

Figure 6.9(a) depicts the distribution of adult *Aedes* when the depths of water-bodies vary between 0 and 100 *mm*. The trajectories of abundance of adults follow patterns of rainfall as expected but with much lower densities. The observed low densities result from the fact that with water-body depths varying between 0 and 100 *mm* there is only a 15% chance of a particular site to be flooded. That is, only 15% of larval habitats would have a chance to satisfy the condition depth minus 'daily water level' less than or equal to zero. In these settings it is as if we have reduced locations suitable for development of immature *Aedes* mosquitoes, that is, location with sufficient accumulated precipitation . This is in good agreement with findings from empirical studies of mosquito larval habitats [237], which have found that the probability of larval habitat presence increased with increasing accumulated precipitation. This can be illustrated by reducing the variability of water-body depths to vary between 0 and 50 *mm* as well as between 0 and 20 *mm*. Figures 6.9(b) and 6.9(c) clearly depict the increase on the density of the distribution of the abundance of adult *Aedes* when decreasing the variability of water-body depths.

6.4.9 Model extension and other applications

Although the model presented here is a comprehensive simulation model of the mosquito life cycle for predicting temporal abundance of mosquitoes, there is still

room for model extension. For example, in the current model mosquito larval habitats are all equally distributed with little modification to account for spatial effects by incorporating variability in the depth of water-bodies. This was meant to extend the model to include variability in the spatial distribution of larval habitats which are known to affect the spatial distribution of adults in order to able to examine its effects on the abundance of adults. Therefore, in order to be able to fully examine the impact of spatial distribution of larval habitats on the spatial distribution of the adult vectors, it would be necessary to extend the model to use a heterogeneous spatial arrangement of the environment with detailed information about the landscape variables. Landscape factors such as topographic wetness index, soil type, land use-land cover, and distance to stream are known to influence the spatial distribution of vectors [237, 238]. With availability of this information it would be possible to embed Geographic Information System (GIS) capabilities with our model such that the model could run based on a real landscape. This could lead to further extension of the model by moving from local spatial scale to a more larger scale with detailed data of weather variables (temperature, precipitation, humidity) and landscape variables of each local site. Such extensions could be useful for analysing the spatial distribution of abundance of RVF mosquitoes for instance at a scale of a country providing useful informative indicators for preventing and controlling disease outbreaks by providing guidance for specific site. In addition, this model could be extended to include variability in the number of mosquito larval habitats driven by seasonal differences in rainfall. This would allow one to investigate links between mosquito larval habitat distribution and RVF adult vectors across seasons. Further, the model could be extended to include livestock and detailed information underlying disease progress in both vector and host. Such a model could be useful for correlating abundance of mosquitoes and disease incidences providing a basis for predicting RVF outbreaks and estimation of important epidemiological parameters.

6.5 Conclusion

In this study we have introduced an IBM phenology model which included important features of the mosquito life cycle such as egg oviposition, egg maturation, diapause phenomenon, developmental stages (egg, larva instar 1 to 4, pupa and adult), temperature, rainfall and dessication dependent survival of immature stages, aquatic habitats, host seeking, engorgement, oviposition site seeking and adults age-dependent survival. Running the model under real daily data sets of temperature and rainfall led us to predict the mosquito population dynamic that closely resembles observations in the field [29, 34]. Combined effects of temperature and rainfall seasonal variations were responsible for creating the intra- and inter-annual variations observed in the abundance of adult mosquitoes which is in good agreement with findings from other studies [79, 213]. Temperature heavily affects the development time of these mosquitoes, while rainfall mainly controls their seasonal variations by controlling the availability of breeding sites, given that these mosquitoes are fresh water breeders. The approximations of their

physiological time by means of heat accumulation in units measured in degree days has enabled us to model the development of immature stages in a manner that closely resembles their growth in nature. This approach has successfully been used for decades for modelling development of exothermic organisms, since their development is highly controlled by environmental temperatures [205, 206]. Low temperatures reduce the rate of development of mosquitoes in a way that if it falls below the critical threshold 10°C, development stops [6, 189]. On the other hand an increase in temperature directly influences the growth rate of insects with optimal development being achieved around a daily temperatures of 30°C [6], such that beyond this threshold, decreases on the rate of development are likely to be registered [239]. Such variability among individuals and high mortality near the lower and upper threshold temperatures poses substantial challenges for measuring temperature-dependent development responses. Hence, models of the mosquito life cycle built under the concept of heat accumulation are of great importance in understanding the ecology of mosquito life histories as they offer unique opportunity for examining the impacts of temperature and other factors on the population dynamics and management of insects. Moreover, both *Aedes* and *Culex* species considered in our model are outdoor species which breed in fresh temporary water [31, 33, 186]. This additional characteristic feature of these mosquitoes calls for a close eye on the impact of rainfall regimes on the population dynamics of these mosquitoes. Reason why RVF outbreaks are highly correlated to heavy rainfall and flooding regimes [1, 14, 34]. These flooding conditions increase the number of breeding sites for mosquitoes, resulting in hatching of dormant *Aedes* eggs with subsequent elevation of *Culex* mosquitoes [13]. Flooding regimes result from a combination of temperature and precipitation effects which leads to permanence of water in the water-bodies [212]. Available information suggests that due to evaporation effect, rainy water may persist in the water-bodies for about 20 to 40 days [210, 211], which is an appropriate time interval for developmental of broods. We have examined the effects of evaporation phenomenon by varying its parameter value. Low values of evaporation rates lead to more days of water persistence, hence facilitating complete development of the insect. This highlights that successful development of *Aedes* and *Culex* mosquitoes mainly depends on a combination of two factors: the presence of water and temperatures at that period [188, 189, 212]. Our results have suggested that even water persistence of about 20 days is sufficient for reproductive ability of the brood, as this duration was found to surpass the effects of dry spells. To further examine the role of precipitation on abundance of mosquitoes, we have examined the time of appearance of the first cohorts of mosquitoes after suitable climatic conditions. Our findings suggest that the first cohort of both *Aedes* and *Culex* adults is likely to be observed around the 6th and 27th day respectively after rainfall which is in good agreement with findings from empirical studies [29]. These results are of great epidemiological importance as they provide crucial knowledge about the timing of appearance of mosquitoes which is essential for vector control. It is worth noting that this control method remains the most important one given that use of vaccine in livestock is not yet reliable for affected countries due to economic reasons [11].

The core part of this study was to thoroughly analyse how each feature of the mosquito life cycle contributes to abundance of adults. The selected features are gonotrophic cycle, number of eggs each adult lays, age-dependence survival, diapause and flight behaviour. Gonotrophic cycle determines how many times a female mosquito would bite its host for blood meal, such that shorter lengths of the gonotrophic cycle increases the frequency of mosquito biting. Hence, the vector's reproductive ability since the female takes blood for egg production which in turn enhances its vectorial capacity [138]. Our analysis on this factor has shown that increasing the duration of the gonotrophic cycle substantially decreases the abundance of the adults and our results highlight an optimal duration of about 8 days. This is in good agreement with results from other studies [138, 213], although in nature this length is likely to vary according to variations in temperature among other factors [138]. In these settings if temperature-dependent survival of adults is known and track of vector parity status is recorded, the length of the gonotrophic cycle can be determined based on these two parameters [231]. The gonotrophic cycle can also be thought of as the time between two acts of egg oviposition. There are a number of factors affecting the number of eggs laid per each gonotrophic cycle including the parity status of the female, egg-laying behaviour, temperature, and availability of several larval habitats [189, 240–242]. Results of the simulation have shown that there is a link between the number of eggs laid at each gonotrohic cycle and abundance of adults such that large numbers of eggs laid are likely to increase the chance of many broods to complete their life cycle up to the adult stage. In addition to this, an important factor is the diapause which allows the survival of broods across generations. Our analysis has shown that without diapause, stochastic extintion of the species is certain and that the time each species goes to diapause it is critical for successful long-term survival of the vectors. However, this aspect itself deserves further investigation.

Several studies have highlighted the importance of vector age-dependent mortality on both abundance and transmission of vector-borne diseases [232, 233, 243]. In fact, small changes in daily mortality can result in relatively large changes in the pathogen transmission cycle [195] and on the population dynamics of the vector. To partially capture the effects of vector senescence on abundance of the adults age-specific mortality rates for all, the adult stages have been implemented. Our findings have suggested that this factor directly correlates with the abundance of adults through a linear relationship in particular for *Aedes* while for *Culex* the relationship was found to be nonlinear. This nonlinearity was found to result from the interplay between degree of mortality deceleration and their adaptive behaviour for surviving during dry spells. The longer a mosquito stays alive not only contributes to its ability to reproduce, but also to its ability to disperse over greater distances. Through its flight behaviour there is high chance of spreading diseases across sites including the virgin ones. We have assessed the impacts of this factor on the abundance of adults, and our findings indicated the ability of a mosquito to find a host for a blood meal enhances the reproduction of the species as expected. However, the success of this adaptive behaviour was found to be linked to the scale of the environment and vector vision's radius. Studies aiming to investigate spatial patterns in the distribution of adult mosquitoes are required to further explore effects of vector flight behaviour on spatial abundance of adults

over different spatial arrangements.

The importance of this study does not rest only on determining the impacts of climatic conditions on a mosquito's life histories, rather it is aimed to establish a holistic framework that can serve as a research tool for entomologists, epidemiologists, ecologists and other expert personnel involved in the fight against the fear posed by these mosquito vectors. Similar tools have been developed for malaria [193–195], and have been successfully used to study several biological questions (for more details see [195] and references therein). Following this perspective we have examined several biological and epidemiological questions, which are of great importance for improving our understanding of vector ecology to better ameliorate vector and disease control interventions. We mainly focussed on major contributions of the mosquito life cycle features on population dynamics of the vectors and on how these are impacted by weather conditions. Within this realm we have systematically investigated the role of the length of the gonotrohic cycle, number of eggs laid by each adult per blood meal, flight behaviour, diapause and adults age-dependent survival. These features are major determinants of species ability to reproduce and survive for the next generation by optimizing the length of time between consecutive blood meals, number of eggs to lay and their diapause ability. By including these features in our model we have laid a foundation reliable for examining other important determinants of the pathogen transmission cycle such as biting rate, infection rate, and more.

Chapter 7

Rift Valley fever Disease Inter-Epidemic Activities in Livestock. Insights from an Individual-based Model of Rift Valley fever Mosquito Life Cycle

7.1 Introduction

Rift Valley fever (RVF) outbreaks (epidemic activities) occur at irregular intervals following heavy rainfall and excessive flooding, in particular in East, South and horn of Africa [1, 14, 34]. However, there is more and more evidence of disease transmission between outbreaks [3, 39, 44–46], which are hereafter referred to as inter-epidemic activities. Such inter-epidemic activities generally pass undetected clinically, but can be revealed where active serological surveillance is regularly carried out in livestock [39]. For instance, RVF virus (RVFV) transmission has been reported without noticeable outbreaks or clinical cases in cattle in Mayotte [40, 41], in sheep and goats in Senegal [42] and Mozambique [43], in cattle, sheep and goats in Tanzania [3, 39] and Kenya [44–46]. Despite this detection of virus activities through molecular epidemiology, RVF maintenance in nature between epidemics both in the mammalian host and vector populations has not yet been fully explained [45, 46]. This is partly due to the limited evidence that has been gathered and the knowledge of the other factors driving its maintenance in a particular geographical scale. For example, the vectors thought to maintain virus circulation during inter-epidemic periods in East Africa belong to *Aedes* subgenus Neomelaniconion, however in West Africa they are a combination of this and subgenus Aedimorphus [42]. Furthermore, heavy rainfall which normally correlates with disease outbreaks in eastern and southern Africa was not often associated with RVF outbreaks in West Africa [11]. Hence, the interplay between the changing ecosystems, climate, emergence of infections and vector ecology pose a substantial

challenge for identifying viable control options against RVF [45].

The present study makes use of an individual-based model (IBM) of RVF mosquito life cycle (see Chapter 6) to incorporate effects of vertical transmission on *Aedes* mosquitoes including livestock for investigating disease activities between outbreaks. The core model includes important features of both the mosquito life cycle such as: oviposition, egg maturation, diapause, developmental stages (egg, larva instar 1 to 4, pupa and adult), development and mortality in all different stages, aquatic habitats, host seeking, engorgement and oviposition site seeking, adults age-dependent mortality and flight behaviour. Our goal in conducting this research is to examine how the above important features of the mosquito life cycle and effects of vertical transmission in *Aedes* mosquitoes contribute to disease transmission in livestock during the inter-epidemic period (IEP). The IBM allows one to include detailed processes of disease development in both vector and livestock populations which is important for estimating important epidemiological parameters. Additionally, we aim to examine impacts of the interplay between vertical transmission and mosquito diapause mechanism on the prevalence of disease inter-epidemic activities. Based on RVF reported cases during the IEP between 2009 and 2011 (after the major 2006-2007 outbreak in East Africa) collected from Sangailu, Ijara District of Kenya [46] including weather data (temperature and precipitation), our focus is to correlate abundance of mosquitoes with the number of RVF reported cases in livestock during the inter-epidemic period. Our efforts will be capitalized on answering the following four questions: (1) Is there any correlation between abundance of mosquitoes and RVF incidences? (2) What are the factors during the mosquito life cycle that contribute to transmission of the disease? (3) What are the necessary levels of vertical transmission to maintain the disease between outbreaks? This way not only are we interested in obtaining knowledge about mechanisms underlying disease inter-epidemic activities but also to establish the type of feedback mechanisms that exist within entities involved in the transmission of RVF during the IEP. Our results provide important insights regarding the correlation between abundance of *Aedes* mosquitoes and RVF incidence cases during the IEP. Additionally, we have found important features of the RVF mosquito life cycle that heavily influence the dynamics of the disease.

7.1.1 Study site and data

Our focus is Sangaiulu, where detailed studies on vector abundance and virus circulation on sheep and goats have been conducted, for the period between 2009 and 2011 [45, 46]. Minimum, average and maximum temperature and precipitation were recorded daily. Selected domestic livestock were tagged with identification collars and then left to continue grazing together with the rest of the ruminants and the sero-survey activities were scheduled during the rainy season when the mosquito's activity was presumed to be higher [45, 46]. Row data about the sero-prevalence of the disease on livestock was provided by Drs Sang and Kasiiti, which was then used to compare with model disease predictions.

7.2 The Model

The model was developed using Netlogo 5.2 software (http://ccl.northwestern.edu/netlogo/.) [216], combined with *R* extension (RNetlogo) for model analysis [217, 218] and Matlab was used for graphical outputs. The model description follows the ODD (Overview, Design concepts, Details) protocol for describing individual- and agent-based models [219]. A complete schematic representation outlining all processes and algorithms of the RVF mosquito life cycle model which consists of both aquatic and terrestial (adult) mosquitoes coupled with disease dynamics within livestock is shown in Figure 7.1. A summary of all model input parameters included within the simulation model is given in Table 7.1.

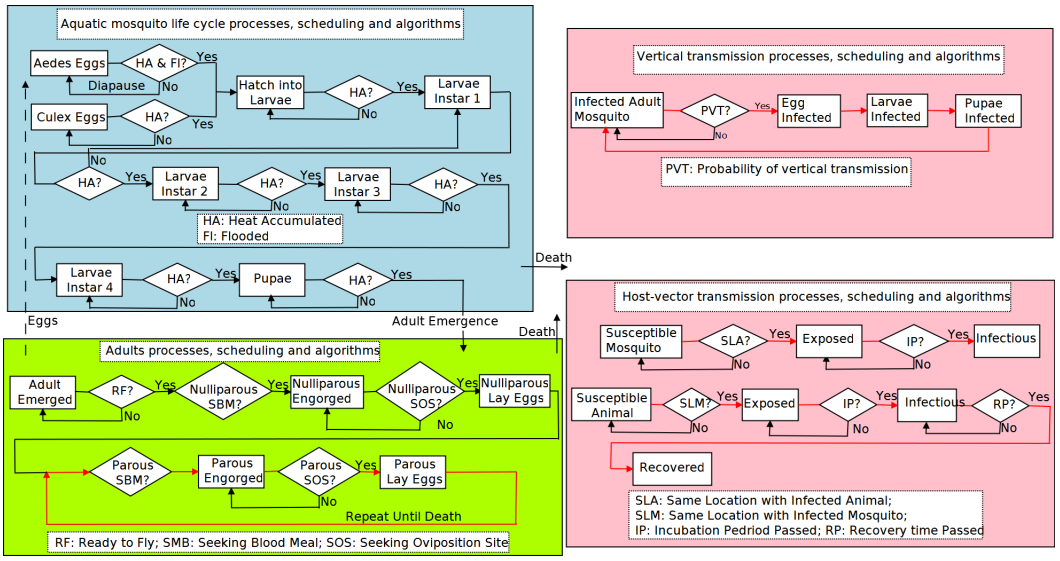

FIGURE 7.1: Outline of model processes and scheduling of the sub-models algorithms. The rectangular boxes represent the process (a state) of a given entity while the rhombus represents a decision point. Details on the decision processes are discussed in Section 6.2.7 of Chapter 6.

7.2.1 Purpose

This model aims to apply an IBM of the RVF mosquito life cycle to assess correlation between abundance of mosquitoes and RVF incidences for investigating mosquito life cycle features leading to disease circulation in livestock during the inter-epidemic period.

7.2.2 Entities, State Variables and Scales

We have five groups of entities in the model: aquatic mosquitoes (eggs, larvae and pupae), terrestrial mosquitoes (adult mosquitoes), livestock, mosquito habitats

(water-bodies and edges of water-bodies) and the model environment. Details about entities and state variables of the mosquito life cycle model can be found in Section 6.2.2 of Chapter 6). Regarding the dynamics of the disease adult mosquitoes are categorized in three groups: susceptible S, exposed but not yet infectious E and infectious I as an SEI type model [4, 69, 244]. Once a mosquito is infected it remains infected for life and disease persistence is driven by female *Aedes* mosquitoes. Hence, in turn *Aedes* immature stages are either infected or not. Livestock are the source of blood meals for adult mosquitoes and they have a static variable, that is, their location. Additionally, livestock entities in terms of the infection are considered to be in one of four states representing the progression of the disease, based on an $SEIR$ type model [21, 59, 167], where S is for susceptible to infectious mosquitoes, E exposed but not yet infectious, I infectious to susceptible mosquitoes, and R recovered with immunity developed against RVF virus. For the period that the model is simulated we ignore birth and death processes so that the population of livestock is in equilibrium.
The model does not use real geographic space, but instead represents the environment as a two-dimensional space of 10201 m^2 grid with 20 m x 20 m grid squares corresponding to an area of 2 Km x 2 Km. A scale of 20 m x 20 m grids (patches in the Netlogo language) was chosen, as 20 m represents the minimum distance from which mosquito can identify a mammalian host [189] such that mosquito host-seeking behaviour is approximated at this scale. The model is set so that one time step in the model represents one day and it is run for almost two years from 15 January 2009 to 15 October 2010.

7.2.3 Process Overview and Scheduling

This model simulates a complete RVF mosquito (*Aedes* and *Culex* spp.) life cycle and transmission of the RVF virus in livestock during the inter-epidemic period. Time is modelled in discrete time steps where each time step corresponds to one day of activities. A time step of one day was chosen because the mosquito life cycle model is on daily time steps and disease progression patterns in both livestock and mosquitoes are better described on a daily basis [5, 69]. Within each time step for the mosquito life cycle model each entity will go through its developmental stages, while first checking survivability followed by its underlying life cycle activities (for more details see Section 6.2.7 of Chapter 6). For disease transmission an entity either contracts infection or recovers from infection and *Aedes* eggs may acquire infection transovarially. A detailed description of all model processes is given in Section 7.2.7.

7.2.4 Design Concepts

7.2.4.1 Basic Principles

The construction of the mosquito life cycle model and its underlying design concepts followed the framework of Pattern Oriented Modelling (POM) [65, 201, 202]. However, the disease dynamics added to this model are based on results from surveillance and experimental studies of both vector and host ecology and epidemiology. A summary of detailed information about the ecology and epidemiology of both the vector and host is given in [11]. This approach has been successfully applied in other simulation models of disease dynamics [67, 204]. The dynamic of disease spread and persistence is strongly affected by vertical transmission on *Aedes* species, diapause, mosquito's flight behaviour and presence of cohorts of adult mosquitoes which in turn affect transmission rates.

7.2.4.2 Emergence

Vertical transmission and diapause combined with a mosquito's flight behaviour when searching for a host lead to emergence of adult infected mosquitoes and infected livestock. Disease spreads among livestock through proximity of infected adult mosquitoes with susceptible mammalian hosts. Livestock are not mobile in our model and contract infection when bitten by an infectious adult mosquito moving around looking for a blood meal. This results in the emergence of host-vector disease dynamics.

7.2.4.3 Adaptation

For details regarding adaptive behaviour see Section 6.2.4 of Chapter 6.

7.2.4.4 Fitness

For details regarding entities fitness mechanism see Section 6.2.4 of Chapter 6.

7.2.4.5 Sensing

For details regarding sensing see Section 6.2.4 of Chapter 6.

7.2.4.6 Interaction

Both adult species interact with the host through feeding behaviour. An infected adult mosquito may infect a given susceptible host and a susceptible mosquito

may acquire infection while feeding on the same host. For more details regarding host-vector interactions see Section 6.2.4 of Chapter 6.

7.2.4.7 Stochasticity

Disease transmission from infected vector to susceptible host and from infected host to susceptible vector occurs when a vector feeds on a host and it is probabilistic. Progression of infection and recovery are also stochastic processes. This represents our uncertainty in the events leading to successful transmission or recovery from the virus.

7.2.5 Initialization

In order to be able to perform the simulation a model environment of 10201 m^2 grid with 20 m x 20 m grid squares is set. Then water-bodies and water-body edges are created and distributed over the world with different depths ranging from 16 mm to 100 mm. Both aquatic and terrestrial (only *Aedes* eggs and *Culex* adults) and livestock breeders are created when the model is initialized; the total number of each is specified via parameters: 'initial-number-Aedes-eggs', 'initial-number-Aedes-adult', 'initial-number-Culex-adult' and 'initial-number-livestock'. Note that the mosquito variables represent only female mosquitoes since only females bite for a blood meal. A proportion of *Aedes* infected eggs is also initialized and is set by the parameter 'vertical transmission'. A total of 200 susceptible livestock is initialized as we aim to reproduce the distribution of infection patterns observed from the data [45, 46]. Note however, that during the sero-survey study about only 90 domestic livestock were monitored for virus detection but were left to continue grazing with the others. Therefore, our assumption of 200 ruminants is reasonable to account for the contribution of other ruminants that were not targeted during the study. At the start of simulation a certain proportion of *Aedes* eggs governed by the parameter 'vertical transmission' is randomly given a chance to start off infected in order to initiate the disease transmission process. *Aedes* eggs are initialized and distributed uniformly in water-body edges while both *Aedes* and *Culex* adults are initialized and distributed uniformly over the entire world. Note that *Culex* eggs are not initialized since they only breed in water. A complete description of all model parameters is given in Table 7.1.

Agent/Individual	Parameter	Baseline Value	Range	Units	References
Aedes & *Culex* adults	Gonotrophic time	8	4 - 12	Days	[138, 213]
	Aedes number of eggs	59	50 - 150	-	[195]
	Culex number of eggs	60	50 - 200	-	Estimated
	Resting time after emergence	-	1 - 3	Days	[189]
	Resting time after oviposition	-	1 -3	Days	[189]
	Search radius	60	20 -	Meters	[189]
	Successful blood feeding	0.8	0.5 - 1	-	Estimated
	Incubation period	6	4 - 8	Days	[69, 245]
	Vector to host probability of transmission	0.38	0.1 - 0.54	-	[11, 23, 99]
	Vertical transmission	0.1	0.01 - 1	-	[**?**]
Livestock	Incubation period	4	1 - 6	Days	[76]
	Recovery time	6	3 - 7	Days	[11]
	Host to vector probability of transmission	0.61	0.3 - 0.9	-	[11, 23, 99, 246]
Water-bodies	Evaporation rate	0.1	0.05 - 0.20	$Days^{-1}$	[210, 211]

TABLE 7.1: Model input parameters: calibrated and non-calibrated.

7.2.6 Input Data

Rainfall and temperature daily time series data are used for quantifying the development, hatching of eggs, survival of aquatic mosquitoes (egg, larvae and pupae), water level of water-bodies and moisture index.

7.2.7 Submodels

Here we present details of the model processes. It is worth noting that sub-models regarding the mosquito life cycle model are not included but they are given in Section 6.2.7 of Chapter 6.

7.2.7.1 Adult *Aedes* and *Culex* blood feeding and disease transmission

Blood and its protein ingredients are essential for egg-production [189]. Blood feeding takes place once a female adult mosquito has found a host, that is, sharing the same patch with the ruminant. Then a uniform random number between zero and one is drawn, and if it is less than the parameter 'successful blood feeding' then the mosquito has successfully acquired a blood meal enough for egg maturation such that it becomes engorged and will only take another blood meal after egg oviposition. Disease transmission occurs during this process of biting a livestock for a blood meal and details about rules governing either livestock infection or mosquito infection are given in sections 7.2.7.2 and 7.2.7.3.

7.2.7.2 Vertical transmission and vector to host transmission

The virus is introduced into our system through vertical transmission by a female *Aedes* mosquito as she is capable of passing the virus to its eggs [11, 33]. Vertical transmission efficiency is set as a proportion of *Aedes* infected laid eggs and it is governed by the parameter 'vertical transmission' see Table 7.1. Once the virus has been introduced, newly emerged infected adults will successively spread the disease by infecting susceptible livestock while biting for a blood meal according to a transmission probability parameter (see Table 7.1). A uniform random number between zero and one is drawn, and if it is less than the parameter 'vector to host probability of transmission' the livestock becomes infected, otherwise it remains susceptible. Once transmission has occurred, the livestock will go through its incubation period only becoming infectious after the incubation period has elapsed. This period is drawn from a normal distribution with $mean = 3$ and $standard\ deviation = 1$ within a minimum of 1 day and a maximum of 6 days [76].

7.2.7.3 Host to vector transmission

After the virus has been introduced into the livestock community this in turn amplifies spread of the disease by infecting other mosquitoes. A susceptible adult mosquito may become infected when feeding on an infected ruminant according to a transmission probability (see Table 7.1). A uniform random number between zero and one is drawn, and if it is less than the parameter 'host to vector probability of transmission' the mosquito becomes infected, otherwise it remains susceptible. Once transmission has occurred, the mosquito will go through its incubation period only becoming infectious after the incubation period has elapsed. This period is drawn from a normal distribution with $mean = 4$ and $standard\ deviation = 2$ within a minimum of 4 days and a maximum of 8 days [245]. Once a mosquito is infected it remains infected for life and infection is not harmful to them [4, 69].

7.2.7.4 Host recovery

In this study we do not model vital dynamics in livestock, that is, we ignore birth and death processes since our aim is to compare the distribution of infected livestock from our model with those of reported cases in Sangailu during the inter-epidemic period after the 2006-2007 major outbreak in East Africa. In this setting infected livestock recover from infection after the recovery time has elapsed. This time is accumulated since the day of virus infection, and the virus is cleared after about 15 days [11] and it is drawn from a normal distribution around this value We assume that infection with RVFV induces life-long immunity in livestock population since the duration of this immunity is not known with certainty [11].

7.2.8 Model predictions and observations

The mosquito life cycle model was built and parametrized based on two approaches: 'model cycling' and pattern oriented modelling (POM) [65, 201, 202]. This methodology allowed us to compare patterns of the simulation model to selected performance criteria which are geared towards aspects of a predictive model that is able to capture seasonal variations observed in RVF mosquito population dynamics (for details see Section 6.2.8 of Chapter 6). When disease dynamics are included further model performance criteria are defined and evaluated. Vertical transmission in *Aedes* is the main mechanism by which disease is introduced in the eco-system [11, 33], leading to occurrence of epizootics/epidemics and virus circulation between outbreaks [3, 39, 44–46]. Using this parameter we evaluate our disease transmission model in two important ways: 1) Do RVF inter-epidemic activities correlate to abundance of adult mosquitoes and weather conditions? 2) What are the necessary levels of vertical transmission for sustaining disease inter-epidemic activities? The latter is mainly examined by comparing our model prediction with data of ruminants that tested positive for RVFV in Sangailu, Ijara district of Kenya during 2009 and 2010. This way we were able to test that our simulation model could adequately reproduce patterns of disease inter-epidemic activities in Ijara district (see Fig.7.4).

7.3 Model Analysis

We used our model to address the following questions: (1) What are the factors during the mosquito life cycle that contribute to transmission of the disease during the IEP leading to sporadic outbreaks? (2) What are the necessary levels of vertical transmission to maintain disease activities between outbreaks? These questions were addressed by: investigating how specific the mosquito life cycle features affect spread of the disease; the correlation between abundance of mosquitoes and RVF incidences; examining effects of vertical transmission, diapause and disease progression factors (incubation and recovery) in the spread and maintenance of the virus between outbreaks.

7.4 Results and Discussion

7.4.1 Effects of temperature and rainfall

Temperature influences every aspects of the mosquito life cycle since temperature affects both development and mortality of all larval stages (see equations (6.10) and (6.11) in Chapter 6). Increasing the value of accumulated degree-days required for transition from one stage to another linearly increases the developmental time, but the overall relationship between temperature and development rate of

immature stages is nonlinear [220]. These fluctuations on temperature significantly induce variations in the development of immature stages and emergence of adults. However, temperature was not responsible for creating the intra- and inter-annual variation on adults abundance. This was mainly driven by variations on rainfall regimes. Rainfall affects the dynamics of the mosquito population in two aspects: creates suitable breeding sites for immature stages and influences their survival. A daily water level of 16 *mm* was set as the minimum amount of water required to keep water-bodies suitable for immature stages development. However, periods of drought would reduce their survival and *Culex* appeared to be more sensitive to drought compared to *Aedes*. This phenomenon may result from the fact that during unfavourable seasons *Aedes* go diapause in the form of eggs and the adult is able to continue to lay eggs even if the water-bodies are not flooded [189], while *Culex* adults can only lay eggs if water-bodies are flooded [187, 189]. Therefore, successful development of new cohorts of both *Aedes* and *Culex* is dependent on two main factors: temperature and rainfall.

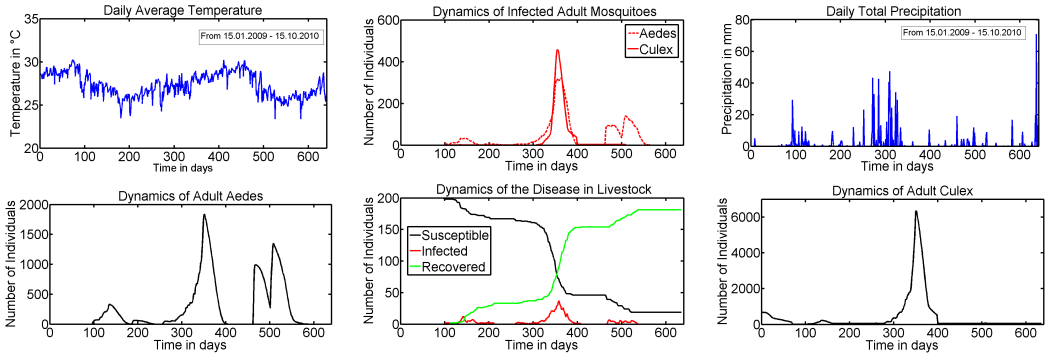

FIGURE 7.2: A one time simulation model output under baseline parameter settings. The output outines the abundance of both *Aedes* and *Culex* mosquitoes and the dynamics of the disease on both mosquitoes and livestock. Temperature and rainfall data are also plotted.

7.4.2 Correlation between abundance of mosquitoes and RVF incidences

To investigate the correlation between abundance of mosquitoes and RVF incidences we plot times series of the dynamics of the disease in both vector and mammalian host. Figure 7.3 (left) shows the dynamics of infected adult *Aedes* mosquitoes which are highly correlated to patterns of the species population dynamics. Similar trends are observed within *Culex* mosquitoes see Fig. 7.3 (right) confirming that disease activities correlate with abundance of mosquitoes even during inter-epidemic period [44]. These results highlight that the distribution of infections follows the patterns of temperature and rainfall with major emphasis on rainfall seasonal variations. A striking feature is observed within the distribution of RVF cases in livestock Fig. 7.3 (center). The dynamics of RVF cases heavily follows the dynamics of *Aedes* mosquito population such that abundance of infected mosquitoes correlates the

abundance of disease cases. This feature highlights the importance of *Aedes* species as disease primary vectors for the spread of the disease. This feature is central for initiating and maintaining the spread of the disease [44] even in a situation of short rains with dry spells such as the period between day 100 and day 200. Another interesting feature is that the peak of disease cases in livestock coincides with that of both infected *Aedes* and infected *Culex* adults. This emphasizes the contribution of the latter species as secondary vectors or disease amplifiers [13]. The emergence and abundance of the *Culex* result from the fact that during this period the rainfall persisted long enough to ensure complete development of species which leads to subsequent emergence of new cohorts of adults. These adults when feeding on infected ruminant further spread the virus.

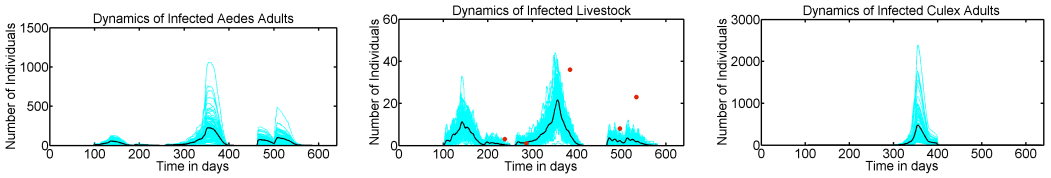

FIGURE 7.3: Dynamics of the spread of RVF in both vector and mammalian host population. (Left:) Distribution of the number of infected *Aedes* adults and distribution of the number of infected *Culex* adults (right). Distribution of the number of infected livestock and the red dots represent the data (center). The dark line represents the average of 200 replicates.

7.4.3 Effects of vertical transmission and diapause

Vertical transmission is a mechanism by which the RVFV is introduced into the host-vector community. The *Aedes* species are the ones responsible for this process. With their eggs which are able to withstand several periods of dessication from days to years [187], if carrying the virus new cohorts of infected adult mosquitoes will emerge when suitable flooding conditions are met. Then, the virus is amplified when these adults feed on vulnerable mammalian hosts leading to disease endemicity. Furthermore, it likely that an independent transmission loop within the mosquito population can maintain the virus even in situations where mammalian host infections are absent. However, the actual contribution of vertical transmission to virus persistence is less clear. Hence, understanding the efficiency of this parameter for initiating and maintaining disease transmission is central to our understanding of disease inter-epidemic activities. Figure 7.4 shows the results of the effects of different vertical transmission levels to disease prevalence. The trajectories show seasonal fluctuations followed by periods of zero incidences during unfavourable seasons. There are a number of factors underlying these fluctuations: (1) the stochasticity underlying the model processes of both mosquito life cycle and disease features. (2) the virus must incubate in the mosquito gut to generate sufficient levels for onward transmission as well as in the mammalian host. A combination of mosquito incubation period and mosquito life expectancy may lead to fluctuations in transmission efficacy. Therefore, leading to variation

in the number of infected livestock. Another interesting feature is that vertical transmission efficiency correlates with the size of the epidemic such that high levels of this parameter imply high prevalence of the disease. Additionally, very low levels of vertical transmission efficiency may lead to stochastic extinction, suggesting that a minimum of 10% may be required to keep disease circulation going. This might result from the fact that the mosquito life-cycle is relatively short and vertically acquired infections are likely to be diluted with every generation [85]. On the other hand the periods of zero incidences are due to the recovery time in livestock which is very rapid and during the unfavourable season the hosts rapidly clear the virus as it quickly develops adaptive immune responses [11]. Additionally, availability of susceptible hosts for subsequent transmission is critical for maintaining the virus, otherwise the virus will go extinct at the end of the favourable season during which mosquitoes go diapause. Diapause is another of the mosquito's adaptive behaviour that further compounds the effects of vertical transmission, since survival of eggs during diapause is higher [187, 189] leading to disease inter-epidemic activities.

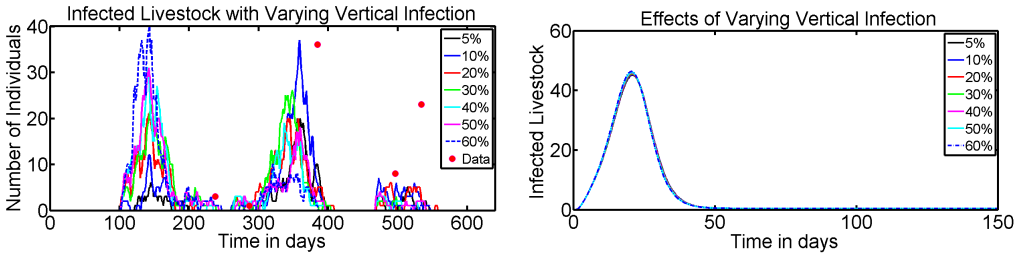

FIGURE 7.4: Effects of varying vertical transmission efficiency on the prevalence of the disease in livestock. (Left) Individual-based model output and (right) deterministic equation-based model output [4].

To further demonstrate the potential of our model compared to equation-based deterministic models, we also plot effects of varying vertical transmission using a deterministic model [4] see Fig.7.4 (right). These results show that effects of this parameter are almost unapparent when using deterministic models and can only be revealed when the effect of this parameter is evaluated using the basic reproduction number (see [80]). This highlights the important role of individual-based models for investigating biological questions as we can easily monitor how macroscale properties emerge form micro dynamics.

7.4.4 Effects of loss of immunity in livestock

The dynamics of disease incidences in livestock is highly sensitive to the recovery time. The recovery time is a function of the virus induced immunity and the time the ruminant stays infected. From the date of infection the virus may persist in the livestock's body for at most for 20 days [11], and after that the ruminant recovers, however, it is not well known for how long the ruminant stays immune and this remains to date an open question. Available information indicates that

the ruminant may stay immune for more than five months [11]. Therefore, to investigate how does the duration of acquired immunity influence the dynamics of the disease, we run the model for four different settings regarding the loss of immunity such that immunity either wanes after 180 days or 365 days or 545 days or 635 days (immune for life in the model sense). For the first 300 days the trajectories overlay each other due to the fact that for the first six months the parameter 'loss of immunity' does not have any effect (see Fig.7.5(left)). One may wonder why even after 200 days trajectories still over lay such that the effect of loss of immunity is unapparent. These results emerge from the fact that during the period between 200 and 300 days there are no adult mosquitoes, it is the unfavourable season and new infections are at a minimum. However, irrespective of this situation differences in the period above 300 days are still not paramount. The results stem from the fact that within this period there is a substantial decline in the number of susceptible individuals. In addition, inherent complexities arising from the ecology of the vector further compounds this situation, suggesting that host immunity waning cannot be evaluated as a single factor but rather as a whole including changes in the environment.

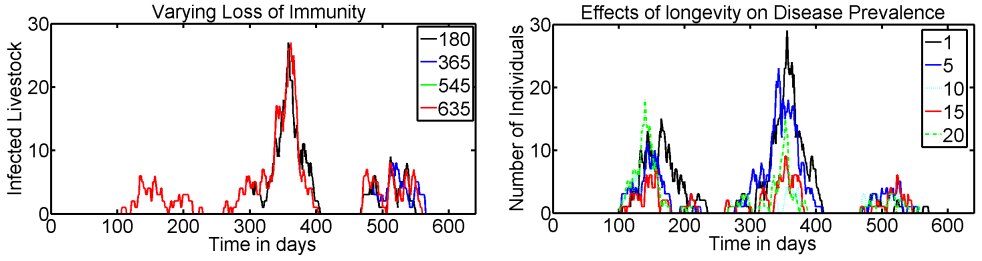

FIGURE 7.5: Left: Effects of varying the time of loss of immunity in livestock disease dynamics. Right: Effects of varying adult mosquito's degree of mortality deceleration on disease prevalence in livestock.

7.4.5 Effects of mosquito's age-dependence mortality

The survival of adult female mosquitoes is a critical component of their ability to transmit diseases. This allows mosquito to survive longer, hence enhancing their reproductivity. To investigate the link between an adult mosquito's longevity and its ability to transmit the virus, we analyse the effects of the degree of mortality deceleration on disease prevalence see Fig.7.5 (right). The relationship between this parameter and the number of infected livestock is somewhat linear and nonlinear, which results from inherited linear and nonlinear effects from *Aedes* and *Culex* respectively. Nevertheless, it is apparent that for small values of the degree of mortality deceleration there is a tendency of expanding the size of the epidemic at least for the first and second waves. This is due to the fact that lower degree of mortality deceleration increases survival of mosquitoes such that they live long enough to become infectious, and then to deliver more infective bites during the remainder of their lifetime. However, for the last wave the same cannot be concluded.

This results from the fact that at this point the decline in the number of susceptible individuals is very substantial in such a way that there are few susceptible hosts and those who have recovered from previous infectious are immune from the virus. Our results indicate that longevity of adult mosquitoes is of considerable epidemiological importance because older mosquitoes are more likely to have survived beyond the virus extrinsic incubation period, which enhances their ability to further disperse the virus.

7.4.6 Disease incidence rates and basic reproduction number, R_0

An important benefit of the IBM relies on its ability to estimate important epidemiological parameters since its model parameters are defined at an individual level and can be related to field measurements. At each model step we estimate the basic reproduction number, R_0 which gives the average number of secondary cases arising as a result of introducing one infected individual into a wholly susceptible population, over the course of the infected individual's contagious period. If $R_0 > 1$ the virus can invade the population, otherwise it cannot. This results from the fact that if an infected individual on average cannot successfully transmit the virus to more than one individual, then the disease cannot spread over the population. At the end of the simulation the quantity R_0 reflects an estimate of the reproduction number, the final size relation that indicates whether there will be (or there was, in the model sense) an epidemic [247]. The basic reproduction number is directly related to the size of susceptible individuals such that for an epidemic to occur the fraction of the initial number of susceptible individuals should be greater than the inverse of this threshold parameter. Therefore, it possible for the livestock population to determine the rate at which new cases are produced by an infectious individual, given that the entire population of livestock is susceptible at the beginning of the simulation [21]. In such a situation the host reproductive number can be estimated from the final size of the epidemic [248] (for more details on the derivation of this threshold see equation (E.4) in Appendix E). Figure 7.6 shows the distribution of this parameter here named host-reproductive rate which gives the maximum reproductive potential of the disease [249]. From this figure we can confirm that the host-reproductive number is above 1 exactly during periods where we have waves of disease outbreaks (see Fig.7.2(center) 'Dynamics of the disease in livestock'). The latter depicts the temporal dynamics of the disease in livestock in which we see the typical 'S curve' where the fraction of susceptible decreases as the fraction of recovered increases and the peak of infected at around the intersection between the susceptible and recovery curves. Another important observation is that the breaks in the chain of transmission does not necessarily occur because of lack of susceptibles, but rather due to the decline or lack of infectives [21], which for our cases are mosquitoes. This decline in mosquito population is due to seasonal variations. In regard to this, the very same principle cannot be applied for obtaining the vector reproductive number in the settings of our model since their population varies with time according to factors that influence their

life cycle. Instead we determine incidence and infection rates that indicate the frequency at which the disease spreads over the population and the average number of new secondary infections per day respectively. Both host and vector infection rates emerge essentially from interactions among the following mosquito life cycle features: duration of gonotrophic cycle, blood feeding behaviour, flight behaviour and longevity which all together contribute to a mosquito's ability to transmit and spread the disease.

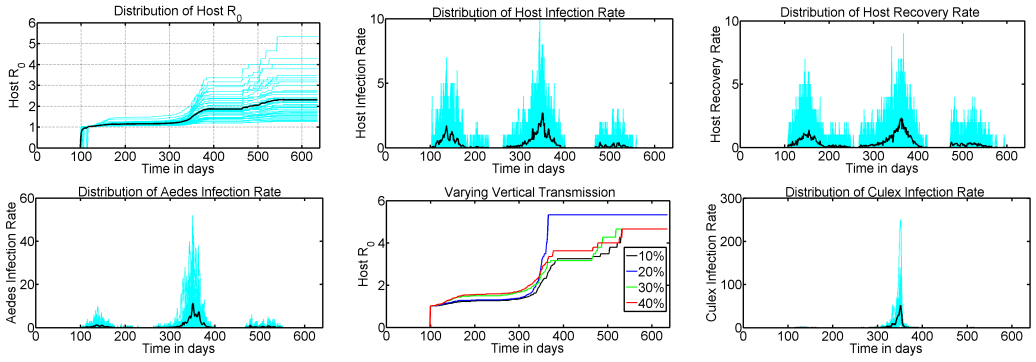

FIGURE 7.6: Top: Distribution of host reproductive rates, host infection rate and host recovery rate respectively. Bottom: Distribution of both *Aedes* and *Culex* infection rates and quantification of the effects of varying vertical trasmission on host reproductive numeber (center).

7.4.7 Model extension and other applications

Here we have extended a comprehensive IBM model of the mosquito life cycle to investigate RVF transmission in livestock during the IEP. This has enabled us to study important biological questions regarding disease inter-epidemic activities at a particular site under changing environmental settings. However, as pointed out in Chapter 6 that extending the model to include Geographic Information System (GIS) capabilities could lead to further important extensions. It was highlighted that with such extension we could move from local spatial scales to much larger scales with realistic landscape variables such as vegetation index which has proven to be an important epidemiological factor. Allowing us to thoroughly study the spatial and temporal variability of emergence of the disease. RVF outbreaks do not start at the same time in every part of a particular country, but rather start from a foci location (local hot spots regions) then progress spatially until reaching virgin areas within a single outbreak. With detailed spatial arrangement such important questions can be further investigated including creation of disease risk maps at different spatial and temporal scales. This presumes that both host and vector population are not uniformly distributed and do not mix homogeneously. Therefore, in this setting we could estimate important parameters such as host-vector ratio which is a critical component of vectorial capacity to transmit diseases [250]. It is believed that outbreaks in virgin areas are mainly introduced by either vector or livestock from sites where the outbreaks started earlier [13]. Additionally,

this phenomenon is stimulated by the direction of climatic gradients which cause patterns of precipitation such that the rain starts at a certain point and with time progresses to other areas [68]. Most RVF outbreaks occur in arid and semi-arid lands where the majority of the population is pastoralist with a nomadic lifestyle such that with the onset of rains, many pastoralists move their herds to areas with new grass growth and water-filled dambos (temporary water bodies) [58]. Through these movements the virus may be introduced in uninfected areas. Therefore, a model with such capabilities could be of great importance for investigating the impacts of migration and migration organization on disease outbreaks and inter-epidemic activities. Also it is of great epidemiological interest to study in detail RVF mosquito larval habitats which are fundamental in providing a basis for understanding the spatial determinates of disease transmission.
In the framework of this transmission model one can be interested in whether after an epizootic takes off, the dominant disease transmission mechanism is still ensured by mosquitoes or is simply by aerosol [11, 68]. Many mammalian species are susceptible to infection with RVFV, including livestock such as cattle, goats, sheep and camels [11], but also wildlife such as giraffe and African buffalo [251], but they do not have the same degree of susceptibility. This variation in their differences on innate immunity can lead to further extensions of the model to investigate how this impacts disease transmission and persistence. When several types of mammalian hosts are taken into consideration we can examine effects of host preference of the vector.

7.5 Conclusion

There is more and more evidence of RVF transmission during the inter-epidemic period (IEP) in some parts of endemic regions [39]. Such virus activities generally occur without clinical cases and with frequency in RVF hotspots. However, factors leading to disease occurrence between outbreaks are not yet fully understood [45, 46]. This situation highlights the necessity of developing comprehensive models to assess and predict potential epidemiological and ecological risks of disease emergence and its maintenance in nature by following reliable informative indicators [79]. For this reason, we have incorporated effects of disease transmission in livestock on an individual-based model (IBM) of the RVF mosquito life cycle (Chapter 6) for correlating abundance of mosquitoes with RVF incidences while investigating disease inter-epidemic activities. We aimed to examine how important features of the mosquito life cycle affects the spread of the disease during the IEP under changing environmental conditions. Our results are summarized with the followings points: (1) disease inter-epidemic activities follow patterns of seasonal abundance of *Aedes* mosquitoes; (2) diapause compounds with vertical transmission mechanisms to sustain sporadic outbreaks during the IEP and a minimum level of 10% of vertical transmission efficiency is necessary to avoid stochastic extinction; mosquito life cycle features such as vector longevity, gonotrophic cycle and flight behaviour heavily affect the dynamics of the disease in livestock; the time livestock stay infectious and immune are important factors for both short and long-term disease

dynamics. Therefore, abundance of *Aedes* mosquitoes can be used as a signal of disease activities and appropriate interventions targeting specific features of the mosquito life cycle should be developed to reduce the burden caused by RVFV.

Chapter 8

Conclusions, Recommendations and Future Directions

8.1 Conclusions

The emergence and re-emergence of infectious diseases have become a great epidemiological concern, especially in the case of vector-borne viral zoonoses that occasionally give rise to human epidemics such as West Nile fever and Rift Valley fever (RVF) [7] just to mention a few. Being able to better understand how vector-borne diseases are propagated and how they may be contained requires knowledge of the many factors that influence their success or failure [15]. The success of vector-borne diseases to invade and persist in a given community poses a unique challenge to public health and veterinary authorities because their epidemiology and ecology are closely linked with environmental factors such as climate, population migration, landscape, and complicated transmission mechanisms [252, 253]. These factors interact in diverse ways such that development and analyses of epidemiological models that would take into account the combination of chance events, time delays, and nonlinearities in varying environmental settings make predicting spread of diseases a daunting task. To tackle this challenge we have used different modelling approaches for answering different biological questions, giving our audience and scientists an opportunity to engage in cross-disciplinary and cross-cultural dialogue about the dynamics of RVF. The methods we have used range from classic deterministic models, stochastic models, to bottom up modelling approaches based on individual-based models. Our efforts have been concentrated on factors underlying disease epidemic and inter-epidemic activities, the temporal characteristic pattern of disease outbreaks (irregular intervals of up to 15 years) and the role of climatic conditions and mosquito life cycle features on the characteristic pattern of disease outbreaks.

In Chapter 2, a deterministic model [4] taking into account *Aedes* mosquito, *Culex* mosquito and livestock populations, mechanism of vertical transmission from *Aedes*

mosquitoes and a class of asymptomatic livestock was proposed. To investigate the role and contribution of vertical transmission from *Aedes* mosquitoes for both disease epidemic and endemic activities a reduced model of juveniles *Aedes* mosquitoes [80] was applied. We found that for low moisture parameters the response of the basic reproduction number, R_0 with respect to vertical transmission was initially very small but strengthened rapidly when the vertical infection efficiency exceeded 20%, while for high moisture parameters the host type reproductive number quickly accelerated even for proportion vertical infection less than 5%, highlighting the importance of vertical transmission and effects of climatic conditions for initial spread and persistence of the disease during endemic activities. Then, uncertainty and sensitivity analysis techniques were employed for quantifying the attribution of model output variations to input parameters over time, providing important information for improving disease management. Furthermore, time varying sensitivity analysis was explored for providing a comprehensive overview of the effects of each model input parameter at all important stages of the epidemic. For deriving conditions for existence of model steady states in Chapter 3 [4], the model in Chapter 2 was used to analytically investigate the stability of both the disease-free and endemic equilibrium. Then, employing techniques of numerical simulations we performed bifurcation and chaos analysis of the model under periodic environment for evaluating the effects of rainfall on the characteristic pattern of disease outbreaks. Studies have revealed that optimum climatic conditions, presence of mosquitoes, international trade of livestock and their products have not completely explained the RVF outbreaks [26], such that other potential vectors such as ticks have been implicated in the transmission of RVFV [28, 29]. In Chapter 4 we proposed a model that extends the model in Chapter 2 to hypothetically evaluate this possibility, pointing out relevant model parameters that require further attention from experimental ecologists and modellers to further determine the actual role of ticks and/or other biting insects in the transmission and endemicity of RVF.

RVF outbreaks occur in irregular intervals of up to 15 years in particular in East Africa and this characteristic pattern of disease outbreaks makes prediction and effective preparedness for disease control a complicated task. In Chapter 5 we proposed a RVF stochastic host-vector model with vertical transmission and analytically determined the dominant period of disease outbreaks with respect to vertical transmission efficiency. These predictions will then be compared with observations if reliable data become available. Using this model we determined novel relationships among vertical transmission, invasion and extinction probabilities and the basic reproduction number. In Chapter 6 we introduced a novel individual-based model (IBM) of the complete mosquito life cycle, built under daily temperature and rainfall data sets. The model was applied for determining correlation between abundance of mosquito populations and rainfall regimes and determining important mosquito life cycle features that influence the population dynamics of mosquitoes. We found that rainfall is indeed responsible for creating the intra- and inter-annual variations observed in the abundance of adult mosquitoes. Regarding mosquito life cycle features, our results showed that the length of gonotrophic cycle, number of eggs laid per blood meal, adults age-dependent survival and flight behaviour are

among the most important features of the mosquito life cycle that substantially induces variability in the abundance of adult mosquitoes. Further, in Chapter 7 we applied the model in Chapter 6 for studying the dynamics of disease inter-epidemic activities in livestock for the period between 2009 and 2011. The model reproduced the observed trend of disease activities during this period and the minimum level of vertical transmission efficiency leading to disease inter-epidemic activities was determined. Abundance of mosquitoes, in particular *Aedes*, was found to have strong correlation with disease incidence cases and mosquito life cycle features such as length of gonotrophic cycle, number of eggs laid per blood meal, adults age-dependent survival and flight behaviour were found to have important influence. These indicators could be of great epidemiological significance by allowing disease control program managers to focus their efforts on specific features of vector life cycle including vertical transmission ability and diapause. With no doubt we affirm that the use of different modelling approaches has enabled us to discuss a broad range of biological questions regarding RVF disease epidemic and inter-epidemic activities providing useful information for improving disease management strategies. Furthermore, we argue that our IBM is an ideal extendible framework useful for further investigations of other relevant host-vector ecological and epidemiological questions for providing additional knowledge important for improving the length and quality of life of humans and domestic livestock.

8.2 Recommendations

The goal of this research study was to develop and analyse mathematical models for improving our understanding of RVF epidemic and inter-epidemic activities and use the outcome for providing knowledge-based disease management strategies. Mathematical epidemic models are formulated in terms of state variables (representing different individuals epidemiological status) and parameters quantifying the rate of change between individuals epidemiological status. Therefore, all the recommendations stated in this section are based on the model structure and its underlying assumptions. All the models developed in this research study (equation-based, stochastic and individual-based models) involve only mosquitoes and mammalian hosts (without differentiating if cattle, sheep or goats). Hence, all disease control strategies discussed are targeting mosquitoes and livestock but they can be extended to humans where applicable. All the three implemented modelling approaches (equation-based, stochastic and individual-based models) outline important disease progression stages which can then be targeted for disease control. An important threshold epidemiological parameter is the basic reproduction number, R_0 which is used for determining the rate at which the disease spreads. In addition, effects of disease control can be assessed using disease related model state variables. We summarize important disease control strategies targeting both mosquitoes and mammalian hosts.

8.2.1 Larval Vector Control

Immature mosquito control is an important component of mosquito control strategies. This is due to the fact that RVF primary vectors such as mosquitoes of genus *Aedes* can also transmit the virus to their eggs which can persist in the ground for long periods of dessication. Analysis of the relationship between vertical transmission and R_0 indicated that for low moisture parameters the response was initially very small but strengthened rapidly when the proportion of vertical infection efficiency exceeded 20% and using a vector type reproductive number, T_1^v we found that vertical infection of about 20% can be responsible for more than 80% of required effort to eliminate the disease. One way to reduce effects of vertical transmission is to implement control programs that target immature mosquitoes. Alternatively, efforts can be directed to factors in the biology of the female adult mosquito that are critical to her ability to pass the virus to her eggs. Further analysis highlighted that the impact of vertical transmission is further compounded with diapause and weather/climatic conditions. For high moisture parameters we found an exponential relationship between vertical transmission and R_0 even for vertical infection efficiency of less than 0.1. Hence, larval mosquito control should take into account how climate variability and climate change impacts vector population dynamics. Anyamba et al.[13] stated that larval mosquito control is useful for preventing any emergence of adult mosquitoes if used prior to flooding or preventing additional production of adults if applied after flooding. Furthermore, applying the mosquito life cycle IBM for studying RVF inter-epidemic activities and fitting the model to livestock incidence data collected in Sangailu, Kenya we determined an optimal proportion of vertical transmission efficiency of 10%. Therefore, efforts that aim to reduce the probability of vertical transmission efficiency below 10% are viable disease control strategies.

8.2.2 Adult Vector Control

Adult mosquitoes-livestock and adult mosquitoes-humans are the predominant mode of RVF transmission during and after the outbreak. One of the most important moments of disease spread is the exponential phase of the outbreak and it can best be analysed by using R_0. Sensitivity analysis of R_0 to disease characteristic parameters can provide important information useful for guiding disease control efforts. Using this technique we found that vertical transmission efficiency (q_1), probability of infection transmission from *Aedes* to livestock per bite (β_{21}), *Aedes* biting rate (σ_1), initial number of susceptible adult *Aedes* mosquitoes (N_1^0) and initial number of susceptible livestock (N_2^0) highly influenced changes in the magnitude of R_0. We discuss the first four parameters ($q_1, \beta_{21}, \sigma_1, N_1^0$) which are related to mosquitoes and positively correlate with R_0. Hence, these are the features that should be targeted in order to quickly reduce spread of the disease. β_{21} and σ_1 are related to mosquitoes vectorial capacity. Hence, factors contributing to their ability to transmit the infection should be targeted through appropriate interventions. N_1^0 refers to the number of adult mosquitoes that are available at

the beginning of the outbreak. Here adult mosquito control interventions that quickly reduce their population are more effective. Reducing the abundance of adult mosquitoes has the potential to reduce RVFV transmission to livestock and humans by interrupting the transmission cycles. Being able to reduce the number of infected adult mosquitoes able to transmit RVFV to livestock and humans and reducing the number of adult mosquitoes able to deposit eggs after a blood meal into immature habitats is critical to success [13]. Using the framework of IBM we found that mosquito life cycle features such as mosquito longevity (effects of vector senescence), gonotrophic cycle, flight behaviour and number of eggs each female lays per blood meal are critical for mosquito population fitness. Therefore, mosquito control efforts targeting these features can be effective adult mosquito control strategies that can effectively reduce their population regardless of either rainy or dry season. In addition to weather conditions the time when potential RVF vectors are active is an important factor when planing interventions.
Applying time dependent sensitivity analysis we found that the effect of some parameters (for example β_{21} and σ_1) change over time. This may be the case when after a certain period of time after the start of the outbreak, other modes of transmission such as livestock to livestock, livestock to human, etc, come into play. This suggests that it is important to also focus attention of control strategies on various infection agents during the course of an outbreak. Further preventive and control measures to mitigate the impact of RVF and reduce its transmission to domestic livestock and humans are discussed in detail in [13].

8.2.3 Livestock control

Unlike other diseases, RVF has no specific treatment. Therefore, efforts to reduce the impact of RVFV transmission in livestock rely on vector control and vaccination of livestock. Currently, two types of vaccines are available for domestic livestock: inactivated whole-virus and live-attenuated Smithburn vaccines [11, 27]. Inactivated vaccines can be applied to ruminants of all ages without causing abortions but they are expensive and repeated doses are required to provide sustained protection, which is difficult to achieve with nomadic herds. Also it is difficult to sustain this vaccine in affected countries for economic reasons. On the other hand, live-attenuated vaccines are cheap and effective. They confer lifelong immunity with a single dose. However, they may lead to fetal abnormalities and abortions in pregnant ruminants and there is the safety concern of reversion to virulence [78]. Therefore, other alternatives are required to help mitigate the impact of the disease in domestic livestock. Sensitivity analysis indicated that their initial number of susceptible livestock (N_2^0) is negatively correlated to R_0, meaning that increasing the size of livestock density that is vulnerable to the disease decreases the magnitude of R_0. This could mean that if livestock remain in herds of large numbers there is a high probability of reducing their vulnerability to infected biting mosquitoes. Thus, in addition to using the inactivated vaccine pastoralists can be advised to keep their herds is large groups. This control option and others including slaughter bans, livestock movement restrictions and vaccination, require pastoralist's cooperation [254].

Another important disease characteristic parameter is the duration of the infectious period in livestock. Our analysis showed that reduction in this parameter significantly reduce the spread of the disease. Thus, control efforts that would target the immune system of a host in order to keep the infectious period much shorter can significantly reduce the impact of RVF transmission. Concluding, RVF prevention and control measures should include active disease surveillance, an early warning system for outbreak predictions, targeted vaccinations in high-risk areas, improved coordination between livestock owners and public health teams and health education and social mobilization programs [13, 254].

8.3 Future Directions

The research presented in this thesis aimed to investigate the dynamics of RVF epidemic and inter-epidemic activities employing a variety of modelling approaches. The methods applied ranged from deterministic models, stochastic models to bottom up modelling techniques belonging to agent-based models. Each approach investigated a specific set of well-defined biological research questions across a variety of dimensions. In Chapter 2 [80] a systematic sensitivity analysis of the deterministic model was undertaken using the Partial Rank Correlation Coefficient (PRCC) technique. The time invariant sensitivity analysis was carried out by considering only one time point corresponding to the peak of the outbreak. Future work could consider not only extending the methods to include others such as Extended Fourier Amplitude Sensitivity Test (eFAST), but could also extend the analyses by considering other time points before and after the peak of the outbreak. This could allow to have estimates of the relative importance of each model parameter before the peak of the outbreak and after the effects of initial conditions have been discarded. Time varying sensitivity analysis could also be extended to include time points beyond the transient region.
While the following Chapters are an extension of the work presented in Chapter 2 there is still room for further work. The model structure in Chapter 4 could be extended to include juveniles stages of ticks and to include other biting insects other than mosquitoes, while Chapter 5 could be extended to consider comparison of the analytically predicted dominant period of disease outbreaks with data if they become available, by using techniques of wavelet analysis. Chapter 6 presented a holistic framework for studying the dynamics of vector-borne diseases under varying environmental conditions while taking into account individual's variability and interactions. In the current model mosquito larval habitats are all equal with differences in the depth of water-bodies. Future work may instead consider a heterogeneous spatial arrangement of the environment with detailed information about the landscape variables (topographic wetness index, soil type, land use-land cover, and distance to stream) [237]. With availability of this information it would be possible to embed Geographic Information System (GIS) capabilities with our model such that the model could run based on a real landscape. This could lead to further extension of the model by moving from local spatial scale to a much larger scale with detailed data of weather variables (temperature, precipitation, humidity)

and landscape variables of each local site. Such extensions could be useful for analysing the spatial distribution of abundance of RVF mosquitoes for instance at a scale of a country providing useful informative indicators for preventing and controlling disease outbreaks by providing specific guidance for a specific site. Further, studies focussing on the impacts of livestock movement and migration are to be explored to better evaluate the potential of the disease to invade temperate countries and North America, as well as its potential for expanding its geographical distribution at local scale in endemic countries.
In Chapter 7 the model in Chapter 6 was applied for studying disease inter-epidemic activities in livestock. Future applications could include implementation of hypothetical vector control interventions to target specific activities in the mosquito life cycle, then evaluate their impacts with the aim to improve disease control strategies. Further, the model could be extended to include demographic livestock details and detailed information underlying disease progress in both vector and host. Such a model could be useful for correlating abundance of mosquitoes and disease incidences providing a basis for predicting RVF outbreaks as well as evaluating other transmission mechanisms such as direct contact with infected livestock body fluids.

Another very interesting question would be to investigate the interplay between livestock recruitment (or movement) and *Aedes* vertical transmission mechanism in maintaining low level disease activities or small outbreaks after a major outbreak. If recruitment of susceptible susceptible livestock coincides with the next rainy season, this would lead to subsequent waves of disease outbreaks [1]. It would be interesting to extend the IBM model to include recruitment of susceptible livestock and investigate the role of recruitment timing on driving subsequent disease outbreaks. Could livestock births play a significant role in disease endemicity and appearance of subsequent waves of disease activities by introducing susceptible livestock into the system?

Appendix A

Model parameter descriptions and their values and ranges

	High Parameters		Low Parameters		
Parameters	**Baseline**	**Range**	**Baseline**	**Range**	**Reference**
$1/d_1$ & $1/b_1$	30	7-50	14	7-20	[57, 74]
$1/d_2$ & $1/b_2$	2190	360-3600	2190	360-3600	[69]
$1/d_3$ & $1/b_3$	30	7-50	14	7-20	[57, 74]
q_1	0.1	0-1	0.1	0-1	[161]
θ_1	0.20	0.1-0.3	0.10	0.1-0.3	Assumed
$1-\theta_2$	0.4	0.3-0.6	0.4	0.3-0.6	[5, 11, 255]
θ_3	0.20	0.1-0.3	0.20	0.1-0.3	Assumed
σ_1	0.33	0.1-0.5	0.25	0.1-0.5	[5, 91]
σ_2	19	0.1-50	19	0.1-50	[5]
σ_3	0.33	0.1-0.5	0.25	0.1-0.5	Assumed
β_{12}	0.7	0.3-0.9	0.7	0.3-0.9	[5, 11, 99]
β_{21}	0.21	0.001-0.54	0.21	0.001-0.54	[5, 11, 99]
β_{23}	0.21	0.001-0.54	0.21	0.001-0.54	Assumed
β_{32}	0.3	0.3-0.9	0.3	0.3-0.9	Assumed
$\tilde{\beta}_{12}$	0.3	0.1-0.5	0.3	0.1-0.5	[5, 11]
$\tilde{\beta}_{32}$	0.3	0.1-0.500	0.3	0.1-0.500	Assumed
$1/\gamma_1$	6	4-8	6	4-8	[69, 246]
$1/\gamma_3$	6	4-8	6	4-8	[69]
$1/\varepsilon_2$	4	1-7	4	1-7	[5, 91, 164, 255]
$1/\tilde{\varepsilon}_2$	4	1-7	4	1-7	[5, 57, 255]
m_2	0.2	0.05-0.3	0.1	0.05-0.3	[5, 57, 255]

TABLE A.1: Parameters for high and low rainfall patterns for the RVF model (2.1-2.3) with values, range and references.

Parameters	**Description and dimension**
b_1/μ_1	Per capita birth/death rate of *Aedes* mosquito species, Day^{-1}
b_2/μ_2	Per capita birth/death rate of livestock, Day^{-1}
b_3/μ_3	Per capita birth/death rate of *Culex* mosquito species, Day^{-1}
q_1	Probability of vertical transmission from an infectious female *Aedes* mosquito mother to its eggs, dimensionless
θ_a	Development rate of mosquitoes, Day^{-1}, where $a = 1$ and $a = 3$
θ_2	Probability of an infected host moving to the symptomatic stage, dimensionless
$(1 - \theta_2)$	Probability of an infected host moving to the asymptomatic stage, dimensionless
$\sigma_1,\ \sigma_3$	Number of times one *Aedes*, *Culex* mosquito would want to bite a host per Day, if livestock were freely available. This is a function of the mosquito's gonotrophic cycle (the amount of time a mosquito requires to produce eggs) and its preference for livestock blood, Day^{-1}
σ_2	The maximum number of mosquito bites a host can sustain per Day. This is a function of the host's exposed surface area, the efforts it takes to prevent mosquito bites (such as switching its tail), and any vector control interventions in place to kill mosquitoes encountering hosts or prevent bites, Day^{-1}
β_{2a}	Probability of transmission of infection from an infectious mosquito to a susceptible host given that a contact between the two occurs, dimensionless, where $a = 1$ and $a = 3$
β_{a2}	Probability of transmission of infection from an infectious host to a susceptible mosquito given that a contact between the two occurs, dimensionless, where $a = 1$ and $a = 3$
$\tilde{\beta}_{a2}$	Probability of transmission of infection from an asymptomatic host to a susceptible mosquito given that a contact between the two occurs, dimensionless
γ_a	Per capita rate of progression of mosquitoes from the exposed state to the infectious state, Day^{-1}. $1/\gamma_a$ is the average duration of the latent period, Days, where $a = 1$ and $a = 3$
ε_2	Per capita recovery rate for livestock from the infectious state to the recovered state, Day^{-1}. $1/\varepsilon_2$ is the average duration of the infectious period, Days
$\tilde{\varepsilon}_2$	Per capita recovery rate for livestock from the asymptomatic state to the recovered state. $1/\tilde{\varepsilon}_2$ is the average duration of the infectious asymptomatic period, Day^{-1}
m_2	Per capita disease-induced death rate for livestock, Day^{-1}

TABLE A.2: The parameters for the RVF model (2.1-2.3) and their dimensions

Appendix B

Computation of the basic reproduction number

B.1 Computation of the basic reproduction number in a non-periodic environment

First, we calculate the basic reproduction number for the vertical transmission route, $R_{0,V}$. For this case, the only compartments involved are the infected eggs, exposed adults, and infectious adults of the *Aedes* population. Thus we have, in the notation of reference [101],

$$\frac{d}{dt}\begin{pmatrix} U_1 \\ E_1 \\ I_1 \end{pmatrix} = F_v - V_v = \begin{pmatrix} 0 \\ 0 \\ \theta_1 U_1 \end{pmatrix} - \begin{pmatrix} \theta_1 U_1 - b_1 q_1 I_1 \\ \gamma_1 E_1 + d_1 \frac{E_1 N_1}{K_1} \\ d_1 \frac{I_1 N_1}{K_1} - \gamma_1 E_1 \end{pmatrix} \tag{B.1}$$

The corresponding Jacobian matrices at the disease free equilibrium of the above system are

$$F_v^0 = \begin{pmatrix} 0 & 0 & 0 \\ 0 & 0 & 0 \\ \theta_1 & 0 & 0 \end{pmatrix}, \quad V_v^0 = \begin{pmatrix} \theta_1 & 0 & -b_1 q_1 \\ 0 & \gamma_1 + \mu_1 & 0 \\ 0 & -\gamma_1 & \mu_1 \end{pmatrix} \tag{B.2}$$

The basic reproduction number for the vertical transmission is calculated as the spectral radius of the next generation matrix, $(F_v V_v^{-1})$

$$R_{0,V} = \frac{b_1 q_1}{\mu_1} = \frac{b_1 q_1 K_1}{d_1 N_1}.$$

Next, we calculate the horizontal transmission basic reproduction number, $R_{0,H}$. For this mode of transmission we must evaluate the exposed and infectious compartments of the *Aedes*, *Culex* and asymptomatic and infectious compartments of the livestock populations. To simplify the calculation of R_0, we transform our system to consider the percent of the population made up by each compartment,

$x_i = \frac{X_i}{N_i}$, where X_i is a compartment of population i,

$$\frac{d}{dt}\begin{pmatrix} e_1 \\ i_1 \\ a_2 \\ i_2 \\ e_3 \\ i_3 \end{pmatrix} = F_H - V_H = \begin{pmatrix} l_1\beta_{12}i_2N_2(1-e_1-i_1)+l_1\tilde{\beta}_{12}a_2N_2(1-e_1-i_1) \\ 0 \\ (1-\theta_2)l_1\beta_{21}i_1N_1(1-a_2-i_2-r_2)+(1-\theta_2)l_3\beta_{23}i_3N_3(1-a_2-i_2-r_2) \\ \theta_2 l_1\beta_{21}i_1N_1(1-a_2-i_2-r_2)+\theta_2 l_3\beta_{23}i_3N_3(1-a_2-i_2-r_2) \\ l_3\beta_{32}i_2N_2(1-e_3-i_3)+l_3\tilde{\beta}_{32}a_2N_2(1-e_3-i_3) \\ 0 \end{pmatrix} - \begin{pmatrix} (\gamma_1+d_1)e_1 \\ b_1i_1-\gamma_1e_1-\theta_1u_1 \\ (\tilde{\varepsilon}_2+d_2)a_2-m_2i_2a_2 \\ (\varepsilon_2+d_2+m_2)i_2-m_2(i_2)^2 \\ (\gamma_3+d_3)e_3 \\ b_3i_3-\gamma_3e_3 \end{pmatrix} \tag{B.3}$$

where $l_1 = \frac{\sigma_1\sigma_2}{\sigma_1N_1+\sigma_2N_2}$ and $l_3 = \frac{\sigma_3\sigma_2}{\sigma_3N_3+\sigma_2N_2}$.

The corresponding Jacobian matrices at the disease free equilibrium of the above system are:

$$F_H^0 = \begin{pmatrix} 0 & 0 & l_1^0\tilde{\beta}_{12}N_2^0 & l_1^0\beta_{12}N_2^0 & 0 & 0 \\ 0 & 0 & 0 & 0 & 0 & 0 \\ 0 & (1-\theta_2)l_1^0\beta_{21}N_1^0 & 0 & 0 & 0 & (1-\theta_2)l_3^0\beta_{23}N_3^0 \\ 0 & \theta_2 l_1^0\beta_{21}N_1^0 & 0 & 0 & 0 & \theta_2 l_3^0\beta_{23}N_3^0 \\ 0 & 0 & l_3^0\tilde{\beta}_{32}N_2^0 & l_3^0\beta_{32}N_2^0 & 0 & 0 \\ 0 & 0 & 0 & 0 & 0 & 0 \end{pmatrix},$$

$$V_H^0 = \begin{pmatrix} \gamma_1+b_1 & 0 & 0 & 0 & 0 & 0 \\ \gamma_1 & b_1 & 0 & 0 & 0 & 0 \\ 0 & 0 & \tilde{\varepsilon}_2+b_2 & 0 & 0 & 0 \\ 0 & 0 & 0 & \varepsilon_2+b_2+m_2 & 0 & 0 \\ 0 & 0 & 0 & 0 & \gamma_3+b_3 & 0 \\ 0 & 0 & 0 & 0 & -\gamma_3 & b_3 \end{pmatrix} \tag{B.4}$$

where $l_1^0 = \frac{\sigma_1\sigma_2}{\sigma_1N_1^0+\sigma_2N_2^0}$ and $l_3^0 = \frac{\sigma_3\sigma_2}{\sigma_3N_3^0+\sigma_2N_2^0}$.

The spectral radius of $F_H^0(V_H^0)^{-1}$ is given by:

$$R_{0,H} = \sqrt{\frac{(1-\theta_2)(l_3^0)^2\beta_{23}\tilde{\beta}_{32}\gamma_3N_2^0N_3^0}{b_3(\tilde{\varepsilon}_2+b_2)(\gamma_3+b_3)} + \frac{(1-\theta_2)(l_1^0)^2\beta_{21}\tilde{\beta}_{12}\gamma_1N_1^0N_2^0}{b_1(\tilde{\varepsilon}_2+b_2)(\gamma_1+b_1)} + \frac{\theta_2(l_3^0)^2\beta_{23}\beta_{32}\gamma_3N_2^0N_3^0}{b_3(\varepsilon_2+b_2+m_2)(\gamma_3+b_3)} + \frac{\theta_2(l_1^0)^2\beta_{21}\beta_{12}\gamma_1N_1^0N_2^0}{b_1(\varepsilon_2+b_2+m_2)(\gamma_1+b_1)}} \tag{B.5}$$

When strictly defined as the reproductive rate of the pathogen, R_0 for the overall model that accounts for both vertical infection and horizontal transmission is given by:

$$R_0 = \frac{b_1q_1}{2\mu_1} + \frac{1}{2}\sqrt{R_{0,V}^2 + 4R_{0,H}^2} \tag{B.6}$$

B.2 Computation of the basic reproduction number in a periodic environment

The concept behind the definition of R_0 in a periodic environment as the spectral operator on space of periodic functions is described below, and for more details see [103, 104].

For all $t \in R$ and $x \geq 0$, let $K(t,x)$ be a nonnegative $n \times n$ matrix. Assume

that $K(t,x)$ is a periodic function of t of period α for all $x \geq 0$. The idea behind the function $K(t,x)$ is an epidemic model with n "infected" compartments $(I_1, I_2, \cdots, I_n)$, which may be infectious or latent. The coefficient $K_{i,j}(t,x)$ in row i and column j represents the expected number of individuals in compartment I_i that one individual in compartment I_j "generates" at the beginning of an epidemic per unit time at time t if it has been in compartment I_j for x units of time. The verb 'generates' cover the case where individuals in compartment I_j infect individuals in compartment I_i, but also the case where individuals in compartment I_j just move to compartment I_i [104].

By linearising the system (3.1-3.3) near the disease-free equilibrium point

$$(\frac{b_1 N_1}{\theta_1}, 0, \frac{b_1 K_1}{d_1}, 0, 0, \frac{b_2 K_2}{d_2}, 0, 0, 0, \frac{b_3 N_3}{\theta_3}, \frac{b_3 K_3}{d_3}, 0, 0)$$

we have:

$$\begin{aligned}
\dot{U}_1(t) &= b_{s1}(t) q_1 I_1 - \theta_1 U_1 \\
\dot{E}_1(t) &= \frac{\sigma_1\sigma_2\beta_{12}}{\sigma_1 N_1 + \sigma_2 N_2} I_2 S_1^0 + \frac{\sigma_1\sigma_2\tilde{\beta}_{12}}{\sigma_1 N_1 + \sigma_2 N_2} A_2 S_1^0 - (\gamma_1 - d_1 \frac{N_1}{K_1}) E_1 \\
\dot{I}_1(t) &= \gamma_1 E_1 + \theta_1 U_1 - d_1 \frac{I_1 N_1}{K_1}, \\
\dot{A}_2(t) &= (1-\theta_2) \frac{\sigma_1\sigma_2\beta_{21}(t)}{\sigma_1 N_1 + \sigma_2 N_2} I_1 S_2^0 + (1-\theta_2) \frac{\sigma_3\sigma_2\beta_{23}(t)}{\sigma_3 N_3 + \sigma_2 N_2} I_3 S_2^0 - (\tilde{\varepsilon}_2 - d_2 \frac{N_2}{K_2}) A_2 \\
\dot{I}_2(t) &= \theta_2 \frac{\sigma_1\sigma_2\beta_{21}(t)}{\sigma_1 N_1 + \sigma_2 N_2} I_1 S_2^0 + \theta_2 \frac{\sigma_3\sigma_2\beta_{23}(t)}{\sigma_3 N_3 + \sigma_2 N_2} I_3 S_2^0 - (\varepsilon_2 + m_2 + d_2 \frac{N_2}{K_2}) I_2 \\
\dot{E}_3(t) &= \frac{\sigma_3\sigma_2\beta_{32}}{\sigma_3 N_3 + \sigma_2 N_2} I_2 S_3^0 + \frac{\sigma_3\sigma_2\tilde{\beta}_{32}}{\sigma_3 N_2 + \sigma_2 N_2} A_2 S_3^0 - (\gamma_3 + d_3 \frac{N_3}{K_3}) E_3 \\
\dot{I}_3(t) &= \gamma_3 E_3 - d_3 \frac{I_3 N_3}{K_3},
\end{aligned} \tag{B.7}$$

The transmissibility number $\bar{R}_0$ is defined through the spectral radius of a linear integral operator on a space of periodic functions, thus the operator $K(t,x)$ is given by:

$$\begin{pmatrix}
0 & 0 & b_1 q_1 e^{-\mu_1 x} & 0 & 0 & 0 & 0 \\
0 & 0 & 0 & l_1^0 \tilde{\beta}_{12} S_1^0 e^{-v_1 x} & l_1^0 \beta_{12} S_1^0 e^{-v_2 x} & 0 & 0 \\
\theta_1 e^{-\theta_1 x} & \gamma_1 e^{-v_3 x} & 0 & 0 & 0 & 0 & 0 \\
0 & 0 & (1-\theta_2) l_1^0 \beta_{21} S_2^0 e^{-\mu_1 x} & 0 & 0 & 0 & (1-\theta_2) l_3^0 \beta_{23} S_2^0 e^{-\mu_3 x} \\
0 & 0 & \theta_2 l_1^0 \beta_{21} S_2^0 e^{-\mu_1 x} & 0 & 0 & 0 & \theta_2 l_3^0 \beta_{23} S_2^0 e^{-\mu_3 x} \\
0 & 0 & 0 & l_3^0 \tilde{\beta}_{32} S_3^0 e^{-v_1 x} & l_3^0 \beta_{32} S_3^0 e^{-v_2 x} & 0 & 0 \\
0 & 0 & 0 & 0 & 0 & \gamma_3 e^{-v_4 x} & 0
\end{pmatrix} \tag{B.8}$$

where $v_1 = (\tilde{\varepsilon}_2 + \mu_2),\ v_2 = (\tilde{\varepsilon}_2 + m_2 + \mu_2), v_3 = (\gamma_1 + \mu_1),\ v_4 = (\gamma_3 + \mu_3)$.
Thus the integral operator G_j gives:

$$\begin{aligned}
G_j = & \frac{b_1 q_1}{\mu_1 + 2\pi j i} \bullet \frac{\theta_1}{\theta_1 + 2\pi j i} + \frac{\gamma_1}{\gamma_1 + \mu_1 + 2\pi j i} \bullet \frac{(l_1^0)^2 \beta_{21} S_2^0 S_1^0}{\mu_1 + 2\pi j i} \left[\frac{(1-\theta_2)\tilde{\beta}_{12}}{\tilde{\varepsilon}_2 + \mu_2 + 2\pi j i} + \frac{\theta_2 \beta_{12}}{\varepsilon_2 + m_2 + \mu_2 + 2\pi j i} \right] \\
& + \frac{\gamma_3}{\gamma_3 + \mu_3 + 2\pi j i} \bullet \frac{(l_3^0)^2 \beta_{23} S_3^0 S_2^0}{\mu_3 + 2\pi j i} \left[\frac{(1-\theta_2)\tilde{\beta}_{32}}{\tilde{\varepsilon}_2 + \mu_2 + 2\pi j i} + \frac{\theta_2 \beta_{32}}{\varepsilon_2 + m_2 + \mu_2 + 2\pi j i} \right]
\end{aligned} \tag{B.9}$$

Appendix C

Basic reproduction number, Stability analysis and Parameter values

C.1 Computation of the basic reproduction number

To compute the analytical expression of R_0, we express the model equations (4.1-4.4) in vector form as the difference between the rate of new infection in compartment i, $\mathcal{F}_i$ and the rate of transfer between compartment i and all other compartments due to other processes, $\mathcal{V}_i$ [101]. In this settings only disease compartments are involved in the computation of the next-generation operator, which are: *Aedes* infected eggs U_1, *Aedes* exposed and infectious adults, infectious livestock, *Culex* exposed and infectious adults and the infectious compartments of tick populations with respect to their attachment status. Thus, the corresponding system in matrix form is

$$\begin{pmatrix} \dot{U_1} \\ E_1 \\ I_1 \\ I_2 \\ E_3 \\ I_3 \\ I_a \\ I_d \end{pmatrix} = \mathcal{F}_i - \mathcal{V}_i = \begin{pmatrix} \mu_1 q_1 I_1 \\ g_1 I_2 S_1 \\ 0 \\ g_3 I_1 S_2 + g_4 I_3 S_2 + \beta_{2t} I_a S_2 \\ g_5 I_2 S_3 \\ 0 \\ \beta_{t2} I_2 S_a \\ 0 \end{pmatrix} - \begin{pmatrix} \theta_1 U_1 \\ (\gamma_1 + \mu_1) E_1 \\ \mu_1 I_1 - \gamma_1 E_1 - \theta_1 U_1 \\ (\varepsilon_2 + m_2 + \mu_2) I_2 \\ (\gamma_3 + \mu_3) E_3 \\ \mu_3 I_3 - \gamma_3 E_3 \\ \delta N_2 I_a - \frac{\alpha N_2 I_d}{1+S_a+I_a} \\ \frac{\alpha N_2 I_d}{1+S_a+I_a} + d_t I_d - \delta N_2 I_a \end{pmatrix}, \tag{C.1}$$

where $g_1 = \dfrac{\sigma_1 \sigma_2 \beta_{12}}{\sigma_1 A_0 + \sigma_2 L_0}$, $g_3 = \dfrac{\sigma_1 \sigma_2 \beta_{21}}{\sigma_1 A_0 + \sigma_2 L_0}$, $g_4 = \dfrac{\sigma_3 \sigma_2 \beta_{23}}{\sigma_3 C_0 + \sigma_2 L_0}$ and $g_5 = \dfrac{\sigma_3 \sigma_2 \beta_{32}}{\sigma_3 C_0 + \sigma_2 L_0}$.

The corresponding Jacobian matrices at the disease free equilibrium of the above

system are:

$$F = \begin{pmatrix} 0 & 0 & \mu_1 q_1 & 0 & 0 & 0 & 0 & 0 \\ 0 & 0 & 0 & g_1 S_1^0 & 0 & 0 & 0 & 0 \\ 0 & 0 & 0 & 0 & 0 & 0 & 0 & 0 \\ 0 & 0 & 0 & g_3 S_2^0 & 0 & 0 & g_4 S_2^0 & \beta_{2t} S_2^0 \quad 0 \\ 0 & 0 & 0 & g_5 S_3^0 & 0 & 0 & 0 & 0 \\ 0 & 0 & 0 & 0 & 0 & 0 & 0 & 0 \\ 0 & 0 & 0 & \beta_{t2} S_a & 0 & 0 & 0 & 0 \\ 0 & 0 & 0 & 0 & 0 & 0 & 0 & 0 \end{pmatrix},$$

$$V = \begin{pmatrix} \theta_1 & 0 & 0 & 0 & 0 & 0 & 0 & 0 \\ 0 & \gamma_1 + \mu_1 & 0 & 0 & 0 & 0 & 0 & 0 \\ -\theta_1 & -\gamma_1 & \mu_1 & 0 & 0 & 0 & 0 & 0 \\ 0 & 0 & 0 & \varepsilon_2 + m_2 + \mu_2 & 0 & 0 & 0 & 0 \\ 0 & 0 & 0 & 0 & \gamma_3 + \mu_3 & 0 & 0 & 0 \\ 0 & 0 & 0 & 0 & -\gamma_3 & \mu_3 & 0 & 0 \\ 0 & 0 & 0 & 0 & 0 & 0 & \delta N_2 & -\frac{\alpha N_2}{1+S_a^0} \\ 0 & 0 & 0 & 0 & 0 & 0 & -\delta N_2 & \frac{\alpha N_2}{1+S_a^0} + dt \end{pmatrix}. \tag{C.2}$$

C.2 Global stability analysis

To check whether matrix $D - CA^{-1}B$ is Metzler stable we repeat lemma 4.3. In our case we have,

$$A = \begin{pmatrix} -(\gamma_3 + \mu_3) & 0 \\ 0 & -\mu_3 \end{pmatrix}, B = \begin{pmatrix} \frac{(\mu_1 - \mu_1 q_1)(\gamma_1 + \mu_1) g_5 \bar{S}_3 \beta_{2t} \bar{S}_2}{1 - R_0^1} & 0 \\ 0 & 0 \end{pmatrix},$$

$$C = \begin{pmatrix} 0 & \frac{(\mu_1 - \mu_1 q_1)(\gamma_1 + \mu_1) \beta_{t2} \bar{S}_a g_4 \bar{S}_2}{1 - R_0^1} \\ 0 & 0 \end{pmatrix}, D = \begin{pmatrix} -\delta N_2 + \frac{(\mu_1 - \mu_1 q_1)(\gamma_1 + \mu_1) \beta_{t2} \bar{S}_a \beta_{2t} \bar{S}_2}{1 - R_0^1} & 0 \\ \delta N_2 & -\frac{\delta N_2}{1 + \bar{S}_a} - d_t \end{pmatrix}.$$

Clearly, A is a Metzler stable matrix and $D - CA^{-1}B = D$, which is a stable Metzler matrix if $\left(-\delta N_2 + \frac{(\mu_1 - \mu_1 q_1)(\gamma_1 + \mu_1) \beta_{t2} \bar{S}_a \beta_{2t} \bar{S}_2}{1 - R_0^1}\right) \times \left(-\frac{\delta N_2}{1 + \bar{S}_a} - d_t\right) \geq 0$.

C.3 Model parameter values

Parameter	Baseline	Range	Reference
β_{t2}	0.03	0.001-0.05	Assumed
β_{2t}	0.0125	0.005-0.02	Assumed
α	0.165	0.03-0.5	Assumed
δ	0.275	0.05-0.5	Assumed
b_t	0.05	0.01-0.1	Assumed
d_t	0.01	0.01-0.1	Assumed

TABLE C.1: Parameters for the RVF model for high rainfall and moderate temperature (wet season) for equations (4.1-4.4) with baseline values, range and references. Details of other model parameters are given in Table A.1 in Appendix A.

Appendix D

Stochastic Processes and Analysis

D.1 Forces of Infection Approximation

Following the approach in Chitnis et al [5] we derive disease forces of infection. Let α_1 be the rate at which a mosquito would bite a ruminant, defined as a function of its gonotrophic cycle. Let also α_2 be the maximum number o bites a particular ruminant can sustain per unit time. Thus, $\alpha_1 N_1$ gives the total number of bites that a mosquito would achieve per unit time and $\alpha_2 N_2$ gives the availability of livestock. Assuming that the total number of mosquito-livestock contacts is defined as half the harmonic mean of $\alpha_1 N_1$ and $\alpha_2 N_2$,

$$a = a(N_1, N_2) = \frac{\alpha_1 N_1 \alpha_2 N_2}{\alpha_1 N_1 + \alpha_2 N_2}. \tag{D.1}$$

Hence, the number of bites per livestock per unit time and the number of bites per mosquito per unit time can be defined as

$$a_2 = a_2(N_1, N_2) = a(N_1, N_2)/N_2 = \frac{\alpha_1 \alpha_2 N_1}{\alpha_1 N_1 + \alpha_2 N_2}, \tag{D.2}$$

$$a_1 = a_1(N_1, N_2) = a(N_1, N_2)/N_1 = \frac{\alpha_1 \alpha_2 N_2}{\alpha_1 N_1 + \alpha_2 N_2}, \tag{D.3}$$

respectively. Therefore, the force of infection from mosquitoes to livestock, λ_{21}, can be defined as the product of the number of mosquito bites that a ruminant can sustain per unit time, a_2, the probability of successful infection transmission from an infected mosquito to a susceptible ruminant, β_{21}, and the prevalence of infectious mosquitoes,I_1/N_1. Then, λ_{21} is given as follows,

$$\lambda_{21} = \beta_{21} \frac{\alpha_1 \alpha_2 N_1}{\alpha_1 N_1 + \alpha_2 N_2} \frac{I_1}{N_1}. \tag{D.4}$$

The force of infection from livestock to mosquitoes, λ_{12}, can be defined as a product of the number of livestock bites one mosquito has per unit time, a_1, the probability of successful infection transmission from n infected ruminant to a susceptible

mosquito, β_{12}, and the prevalence of the disease in livestock, I_2/N_2. Then, λ_{12} is given as follows,

$$\lambda_{12} = \beta_{12}\frac{\alpha_1\alpha_2 N_2}{\alpha_1 N_1 + \alpha_2 N_2}\frac{I_2}{N_2}. \tag{D.5}$$

These forces of infections assume in principle that the total number of mosquito-livestock bites depend on the size of both population species. This formalism implies that both species contributes to the structure of contact rates mainly driven by the ratio mosquitoes to livestock and livestock availability to mosquitoes. However, if we are interested in the situation where mosquitoes bite hosts at a constant rate distributed uniformly among all hosts within an area, we obtain a frequency-dependent transmission mechanism with respect to the host population [21]. Thus, the above forces of infections λ_{21} and λ_{12} can be collapsed into simplified versions, by changing the contact structure,

$$a = a(N_1, N_2) = \frac{\alpha_1 N_1 \alpha_2 N_2}{\alpha_1 N_1 + \alpha_2 N_2} = \frac{\alpha_1\alpha_2 N_1}{\alpha_1(N_1/N_2) + \alpha_2}. \tag{D.6}$$

Since, we are interested on forces of infections in which contact rates or biting rates are expected to be constant irrespective of the number of available hosts, then it is reasonable to find the approximation as N_2 tends to infinity. That is,

$$a' = \lim_{N_2\to\infty} a' = \lim_{N_2\to\infty} \frac{\alpha_1\alpha_2 N_1}{\alpha_1(N_1/N_2) + \alpha_2} = \alpha_1 N_1. \tag{D.7}$$

Hence, the corresponding number of bites per livestock per unit time is then given by $a_2' = a'/N_2 = \alpha_1 N_1/N_2 = \alpha_1 m_0$, where m_0 is the ratio female mosquitoes to livestock. Similarly, the mosquito biting rate, that is, the number of bites per unit time is given by $a_1' = a'/N_1 = \alpha_1$. Denoting, $\alpha_1 = \alpha$, yield the following standard forces of infections for mosquito transmitted diseases, $\lambda_{21}' = \beta_{21}\alpha m_0 \frac{I_1}{N_1}$ and $\lambda_{12}' = \beta_{12}\alpha\frac{I_2}{N_2}$.

D.2 Stochastic Processes

D.2.1 Branching process approximation

Branching processes play a fundamental role in epidemic theory, underpinning our understanding of the threshold behaviour of epidemics and the calculation of both probability of disease extinction and invasion, while providing a simple way for modelling the spread of an infection at early stages of the epidemic [150, 256]. In multi-type branching process, individuals in the population are categorised into a finite number of types and each individual behaves independently. An individual of given type can produce offspring of possibly all types and individuals of the same type have the same offspring distribution [173, 174]. Given that infectious hosts and infectious vectors are the only sources of infection, the branching process is applied only to these infectious groups keeping the susceptibles at disease-free steady state

[257]. Infectious vectors produce infected host when they bite a susceptible animal as well as infected vector through vertical transmission. Infectious hosts produce infected vectors when bitten by susceptible vector. Therefore, the number of infectives in the host-vector system during the early stages of the epidemic process is approximated by a two type branching process. Here infectious vectors are of type 1 and infectious hosts are of type 2. Note that first we consider the host-vector dynamics then later the vector-vector transmission.

D.2.2 Disease threshold conditions

Using the theory of multitype branching processes we have approximated the nonlinear stochastic model near the disease-free equilibrium (DFE). With this approximation we can now derive an estimate for the probability of disease extinction or a major outbreak after introduction of a single infective individual. Recall that we have two types of infective individuals: type 1 infective vectors and type 2 infective animals. Let $\{X_{ij}, i, j = 1, 2\}$ be the number of infectives of type j produced by an infective of type i and $m_{ij} = E[X_{ij}]$. We now derive the offspring distributions and expected numbers for the approximating branching process.
An infectious *Aedes* mosquito produces at most one single infectious host, but no other offspring, hence $X_{11} \equiv 0$. While on the ground an infectious *Aedes* either dies at rate μ_1 before surviving the intrinsic incubation period that is exponentially distributed with intensity γ_1, thus $P(X_{12} = 0) = \frac{\mu_1}{\gamma_1+\mu_1}$. Or the infected *Aedes* mosquito survives the intrinsic incubation period with probability $\frac{\gamma_1}{\gamma_1+\mu_1}$ and infects a susceptible host according to a Poisson process with intensity $\frac{\alpha_1\alpha_2\beta_{21}}{\alpha_1 N_1+\alpha_2 N_2}$ within a period of time $T_1 = \frac{1}{\mu_1}$, since a mosquito once infected remains infected throughout its lifespan. For mathematical tractability this intermediate stage (incubation period) is not accounted for in this study.
Here we make the simplifying assumption that the number of infectious *Aedes* mosquitoes is very small, that is $I_1 = 1$.
Conditioning on T_1, the *Aedes* mosquito lifespan, the expected number of susceptible hosts that are infected before this period ends is

$$\begin{aligned} E[X_{12}] &= E(E[X_{12}|T_1]) = E\left(\tfrac{\alpha_1\alpha_2\beta_{21}}{\alpha_1 N_1+\alpha_2 N_2} S_2^0 T_1\right) = \tfrac{\alpha_1\alpha_2\beta_{21}}{\alpha_1 N_1+\alpha_2 N_2} S_2^0 E[T_1] \\ &= \tfrac{\alpha_1\alpha_2\beta_{21}}{\alpha_1 N_1+\alpha_2 N_2} S_2^0 \tfrac{1}{\mu_1} \end{aligned} \tag{D.8}$$

Next, an infectious host produces one infected *Aedes* mosquito if bitten by susceptible *Aedes* mosquito, hence $X_{22} \equiv 0$. A host is infectious for a time period that is exponentially distributed with intensity $\epsilon_2 + \mu_2$ (either it dies naturally at rate μ_2 or it recovers at the rate ϵ_2). During this period it infects susceptible *Aedes* according to a Poisson process with intensity $\frac{\alpha_1\alpha_2\beta_{12}}{\alpha_1 N_1+\alpha_2 N_2}$. Here we make the simplifying assumption that the number of infectious host is very small, that is $I_2 = 1$.
Thus, conditioning on $T_2 = \epsilon_2 + \mu_2$, the length of infectious period of a host, the

expected number of susceptible *Aedes* that are infected before this period ends is

$$\begin{aligned} E[X_{21}] &= E(E[X_{21}|T_2]) = E\left(\tfrac{\alpha_1\alpha_2\beta_{12}}{\alpha_1N_1+\alpha_2N_2}S_1^0T_2\right) = \tfrac{\alpha_1\alpha_2\beta_{12}}{\alpha_1N_1+\alpha_2N_2}S_1^0E[T_2] \\ &= \tfrac{1}{\epsilon_2+\mu_2}\tfrac{\alpha_1\alpha_2\beta_{12}}{\alpha_1N_1+\alpha_2N_2}S_1^0. \end{aligned} \tag{D.9}$$

Let $\{m_{ij}\}_{ij=1}^2$ be the expected matrix of the form

$$M = \begin{pmatrix} 0 & \frac{\alpha_1\alpha_2\beta_{21}}{\alpha_1N_1+\alpha_2N_2}S_2^0\frac{1}{\mu_1} \\ \frac{1}{\epsilon_2+\mu_2}\frac{\alpha_1\alpha_2\beta_{12}}{\alpha_1N_1+\alpha_2N_2}S_1^0 & 0 \end{pmatrix} \tag{D.10}$$

If the largest real-valued eigenvalue of M is less than or equal to unity, the epidemic dies out fairly quickly, while if the largest real-valued eigenvalue of M is greater than unity, there is a positive probability that the epidemic will take off [174].
The eigenvalues of M are the roots of the characteristic polynomial of matrix M. Since M is a regular matrix, it has all positive entries, then M has a positive eigenvalue λ that is larger than any other eigenvalue, which is given by

$$\lambda = \sqrt{\frac{\alpha_1\alpha_2\beta_{21}}{\alpha_1N_1+\alpha_2N_2}S_2^0\frac{1}{\mu_1}\frac{1}{\epsilon_2+\mu_2}\frac{\alpha_1\alpha_2\beta_{12}}{\alpha_1N_1+\alpha_2N_2}S_1^0} \tag{D.11}$$

$R_{0,H} = \sqrt{R_{21}R_{12}}$ is the horizontal basic reproduction number, $R_{12} = \frac{1}{\epsilon_2+\mu_2}\frac{\alpha_1\alpha_2\beta_{12}}{\alpha_1N_1+\alpha_2N_2}S_1^0$ is the number of new infections in *Aedes* mosquitoes generated by single infected livestock and $R_{21} = \frac{\alpha_1\alpha_2\beta_{21}}{\alpha_1N_1+\alpha_2N_2}S_2^0\frac{1}{\mu_1}$ is the number of new infections in livestock generated by single infected *Aedes* mosquito.
Since we are interested in the case where the largest eigenvalue is greater than unity, then $\lambda > 1$ implies that $\lambda^2 > 1$. This yields the following: $R_{0,H} = R_{21}R_{12}$.
We now relax the above assumption about transovarial transmission in *Aedes* mosquito species. Infectious female *Aedes* may infect their offspring during their life time which is exponentially distributed with intensity d_1, with the proportion q_1b_1, hence the $P(X_{11} > 1) = q_1b_1$ and the expected number of infected *Aedes* mosquitoes produced by a parent is

$$m_{11} = E[X_{11}] = \frac{q_1b_1}{\mu_1} = q_1 \tag{D.12}$$

since at early stage of the epidemic the system is at equilibrium. Now, the threshold Γ can be written as

$$\Gamma = \frac{q_1}{2} + \frac{1}{2}\sqrt{q_1^2 + R_{0,H}^2} \tag{D.13}$$

Γ is the threshold quantity when the system is in equilibrium at the time of disease introduction. From equation (D.13) we notice that Γ has a monotonic dependence on all model parameters. When $\Gamma \leq 1$, the epidemic dies out fairly quickly since the probability of extinction is one and when $\Gamma > 1$, the epidemic may take off in the system and has a chance of becoming endemic since there is a positive probability of infection survival.

D.2.3 Probability of a major outbreak and disease extinction

With branching process theory we know that the likelihood of invasion depends not only on the average number of secondary infections (i.e. R_0), but also on their distribution [150]. Let the probability generating function of the offspring distribution of infectives produced by an infective of type $i(i = 1, 2)$, be $G_i(s) = E[\prod_{j=1}^{2} s_j^{X_{ij}}]$, where X_{ij} is as defined in the previous section and $s = (s_1, s_2)$.
The probability that a minor outbreak of the disease occurs given that there are a_j infectives initially of each of the two types is $\pi = \pi_1^{a_1}\pi_2^{a_2}$. Since M is irreducible, we know that $\pi_1 = \pi_2$ if $\Gamma \leq 1$ or that $\varphi(\pi_1, \pi_2)$ is the unique root of $s = G(s)$ that satisfies $\pi_1 < 1$ and $\pi_2 < 1$ if $\Gamma > 1$.
Since $X_{11} \equiv 0$ in the horizontal transmission and X_{12} is Poisson distributed conditioned on the infectious period $T_1 = t$ (as explained in the previous section), the probability generating function of offspring produced by one infected *Aedes* mosquito is

$$\begin{aligned} G_1(s) &= E[s_1^{X_{11}} s_2^{X_{12}}] = \textstyle\sum_x s_2^x P(X_{12} = x) = \sum_x s_2^x \int_0^\infty \mu_1 e^{-\mu_1 t} \frac{e^{-g_3 N_2 t}(g_3 N_2 t)^x}{x!} dt \\ &= \mu_1 \textstyle\int_0^\infty e^{-(\mu_1 + g_3 N_2)t} \left\{ \sum_{x=0}^\infty \frac{(g_3 N_2 s_2 t)^x}{x!} \right\} dt = \mu_1 \int_0^\infty e^{-(\mu_1 + g_3 N_2)t} e^{g_3 N_2 s_2 t} dt \\ &= \tfrac{\mu_1}{\mu_1 + g_3 N_2 - g_3 N_2 s_2} = \tfrac{1}{1 + R_{21}(1 - s_2)} \end{aligned} \tag{D.14}$$

Now in the presence of vertical transmission, that is, $X_{22} \neq 0$ and applying formula (4.8) in [150] we obtain that

$$G_1(s) = E[s_1^{X_{11}} s_2^{X_{12}}] = \frac{1}{1 + R_{11}(1 - s_1) + R_{21}(1 - s_2)}. \tag{D.15}$$

As $X_{22} \equiv 0$ and X_2 is Poisson distributed conditioned on the infectious period $T_2 = t$, the probability generating function of *Aedes* offspring produced by one infectious host is

$$\begin{aligned} G_2^1(s) &= E[s_1^{X_{21}}] = \textstyle\sum_x s_1^x P(X_{21} = x) \\ &= \textstyle\sum_x s_1^x \int_0^\infty (\epsilon_2 + \mu_2) e^{-(\epsilon_2 + \mu_2)t} \frac{e^{-g_2 N_1 t}[g_2 N_1 t]^x}{x!} dt \\ &= (\epsilon_2 + m_2 + \mu_2) \textstyle\int_0^\infty e^{-[\epsilon_2 + \mu_2 + g_2 N_1]t} \left\{ \sum_{x=0}^\infty \frac{[g_2 N_1 s_1 t]^x}{x!} \right\} dt \\ &= (\epsilon_2 + \mu_2) \textstyle\int_0^\infty e^{-[\epsilon_2 + \mu_2 + g_2 N_1]t} e^{g_2 N_1 s_1 t} dt \\ &= \tfrac{\epsilon_2 + \mu_2}{\epsilon_2 + \mu_2 + g_2 N_1 - g_2 N_1 s_1} = \tfrac{1}{1 + R_{12}(1 - s_1)} \end{aligned} \tag{D.16}$$

In order to solve for extinction probabilities and probabilities of a major outbreak, we need to find the solution of the following system of two equations

$$G_1(s_1, s_2) = s_1 \texttt{ and } G_2(s_1, s_2) = s_2. \tag{D.17}$$

Given that we have a two-step life cycle from one type to another and then back to the original [150], the generating functions can be written as a composition function of the two single step generating functions [258]. Therefore, instead of

solving equations (D.17) we solve the following equations:

$$G_1(G_2(s_1)) = s_1 \text{ and } G_2(G_1(s_1, s_2)) = s_2. \tag{D.18}$$

The vector $(s_1, s_2) = (1, 1)$ is always a solution. If $\Gamma \leq 1$ it is the only solution, whereas if $\Gamma > 1$ there are another solutions with all the components of the vector less than 1 [259], thus, the extinction probabilities are given by $\pi_i = min\{1, s_i\}$ for $i = 1, 2$.

D.3 Analytical Analysis of the Stochastic Model

In this appendix we present an elegant mathematical formulation of the stochastic dynamics due to van Kampen's [157] system-size expansion method. In the first part we present the details of the mean-field version of the stochastic model. In the second part, the details of the calculation of the power spectral density from a stochastic Fokker-Planck equation. Then, stability analysis of the fixed points of the derived deterministic model.

The deterministic limit

First we write the master equation (5.4) in its generalized form Detailed expansion about the master equation (5.4) is

$$\begin{aligned}
&\tfrac{dP(s_2,i_2,i_1;t)}{dt} = \\
&T(s_2, i_2, i_1|s_2 + 1, i_2 - 1, i_1)P(s_2 + 1, i_2 - 1, i_1; t) + T(s_2, i_2, i_1|s_2, i_2, i_1 - 1)P(s_2, i_2, i_1 - 1; t) \\
&+T(s_2, i_2, i_1|s_2 - 1, i_2, i_1)P(s_2 - 1, i_2, i_1; t) + T(s_2, i_2, i_1|s_2 + 1, i_2, i_1)P(s_2 + 1, i_2, i_1; t) \\
&+T(s_2, i_2, i_1|s_2, i_2, i_1 + 1)P(s_2, i_2, i_1 + 1; t) + T(s_2, i_2, i_1|s_2, i_2 + 1, i_1)P(s_2, i_2 + 1, i_1; t) \\
&-[T(s_2 - 1, i_2 + 1, i_1|s_2, i_2, i_1) + T(s_2, i_2, i_1 + 1|s_2, i_2, i_1) + T(s_2 + 1, i_2, i_1|s_2, i_2, i_1) \\
&+T(s_2 - 1, i_2, i_1|s_2, i_2, i_1) + T(s_2, i_2, i_1 - 1|s_2, i_2, i_1) + T(s_2, i_2 - 1, i_1|s_2, i_2, i_1)]P(s_2, i_2, i_1; t).
\end{aligned} \tag{D.19}$$

This gives a complete description of the time evolution of the temporal model, from which we can obtain the deterministic analogues [169]. Following the notation and elaboration in [146], a straight forward way is to multiply (D.19) by s_2, i_2 and i_1 in turn and subsequently to sum over all allowed values of s_2, i_2 and i_1, and to take all the boundary values zero [169]. This gives equations for the mean $S_2 = \langle s_2 \rangle$, $I_2 = \langle i_2 \rangle$ and $I_1 = \langle i_1 \rangle$. For $S_2 = \langle s_2 \rangle = \sum_{s_2,i_2=0}^{N_2} \sum_{i_1=0}^{N_1} s_2 P(s_2, i_2, i_1; t)$, the mean-field theory takes the form

$$\begin{aligned}
&\tfrac{dS_2}{dt} = \tfrac{d\langle s_2 \rangle}{dt} = \\
&\sum_{s_2,i_2=0}^{N_2} \sum_{i_1=0}^{N_1} T(s_2 + 1, i_2, i_1|s_2, i_2, i_1)P(s_2, i_2, i_1; t) \\
&- \sum_{s_2,i_2=0}^{N_2} \sum_{i_1=0}^{N_1} [T(s_2 - 1, i_2 + 1, i_1|s_2, i_2, i_1) + T(s_2 - 1, i_2, i_1|s_2, i_2, i_1)]P(s_2, i_2, i_1; t)
\end{aligned} \tag{D.20}$$

A similar way gives the equations for $I_2 = \langle i_2 \rangle$ and $I_1 = \langle i_1 \rangle$:

$$\frac{dI_2}{dt} = \frac{d\langle i_2 \rangle}{dt} = \tag{D.21}$$

$$\sum_{s_2,i_2=0}^{N_2} \sum_{i_1=0}^{N_1} [T(s_2 - 1, i_2 + 1, i_1 | s_2, i_2, i_1) - T(s_2, i_2 - 1, i_1 | s_2, i_2, i_1)] P(s_2, i_2, i_1; t) \tag{D.22}$$

and

$$\frac{dI_1}{dt} = \frac{d\langle i_1 \rangle}{dt} = \tag{D.23}$$

$$\sum_{s_2,i_2=0}^{N_2} \sum_{i_1=0}^{N_1} [T(s_2, i_2, i_1 + 1 | s_2, i_2, i_1) - T(s_2, i_2, i_1 - 1 | s_2, i_2, i_1)] P(s_2, i_2, i_1; t) \tag{D.24}$$

Given the derived equations (D.20)-(D.24), we now take the mean-field limits, $N_1, N_2 \to \infty$, which allows us to take the replacement $\langle i_1 s_2 \rangle = \langle i_1 \rangle \langle s_2 \rangle$ and $\langle i_2 (N_1 - i_1) \rangle = \langle i_2 \rangle \langle N_1 - i_1 \rangle$ [146, 169]. When applying the following fractional variables

$$\phi_1 = \lim_{N_2 \to \infty} \frac{S_2}{N_2}, \quad \phi_2 = \lim_{N_2 \to \infty} \frac{I_2}{N_2}, \quad \psi = \lim_{N_1 \to \infty} \frac{I_1}{N_1} \tag{D.25}$$

yield the following set of deterministic equations:

$$\begin{aligned} \tfrac{d\phi_1}{dt} &= -\beta_{21} \alpha' m_0 \psi \phi_1 + \mu_2 (1 - \phi_1), \\ \tfrac{d\phi_2}{dt} &= \beta_{21} \alpha' m_0 \psi \phi_1 - (\epsilon_2 + \mu_2) \phi_2, \\ \tfrac{d\psi}{dt} &= \beta_{12} \alpha' \phi_2 (1 - \psi) + \mu_1 q_1 \psi - \mu_1 \psi. \end{aligned} \tag{D.26}$$

D.3.1 The system-size expansion and analysis of the fluctuations

van Kampen's system expansion method [157], is an appropriate technique for characterizing disease fluctuations in order to investigate the effects of stochasticity in our model and for finding stochastic corrections to the resulting deterministic equations for large N_1 and N_2 [169]. To do so, we transform the stochastic discrete variables $\sigma = (s_2, i_2, i_1)$ to depend into new stochastic variables $\zeta = (x_1, x_2, x_3)$ as follows:

$$\begin{aligned} s_2 &= N_2 \phi_1 + \sqrt{N_2} x_1, \\ i_2 &= N_2 \phi_2 + \sqrt{N_2} x_2, \\ i_1 &= N_1 \psi + \sqrt{N_1} x_3. \end{aligned}$$

Then, the probability distribution $P(s_2, i_2, i_1; t)$ is now written as a function of the new variables x_1, x_2, x_3 as follows:

$$\frac{dP}{dt} = \frac{\partial \Pi}{\partial t} - \sqrt{N_2}\frac{d\phi_1}{dt}\frac{\partial \Pi}{\partial x_1} - \sqrt{N_2}\frac{d\phi_2}{dt}\frac{\partial \Pi}{\partial x_2} - \sqrt{N_1}\frac{d\psi}{dt}\frac{\partial \Pi}{\partial x_3}. \tag{D.27}$$

Before going further, we introduce an operator in the following form

$$\varepsilon_{\zeta}^{\pm 1} = 1 \pm \frac{1}{\sqrt{N_2}}\frac{\partial}{\partial \zeta} + \frac{1}{2N_2}\frac{\partial^2}{\partial \zeta^2},$$

which yield the following step operators [157, 169],

$$\begin{aligned}
\varepsilon_{s_2}^{\pm 1} f(s_2, i_2, i_1) &= f(s_2 \pm 1, i_2, i_1), \\
\varepsilon_{i_2}^{\pm 1} f(s_2, i_2, i_1) &= f(s_2, i_2 \pm 1, i_1), \\
\varepsilon_{i_1}^{\pm 1} f(s_2, i_2, i_1) &= f(s_2, i_2, i_1 \pm 1),
\end{aligned}$$

which are then used to rewrite the master equation (D.19) with transition rates of equations (5.1-5.2) as

$$\begin{aligned}
&\tfrac{dP(s_2,i_2,i_1;t)}{dt} = \\
&[(\varepsilon_{s_2}\varepsilon_{i_2}^{-1} - 1)T(s_2 - 1, i_2 + 1, i_1 | s_2, i_2, i_1) + (\varepsilon_{i_1}^{-1} - 1)T(s_2, i_2, i_1 + 1 | s_2, i_2, i_1) \\
&+(\varepsilon_{s_2}^{-1} - 1)T(s_2 + 1, i_2, i_1 | s_2, i_2, i_1) + (\varepsilon_{s_2} - 1)T(s_2 - 1, i_2, i_1 | s_2, i_2, i_1) \\
&+(\varepsilon_{i_1} - 1)T(s_2, i_2, i_1 - 1 | s_2, i_2, i_1) + (\varepsilon_{i_2} - 1)T(s_2, i_2 - 1, i_1 | s_2, i_2, i_1)]P(s_2, i_2, i_1; t) \\
&= \Big\{(\varepsilon_{s_2}\varepsilon_{i_2}^{-1} - 1)\beta_{21}\alpha' m_0 i_1 s_2 + (\varepsilon_{i_1}^{-1} - 1)[\beta_{12}\alpha' i_2(N_1 - i_1) + \mu_1 q_1 i_1] \\
&+(\varepsilon_{s_2}^{-1} - 1)\mu_2 N_2 + (\varepsilon_{s_2} - 1)\mu_2 s_2 + (\varepsilon_{i_2} - 1)(\epsilon_2 + \mu_2) i_2 + (\varepsilon_{i_1} - 1)\mu_1 i_1 \Big\} P(s_2, i_2, i_1; t).
\end{aligned} \tag{D.28}$$

Expanding the step operators $\varepsilon_{s_2}^{\pm 1}$ and $\varepsilon_{i_2}^{\pm 1}$ in a power series in $N_2^{-1/2}$, $\varepsilon_{i_1}^{\pm 1}$ in $N_1^{-1/2}$, respectively,

$$\begin{aligned}
\varepsilon_{s_2}^{\pm 1} &= 1 \pm \frac{1}{\sqrt{N_2}}\frac{\partial}{\partial x_1} + \frac{1}{2N_2}\frac{\partial^2}{\partial x_1^2}, \\
\varepsilon_{i_2}^{\pm 1} &= 1 \pm \frac{1}{\sqrt{N_2}}\frac{\partial}{\partial x_2} + \frac{1}{2N_2}\frac{\partial^2}{\partial x_2^2}, \\
\varepsilon_{i_1}^{\pm 1} &= 1 \pm \frac{1}{\sqrt{N_1}}\frac{\partial}{\partial x_3} + \frac{1}{2N_1}\frac{\partial^2}{\partial x_3^2},
\end{aligned}$$

and then substituting these operators into equation (D.28), we get

$$\begin{aligned}
&\frac{dP}{dt} = \\
&\Bigg\{ \left[\left(1 + \frac{1}{\sqrt{N_2}}\frac{\partial}{\partial x_1} + \frac{1}{2N_2}\frac{\partial^2}{\partial x_1^2}\right)\left(1 - \frac{1}{\sqrt{N_2}}\frac{\partial}{\partial x_2} + \frac{1}{2N_2}\frac{\partial^2}{\partial x_2^2}\right) - 1 \right] \beta_{21}\alpha' m_0 i_1 s_2 \\
&+ \left(-\frac{1}{\sqrt{N_1}}\frac{\partial}{\partial x_3} + \frac{1}{2N_1}\frac{\partial^2}{\partial x_3^2}\right)\left[\beta_{12}\alpha' i_2(N_1 - i_1) + \mu_1 q_1 i_1\right] + \left(-\frac{1}{\sqrt{N_2}}\frac{\partial}{\partial x_1} + \frac{1}{2N_2}\frac{\partial^2}{\partial x_1^2}\right)\mu_2 N_2 \\
&+ \left(\frac{1}{\sqrt{N_2}}\frac{\partial}{\partial x_1} + \frac{1}{2N_2}\frac{\partial^2}{\partial x_1^2}\right)\mu_2 s_2 + \left(\frac{1}{\sqrt{N_2}}\frac{\partial}{\partial x_2} + \frac{1}{2N_2}\frac{\partial^2}{\partial x_2^2}\right)(\epsilon_2 + \mu_2) i_2 \\
&+ \left(\frac{1}{\sqrt{N_1}}\frac{\partial}{\partial x_3} + \frac{1}{2N_1}\frac{\partial^2}{\partial x_3^2}\right)\mu_1 i_1 \Bigg\} \Pi(x_1, x_2, x_3; t).
\end{aligned} \tag{D.29}$$

Then, expanding Eq.D.29 and ignoring higher order terms and drawing a comparison of which with equation (D.27) order by order yields the so-called macroscopic equations

$$\frac{d\phi}{dt} = f_1(\phi_1, \phi_2, \psi), \qquad \frac{d\phi_2}{dt} = f_2(\phi_1, \phi_2, \psi), \qquad \frac{d\psi}{dt} = (\phi_1, \phi_2, \psi), \tag{D.30}$$

to leading order, where

$$\begin{aligned}
f_1(\phi_1, \phi_2, \psi) &= -\beta_{21}\alpha' m_0 \psi\phi_1 + \mu_2(1 - \phi_1), \\
f_2(\phi_1, \phi_2, \psi) &= \beta_{21}\alpha' m_0 \psi\phi_1 - (\epsilon_2 + \mu_2)\phi_2, \\
f_3(\phi_1, \phi_2, \psi) &= \beta_{12}\alpha'\phi_2(1 - \psi) + \mu_1 q_1 \psi - \mu_1 \psi,
\end{aligned} \tag{D.31}$$

which are indeed the equations (D.26). The next-to-leading order gives rise to a Fokker-Planck equation for the fluctuation variables x_1, x_2, x_3

$$\frac{\partial \Pi}{\partial t} = -\sum_{k,l=1}^{3} A_{kl}\frac{\partial(x_l \Pi)}{\partial x_k} + \frac{1}{2}\sum_{k,l=1}^{3} B_{kl}\frac{\partial^2 \Pi}{\partial x_k \partial x_l}. \tag{D.32}$$

To obtain the coefficients A_{kl} and B_{kl} we expand the equation (D.32) and draw comparison order by order with equation (D.29). Since we are interested in fluctuations about the endemic equilibrium point $E^* = (\phi_1^*, \phi_2^*, \psi^*)$ defined in equation (D.26) of the deterministic model, both matrix $\mathcal{A} = (A_{kl})_{3\times 3}$ and $\mathcal{B} = (B_{kl})_{3\times 3}$ are evaluated at this fixed point, whose explicit form are found to be

$$\mathcal{A} = \begin{pmatrix} \frac{\partial f_1}{\partial \phi_1} & 0 & \sqrt{1/m_0}\frac{\partial f_1}{\partial \psi} \\ \frac{\partial f_2}{\partial \phi_1} & \frac{\partial f_2}{\partial \phi_2} & \sqrt{1/m_0}\frac{\partial f_2}{\partial \psi} \\ 0 & \sqrt{m_0}\frac{\partial f_3}{\partial \phi_2} & \frac{\partial f_3}{\partial \psi} \end{pmatrix}_{\phi_1=\phi_1^*, \phi_2=\phi_2^*, \psi=\psi^*} \quad \text{and } \mathcal{B} = \begin{pmatrix} B_{11} & B_{12} & 0 \\ B_{21} & B_{22} & 0 \\ 0 & 0 & B_{33} \end{pmatrix}_{\phi_1=\phi_1^*, \phi_2=\phi_2^*, \psi=\psi^*} \tag{D.33}$$

with

$$\begin{aligned}
B_{11} &= \beta_{21}\alpha' m_0 \psi\phi_1 + \mu_2(1 + \phi_1), \\
B_{12} &= B_{21} = -2\beta_{21}\alpha' m_0 \psi\phi_1, \\
B_{22} &= \beta_{21}\alpha' m_0 \psi\phi_1 + (\epsilon_2 + \mu_2)\phi_2, \\
B_{33} &= \beta_{12}\alpha'\phi_2(1 - \psi) + \mu_1 q_1 \psi + \mu_1 \psi.
\end{aligned}$$

D.3.2 Power spectral calculation and its peak

To calculate the power spectra of the fluctuations around the stationary state, we have to make a Fourier analysis, so it is first essential to formulate a set of Langevin equations of the stochastic variables $x_k(t), (k = 1, 2, 3)$. The Langevin equations corresponding to equation (D.32) are

$$\frac{dx_k}{dt} = \sum_{l=1}^{3} A_{kl}x_l + \xi_k(t), \quad (k, l = 1, 2, 3) \tag{D.34}$$

which are three differential equations describing the stochastic behaviour of the model at large but finite N. The variables $x_l(l = 1, 2, 3)$ are stochastic corrections to the deterministic variables s_2, i_2, i_1, and $\xi_k(t)(k = 1, 2, 3)$ are Gaussian white noises with zero mean and a correlation function given by

$$\langle \xi_k(t)\xi_l(t')\rangle = B_{kl}\delta(t - t').$$

Taking the temporal Fourier transform $\tilde{x}_k(\omega) = \int_{-\infty}^{\infty} e^{-i\omega t}x_k(t)dt$ of (D.34) gives

$$-i\omega\tilde{x}_k(\omega) = \sum_{l=1}^{3} A_{kl}\tilde{x}_l(\omega) + \tilde{\xi}_k(\omega), \quad (k, l = 1, 2, 3) \tag{D.35}$$

with

$$\langle \tilde{\xi}_k(\omega)\tilde{\xi}_l(\omega')\rangle = B_{kl}(2\pi)\delta(\omega + \omega').$$

Actually, this Fourier transform is a system with three coupled linear algebraic equations which can be used to obtain a closed form expression for the power spectra. Therefore, solving equation (D.35), we obtain

$$\begin{aligned}
\tilde{x}_1(\omega) &= \tfrac{(A_{23}A_{32}-A_{22}A_{33})\tilde{\xi}_1-A_{13}A_{32}\tilde{\xi}_2+A_{13}A_{22}\tilde{\xi}_3+\omega^2\tilde{\xi}_1+i\omega[-(A_{22}+A_{33})\tilde{\xi}_1+A_{13}\tilde{\xi}_3]}{\mathcal{D}(\omega)},\\
\tilde{x}_2(\omega) &= \tfrac{A_{21}A_{33}\tilde{\xi}_1-A_{11}A_{33}\tilde{\xi}_2+(A_{11}A_{23}-A_{21}A_{13})\tilde{\xi}_3+\omega^2\tilde{\xi}_2+i\omega[A_{21}\tilde{\xi}_1-(A_{11}+A_{33})\tilde{\xi}_2+A_{23}\tilde{\xi}_3]}{\mathcal{D}(\omega)},\\
\tilde{x}_3(\omega) &= \tfrac{A_{21}A_{32}\tilde{\xi}_1+A_{11}A_{32}\tilde{\xi}_2-A_{11}A_{22}\tilde{\xi}_3+\omega^2\tilde{\xi}_3+i\omega[A_{32}\tilde{\xi}_2-(A_{11}+A_{22})\tilde{\xi}_3]}{\mathcal{D}(\omega)}
\end{aligned} \tag{D.36}$$

where the denominator $\mathcal{D}$ is given by

$$\begin{aligned}
\mathcal{D}(\omega) &= (i\omega)^3 + tr\mathcal{A}(i\omega)^2 + \Theta(i\omega) + det\mathcal{A},\\
tr\mathcal{A} &= A_{11} + A_{22} + A_{33},\\
\Theta &= A_{11}A_{22} + A_{11}A_{33} + A_{22}A_{33} - A_{23}A_{32},\\
det\mathcal{A} &= A_{11}A_{22}A_{33} - A_{11}A_{23}A_{32} + A_{21}A_{13}A_{32}.
\end{aligned}$$

Averaging the squared moduli of $\tilde{x}_k(k=1,2,3)$ gives the power-spectra of variables S_2, I_2 and I_1:

$$\begin{aligned} P_{S_2}(\omega) &= \langle|\tilde{x}_1(\omega)|^2\rangle = \frac{B_{11}\omega^4+\Gamma_{S_2}\omega^2+\chi_{S_2}}{|\mathcal{D}(\omega)|^2}, \\ P_{I_2}(\omega) &= \langle|\tilde{x}_2(\omega)|^2\rangle = \frac{B_{22}\omega^4+\Gamma_{I_2}\omega^2+\chi_{I_2}}{|\mathcal{D}(\omega)|^2}, \\ P_{I_1}(\omega) &= \langle|\tilde{x}_3(\omega)|^2\rangle = \frac{B_{33}\omega^4+\Gamma_{I_1}\omega^2+\chi_{I_1}}{|\mathcal{D}(\omega)|^2}, \end{aligned} \tag{D.37}$$

where

$$\begin{aligned} |\mathcal{D}(\omega)|^2 &= (\omega^3-\Theta\omega)^2+(det\mathcal{A}-tr\mathcal{A}\omega^2)^2, \\ \chi_{S_2} &= (A_{23}A_{32}-A_{22}A_{33})^2B_{11}-2A_{13}A_{32}(A_{23}A_{32}-A_{22}A_{33})B_{12}+(A_{13}A_{32})^2B_{22} \\ &\quad +(A_{13}A_{22})^2B_{33}, \\ \Gamma_{S_2} &= 2(A_{23}A_{32}-A_{22}A_{33})B_{11}-2A_{13}A_{32}B_{12}+(A_{22}+A_{33})^2B_{11}+A_{13}^2B_{33}, \\ \chi_{I_2} &= (A_{21}A_{33})^2B_{11}+(A_{11}A_{33})^2B_{22}+(A_{11}A_{23}-A_{21}A_{13})^2B_{33}-2A_{11}A_{21}A_{33}^2B_{12}, \\ \Gamma_{I_2} &= 2A_{21}A_{33}B_{12}-2A_{11}A_{33}B_{22}+A_{21}^2B_{11}-2A_{21}(A_{11}+A_{33})B_{12}+(A_{11}+A_{33})^2B_{22} \\ &\quad +A_{32}^2B_{33}, \\ \chi_{I_1} &= (A_{21}A_{32})^2B_{11}+(A_{11}A_{32})^2B_{22}+(A_{11}A_{22})^2B_{33}+2A_{11}A_{21}A_{32}^2B_{12}, \\ \Gamma_{I_1} &= A_{32}^2B_{22}+(A_{11}+A_{22})^2B_{33}-2A_{11}A_{22}B_{33}. \end{aligned}$$

By using these methods, we can analytically predict the epidemic outbreaks and fade-outs on a certain disease, as done for several childhood diseases [149].

D.4 Stability analysis of fixed points E^0 and E^* of system (D.26)

First, we give the stability analysis of the disease-free equilibria $E^0=(1,0,0)$, the Jacobian matrix of which is given by

$$J^0=\begin{bmatrix} -\mu_2 & 0 & -a \\ 0 & -g & a \\ 0 & b & -\mu_1(1-q_1) \end{bmatrix} \tag{D.38}$$

where $a=\beta_{21}\alpha' m_0,\quad b=\beta_{12}\alpha',\quad g=\epsilon_2+\mu_2$.
From the first column of the Jacobian matrix (D.38) we observe that the matrix has the eigenvalue $\lambda_1=\mu_2$, and the remaining eigenvalues will be derived from the reduced 2×2 Jacobian matrix $J_1^0=\left[\begin{smallmatrix} -g & a \\ b & -\mu_1(1-q_1) \end{smallmatrix}\right]$, from which we obtain the trace, $tr(J_1^0)=-g-\mu_1(1-q_1)$, which is negative and its determinant is $det(J_1^0)=g\mu_1(1-q_1)-ab$.
Since for local stability it is sufficient to have $tr(J_1^0)<0$ and $det(J_1^0)>0$, so for determinant to be positive, we need to show that $g\mu_1(1-q_1)-ab>0$, that is $1-\frac{ab}{g\mu_1(1-q_1)}>0$. Thus, $\frac{ab}{g\mu_1(1-q_1)}<1$, which is the condition for basic reproduction number, i.e., $R_0<1$, and $R_0=\frac{1}{1-q_1}\frac{\beta_{21}\alpha' m_0}{\mu_1}\frac{\beta_{12}\alpha'}{\epsilon_2+\mu_2}$.
Second, the stability analysis of the endemic equilibria $E^*=(\phi_1^*,\phi_2^*,\psi^*)$, with

$\phi_1^* = \frac{\mu_2 R_0 + a}{(a+\mu_2)R_0}$, $\phi_2^* = \frac{\mu_1\mu_2(1-q_1)(R_0-1)}{b(a+\mu_2)}$, $\psi^* = \frac{\mu_1\mu_2 g(1-q_1)(R_0-1)}{a(b\mu_2+\mu_1 g(1-q_1))}$.
The Jacobian matrix at E^* is

$$J^* = \begin{bmatrix} -\frac{a\mu_2(R_0-1)}{fh} - \mu_2 & 0 & -\frac{af}{bl} \\ \frac{a\mu_2(R_0-1)}{fh} & -g & \frac{af}{bl} \\ 0 & b\left(1 - \frac{\mu_2(R_0-1)}{fh}\right) & -\frac{b\mu_2(R_0-1)}{lm} - \mu_1(1-q_1) \end{bmatrix}$$

with $f = b\mu_2 + \mu_1 g(1-q_1)$, $m = \frac{1}{1-q_1}\frac{b}{\mu_1}$, $h = \frac{1}{1-q_1}\frac{a}{g}$ and $l = a + \mu_2$.
The characteristic polynomial of Jacobian matrix J^* is written as cubic polynomial about λ denoted as $P(\lambda)$:

$$P(\lambda) = \lambda^3 + A\lambda^2 + B\lambda + C, \tag{D.39}$$

all of the coefficients of which are

$$A = \frac{fhb\mu_2(R_0-1) + fhlm\mu_1(1-q_1) + lma\mu_2(R_0-1) + lmgfh + lmfh\mu_2}{lmfh} > 0 \text{ for } R_0 > 1,$$

$$\begin{aligned} B = \frac{1}{lmfh}[&amf\mu_2(R_0-1) + bgfh\mu_2(R_0-1) + ab\mu_2^2(R_0^2-2R_0) + bfh\mu_2^2(R_0-1) + ab\mu_2^2 \\ &+ lmgfh(1-q_1) + alm\mu_1\mu_2(R_0-1)(1-q_1) + lmfh\mu_1\mu_2(1-q_1)lmag\mu_2(R_0-1) \\ &+ glmfh\mu_2] > 0 \quad \text{for} \quad R_0 > 1, \end{aligned}$$

$$\begin{aligned} C = \frac{\mu_2}{lmfh}\{&gab\mu_2(R_0^2-2R_0) + bgfh\mu_2(R_0-1) + glma\mu_1(R_0-1)(1-q_1) \\ &+ lmgfh\mu_1(1-q_1) + amf[\mu_2(R_0-1) - fh]\}. \end{aligned}$$

$C > 0$ if and only if $R_0 > 1$, given that $\psi^* > 0$. Here $A > 0, B > 0$ and $C > 0$ for $R_0 > 1$. Thus equation (D.39) has no root which is positive or zero (Descartes' rule of sign). The equation (D.39) will only have negative roots or complex roots with negative real part if $AB - C > 0$ according to the (Routh-Hurwitz criteria). Thus the system is stable about the interior equilibrium point E^* whenever it exists and $AB - C > 0$.

Appendix E

Host reproduction number approximation

The well known critical epidemiological parameter in terms of disease spread and control is the basic reproduction number, R_0. This threshold condition gives the average number of secondary cases produced by a single infective individual during the course of his infectious period in an entirely susceptible population. The value of this parameter results from the product of three factors: number of susceptible individuals, transmission rate and infectious period of the infective individual. From this definition one can easily pick up the relation between R_0 and the number of initial susceptible individuals such that R_0 can be estimated from the final size of the epidemic [248].
Since the progress of infection in livestock can be approximated by an *SIR* model describing a closed system without vital dynamics, then the average dynamics of the system can be approximated by the following equations:

$$\begin{array}{l} \frac{dX}{dt} = \frac{-\beta SI}{N}, \\ \frac{dY}{dt} = \frac{\beta SI}{N} - \gamma I, \\ \frac{dZ}{dt} = \gamma I, \end{array} \tag{E.1}$$

where X, Y `and` Z correspond to S, I `and` R which represent the fraction of susceptible, infected and recovered respectively. The parameters β, γ represent the transmission and recovery rates. Given that the total population of livestock is constant, then Z can be obtained when X and Y are known. In this setting equation (E.1) reduces to

$$\begin{array}{l} \frac{dX}{dt} = \frac{-\beta SI}{N}, \\ \frac{dY}{dt} = \frac{\beta SI}{N} - \gamma I. \end{array} \tag{E.2}$$

From the latter, if we divide the second equation by the first we then obtain $\frac{dY}{dX} = -1 + \frac{N}{R_0 X}$, which we can integrate w.r.t X to yield

$$X(0) - X(\infty) + \frac{N}{R_0} ln \frac{X(\infty)}{X(0)} = Y(\infty) - Y(0) = 0. \tag{E.3}$$

If $X(0) = N$, the $N - X(\infty)$ is the final size of the outbreak and the fraction of ultimately infected individuals is given by $f = 1 - \frac{X(\infty)}{N}$ such that

$$R_0 = -\frac{ln(1-f)}{f}. \tag{E.4}$$

Bibliography

[1] R M Murithi, P Munyua, P M Ithondeka, J M Macharia, A Hightower, E T Luman, R F Breiman, and M Kariuki Njenga. Rift Valley fever in Kenya: history of epizootics and identification of vulnerable districts. *Epidemiology and Infection*, 139(3):372–380, 2011. ISSN 0950-2688. doi: 10.1017/S0950268810001020.

[2] Nicolaas J. Pienaar and Peter N. Thompson. Temporal and spatial history of Rift Valley fever in South Africa : 1950 to 2011. *Onderstepoort Journal of Veterinary Research*, 80:1–13, 2013. ISSN 0030-2465. doi: 10.4102/ojvr.v80i1.384.

[3] Calvin Sindato, Esron D. Karimuribo, Dirk U. Pfeiffer, Leonard E G Mboera, Fredrick Kivaria, George Dautu, Bett Bernard, and Janusz T. Paweska. Spatial and temporal pattern of rift valley fever outbreaks in Tanzania; 1930 to 2007. *PLOS ONE*, 9(2), 2014. ISSN 19326203. doi: 10.1371/journal.pone.0088897.

[4] Sansao A Pedro, Shirley Abelman, Frank T Ndjomatchoua, Rosemary Sang, and Henri E Z Tonnang. Stability, bifurcation and chaos analysis of vector-borne disease model with application to rift valley Fever. *PLOS ONE*, 9(10): e108172, 2014. ISSN 1932-6203. doi: 10.1371/journal.pone.0108172. URL http://dx.plos.org/10.1371/journal.pone.0108172.

[5] Nakul Chitnis, James M. Hyman, and Carrie A. Manore. Modelling vertical transmission in vector-borne diseases with applications to Rift Valley fever. *Journal of Biological Dynamics*, 7:11–40, 2013. ISSN 1751-3758. doi: 10.1080/17513758.2012.733427.

[6] L M Rueda, K J Patel, R C Axtell, and R E Stinner. Temperature-dependent development and survival rates of Culex quinquefasciatus and Aedes aegypti (Diptera: Culicidae). *Journal of Medical Entomology*, 27(5):892–898, 1990. ISSN 0022-2585.

[7] V Chevalier, S de la Rocque, T Baldet, L Vial, and F Roger. Epidemiological processes involved in the emergence of vector-borne diseases: West Nile fever, Rift Valley fever, Japanese encephalitis and Crimean-Congo haemorrhagic fever. *Revue scientifique et technique (International Office of Epizootics)*, 23 (2):535–555, 2004. ISSN 0253-1933.

[8] Karl M Rich and Francis Wanyoike. An assessment of the regional and national socio-economic impacts of the 2007 Rift Valley fever outbreak in Kenya. *The American Journal of Tropical Medicine and Hygiene*, 83(2 Suppl): 52–57, 2010. ISSN 1476-1645. doi: 10.4269/ajtmh.2010.09-0291.

[9] Véronique Chevalier, Renaud Lancelot, Yaya Thiongane, Baba Sall, Amadou Diaité, and Bernard Mondet. Rift Valley Fever in small ruminants, Senegal, 2003. *Emerging Infectious Diseases*, 11:1693–1700, 2005. ISSN 10806040. doi: 10.3201/eid1111.050193.

[10] Hanan H. Balkhy and Ziad A. Memish. Rift Valley fever: An uninvited zoonosis in the Arabian peninsula. *International Journal of Antimicrobial Agents*, 21(2):153–157, 2003. ISSN 09248579. doi: 10.1016/S0924-8579(02) 00295-9.

[11] Michel Pepin, Michèle Bouloy, Brian H. Bird, Alan Kemp, and Janusz Paweska. Rift Valley fever virus (Bunyaviridae: Phlebovirus): An update on pathogenesis, molecular epidemiology, vectors, diagnostics and prevention. *Veterinary Research*, 41(6), 2010. ISSN 09284249. doi: 10.1051/vetres/ 2010033.

[12] Sara Moutailler, Ghazi Krida, Francis Schaffner, Marie Vazeille, and Anna-Bella Failloux. Potential vectors of Rift Valley fever virus in the Mediterranean region. *Vector borne and zoonotic diseases (Larchmont, N.Y.)*, 8(6):749–753, 2008. ISSN 1557-7759. doi: 10.1089/vbz.2008.0009.

[13] Assaf Anyamba, Kenneth J. Linthicum, Jennifer Small, Seth C. Britch, Edwin Pak, Stephane De La Rocque, Pierre Formenty, Allen W. Hightower, Robert F. Breiman, Jean Paul Chretien, Compton J. Tucker, David Schnabel, Rosemary Sang, Karl Haagsma, Mark Latham, Henry B. Lewandowski, Salih Osman Magdi, Mohamed Ally Mohamed, Patrick M. Nguku, Jean Marc Reynes, and Robert Swanepoel. Prediction, assessment of the Rift Valley fever activity in east and southern Africa 2006-2008 and possible vector control strategies. *American Journal of Tropical Medicine and Hygiene*, 83(2 SUPPL.):43–51, 2010. ISSN 00029637. doi: 10.4269/ajtmh.2010.09-0289.

[14] A Desiree LaBeaud, Yoshitsugu Ochiai, C J Peters, Eric M Muchiri, and Charles H King. Spectrum of Rift Valley fever virus transmission in Kenya: insights from three distinct regions. *The American Journal of Tropical Medicine and Hygiene*, 76(5):795–800, 2007. ISSN 0002-9637.

[15] Bruce Hannon and Matthias Ruth. *Dynamic Modeling of Diseases and Pests*, volume VIII. 2009. doi: 10.1007/978-0-387-09560-8.

[16] WHO. Vector-Borne Diseases Fact Sheet 387, 2014. *World Health Organization, Media Centre*, 2014. Accessed 19/01/2016. doi: http://www.who.int/ mediacentre/factsheets/fs387/en/.

[17] D. J. Gubler. Resurgent vector-borne diseases as a global health problem. *Emerging Infectious Diseases*, 4(3):442–450, 1998. ISSN 1080-6040. doi: 10.3201/eid0403.980326.

[18] Maia Martcheva and Olivia Prosper. Unstable dynamics of vector-borne diseases: Modeling through delay-differential equations. In Vadrevu Sree Hari Rao and Ravi Durvasula, editors, *Dynamic Models of Infectious Diseases*, pages 43–75. Springer New York, 2013. ISBN 978-1-4614-3960-8. doi: 10.1007/978-1-4614-3961-5_2. URL http://dx.doi.org/10.1007/978-1-4614-3961-5_2.

[19] Calvin Sindato, Esron Karimuribo, and E.G. Mboera. The epidemiology and socio-economic impact of Rift Valley fever epidemics in Tanzania: A review. *Journal of Veterinary Research*, 79(2), 2012. ISSN 0030-2465. doi: 10.4102/ojvr.v79i2.467.

[20] Jeffrey C. Glaubitz, Terry M Casstevens, Fei Lu, James Harriman, Robert J. Elshire, Qi Sun, Edward S. Buckler, and et al. Wright. Diseases of humans and their domestic mammals: pathogen characteristics, host range and the risk of emergence. *Proceedings. Biological sciences / The Royal Society*, 11(2):629–37, 2010. ISSN 0962-8452. doi: 10.1016/j.tree.2006.08.001. URL http://www.ncbi.nlm.nih.gov/pubmed/21239391$\delimiter"026E30F$nhttp://doi.wiley.com/10.1002/zoo.1430050212$\delimiter"026E30F$nhttp://www.ncbi.nlm.nih.gov/pubmed/20847747$\delimiter"026E30F$nhttp://rspb.royalsocietypublishing.org/content/early/2010/09/29/rspb.2010.1920.full$\delimiter"026E30F$nhttp://link.springer.com/10.1007/s10592-009-0006-y$\delimiter"026E30F$nhttp://www.ncbi.nlm.nih.gov/pubmed/18007600$\delimiter"026E30F$nhttp://www.ncbi.nlm.nih.gov/pubmed/14635837$\delimiter"026E30F$nhttp://www.ncbi.nlm.nih.gov/pubmed/11112176$\delimiter"026E30F$nhttp://www.ncbi.nlm.nih.gov/pubmed/22008237$\delimiter"026E30F$nhttp://rstb.royalsocietypublishing.org/content/356/1411/9.

[21] Matthew James Keeling and Pejman Rohani. *Modeling Infectious Diseases in Humans and Animals*, volume 47. 2007. ISBN ISBN: 9781400841035. doi: ISBN:978-0-691-11617--4. URL http://www.modelinginfectiousdiseases.org/.

[22] Fangling Xu, Dongying Liu, Marcio R T Nunes, Amelia P A Travassos Da Rosa, Robert B. Tesh, and Shu Yuan Xiao. Antigenic and genetic relationships among Rift Valley fever virus and other selected members of the genus phlebovirus (Bunyaviridae). *American Journal of Tropical Medicine and Hygiene*, 76(6):1194–1200, 2007. ISSN 00029637. doi: 76/6/1194[pii].

[23] P. G. Jupp, A. Kemp, A. Grobbelaar, P. Leman, F. J. Burt, A. M. Alahmed, D. Al Mujalli, M. Al Khamees, and R. Swanepoel. The 2000 epidemic of Rift Valley fever in Saudi Arabia: Mosquito vector studies. *Medical and Veterinary Entomology*, 16(3):245–252, 2002. ISSN 0269283X. doi: 10.1046/j.1365-2915.2002.00371.x.

[24] Raphaëlle Métras, Lisa M Collins, Richard G White, Silvia Alonso, Véronique Chevalier, Christine Thuranira-McKeever, and Dirk U Pfeiffer. Rift Valley

fever epidemiology, surveillance, and control: what have models contributed? *Vector Borne and Zoonotic Diseases (Larchmont, N.Y.)*, 11(6):761–771, 2011. ISSN 1557-7759. doi: 10.1089/vbz.2010.0200.

[25] F G Davies. Observations on the epidemiology of Rift Valley fever in Kenya. *The Journal of Hygiene*, 75(2):219–230, 1975. ISSN 0022-1724. doi: 10.1017/S0022172400047252.

[26] F. Nchu and A. Rand. Rift valley fever outbreaks: Possible implication of hyalomma truncatum (acari: Ixodidae). *Afr. J. Microbiol. Res.*, 7(30): 3891–3894, 2013. URL DOI:10.5897/AJMR12.2144.

[27] F Glyn Davies and Vincent Martin. Recognizing Rift Valley Fever. *Veterinaria Italiana*, 42:31–53, 2006. ISSN 1828-1427. URL http://www.ncbi.nlm.nih.gov/pubmed/20429078.

[28] K. J. Linthicum, T. M. Logan, C. L. Bailey, D. J. Dohm, and J. R. Moulton. Transstadial and horizontal transmission of Rift Valley fever virus in Hyalomma truncatum. *American Journal of Tropical Medicine and Hygiene*, 41 (4):491–496, 1989. ISSN 00029637.

[29] Didier Fontenille, M. Traore-Lamizana, M. Diallo, J. Thonnon, J. P. Digoutte, and H. G. Zeller. New vectors of Rift Valley fever in West Africa. *Emerging Infectious Diseases*, 4(2):289–293, 1998. ISSN 10806040. doi: 10.3201/eid0402.980218.

[30] The Foreign Animal Disease Preparedness and Response Plan (FAD PReP). Disease response strategy: Rift valley fever. 2013. URL www.aphis.usda.gov/animal-health/emergency-management/downloads/ppr-rvf-disease-strategy.pdf.

[31] D. Fontenille, M. Traore-Lamizana, H. Zeller, M. Mondo, M. Diallo, and J. P. Digoutte -. Short report: Rift valley fever in Western Africa: Isolations from Aedes mosquitoes during an interepizootic period. *American Journal of Tropical Medicine and Hygiene*, 52(5):403–404, 1995. ISSN 00029637.

[32] Gear J, De Meillon B, Le Roux AF, Kofsky R, Innes RR, Steyn JJ, Oliff WD, and Schulz KH. Rift valley fever in south africa; a study of the 1953 outbreak in the orange free state, with special reference to the vectors and possible reservoir hosts. *S Afr Med J.*, 29(22):514–8, May 28 1955.

[33] BM McIntosh and PG Jupp. Epidemiological aspects of rift valley fever in south africa with reference to vectors. *Contrib. Epidemiol. Biostat.*, 3:92–99, 1981.

[34] K J Linthicum, A Anyamba, C J Tucker, P W Kelley, M F Myers, and C J Peters. Climate and satellite indicators to forecast Rift Valley fever epidemics in Kenya. *Science (New York, N.Y.)*, 285(5426):397–400, 1999. ISSN 00368075. doi: 10.1126/science.285.5426.397.

[35] K J Linthicum, F G Davies, a Kairo, and C L Bailey. Rift Valley fever virus (family Bunyaviridae, genus Phlebovirus). Isolations from Diptera collected during an inter-epizootic period in Kenya. *The Journal of Hygiene*, 95(1): 197–209, 1985. ISSN 0022-1724. doi: 10.1017/S0022172400062434.

[36] T M Logan, K J Linthicum, F G Davies, Y S Binepal, and C R Roberts. Isolation of Rift Valley fever virus from mosquitoes (Diptera: Culicidae) collected during an outbreak in domestic animals in Kenya. *J Med Entomol*, 28(2):293–295, 1991. ISSN 0022-2585. URL http://www.ncbi.nlm.nih.gov/pubmed/1676073.

[37] Rosemary Sang, Elizabeth Kioko, Joel Lutomiah, Marion Warigia, Caroline Ochieng, Monica O'Guinn, John S. Lee, Hellen Koka, Marvin Godsey, David Hoel, Hanafi Hanafi, Barry Miller, David Schnabel, Robert F. Breiman, and Jason Richardson. Rift Valley fever virus epidemic in Kenya, 2006/2007: The entomologic investigations. *American Journal of Tropical Medicine and Hygiene*, 83(2 SUPPL.):28–37, 2010. ISSN 00029637. doi: 10.4269/ajtmh.2010.09-0319.

[38] Center for Disease Control and Prevention. Rift valley fever fact sheet. Retrieved on the 17 January 2014. URL www.cdc.gov/ncidod/.../Fact_Sheets/Rift_Valley_Fever_Fact_Sheet.pdf.

[39] Robert D. Sumaye, Eveline Geubbels, Edgar Mbeyela, and Dirk Berkvens. Inter-epidemic Transmission of Rift Valley Fever in Livestock in the Kilombero River Valley, Tanzania: A Cross-Sectional Survey. *PLOS Neglected Tropical Diseases*, 7(8), 2013. ISSN 19352727. doi: 10.1371/journal.pntd.0002356.

[40] Catherine Cêtre-Sossah, Aurélie Pédarrieu, Hélène Guis, Cédric Defernez, Michèle Bouloy, Jacques Favre, Sébastien Girard, Eric Cardinale, and Emmanuel Albina. Prevalence of rift valley fever among ruminants, Mayotte. *Emerging Infectious Diseases*, 18:972–975, 2012. ISSN 10806040. doi: 10.3201/eid1806.111165.

[41] Daouda Sissoko, Claude Giry, Philippe Gabrie, Arnaud Tarantola, François Pettinelli, Louis Collet, Eric D'Ortenzio, Philippe Renault, and Vincent Pierre. Rift valley fever, mayotte, 2007-2008. *Emerging Infectious Diseases*, 15(4):568–570, 2009. ISSN 10806040. doi: 10.3201/eid1504.081045.

[42] Herve G. Zeller, Didier Fontenille, Moumouni Traore-Lamizana, Yaya Thiongane, and Jean Pierre Digoutte. Enzootic activity of rift valley fever virus in Senegal. *American Journal of Tropical Medicine and Hygiene*, 56(3): 265–272, 1997. ISSN 00029637.

[43] José Fafetine, Luis Neves, Peter N. Thompson, Janusz T. Paweska, Victor P M G Rutten, and J. A W Coetzer. Serological Evidence of Rift Valley Fever Virus Circulation in Sheep and Goats in Zambézia Province, Mozambique. *PLOS Neglected Tropical Diseases*, 7(2), 2013. ISSN 19352727. doi: 10.1371/journal.pntd.0002065.

[44] A. Desiree LaBeaud, Eric M. Muchiri, Malik Ndzovu, Mariam T. Mwanje, Samuel Muiruri, Clarence J. Peters, and Charles H. King. Interepidemic Rift Valley fever virus seropositivity, northeastern Kenya. *Emerging Infectious Diseases*, 14(8):1240–1246, 2008. ISSN 10806040. doi: 10.3201/eid1408.080082.

[45] Nelson O Owange, William O Ogara, Hippolyte Affognon, Gathura B Peter, Jacqueline Kasiiti, Sam Okuthe, W Onyango-Ouma, Tobias Landmann, Rosemary Sang, and Murithi Mbabu. Occurrence of rift valley fever in cattle in Ijara district, Kenya. *Preventive Veterinary Medicine*, 117(1):121–8, 2014. ISSN 1873-1716. doi: 10.1016/j.prevetmed.2014.08.008. URL http://www.sciencedirect.com/science/article/pii/S0167587714002608.

[46] Jacqueline Kasiiti Lichoti, Absolomon Kihara, Abuu a Oriko, Leonard Ateya Okutoyi, James Ogaa Wauna, David P Tchouassi, Caroline C Tigoi, Steve Kemp, Rosemary Sang, and Rees Murithi Mbabu. Detection of rift valley Fever virus interepidemic activity in some hotspot areas of kenya by sentinel animal surveillance, 2009-2012. *Veterinary Medicine International*, 2014:379010, 2014. ISSN 2090-8113. doi: 10.1155/2014/379010. URL http://www.pubmedcentral.nih.gov/articlerender.fcgi?artid=4147350&tool=pmcentrez&rendertype=abstract.

[47] R. Daubney, J.R. Hudson, and P.C. Garnham. Enzootic hepatitis of rift valley fever, an undescribed virus disease of sheep, cattle and man from east africa. *Journal of Pathology and Bacteriology*, 34:545–579, 1931.

[48] Saul C. Mpeshe, Heikki Haario, and Jean M. Tchuenche. A Mathematical Model of Rift Valley Fever with Human Host. *Acta Biotheoretica*, 59(3-4):231–250, 2011. ISSN 00015342. doi: 10.1007/s10441-011-9132-2.

[49] V Chevalier, M Pépin, L Plée, and R Lancelot. Rift Valley fever–a threat for Europe? *Euro surveillance : bulletin europeen sur les maladies transmissibles = European Communicable Disease Bulletin*, 15(10):19506, 2010. ISSN 1560-7917.

[50] A. Adam, M. Karsany, and I. Adam. Manifestations of severe rift valley fever in sudan. *Int J Infect Dis*, 14:179–180, 2010.

[51] Soa F. Andriamandimby, A. E. Randrianarivo-Solofoniaina, Elisabeth M. Jeanmaire, Lisette Ravololomanana, Lanto Tiana Razafimanantsoa, Tsanta Rakotojoelinandrasana, Josette Razainirina, Jonathan Hoffmann, Jean Pierre Ravalohery, J. T. Rafisandratantsoa, Pierre E. Rollin, and Jean Marc Reynes. Rift valley fever during rainy seasons, Madagascar, 2008 and 2009. *Emerging Infectious Diseases*, 16(6):963–970, 2010. ISSN 10806040. doi: 10.3201/eid1606.091266.

[52] OIE-WAHID. Rift valley fever in south africa. 2010. URL http://www.oie.int/wahis/public.php?page=singlereportpop=1reported=9491.

[53] OIE-WAHID:. Rift valley fever. 2010. URL http://www.oie.int/wahis/public.php?page=singlereport$pop=1$reported=9947.

[54] OIE-WAHID. Rift valley fever. 2010. URL http://web.oie.int/wahis/public.php?page=single-reportpop=1reported=925811.

[55] Ahmed B. Ould El Mamy, Mohamed Ould Baba, Yahya Barry, Katia Isselmou, Mamadou L. Dia, Ba Hampate, Mamadou Y. Diallo, Mohamed Ould Brahim El Kory, Mariam Diop, Modou Moustapha Lo, Yaya Thiongane, Mohammed Bengoumi, Lilian Puech, Ludovic Plee, Filip Claes, Stephane de la Rocque, and Baba Doumbia. Unexpected rift valley fever outbreak, Northern Mauritania, 2011. ISSN 10806040.

[56] V. Chevalier, B. Mondet, A. Diaite, R. Lancelot, A. G. Fall, and N. Ponçon. Exposure of sheep to mosquito bites: Possible consequences for the transmission risk of Rift Valley Fever in Senegal. *Medical and Veterinary Entomology*, 18(3):247–255, 2004. ISSN 0269283X. doi: 10.1111/j.0269-283X.2004.00511.x.

[57] Thomas R Kasari, Deborah A Carr, Tracey V Lynn, and J Todd Weaver. Evaluation of pathways for release of Rift Valley fever virus into domestic ruminant livestock, ruminant wildlife, and human populations in the continental United States. *Journal of the American Veterinary Medical Association*, 232(4):514–529, 2008. ISSN 0003-1488. doi: 10.2460/javma.232.4.514.

[58] Peninah Munyua, Rees M. Murithi, Sherrilyn Wainwright, Jane Githinji, Allen Hightower, David Mutonga, Joseph Macharia, Peter M. Ithondeka, Joseph Musaa, Robert F. Breiman, Peter Bloland, and M. Kariuki Njenga. Rift Valley fever outbreak in livestock in Kenya, 2006-2007. *American Journal of Tropical Medicine and Hygiene*, 83(2 SUPPL.):58–64, 2010. ISSN 00029637. doi: 10.4269/ajtmh.2010.09-0292.

[59] H W Hethcote, H W Stech, and P van den Driessche. Stability analysis for models of diseases without immunity. *Journal of Mathematical Biology*, 13 (2):185–198, 1981. ISSN 0303-6812. doi: 10.1007/BF00275213.

[60] Darci R Smith, Brian H Bird, Bridget Lewis, Sara C Johnston, Sarah McCarthy, Ashley Keeney, Miriam Botto, Ginger Donnelly, Joshua Shamblin, César G Albariño, Stuart T Nichol, and Lisa E Hensley. Development of a novel nonhuman primate model for Rift Valley fever. *Journal of Virology*, 86(4):2109–20, 2012. ISSN 1098-5514. doi: 10.1128/JVI.06190-11. URL http://www.pubmedcentral.nih.gov/articlerender.fcgi?artid=3302397&tool=pmcentrez&rendertype=abstract.

[61] JAP Heesterbeek. *Mathematical Epidemiology of Infectious Diseases: Model Building, Analysis and Interpretation*, volume 26 Suppl 4. 2000. URL http://books.google.com/books?hl=en&lr=&id=5VjSaAf35pMC&oi=fnd&pg=PR11&dq=Mathematical+Epidemiology+of+Infectious+Diseases:+Model+Building,+Analysis,+and+Interpretation&ots=c0Va_SdseJ&sig=Nmbccgwx6CEAJ-obdy99k5NXw3w$\delimiter"026E30F$nhttp://books.google.com/books?hl=en&lr.

[62] R Axelrod and W D Hamilton. The evolution of cooperation. *Science (New York, N.Y.)*, 211(4489):1390–1396, 1981. ISSN 0036-8075. doi: 10.1126/science.7466396.

[63] Christopher W. Woods, Adam M. Karpati, Thomas Grein, Noel McCarthy, Peter Gaturuku, Eric Muchiri, Lee Dunster, Alden Henderson, Ali S. Khan, Robert Swanepoel, Isabelle Bonmarin, Louise Martin, Philip Mann, Bonnie L. Smoak, Michael Ryan, Thomas G. Ksiazek, Ray R. Arthur, Andre Ndikuyeze, Naphtali N. Agata, and Clarence J. Peters. An outbreak of Rift Valley fever in Northeastern Kenya, 1997-98. *Emerging Infectious Diseases*, 8(2):138–144, 2002. ISSN 10806040. doi: 10.3201/eid0802.010023.

[64] Jacques Ferber. *Multi-Agent Systems: An Introduction to Distributed Artificial Intelligence*, volume 222. 1999. ISBN 0201360489. URL http://jasss.soc.surrey.ac.uk/4/2/reviews/rouchier.html.

[65] V Grimm and Sf Railsback. *Individual-based Modeling and Ecology*. 2005. ISBN 069109666X. doi: 10.1111/j.1467-2979.2008.00286.x.

[66] Stephen Eubank, Hasan Guclu, V S Anil Kumar, Madhav V Marathe, Aravind Srinivasan, Zoltán Toroczkai, and Nan Wang. Modelling disease outbreaks in realistic urban social networks. *Nature*, 429(6988):180–184, 2004. ISSN 0028-0836. doi: 10.1038/nature02541.

[67] Benjamin Roche, Jean-François Guégan, and François Bousquet. Multi-agent systems in epidemiology: a first step for computational biology in the study of vector-borne disease transmission. *BMC Bioinformatics*, 9:435, 2008. ISSN 1471-2105. doi: 10.1186/1471-2105-9-435.

[68] Charly Favier, Karine Chalvet-Monfray, Philippe Sabatier, Renaud Lancelot, Didier Fontenille, and Marc A Dubois. Rift Valley fever in West Africa: the role of space in endemicity. *Tropical Medicine & International Health : TM & IH*, 11(12):1878–1888, 2006. ISSN 1360-2276. doi: 10.1111/j.1365-3156.2006.01746.x.

[69] Holly D. Gaff, David M. Hartley, and Nicole P. Leahy. An epidemiological model of rift valley fever. *Electronic Journal of Differential Equations*, 2007: 1–12, 2007. ISSN 10726691. doi: 10.1155/2012/138757.

[70] Holly Gaff, Colleen Burgess, Jacqueline Jackson, Tianchan Niu, Yiannis Papelis, and David Hartley. Mathematical Model to Assess the Relative Effectiveness of Rift Valley Fever Countermeasures. *International Journal of Artificial Life Research*, 2(2):1–18, 2011. ISSN 1947-3087. doi: 10.4018/jalr.2011040101. URL http://services.igi-global.com/resolvedoi/resolve.aspx?doi=10.4018/jalr.2011040101.

[71] Tianchan Niu, Holly D. Gaff, Yiannis E. Papelis, and David M. Hartley. An epidemiological model of rift valley fever with spatial dynamics. *Computational and Mathematical Methods in Medicine*, 2012, 2012. ISSN 1748670X. doi: 10.1155/2012/138757.

[72] Ling Xue, H. Morgan Scott, Lee W. Cohnstaedt, and Caterina Scoglio. A network-based meta-population approach to model Rift Valley fever epidemics. *Journal of Theoretical Biology*, 306:129–144, 2012. ISSN 00225193. doi: 10.1016/j.jtbi.2012.04.029.

[73] Ling Xue, Lee W. Cohnstaedt, H. Morgan Scott, and Caterina Scoglio. A Hierarchical Network Approach for Modeling Rift Valley Fever Epidemics with Applications in North America. *PLOS ONE*, 8(5), 2013. ISSN 19326203. doi: 10.1371/journal.pone.0062049.

[74] Saul C Mpeshe, Livingstone S Luboobi, and Yaw Nkansah-Gyekye. Modeling the impact of climate change on the dynamics of rift valley Fever. *Computational and Mathematical Methods in Medicine*, 2014:627586, 2014. ISSN 1748-6718. doi: 10.1155/2014/627586. URL http://www.pubmedcentral.nih.gov/articlerender.fcgi?artid=3985190&tool=pmcentrez&rendertype=abstract.

[75] P.D. Little. Hidden value on the hoof: Crossborder livestock trade in eastern africa. common market for eastern and southern africa comprehensive african agriculture development program. Technical report, 2009. URL http://www.caadp.net/pdf/COMESA%20CAADP%20Policy%20Brief%202%20Cross%20Border%20Livestock%20Trade%20(2).pdf.

[76] Yousif E Himeidan, Eliningaya J Kweka, Mostafa M Mahgoub, El Amin El Rayah, and Johnson O Ouma. Recent outbreaks of rift valley Fever in East Africa and the middle East. *Frontiers in Public Health*, 2:169, 2014. ISSN 2296-2565. doi: 10.3389/fpubh.2014.00169. URL http://www.pubmedcentral.nih.gov/articlerender.fcgi?artid=4186272{&}tool=pmcentrez{&}rendertype=abstract.

[77] Farida Chamchod, Robert Stephen Cantrell, Chris Cosner, Ali N Hassan, John C Beier, and Shigui Ruan. A modeling approach to investigate epizootic outbreaks and enzootic maintenance of rift valley Fever virus. *Bulletin of Mathematical Biology*, 76(8):2052–72, 2014. ISSN 1522-9602. doi: 10.1007/s11538-014-9998-7. URL http://www.ncbi.nlm.nih.gov/pubmed/25102776.

[78] Tetsuro Ikegami and Shinji Makino. Rift Valley fever vaccines. *Vaccine*, 27 (SUPPL. 4), 2009. ISSN 0264410X. doi: 10.1016/j.vaccine.2009.07.046.

[79] D J Bicout and P Sabatier. Mapping Rift Valley Fever vectors and prevalence using rainfall variations. *Vector Borne and Zoonotic Diseases (Larchmont, N.Y.)*, 4(1):33–42, 2004. ISSN 1530-3667. doi: 10.1089/153036604773082979.

[80] S.A. Pedro, H.E.Z. Tonnang, and S. Abelman. Uncertainty and sensitivity analysis of a rift valley fever model. *Applied Mathematics and Computation*, 279:170 – 186, 2016. ISSN 0096-3003. doi: http://dx.doi.org/10.1016/j.amc.2016.01.003. URL http://www.sciencedirect.com/science/article/pii/S0096300316300030.

[81] Brian H Bird, Jane W K Githinji, Joseph M Macharia, Jacqueline L Kasiiti, Rees M Muriithi, Stephen G Gacheru, Joseph O Musaa, Jonathan S Towner, Serena A Reeder, Jennifer B Oliver, Thomas L Stevens, Bobbie R Erickson, Laura T Morgan, Marina L Khristova, Amy L Hartman, James A Comer, Pierre E Rollin, Thomas G Ksiazek, and Stuart T Nichol. Multiple virus lineages sharing recent common ancestry were associated with a Large Rift Valley fever outbreak among livestock in Kenya during 2006-2007. *Journal of Virology*, 82(22):11152–11166, 2008. ISSN 0022-538X. doi: 10.1128/JVI.01519-08.

[82] J M Heffernan, R J Smith, and L M Wahl. Perspectives on the basic reproductive ratio. *Journal of the Royal Society, Interface / the Royal Society*, 2(4):281–293, 2005. ISSN 1742-5689. doi: 10.1098/rsif.2005.0042.

[83] Simeone Marino, Ian B. Hogue, Christian J. Ray, and Denise E. Kirschner. A methodology for performing global uncertainty and sensitivity analysis in systems biology, 2008. ISSN 00225193.

[84] A Saltelli, K Chan, and E M Scott. *Sensitivity Analysis*. 2000. ISBN 0-471-99892-3. URL http://www.wiley.com/.

[85] Ben Adams and Michael Boots. How important is vertical transmission in mosquitoes for the persistence of dengue? Insights from a mathematical model. *Epidemics*, 2(1):1–10, 2010. ISSN 17554365. doi: 10.1016/j.epidem.2010.01.001.

[86] Carlene Trevennec, Claudia Pittiglio, Sherrilyn Wainwright, Ludovic Plee, Julio Pinto, Juan Lubroth, and Vincent Martin. Rift Valley fever vigilance needed in the coming months. *EMPRES Watch*, 27(December), 2012.

[87] Jing Li, Daniel Blakeley, and Robert J Smith. The failure of r(0). *Computational and Mathematical Methods in Medicine*, 2011:527610, 2011. ISSN 1748-670X. doi: 10.1155/2011/527610.

[88] Md Samsuzzoha, Manmohan Singh, and David Lucy. Uncertainty and sensitivity analysis of the basic reproduction number of a vaccinated epidemic model of influenza. *Applied Mathematical Modelling*, 37(3):903–915, 2013. ISSN 0307904X. doi: 10.1016/j.apm.2012.03.029.

[89] Nakul Chitnis, James M Hyman, and Jim M Cushing. Determining important parameters in the spread of malaria through the sensitivity analysis of a mathematical model. *Bulletin of Mathematical Biology*, 70(5):1272–96, 2008. ISSN 1522-9602. doi: 10.1007/s11538-008-9299-0. URL http://www.ncbi.nlm.nih.gov/pubmed/18293044.

[90] D M Hamby. A review of techniques for parameter sensitivity analysis of environmental models, 1994. ISSN 01676369. URL http://www.scopus.com/inward/record.url?eid=2-s2.0-0028501607&partnerID=tZOtx3y1.

[91] Yamar Ba, Diawo Diallo, Cheikh Mouhamed Fadel Kebe, Ibrahima Dia, and Mawlouth Diallo. Aspects of Bioecology of Two Rift Valley Fever Virus Vectors in Senegal (West Africa): ¡I¿Aedes vexans¡/I¿ and ¡I¿Culex poicilipes¡/I¿ (Diptera: Culicidae). *Journal of Medical Entomology*, 42(5):739–750, 2005. ISSN 00222585. doi: 10.1603/0022-2585(2005)042[0739:AOBOTR]2.0.CO;2. URL http://dx.doi.org/10.1603/0022-2585(2005)042[0739:AOBOTR]2.0.CO;2.

[92] O N Bjø rnstad and B T Grenfell. Noisy clockwork: time series analysis of population fluctuations in animals. *Science (New York, N.Y.)*, 293(5530): 638–643, 2001. ISSN 0036-8075. doi: 10.1126/science.1062226.

[93] B.M. Parker. Hatchability of eggs of Aedes taeniorhynchus (Diptera: Culicidae): effects of different temperatures and photoperiods during embryogenesis. *Ann. Ent. Soc. Amer.*, 79(6):925–930, 1986.

[94] Jan A. Freund, Sebastian Mieruch, Bettina Scholze, Karen Wiltshire, and Ulrike Feudel. Bloom dynamics in a seasonally forced phytoplankton-zooplankton model: Trigger mechanisms and timing effects. *Ecological Complexity*, 3(2):129–139, 2006. ISSN 1476945X. doi: 10.1016/j.ecocom.2005.11.001.

[95] Jon Greenman, Masashi Kamo, and Mike Boots. External forcing of ecological and epidemiological systems: A resonance approach. *Physica D: Nonlinear Phenomena*, 190(1-2):136–151, 2004. ISSN 01672789. doi: 10.1016/j.physd.2003.08.008.

[96] M. Aguiar, R. Paul, A. Sakuntabai, and N. Stollenwork. Are we modelling the correct data? minimizing false prediction for dengue fever in thailand. *Epidemiol. Infect.*, 142(11):2447–59, 2014. URL doi:10.1017/S0950268813003348.

[97] J M Ireland, B D Mestel, and R A Norman. The effect of seasonal host birth rates on disease persistence. *Mathematical Biosciences*, 206(1):31–45, 2007. ISSN 0025-5564. doi: 10.1016/j.mbs.2006.08.028. URL http://www.sciencedirect.com/science/article/pii/S0025556406001520.

[98] William A Geering, F Glyn Davies, and Vincent Martin. *Preparation of Rift Valley fever contingency plans*. Number 15. Food & Agriculture Org., 2002.

[99] M. J. Turell, C. A. Rossi, and C. L. Bailey. Effect of extrinsic incubation temperature on the ability of Aedes taeniorhynchus and Culex pipiens to transmit Rift Valley fever virus. *American Journal of Tropical Medicine and Hygiene*, 34(6):1211–1218, 1985. ISSN 00029637.

[100] O Diekmann, J A Heesterbeek, and J A Metz. On the definition and the computation of the basic reproduction ratio R0 in models for infectious diseases in heterogeneous populations. *Journal of Mathematical Biology*, 28 (4):365–382, 1990. ISSN 0303-6812. doi: 10.1007/BF00178324.

[101] P. Van Den Driessche and James Watmough. Reproduction numbers and sub-threshold endemic equilibria for compartmental models of disease transmission. *Mathematical Biosciences*, 180:29–48, 2002. ISSN 00255564. doi: 10.1016/S0025-5564(02)00108-6.

[102] M Lipsitch, M A Nowak, D Ebert, and R M May. The population dynamics of vertically and horizontally transmitted parasites. *Proceedings. Biological Sciences / The Royal Society*, 260(1359):321–327, 1995. ISSN 0962-8452. doi: 10.1098/rspb.1995.0099.

[103] Nicholas C Grassly and Christophe Fraser. Seasonal infectious disease epidemiology. *Proceedings. Biological sciences / The Royal Society*, 273(1600): 2541–2550, 2006. ISSN 0962-8452. doi: 10.1098/rspb.2006.3604.

[104] Nicolas Bacaër. Approximation of the basic reproduction number R0 for vector-borne diseases with a periodic vector population. *Bulletin of Mathematical Biology*, 69(3):1067–1091, 2007. ISSN 00928240. doi: 10.1007/s11538-006-9166-9.

[105] David Greenhalgh and Martin Griffiths. Backward bifurcation, equilibrium and stability phenomena in a three-stage extended BRSV epidemic model. *Journal of Mathematical Biology*, 59(1):1–36, 2009. ISSN 03036812. doi: 10.1007/s00285-008-0206-y.

[106] C C Chavez, Z Feng, and W Huang. On The Computation Of R_{0} And Its Role On Global Stability. *The IAM Volume in Mathematics an its Applications*, 125:229, 2002.

[107] Andrei Korobeinikov. Global properties of infectious disease models with nonlinear incidence. *Bulletin of Mathematical Biology*, 69(6):1871–1886, 2007. ISSN 00928240. doi: 10.1007/s11538-007-9196-y.

[108] J.P. La Salle. *The Stability of Dynamical Systems*. Society for Industrial and Applied Mathematics, 1976. doi: 10.1137/1.9781611970432. URL http://epubs.siam.org/doi/abs/10.1137/1.9781611970432.

[109] B.A. Fuchs and B.V. Shabat. In B.A. Fuchs and B.V. Shabat, editors, *Functions of a Complex Variable and Some of their Applications*, volume 2 of *International Series of Monographs on Pure and Applied Mathematics*. Pergamon, 1964. doi: http://dx.doi.org/10.1016/B978-0-08-009404-5.50013-1. URL http://www.sciencedirect.com/science/article/pii/B9780080094045500131.

[110] S. A. Pedro and J. M. Tchuenche. HIV/AIDS dynamics: Impact of economic classes with transmission from poor clinical settings. *Journal of Theoretical Biology*, 267(4):471–485, 2010. ISSN 00225193. doi: 10.1016/j.jtbi.2010.09.019.

[111] Eric Ziegel, William Press, Brian Flannery, Saul Teukolsky, and William Vetterling. Numerical Recipes: The Art of Scientific Computing. *Technometrics*, 29(4):501, 1987. ISSN 00401706. doi: 10.2307/1269484. URL http://www.jstor.org/stable/1269484?origin=crossref.

[112] T S Parker and L O Chua. Practical numerical algorithms for chaotic systems, 1990. ISSN 03784754.

[113] H. Gould and J. Tobochnik. An introduction to computer simulation methods: Applications to physical systems. *Addison-Wesley, New-York*, Second edition, 1996.

[114] Kathleen T. Alligood, Tim D. Sauer, James a. Yorke, and J. D. Crawford. *Chaos: An Introduction to Dynamical Systems*, volume 50. 1997. ISBN 0387946772. doi: 10.1063/1.882006. URL http://scitation.aip.org/content/aip/magazine/physicstoday/article/50/11/10.1063/1.882006.

[115] Edward Ott. Strange attractors and chaotic motions of dynamical systems. *Reviews of Modern Physics*, 53(4):655–671, 1981. ISSN 00346861. doi: 10.1103/RevModPhys.53.655.

[116] Alan Hastings. Chaos in dynamical systems, 1995. ISSN 0092-8240.

[117] F. G. Davies, K. J. Linthicum, and A. D. James. Rainfall and epizootic Rift Valley fever. *Bulletin of the World Health Organization*, 63(5):941–943, 1985. ISSN 00429686.

[118] F G Davies, E Kilelu, K J Linthicum, and R G Pegram. Patterns of Rift Valley fever activity in Zambia. *Epidemiology and Infection*, 108(1):185–191, 1992. ISSN 0950-2688. doi: 10.1017/S0950268800049633.

[119] AR Spickler. Rift valley fever: infectious enzootic hepatitis of sheep and cattle, 2006. URL http://www.cfsph.iastate.edu/Factsheets/pdfs/riftvalleyfever.pdf.

[120] Henry G Mwambi. Ticks and tick-borne diseases in Africa: a disease transmission model. *IMA journal of Mathematics Applied in Medicine and Biology*, 19(2002):275–292, 2002. ISSN 0265-0746.

[121] S. R. Magano, D .A. Els, and S. L. Chown. Feeding patterns of immature stages of Hyalomma truncatum and Hyalomma marginatum rufipes on different hosts. *Experimental & Applied Acarology*, 24(4):301–13, 2000. ISSN 0168-8162. URL http://www.ncbi.nlm.nih.gov/pubmed/11110240.

[122] PG G Jupp and AJ J Cornel. Vector competence tests with Rift Valley fever virus and five South African species of mosquitoes. *Journal of the American Mosquito Control Association*, 4(1):4–8, 1988. ISSN 8756-971X. URL http://ukpmc.ac.uk/abstract/MED/2903903$\delimiter"026E30F$nhttp://citebank.org/sites/default/files/JAMCA_V04_N1_P004-008.pdf.

[123] Dmitry A. Apanaskevich and Ivan G. Horak. The genus Hyalomma. VI. Systematics of H. (Euhyalomma) truncatum and the closely related species, H. (E.) albiparmatum and H. (E.) nitidum (Acari: Ixodidae). *Experimental and Applied Acarology*, 44(2):115–136, 2008. ISSN 01688162. doi: 10.1007/s10493-008-9136-z.

[124] Diop Gora, Thiongane Yaya, Thonnon Jocelyn, Fontenille Didier, Diallo Maoulouth, Sall Amadou, Theodore D. Ruel, and Jean Paul Gonzalez. The potential role of rodents in the enzootic cycle of Rift Valley fever virus in Senegal. *Microbes and Infection*, 2(4):343–346, 2000. ISSN 12864579. doi: 10.1016/S1286-4579(00)00334-8.

[125] D.E. Sonenshine. Biology of Ticks. In *Biology of Ticks Volume ll*, pages 3–65. 1993. ISBN 0195059107.

[126] C. R. Davies, L. D. Jones, and P. A. Nuttall. Experimental studies on the transmission cycle of Thogoto virus, a candidate orthomyxovirus, in Rhipicephalus appendiculatus. *American Journal of Tropical Medicine and Hygiene*, 35(6):1256–1262, 1986. ISSN 00029637.

[127] M Labuda and P A Nuttall. Tick-borne viruses. *Parasitology*, 129 Suppl: S221–S245, 2004. ISSN 0031-1820. doi: 10.1017/S0031182004005220.

[128] Centers for Disease Control (CDC) and Prevention. Rift Valley fever outbreak–Kenya, November 2006-January 2007. *MMWR. Morbidity and mortality weekly report*, 56(4):73–76, 2007. ISSN 1545-861X. doi: mm5604a3[pii]. URL http://ovidsp.ovid.com/ovidweb.cgi?T=JS&PAGE=reference&D=med5&NEWS=N&AN=17268404.

[129] Patrick M. Nguku, S. K. Sharif, David Mutonga, Samuel Amwayi, Jared Omolo, Omar Mohammed, Eileen C. Farnon, L. Hannah Gould, Edith Lederman, Carol Rao, Rosemary Sang, David Schnabel, Daniel R. Feikin, Allen Hightower, M. Kariuki Njenga, and Robert F. Breiman. An investigation of a major outbreak of rift valley fever in Kenya: 2006-2007. *American Journal of Tropical Medicine and Hygiene*, 83(2 SUPPL.):5–13, 2010. ISSN 00029637. doi: 10.4269/ajtmh.2010.09-0288.

[130] H G Mwambi, J Baumgartner, K P Hadeler, and J Baumgartner. Ticks and tick-borne diseases: a vector-host interaction model for the brown ear tick (Rhipicephalus appendiculatus). *Statistical Methods in Medical Research*, 9 (3):279–301, 2000. ISSN 0962–2802. doi: 10.1177/096228020000900307. URL http://smm.sagepub.com/cgi/doi/10.1177/096228020000900307.

[131] Roberto Rosà and Andrea Pugliese. Effects of tick population dynamics and host densities on the persistence of tick-borne infections. *Mathematical Biosciences*, 208:216–240, 2007. ISSN 00255564. doi: 10.1016/j.mbs.2006.10.002.

[132] M.Y.Yi Li and James S Muldowney. On Bendixson's criterion. *J. Differ. Equations*, 106(1):27–39, 1993. ISSN 00220396. doi: 10.1006/jdeq.1993.1097.

[133] Jean Claude Kamgang and Gauthier Sallet. Computation of threshold conditions for epidemiological models and global stability of the disease-free equilibrium (DFE). *Mathematical Biosciences*, 213:1–12, 2008. ISSN 00255564. doi: DOI:10.1016/j.mbs.2008.02.005. URL http://dx.doi.org/10.1016/j.mbs.2008.02.005.

[134] Y. Dumont, F. Chiroleu, and C. Domerg. On a temporal model for the Chikungunya disease: Modeling, theory and numerics. *Mathematical Biosciences*, 213(1):80–91, 2008. ISSN 00255564. doi: 10.1016/j.mbs.2008.02.008.

[135] J. C. Helton, J. D. Johnson, C. J. Sallaberry, and C. B. Storlie. Survey of sampling-based methods for uncertainty and sensitivity analysis. *Reliability Engineering and System Safety*, 91(10-11):1175–1209, 2006. ISSN 09518320. doi: 10.1016/j.ress.2005.11.017.

[136] M. D. McKay, R. J. Beckman, and W. J. Conover. Comparison of Three Methods for Selecting Values of Input Variables in the Analysis of Output from a Computer Code. *Technometrics*, 21(2):239–245, 1979. ISSN 0040-1706. doi: 10.1080/00401706.1979.10489755. URL http://www.tandfonline.com/doi/abs/10.1080/00401706.1979.10489755.

[137] E Massad, F A B Coutinho, M N Burattini, and M Amaku. Estimation of R0 from the initial phase of an outbreak of a vector-borne infection. *Tropical Medicine & International Health*, 15:120–126, 2010. ISSN 13602276. doi: 10.1111/j.1365-3156.2009.02413.x. URL http://dx.doi.org/10.1111/j.1365-3156.2009.02413.x.

[138] Frédéric J Lardeux, Rosenka H Tejerina, Vicente Quispe, and Tamara K Chavez. A physiological time analysis of the duration of the gonotrophic cycle of Anopheles pseudopunctipennis and its implications for malaria transmission in Bolivia. *Malaria Journal*, 7:141, 2008. ISSN 1475-2875. doi: 10.1186/1475-2875-7-141.

[139] FAO. Rift valley Fever vaccine development, progress and constraints. In *GF-TADs meeting*, volume 17, page 42, 2011. ISBN 9789251069219. doi: 10.3201/eid1709.110506. URL http://www.ncbi.nlm.nih.gov/pubmed/21888781.

[140] Holly D. Gaff, Elsa Schaefer, and Suzanne Lenhart. Use of optimal control models to predict treatment time for managing tick-borne disease. *Journal of Biological Dynamics*, 5(5):517–530, 2011. ISSN 1751-3758. doi: 10.1080/17513758.2010.535910.

[141] F G Davies. Risk of a rift valley fever epidemic at the haj in Mecca, Saudi Arabia. *Revue scientifique et technique (International Office of Epizootics)*, 25(1):137–147, 2006. ISSN 0253-1933.

[142] Egil Aj Fischer, Gert Jan Boender, Gonnie Nodelijk, Aline A. De Koeijer, and Herman Jw Van Roermund. The transmission potential of Rift Valley fever virus among livestock in the Netherlands: A modelling study. *Veterinary Research*, 44(1), 2013. ISSN 09284249. doi: 10.1186/1297-9716-44-58.

[143] David M Hartley, Jennifer L Rinderknecht, Terry L Nipp, Neville P Clarke, and Gary D Snowder. Potential effects of Rift Valley fever in the United States. *Emerging Infectious Diseases*, 17(8), 2011. ISSN 1080-6059. doi: 10.3201/eid1708.101088. URL http://www.pubmedcentral.nih.gov/articlerender.fcgi?artid=3381545&tool=pmcentrez&rendertype=abstract.

[144] Raphaelle Metras, Thibaud Porphyre, Dirk U. Pfeiffer, Alan Kemp, Peter N. Thompson, Lisa M. Collins, and Richard G. White. Exploratory Space-Time Analyses of Rift Valley Fever in South Africa in 2008-2011. *PLOS Neglected Tropical Diseases*, 6(8), 2012. ISSN 19352727. doi: 10.1371/journal.pntd.0001808.

[145] Pejman Rohani, Matthew J Keeling, and Bryan T Grenfell. The interplay between determinism and stochasticity in childhood diseases. *The American Naturalist*, 159(5):469–481, 2002. ISSN 0003-0147. doi: 10.1086/339467.

[146] Rong Hua Wang, Zhen Jin, Quan Xing Liu, Johan van de Koppel, and David Alonso. A simple stochastic model with environmental transmission explains multi-year periodicity in outbreaks of avian flu. *PLOS ONE*, 7(2), 2012. ISSN 19326203. doi: 10.1371/journal.pone.0028873.

[147] Andrew J. Black and Alan J. McKane. Stochastic amplification in an epidemic model with seasonal forcing. *Journal of Theoretical Biology*, 267(1):85–94, 2010. ISSN 00225193. doi: 10.1016/j.jtbi.2010.08.014.

[148] M S Bartlett. Measles periodicity and community size. *J R Stat Soc A*, 120: 48–70, 1957. ISSN 00359238. doi: 10.2307/2342553.

[149] David Alonso, Alan J McKane, and Mercedes Pascual. Stochastic amplification in epidemics. *Journal of the Royal Society, Interface / the Royal Society*, 4(14):575–582, 2007. ISSN 1742-5689. doi: 10.1098/rsif.2006.0192.

[150] Alun L Lloyd, Ji Zhang, and A Morgan Root. Stochasticity and heterogeneity in host-vector models. *Journal of the Royal Society, Interface / the Royal Society*, 4(16):851–863, 2007. ISSN 1742-5689. doi: 10.1098/rsif.2007.1064.

[151] M.S. Bartlett. Deterministic and stochastic models for recurrent epidemics. *In Proc. Third Berkeley Symp. Mathematical statistics and probability, Berkeley, CA: University of California Press*, 4:81–109, 1956.

[152] K. B. Athreya and A. N. Vidyashankar. *Branching processes*, volume 19. 2001. doi: 10.1016/S0169-7161(01)19004-8.

[153] Krishna B Athreya and Peter E Ney. *Branching Processes*, volume 39. 2004. ISBN 0486434745. doi: 10.1007/BF01086176.

[154] L Sparks Donald. *Branching Processes in Biology*, volume Volume 96. 2007. ISBN 0065-2113. doi: 10.1016/S0070-2153(06)75012-8. URL http://www.sciencedirect.com/science/article/B7CSX-4PWJ47G-D/2/4d1b1fee906e4416f39d69b0a4def5a6.

[155] Linda J S Allen. An Introduction to Stochastic Epidemic Models. *Mathematical Epidemiology*, 1945(3):81–130, 2008. ISSN 00758434. doi: 10.1007/978-3-540-78911-6_3. URL http://dx.doi.org/10.1007/978-3-540-78911-6_3.

[156] Ira B Schwartz. Multiple stable recurrent outbreaks and predictability in seasonally forced nonlinear epidemic models. *Journal of Mathematical Biology*, 21(3):347–361, 1985. ISSN 0303-6812. doi: 10.1007/BF00276232.

[157] N.G. Van Kampen. Stochastic Processes in Physics and Chemistry, 2007. URL http://www.sciencedirect.com/science/article/pii/B9780444529657500076.

[158] M Simões, M M Telo da Gama, and a Nunes. Stochastic fluctuations in epidemics on networks. *Journal of the Royal Society, Interface / the Royal Society*, 5(22):555–566, 2008. ISSN 1742-5689. doi: 10.1098/rsif.2007.1206.

[159] Andrew J Black and Alan J McKane. Stochasticity in staged models of epidemics: quantifying the dynamics of whooping cough. *Journal of the Royal Society, Interface / the Royal Society*, 7(49):1219–1227, 2010. ISSN 1742-5689. doi: 10.1098/rsif.2009.0514.

[160] G. Rozhnova and A. Nunes. Stochastic effects in a seasonally forced epidemic model. *Physical Review E - Statistical, Nonlinear, and Soft Matter Physics*, 82(4), 2010. ISSN 15393755. doi: 10.1103/PhysRevE.82.041906.

[161] Ws Romoser, Mn Oviedo, K Lerdthusnee, La Patrican, Mj Turell, Dj Dohm, Kj Linthicum, and Cl Bailey. Rift Valley fever virus-infected mosquito ova and associated pathology: possible implications for endemic maintenance. *Research and Reports in Tropical Medicine*, 2:121–127, 2011. URL http://www.dovepress.com/getfile.php?fileID=11003.

[162] DV Canyon, JLK Hii, and R Muller. The frequency of host biting and its effect on oviposition and survival in Aedes aegypti (Diptera: Culicidae). *Bulletin of Entomological Research*, 89(01):35–39, 1999. ISSN 0007-4853. doi: 10.1017/S000748539900005X.

[163] B.H. Bird, T.G. Ksiazek, S.T. Nichol, and N.J. MacLachlan. Rift valley fever virus. *J. Am. Vet. Med. Assoc.*, 234(7):883–893, 2009.

[164] V Martin, V Chevalier, P Ceccato, A Anyamba, L De Simone, J Lubroth, S de La Rocque, and J Domenech. The impact of climate change on the epidemiology and control of Rift Valley fever. *Revue scientifique et technique (International Office of Epizootics)*, 27(2):413–426, 2008. ISSN 0253-1933.

[165] S Gupta, J Swinton, and R M Anderson. Theoretical studies of the effects of heterogeneity in the parasite population on the transmission dynamics of malaria. *Proceedings of the Royal Society B: Biological Sciences*, 256(1347): 231–238, 1994. ISSN 0962-8452. doi: 10.1098/rspb.1994.0075.

[166] N G Van Kampen. *Stochastic Processes in Physics and Chemistry*, volume 11. 1992. ISBN 0444893490. doi: 10.2307/2984076. URL http://books.google.com/books?hl=en{&}lr={&}id=3e7XbMoJzmoC{&}pgis=1.

[167] R M Anderson. Population dynamics of infectious diseases: theory and applications. *Population dynamics of infectious diseases: theory and applications*, 368, 1982. URL http://ovidsp.ovid.com/ovidweb.cgi?T=JS&NEWS=N&PAGE=fulltext&AN=19832702527&D=cagh0.

[168] M.S. Bartlett. Stochastic population models. *London,UK: Methuen*, 1960.

[169] A. McKane and T. Newman. Stochastic models in population biology and their deterministic analogs. *Physical Review E*, 70(4), 2004. ISSN 1539-3755. doi: 10.1103/PhysRevE.70.041902.

[170] F. Ball. The threshold behaviour of epidemic models. *J Appl. Prob.*, 20: 227–242, 1983.

[171] M S Bartlett. The Relevance of Stochastic Models for Large-Scale Epidemiological Phenomena. *Journal of the Royal Statistical Society. Series C (Applied Statistics)*, 13(1):2–8, 1964. ISSN 00359254. doi: 10.2307/2985217. URL http://www.jstor.org/stable/2985217.

[172] D.A. Griffiths. A bivariate birth-death process which approximates to the spread of a disease involving a vector. *J. Appl. Prob.*, 9:65–75, 1972. URL doi:10.2307/3212637.

[173] P. Jagers. Branching processes with biological applications. *New York: Wiley*, 1975.

[174] S. Karlin and H. Taylor. A first course in stochastic processes. *New York: Academic Press*, 2nd ed., 1975.

[175] Sarabjeet Singh, David J. Schneider, and Christopher R. Myers. Using multitype branching processes to quantify statistics of disease outbreaks in zoonotic epidemics. *Physical Review E*, 89, 2014. doi: 10.1103/PhysRevE.89.032702.

[176] Daniel T. Gillespie. A general method for numerically simulating the stochastic time evolution of coupled chemical reactions. *Journal of Computational Physics*, 22(4):403–434, 1976. ISSN 00219991. doi: 10.1016/0021-9991(76)90041-3. URL http://www.sciencedirect.com/science/article/pii/0021999176900413.

[177] Bernard Cazelles, Mario Chavez, Guillaume Constantin de Magny, Jean-Francois Guégan, and Simon Hales. Time-dependent spectral analysis of epidemiological time-series with wavelets. *Journal of the Royal Society, Interface / the Royal Society*, 4(15):625–636, 2007. ISSN 1742-5689. doi: 10.1098/rsif.2007.0212.

[178] J. Morvan, P. E. Rollin, S. Laventure, and J. Roux. Duration of immunoglobulin M antibodies against rift valley fever virus in cattle after natural infection. *Transactions of the Royal Society of Tropical Medicine and Hygiene*, 86(6), 1992. ISSN 0035-9203. URL http://cat.inist.fr/?aModele=afficheN{&}cpsidt=4473821.

[179] C.J. Peters, J.A. Reynolds, T.W. Slone, D.E. Jones, and E.L. Stephen. Prophylaxis of rift valley fever with antiviral drugs, immune serum, an interferon inducer, and a macrophage activator. *Antiviral Research*, 6(5):285 – 297, 1986. ISSN 0166-3542. doi: http://dx.doi.org/10.1016/0166-3542(86)90024-0. URL http://www.sciencedirect.com/science/article/pii/0166354286900240.

[180] O Tomori. Clinical, virological and serological response of the West African dwarf sheep to experimental infection with different strains of Rift Valley fever virus. *Res Vet Sci*, 26(2):152–159, 1979.

[181] M. I. Moussa, K. S E Abdel-Wahab, and O. L. Wood. Experimental infection and protection of lambs with a minute plaque variant of Rift Valley fever virus. *American Journal of Tropical Medicine and Hygiene*, 35(3):660–662, 1986. ISSN 00029637.

[182] B R Miller, M S Godsey, M B Crabtree, H M Savage, Y Al-Mazrao, M H Al-Jeffri, A M Abdoon, S M Al-Seghayer, A M Al-Shahrani, and T G Ksiazek. Isolation and genetic characterization of Rift Valley fever virus from Aedes vexans arabiensis, Kingdom of Saudi Arabia. *Emerg Infect Dis*, 8(12):1492–1494, 2002.

[183] D J D Earn, P Rohani, B M Bolker, and B T Grenfell. A simple model for complex dynamical transitions in epidemics. *Science*, 287(5453):667–670, 2000. ISSN 0036-8075. doi: 10.1126/science.287.5453.667. URL http://www.ncbi.nlm.nih.gov/pubmed/10650003.

[184] Antoinette A. Grobbelaar, Jacqueline Weyer, Patricia A. Leman, Alan Kemp, Janusz T. Paweska, and Robert Swanepoel. Molecular epidemiology of rift valley fever virus. *Emerging Infectious Diseases*, 17(12):2270–2276, 2011. ISSN 10806040. doi: http://dx.doi.org/10.3201/eid1712.111035.

[185] A Anyamba, K J Linthicum, and C J Tucker. Climate-disease connections: Rift Valley Fever in Kenya. *Cadernos de Saude Publica / Ministerio da Saude, Fundacao Oswaldo Cruz, Escola Nacional de Saude Publica*, 17 Suppl: 133–140, 2001. ISSN 0102-311X. doi: 10.1590/S0102-311X2001000700022.

[186] D. Fontenille, M. Traore-Lamizana, J. Trouillet, A. Leclerc, M. Mondo, Y. Ba, J. P. Digoutte, and H. G. Zeller. First isolations of arboviruses from phlebotomine sand flies in West Africa. *American Journal of Tropical Medicine and Hygiene*, 50(5):570–574, 1994. ISSN 00029637.

[187] WR Horsfall, HW Fowler, Moretti LJ, and Larsen JR. Bionomics and embryology of the inland flood water mosquito aedes vexans. *University of Illinois Press, Urbana*, page 211.

[188] Francisco F. Ludueña Almeida and David E. Gorla. The biology of Aedes (Ochlerotatus) albifasciatus Macquart, 1838 (Diptera: Culicidae) in Central Argentina. *Memórias do Instituto Oswaldo Cruz*, 90(4):463–468, 1995. ISSN 0074-0276. doi: 10.1590/S0074-02761995000400006.

[189] Norbert Becker, Dusan Petric, Marija Zgomba, Clive Boase, Madon Minoo, Christine Dahl, and Achim Kaiser. *Mosquitoes and Their Control*. Springer Science & Business Media, 2010.

[190] R. M. Gleiser, J. Urrutia, and D. E. Gorla. Body size variation of the floodwater mosquito Aedes albifasciatus in Central Argentina. *Medical and Veterinary Entomology*, 14:38–43, 2000. ISSN 0269283X. doi: 10.1046/j.1365-2915.2000.00217.x.

[191] R M Gleiser, D E Gorla, and F F L Almeida. Monitoring the abundance of Aedes (Ochlerotatus) albifasciatus (Macquart 1838) (Diptera: Culicidae)to the south of Mar Chiquita Lake, central Argentina, with the aid of remote sensing. *Annals of Tropical Medicine and Parasitology*, 91:917–926, 1997. ISSN 0003-4983. doi: 10.1080/00034989760301. URL http://www.ingentaconnect.com/content/routledg/catm/1997/00000091/00000008/art00003.

[192] Muaz Niazi and Amir Hussain. Agent-based computing from multi-agent systems to agent-based models: A visual survey. *Scientometrics*, 89(2):479–499, 2011. ISSN 01389130. doi: 10.1007/s11192-011-0468-9.

[193] Ying Zhou, S M Niaz Arifin, James Gentile, Steven J Kurtz, Gregory J Davis, and Barbara A Wendelberger. An agent-based model of the Anopheles gambiae mosquito life cycle. In *Proceedings of the 2010 Summer Computer Simulation Conference*, pages 201–208, 2010.

[194] S M Niaz Arifin, Gregory R Madey, and Frank H Collins. Examining the impact of larval source management and insecticide-treated nets using a spatial agent-based model of Anopheles gambiae and a landscape generator tool. *Malaria Journal*, 12:290, 2013. ISSN 1475-2875. doi: 10.1186/1475-2875-12-290. URL http://www.pubmedcentral.nih.gov/articlerender.fcgi?artid=3765353&tool=pmcentrez&rendertype=abstract.

[195] S M Niaz Arifin, Ying Zhou, Gregory J Davis, James E Gentile, Gregory R Madey, and Frank H Collins. An agent-based model of the population dynamics of Anopheles gambiae. *Malaria Journal*, 13(1):424, 2014. ISSN 1475-2875. doi: 10.1186/1475-2875-13-424. URL http://www.malariajournal.com/content/13/1/424.

[196] Barry W. Alto and Steven a. Juliano. Precipitation and Temperature Effects on Populations of Aedes albopictus (Diptera: Culicidae): Implications for Range Expansion. *Journal of Medical Entomology*, 38(5):646–656, 2001. ISSN 0022-2585. doi: 10.1603/0022-2585-38.5.646.

[197] Sandro Jerônimo De Almeida, Ricardo Poley Martins Ferreira, Álvaro E. Eiras, Robin P. Obermayr, and Martin Geier. Multi-agent modeling and

simulation of an Aedes aegypti mosquito population. *Environmental Modelling and Software*, 25(12):1490–1507, 2010. ISSN 13648152. doi: 10.1016/j.envsoft.2010.04.021. URL http://dx.doi.org/10.1016/j.envsoft.2010.04.021.

[198] Nuraini Yusoff, Harun Budin, and Salemah Ismail. Simulation of Population Dynamics of Aedes aegypti using Climate Dependent Model. *World Academy of Science, Engineering and Technology*, 62(2):477–482, 2012.

[199] Annelise Tran, Grégory L'Ambert, Guillaume Lacour, Romain Benoît, Marie Demarchi, Myriam Cros, Priscilla Cailly, Mélaine Aubry-Kientz, Thomas Balenghien, and Pauline Ezanno. A rainfall- and temperature-driven abundance model for Aedes albopictus populations. *International Journal of Environmental Research and Public Health*, 10(5):1698–1719, 2013. ISSN 16617827. doi: 10.3390/ijerph10051698.

[200] Hongfei Gong, Arthur Degaetano, and Laura C Harrington. A climate based mosquito population model. *Proceedings of the World Congress on Engineering and Computer Science*, pages 24–27, 2007. ISSN 20780958.

[201] Steven F. Railsback and Volker Grimm. *Agent-Based and Individual-Based Modeling: A Practical Introduction*. 2011.

[202] Volker Grimm, Eloy Revilla, Uta Berger, Florian Jeltsch, Wolf M Mooij, Steven F Railsback, Hans-Hermann Thulke, Jacob Weiner, Thorsten Wiegand, and Donald L DeAngelis. Pattern-oriented modeling of agent-based complex systems: lessons from ecology. *Science (New York, N.Y.)*, 310(5750):987–91, 2005. ISSN 1095-9203. doi: 10.1126/science.1116681. URL http://www.ncbi.nlm.nih.gov/pubmed/16284171.

[203] H. C. Giacomini, Paulo De Marco, and Miguel Petrere. Exploring community assembly through an individual-based model for trophic interactions. *Ecological Modelling*, 220(1):23–39, 2009. ISSN 03043800. doi: 10.1016/j.ecolmodel.2008.09.005.

[204] Tyler R. Bonnell, Raja R. Sengupta, Colin A. Chapman, and Tony L. Goldberg. An agent-based model of red colobus resources and disease dynamics implicates key resource sites as hot spots of disease transmission. *Ecological Modelling*, 221(20):2491–2500, 2010. ISSN 03043800. doi: 10.1016/j.ecolmodel.2010.07.020. URL http://www.sciencedirect.com/science/article/pii/S0304380010003753.

[205] Brian Dennis, William P Kemp, and R O Y C Beckwith. Stochastic Model of Insect Phenology: Estimation and Testing. *Environmental Entomology*, 546:540–546, 1986.

[206] David W Hilbert. Growth-based approach to modeling the developmental rate of arthropods. *Environmental Entomology*, 24(4):771–778, 1995. ISSN 0046-225X U6 - Journal Article.

[207] C.Y. Arnold. Maximum-minimum temperatures as a basis for computing heat units. *Proceedings of American Society for Horticultural Science*, 76: 682–692, 1960.

[208] G. L. Baskerville and P. Emin. Rapid Estimation of Heat Accumulation from Maximum and Minimum Temperatures. *Ecology*, 50(3):514–517, 1969. ISSN 00129658. doi: 10.2307/1933912.

[209] Lg Higley, Lp Pedigo, and Kr Ostlie. DEGDAY: a program for calculating degree-days, and assumptions behind the degree-day approach. *Environmental Entomology*, 15(5):999–1016, 1986. ISSN 0046225X. doi: 10.1093/ee/15.5.999. URL http://www.ingentaconnect.com/content/esa/envent/1986/00000015/00000005/art00001.

[210] Noboru Minakawa, Clifford M. Mutero, John I. Githure, John C. Beier, and Guiyun Yan. Spatial distribution and habitat characterization of anopheline mosquito larvae in western Kenya. *American Journal of Tropical Medicine and Hygiene*, 61(6):1010–1016, 1999. ISSN 00029637.

[211] J E Gimnig, M Ombok, L Kamau, and W a Hawley. Characteristics of larval anopheline (Diptera: Culicidae) habitats in Western Kenya. *Journal of Medical Entomology*, 38:282–288, 2001. ISSN 0022-2585. doi: 10.1603/0022-2585-38.2.282.

[212] M. Soledad Fontanarrosa, M. Cristina Marinone, Sylvia Fischer, Pablo W. Orellano, and Nicolás Schweigmann. Effects of Flooding and Temperature on Aedes albifasciatus Development Time and Larval Density in Two Rain Pools at Buenos Aires University City. *Memorias do Instituto Oswaldo Cruz*, 95 (6):787–793, 2000. ISSN 0074-0276. doi: 10.1590/S0074-02762000000600007.

[213] Jorge A Ahumada, Dennis Lapointe, and Michael D Samuel. Modeling the population dynamics of Culex quinquefasciatus (Diptera: Culicidae), along an elevational gradient in Hawaii. *Journal of Medical Entomology*, 41(6): 1157–1170, 2004. ISSN 0022-2585. doi: 10.1603/0022-2585-41.6.1157.

[214] Oliver J Brady, Michael a Johansson, Carlos a Guerra, Samir Bhatt, Nick Golding, David M Pigott, Hélène Delatte, Marta G Grech, Paul T Leisnham, Rafael Maciel-de Freitas, Linda M Styer, David L Smith, Thomas W Scott, Peter W Gething, and Simon I Hay. Modelling adult Aedes aegypti and Aedes albopictus survival at different temperatures in laboratory and field settings. *Parasites & Vectors*, 6:351, 2013. ISSN 1756-3305. doi: 10.1186/1756-3305-6-351. URL http://www.pubmedcentral.nih.gov/articlerender.fcgi?artid=3867219&tool=pmcentrez&rendertype=abstract.

[215] J Sutcliffe. Distance orientation of biting flies to their hosts. *International Journal of Tropical Insect Science*, 8(4):611–616, 1987.

[216] U Wilensky. NetLogo. http://ccl.northwestern.edu/netlogo/. *Center for Connected Learning and ComputerBased Modeling Northwestern University Evanston IL*, 2009(26.02.2009):Evanston, IL, 1999. URL http://ccl.northwestern.edu/netlogo/.

[217] Jan C. Thiele and Volker Grimm. NetLogo meets R: Linking agent-based models with a toolbox for their analysis. *Environmental Modelling and Software*, 25(8):972–974, 2010. ISSN 13648152. doi: 10.1016/j.envsoft.2010.02.008. URL http://dx.doi.org/10.1016/j.envsoft.2010.02.008.

[218] Jan C. Thiele, Winfried Kurth, and Volker Grimm. RNetLogo: An R package for running and exploring individual-based models implemented in NetLogo. *Methods in Ecology and Evolution*, 3(3):480–483, 2012. ISSN 2041210X. doi: 10.1111/j.2041-210X.2011.00180.x.

[219] Volker Grimm, Uta Berger, Finn Bastiansen, Sigrunn Eliassen, Vincent Ginot, Jarl Giske, John Goss-Custard, Tamara Grand, Simone K. Heinz, Geir Huse, Andreas Huth, Jane U. Jepsen, Christian Jø rgensen, Wolf M. Mooij, Birgit Müller, Guy Pe'er, Cyril Piou, Steven F. Railsback, Andrew M. Robbins, Martha M. Robbins, Eva Rossmanith, Nadja Rüger, Espen Strand, Sami Souissi, Richard a. Stillman, Rune Vabø, Ute Visser, and Donald L. DeAngelis. A standard protocol for describing individual-based and agent-based models. *Ecological Modelling*, 198(1-2):115–126, 2006. ISSN 03043800. doi: 10.1016/j.ecolmodel.2006.04.023.

[220] M N Bayoh and S W Lindsay. Effect of temperature on the development of the aquatic stages of ¡i¿Anopheles gambiae¡/i¿ sensu stricto (Diptera: Culicidae). *Bull Entomol Res*, 93(5):375–381, 2003.

[221] C J M Koenraadt and L C Harrington. Flushing effect of rain on container-inhabiting mosquitoes Aedes aegypti and Culex pipiens (Diptera: Culicidae). *Journal of medical entomology*, 45(1):28–35, 2008. ISSN 0022-2585. doi: 10.1603/0022-2585(2008)45.

[222] J Hayes and T D Downs. Seasonal changes in an isolated population of Culex pipiens quinquefasciatus (Diptera: Culicidae): A time series analysis. *Journal of Medical Entomology*, 17(1):63–69, 1980. URL http://www.scopus.com/inward/record.url?eid=2-s2.0-0018903518&partnerID=40&md5=b81a578a3ded77debda274738559987d.

[223] Leon E. Hugo, Jason A L Jeffery, Brendan J. Trewin, Leesa F. Wockner, Nguyen Thi Yen, Nguyen Hoang Le, Le Trung Nghia, Emma Hine, Peter A. Ryan, and Brian H. Kay. Adult Survivorship of the Dengue Mosquito Aedes aegypti Varies Seasonally in Central Vietnam. *PLOS Neglected Tropical Diseases*, 8(2), 2014. ISSN 19352735. doi: 10.1371/journal.pntd.0002669.

[224] P F Verhulst. Notice sur la loi que la population suit dans son accroissement. *Corr Math et Phys*, 10(10):113–121, 1838. URL http://scholar.google.com/scholar?hl=en&btnG=Search&q=intitle:Notice+sur+la+loi+que+la+population+suit+dans+son+accroissement#0.

[225] Peijian Shi, Feng Ge, Yucheng Sun, and Chunli Chen. A simple model for describing the effect of temperature on insect developmental rate. *Journal of Asia-Pacific Entomology*, 14(1):15–20, 2011. ISSN 12268615. doi: 10.1016/j.aspen.2010.11.008.

[226] Edward E. Davis. Development of lactic acid-receptor sensitivity and host-seeking behaviour in newly emerged female Aedes aegypti mosquitoes. *Journal of Insect Physiology*, 30(3):211–215, 1984. ISSN 00221910. doi: 10.1016/0022-1910(84)90005-2.

[227] Maryland.gov department of agriculture. URL http:$//mda.maryland.gov/plants-pests/Pages/mosquitoes_host_attractants.aspx$. Accessed: 2015-06-30.

[228] S.J. Lee. Major factors affecting mosquito oviposition. *Chin. J. Entomol*, 6, 1991.

[229] Anthony a. James. *The Biology of Mosquitoes, Vol. I; Development, nutrition and reproduction*, volume 9. 1993. ISBN 0851993745. doi: 10.1016/0169-4758(93)90183-G.

[230] M J Klowden and H Briegel. Mosquito gonotrophic cycle and multiple feeding potential: contrasts between Anopheles and Aedes (Diptera: Culicidae). *Journal of Medical Entomology*, 31:618–622, 1994. ISSN 0022-2585.

[231] G Davidson. Estimation of the survival rate of anopheline mosquitoes in nature. *Nature*, 174:792–793, 1954.

[232] a.N. Clements and G.D. Paterson. The analysis of mortality and survival rates in wild populations of mosquitoes. *Journal of Applied Ecology*, 18(2):373–399, 1981. ISSN 00218901. doi: 10.2307/2402401.

[233] Linda M. Styer, James R. Carey, Jane Ling Wang, and Thomas W. Scott. Mosquitoes do senesce: Departure from the paradigm of constant mortality. *American Journal of Tropical Medicine and Hygiene*, 76(1):111–117, 2007. ISSN 00029637. doi: 10.1016/j.biotechadv.2011.08.021.Secreted.

[234] Edward T. Linacre. A simple formula for estimating evaporation rates in various climates, using temperature data alone. *Agricultural Meteorology*, 18(6):409–424, 1977. ISSN 00021571. doi: 10.1016/0002-1571(77)90007-3.

[235] J. M C Ribeiro, F. Seulu, T. Abose, G. Kidane, and A. Teklehaimanot. Temporal and spatial distribution of anopheline mosquitos in an Ethiopian village: Implications for malaria control strategies. *Bulletin of the World Health Organization*, 74(3):299–305, 1996. ISSN 00429686.

[236] Guofa Zhou, Noboru Minakawa, Andrew Githeko, and Guiyun Yan. Spatial distribution patterns of malaria vectors and sample size determination in spatially heterogeneous environments: a case study in the west Kenyan highland. *Journal of Medical Entomology*, 41(6):1001–1009, 2004. ISSN 0022-2585. doi: 10.1603/0022-2585-41.6.1001.

[237] Robert S McCann, Joseph P Messina, David W MacFarlane, M Nabie Bayoh, John M Vulule, John E Gimnig, and Edward D Walker. Modeling larval malaria vector habitat locations using landscape features and cumulative precipitation measures. *International Journal of Health Geographics*, 13(1): 17, 2014. ISSN 1476-072X. doi: 10.1186/1476-072X-13-17. URL http://www.ncbi.nlm.nih.gov/pubmed/24903736.

[238] Justin M Cohen, Kacey C Ernst, Kim a Lindblade, John M Vulule, Chandy C John, and Mark L Wilson. Local topographic wetness indices predict household malaria risk better than land-use and land-cover in the western Kenya highlands. *Malaria Journal*, 9:328, 2010. ISSN 1475-2875. doi: 10.1186/1475-2875-9-328.

[239] Jacques Régnière, James Powell, Barbara Bentz, and Vincent Nealis. Effects of temperature on development, survival and reproduction of insects: Experimental design, data analysis and modeling. *Journal of Insect Physiology*, 58 (5):634–647, 2012. ISSN 00221910. doi: 10.1016/j.jinsphys.2012.01.010.

[240] C. J M Koenraadt and Willem Takken. Cannibalism and predation among larvae of the Anopheles gambiae complex. *Medical and Veterinary Entomology*, 17(1):61–66, 2003. ISSN 0269283X. doi: 10.1046/j.1365-2915.2003.00409.x.

[241] Constantianus J M Koenraadt, Krijn P Paaijmans, Andrew K Githeko, Bart G J Knols, and Willem Takken. Egg hatching, larval movement and larval survival of the malaria vector Anopheles gambiae in desiccating habitats. *Malaria Journal*, 2:20, 2003. ISSN 1475-2875. doi: 10.1186/1475-2875-2-20.

[242] Yousif E Himeidan, Emmanuel A Temu, El Amin El Rayah, Stephen Munga, and Eliningaya J Kweka. Chemical cues for malaria vectors oviposition site selection: challenges and opportunities. *Journal of Insects*, 2013, 2013.

[243] Steve E. Bellan. The importance of age dependent mortality and the extrinsic incubation period in models of mosquito-borne disease transmission and control. *PLOS ONE*, 5(4), 2010. ISSN 19326203. doi: 10.1371/journal.pone.0010165.

[244] J C Koella and R Antia. Epidemiological models for the spread of anti-malarial resistance. *Malaria Journal*, 2:3, 2003. ISSN 1475-2875. doi: 10.1186/1475-2875-2-3.

[245] M J Turell and B H Kay. Susceptibility of selected strains of Australian mosquitoes (Diptera: Culicidae) to Rift Valley fever virus. *Journal of Medical Entomology*, 35(2):132–135, 1998. ISSN 0022-2585.

[246] Michael J Turell, Kenneth J Linthicum, Lisa A Patrican, F Glyn Davies, Alladin Kairo, and Charles L Bailey. Vector competence of selected African mosquito (Diptera: Culicidae) species for Rift Valley fever virus. *Journal of medical entomology*, 45(1):102–108, 2008. ISSN 0022-2585. doi: 10.1603/0022-2585(2008)45[102:VCOSAM]2.0.CO;2.

[247] C. Yang and U. Wilensky. NetLogo epiDEM Basic model. *Center for Connected Learning and ComputerBased Modeling Northwestern University Evanston IL*, pages Evanston, IL, 2011. URL http://ccl.northwestern.edu/netlogo/models/epiDEMBasic.

[248] R F Grais, M J Ferrari, C Dubray, O N Bjø rnstad, B T Grenfell, A Djibo, F Fermon, and P J Guerin. Estimating transmission intensity for a measles epidemic in Niamey, Niger: lessons for intervention. *Transactions of the Royal Society of Tropical Medicine and Hygiene*, 100(9):867–873, 2006. ISSN 00359203. doi: 10.1016/j.trstmh.2005.10.014.

[249] Diekmann and Jap Heesterbeek. *Mathematical Epidemiology of Infectious Diseases: Model Building, Analysis and Interpretation - O. Diekmann, J. A. P. Heesterbeek*. 2000. ISBN 9780471492412. URL http://eu.wiley.com/WileyCDA/WileyTitle/productCd-0471492418.html.

[250] C. Garrett-Jones and G. R. Shidrawi. Malaria vectorial capacity of a population of Anopheles gambiae: an exercise in epidemiological entomology. *Bulletin of the World Health Organization*, 40(4):531–545, 1969. ISSN 00429686.

[251] A Evans, F Gakuya, J T Paweska, M Rostal, L Akoolo, P J Van Vuren, T Manyibe, J M Macharia, T G Ksiazek, D R Feikin, R F Breiman, and M Kariuki Njenga. Prevalence of antibodies against Rift Valley fever virus in Kenyan wildlife. *Epidemiology and Infection*, 136(9):1261–1269, 2008. ISSN 0950-2688. doi: 10.1017/S0950268807009806.

[252] H.M. Wei, X.Z. Li, and Maia Martcheva. An epidemic model of a vector-borne disease with direct transmission and time delay. *Journal of Mathematical Analysis and Applications*, 342(2):895–908, 2008. ISSN 0022-247X. doi: DOI:10.1016/j.jmaa.2007.12.058. URL http://linkinghub.elsevier.com/retrieve/pii/S0022247X07014515.

[253] a. Marm Kilpatrick and Sarah E. Randolph. Drivers, dynamics, and control of emerging vector-borne zoonotic diseases. *The Lancet*, 380(9857):1946–1955, 2012. ISSN 01406736. doi: 10.1016/S0140-6736(12)61151-9. URL http://dx.doi.org/10.1016/S0140-6736(12)61151-9.

[254] Eric Millstone, Hannington Odame, and Oscar Okumu. Rift valley fever in kenya: Policies to prepare and respond. 2015.

[255] BH1 Bird, TG Ksiazek, ST Nichol, and NJ. Maclachlan. Rift valley fever virus. *J Am Vet Med Assoc.*, 7(234):883–93, April 1 2009. URL doi:10.2460/javma.234.7.883.

[256] C P Farrington, M N Kanaan, and N J Gay. Branching process models for surveillance of infectious diseases controlled by mass vaccination. *Biostatistics (Oxford, England)*, 4(2):279–295, 2003. ISSN 1465-4644. doi: 10.1093/biostatistics/4.2.279.

[257] Glenn E. Lahodny and Linda J S Allen. Probability of a Disease Outbreak in Stochastic Multipatch Epidemic Models. *Bulletin of Mathematical Biology*, 75(7):1157–1180, 2013. ISSN 00928240. doi: 10.1007/s11538-013-9848-z.

[258] G.R. Grimmett and D.R. Stirzaker. Probability and random processes. *Oxford, UK: Oxford University Press*, 1992.

[259] K.B. Athreya and P.E. Ney. Branching processes. *Berlin, Germany: Springer.*, 1972.